The Dissertation Committee for Yun Gon Kim Certifies that this is the approved version of the following dissertation:

Shear Behavior of Reinforced Concrete T-Beams Strengthened with Carbon Fiber Reinforced Polymer (CFRP) Sheets and CFRP Anchors

Committee:

James O. Jirsa, Supervisor

Wassim Ghannoum, Co-Supervisor

Sharon L. Wood

Oguzhan Bayrak

Kenneth Liechti

Shear Behavior of Reinforced Concrete T-Beams
Strengthened with Carbon Fiber Reinforced Polymer (CFRP) Sheets
and CFRP Anchors

by

Yun Gon Kim, B.S., M.S.

Dissertation

Presented to the Faculty of the Graduate School of

The University of Texas at Austin

in Partial Fulfillment

of the Requirements

for the Degree of

Doctor of Philosophy

The University of Texas at Austin
December, 2011

Dedication

To my baby boy

Acknowledgements

Shear Behavior of Reinforced Concrete Beams
Strengthened with Carbon Fiber Reinforced Polymer (CFRP) Sheets
and CFRP Anchors

Publication No._____

Yun Gon Kim, Ph.D.

The University of Texas at Austin, 2011

Supervisor: James O. Jirsa

Co-supervisor: Wassim Ghannoum

The objective of this research is the evaluation of shear behavior of full-scale reinforced concrete T-beams strengthened with carbon fiber reinforced polymer (CFRP) sheets and CFRP anchors. Although the CRFP material has high tensile strength, premature failure due to debonding CFRP sheets prevents utilizing that strength. The use of CFRP anchors prevents this failure, so the CFRP sheets are able to reach ultimate strain.

The current shear design is based on plasticity, which assumes that all steel (ductile material) stirrups, across the critical section yield at ultimate. However the strain in the CFRP (brittle material), is essential to estimate the shear contribution of CFRP. To evaluate the validity of CFRP strengthening for shear, 24 tests were conducted with

several parameters including shear-span-to-depth ratio, depth of beams, different transverse reinforcement ratios, and the layout of CFRP strips. In addition, a simple shear behavior model was developed to explain the differences between ductile and brittle material.

From test observation, the use of CFRP anchors resulted in U-wrap application to perform like continuous wrapping which implies that a CFRP strip reached rupture strain because the anchors prevented debonding failure. However, all FRP strips did not rupture simultaneously because the strain distribution across a critical crack was not uniform. The average strain across the critical crack was about 0.005. Therefore a conservative value of effective strain (0.004) was selected for design purposes.

In addition, when a beam is strengthened with CFRP, interactions between the contributions of the CFRP, steel or concrete must be taken into account. Factors k_a, k_s, and k_f were introduced in the proposed shear design equations. Factor k_a reflects the change in the material contributions as the shear span to depth ratio (a/d ratio) changes in deep beams. Factors k_s and k_f account for the change in steel or CFRP shear contribution due to the change in the critical crack angle as well as the interactions between the steel and FRP transverse reinforcement. As the amount of either steel or FRP material increase, the efficiency of the other material decreases.

Table of Contents

xiii

List of Tables

List of Figures

xviii

xxiii

CHAPTER 1

Introduction

1.1 OVERVIEW

Carbon Fiber Reinforced Polymers (CFRP) is a suitable material for strengthening and rehabilitating RC structures because of its light-weight and flexibility and ease of installation. The material must be attached to the concrete using epoxy resins. However, debonding of the CFRP prevents the development of the full material capacity, leading to premature failure. CFRP anchors may provide a solution to such failure. This research is focused on shear strengthening of reinforced concrete elements using CFRP sheets and CFRP anchors.

1.1.1 Necessity of Rehabilitation

As many reinforced concrete structures become obsolete, repair and strengthening techniques become more important. While replacement may be a fundamental and permanent solution, in many cases, non-construction costs associated with demolishing old structures may lead to rehabilitation as a viable option. For example, destruction of a bridge which is located at a river crossing a congested urban area will create traffic problems while a new bridge is built, whereas rehabilitation can relieve this problem by remaining, at least partially, in operation. The cost of traffic congestion cannot be neglected and rehabilitation may have benefits over new construction.

The main reasons for strengthening are increases in the required loads due to change in use, increase in permitted load, or more stringent code requirement and decreases in the capacity of elements due to corrosion, fabrication errors, damage by impact load, and material deterioration with time or under adverse environmental

condition. The repair/ strengthening techniques have more limitations than new construction in several aspects. Therefore, the ability to quickly apply the materials with a minimum of disruption to the use of a structure and with virtually no change in the geometry or weight of the element makes Fiber Reinforced Polymers a viable and attractive method for strengthening existing elements. For these reason, a large amount of research has been conducted on the use of FRP materials for structural strengthening and Carbon Fiber Reinforced Polymers (CFRP) are widely used FRP materials.

1.1.2   CFRP Anchors in Shear Applications

In most of the studies reported in the literature, the forces are transferred from the concrete member into the CFRP through interface bond. As a result, it has been found that although the CRFP material has high tensile strength, only about 40 to 50% of that strength can be realized because premature failure occurred through delamination of CFRP sheets. Therefore, the designer must take a conservative approach to avoid unexpected and premature failure. The use of CFRP anchors provides a means of precluding debonding failure, so that the CFRP sheets are able to reach their ultimate strain. Recently, the effect of CFRP anchors in flexural application was verified by Kim (2008) and Orton (2007), who reported that the failure of members strengthened using FRP materials was due to fracture of the FRP fiber. The members with anchors reached much higher capacities than those without anchors. However, it remains unclear whether CFRP anchors are effective in shear applications. Shear behavior is totally different from flexural behavior. The strain in the flexural reinforcement of under-reinforced beams is generally greater than 1%, which is close to ultimate strain of CFRP.

However, the strain in shear reinforcement is not likely to reach 1% because the compression capacity of the concrete in shear is controlled by principal tensile strain. If the shear failure is governed by the deficiency in shear capacity of concrete, the strain in the CFRP may be less than the ultimate strain of CFRP despite the use of CFRP anchors.

In addition, the strain distribution of the FRP sheet across the critical crack of the beam is not likely to be uniform. Unlike steel, the stress-strain relationship of the FRP

material is linear up to failure, which means non-uniform strain distribution results in the non-uniform stress distribution. Therefore, to determine the shear contribution of CFRP materials, it is essential to evaluate the strain of CFRP when the maximum capacity of composite elements is reached. Stress compatibility is a key issue in evaluating the shear contributions of concrete, stirrups and CFRP laminates. For these reasons, investigation of shear strengthening using CFRP and CFRP anchors is required regardless of the result of CFRP anchors in flexural application. Furthermore, shear behavior is not easy to estimate the location of critical section or the direction of crack. Because the strength of CFRP is unidirectional, the location and direction of fiber relative to the stress applied to the concrete determine whether the capacity of the CFRP materials can be developed.

1.1.3   Necessity for Quality Control in Practical Applications

Many requirements have been proposed for surface preparation of the concrete to increase bond stress and delay debonding failure. However, surface preparation is not critical factor with the use of CFRP anchors because CFRP anchors provide an alternative stress transfer path after debonding occurs.

However, the anchorage system must be properly designed and installed for the anchors to be effective. It is essential to develop the specifications for quality control. Because most installation procedures depend on worker's expertise, installation procedures need to be standardized. In addition, the certification of qualified workers will improve the quality of installation.

1.2   OBJECTIVES AND SCOPE

The objective of this research was an evaluation of shear strengthening of full-scale reinforced concrete beams using carbon fiber reinforced polymers (CFRP) and CFRP anchors. To evaluate the validity of CFRP strengthening for shear, tests were conducted considering a number of parameters: shear-span-to-depth ratio, depth of beams, layout of CFRP strips, number of anchors, and surface preparation of concrete. A

simple shear behavior model was developed to explain shear behavior in brittle material. This model was calibrated with test results. Finally, design recommendations for shear strengthening using CFRP anchors were developed. Material and construction specifications were included to assist implementation of CFRP shear strengthening in the field. Figure 1-1 shows the overall organization of this dissertation.

Chapter. 1 Introduction

1.1 Overview
1.2 Objectives and Scope

Chapter. 2 Background

2.1 Carbon Fiber Reinforced Polymers (CFRP)
2.2 Externally Bonded FRP Systems
2.3 Shear Strengthening
2.4 CFRP Anchors

Chapter. 3 Experimental Program

3.1 Design Considerations
3.2 Specimen Configurations
3.3 Material Properties
3.4 Estimate of Beam Capacity
3.4 Test Setup
3.5 Instrumentations

Chapter. 4 Test Results

4.1 Overview of Test Results
4.2 Test Observations
4.3 Evaluation of Shear Contributions
4.4 Test Results
4.5 Result Analysis with Parameters
4.6 Summary of Test Performance at
    Major Events

Chapter. 5 Shear Behavior Model

5.1 Motivation for the Shear Behavior
    Model

5.2 Axial Tensiion

5.3 Bond Behavior

5.4 Shear Behavior of Beam Strength-
    ened with FRP

5.5 Shear Behavior Model for FRP
    RC beams

5.6 Shear Behavior Model Consider-
    ing Bond

5.7 Summary

Chapter. 6 Design Recommendations

6.1 Evaluation of Existing Structure
6.2 Design Equations
6.3 Design Considerations
6.4 Specifications

Chapter. 7 Conclusions

7.1 Conclusions
7.2 Future Study

Figure 1-1 Organization of dissertation

5

CHAPTER 2
Background

CFRP has been widely used in strengthening due to advantages over other materials despite high material cost. Many studies have been conducted to evaluate the behavior of FRP material and to develop procedures for application that will result in reliable performance. Most studies have focused on the flexural strengthening. However the members may also have shear deficiencies. Design or construction errors and changes in loading may produce such deficiencies. However, methods for shear strengthening with CFRP material have not been studied in detail.

Debonding, i.e. separation between FRP sheets and the concrete surfaces complicate FRP composite behavior. If debonding failure is prevented, it may be possible to neglect many parameters that influence bond behavior. Furthermore, debonding failure limits the use of the inherent material capacity by reducing the effective strain in the FRP. Therefore, it is possible to maximize the CFRP material capacity by preventing debonding failure. Several anchorage systems have been tried to prevent debonding failure. CFRP anchors provide a new technique for preventing debonding failure.

2.1 CARBON FIBER REINFORCED POLYMERS (CFRP)

2.1.1 History of FRP Material in Civil Engineering

Fiber Reinforced Polymer (FRP) composite applications have been widely used since the 1940s in many industries, including aerospace, marine, electrical and transportation. FRP composite products were first demonstrated to reinforce concrete structures in the mid-1950. In the 1980s, FRP reinforcing bars was used to reinforce concrete where nonmagnetic properties were required or applied to areas that were

subjected to severe chemical attack. However, the most extreme use of FRP for civil engineering structure has been the application of externally bonded FRP for rehabilitation and strengthening of concrete structures. FRP materials have an advantage over steel due to their resistance to corrosion, high strength-to-weight ratios, and ease of application in spite of high material cost and a stiffness that is less than that of steel.

2.1.2 CFRP Material

2.1.2.1 FRP materials: GFRP, AFRP, CFRP

FRP materials are composite materials that typically consist of fibers embedded in a resin matrix. The most common fibers are glass, aramid and carbon. Typical tensile properties are shown in Table 2-1. Matrixes are typically epoxies, polyesters, vinylesters, or phenolics. Epoxy resin is typically used.

Table 2-1 Typical tensile properties of fibers used in FRP systems (ACI 440.2R)

Fiber type	Elastic modulus (ksi)	Ultimate strength (ksi)	Rupture strain Minimum
Carbon (High-strength)	32000 ~ 34000	550 ~ 700	0.014
Glass (E-glass)	10000 ~ 10500	270 ~ 390	0.045
Aramid (High-performance)	16000 ~ 18000	500 ~ 600	0.016

Table 2-2 Typical tensile properties of FRP laminates (ACI 440.2R)

FRP system (w/epoxy)	Young's modulus (ksi)	Ultimate strength (ksi)	Rupture strain
Carbon (High-strength)	15000 ~ 21000	150 ~ 350	0.010 ~ 0.015
Glass (E-glass)	3000 ~ 6000	75 ~ 200	0.015 ~ 0.030
Aramid (High-performance)	7000 ~ 10000	100 ~ 250	0.020 ~ 0.030

Note. The fiber volume fraction of the laminate is about 40 to 60 percent.

Comparing the properties from Table 2-1 and Table 2-2, tensile properties of FRP laminates are less than those of FRP fibers. In general, FRP bars have fiber volumes of 50

to 70%, precured systems have fiber volumes of 40 to 60%, and wet lay-up systems have fiber volumes of 25 to 40%. Because the fiber volume influences the gross-laminate properties, precured laminates usually have higher mechanical properties than laminates created using the wet layup technique. (ACI 440.2R)

2.1.2.2 CFRP

Of the three FRP materials, Carbon Fiber Reinforced Polymer (CFRP) is widely used for structural purposes despite being the most expensive. First, CFRP has relatively high tensile modulus, durability. In addition, CFRP performs well when subjected to fatigue loads. CFRP does not absorb moisture and has a very low coefficient of thermal expansion in the longitudinal direction. Therefore, CFRP is considered to be the most durable of those materials. In field application, durability is an important factor because the quality of material may be affected by environmental conditions such as thermal changes, moisture, fatigue load, and corrosive condition. As shown in Table 2-3, ACI 440.2R uses an environmental reduction factor (C_E). CFRP has the highest factor (C_E) of the three materials, which implies that the strength reduction due to environmental conditions is the least in CFRP. However, FRP materials are sensitive to heat because of their thermal conductivity. As a result, a fire proof treatment may need to be considered.

Table 2-3 Environmental reduction factor for various exposure conditions (ACI 440.2R)

Exposure conditions	Fiber type	Environmental reduction factor C_E
Interior exposure	Carbon	0.95
	Glass	0.75
	Aramid	0.85
Exterior exposure (bridges, piers, and unenclosed parking garages)	Carbon	0.85
	Glass	0.65
	Aramid	0.75
Aggressive environment (chemical plants and wastewater treatment plants)	Carbon	0.85
	Glass	0.50
	Aramid	0.70

2.1.2.3 *Advantages as a strengthening material compared with steel*

For reinforcing concrete, CFRP materials do not have much benefit over steel because steel has a higher elastic modulus and is less expensive. However, CFRP material is often more attractive than steel for retrofit in structures because of its light-weight and quick application.

2.1.3 Material Property of CFRP

2.1.3.1 *Mechanical properties of CFRP compared with steel*

CFRP is an uniaxial and brittle material which has no yield stress plateau. CFRP has a linear stress-strain relationship up to failure. Figure 2-1 shows the nominal material properties of Grade 60 steel and CFRP laminate used in this research Compared to reinforcing steel, the stiffness of CFRP (14800 ksi) is roughly half and the ultimate stress of CFRP (154 ksi) is two and a half times assuming that its rupture strain (0.0105) is reached.
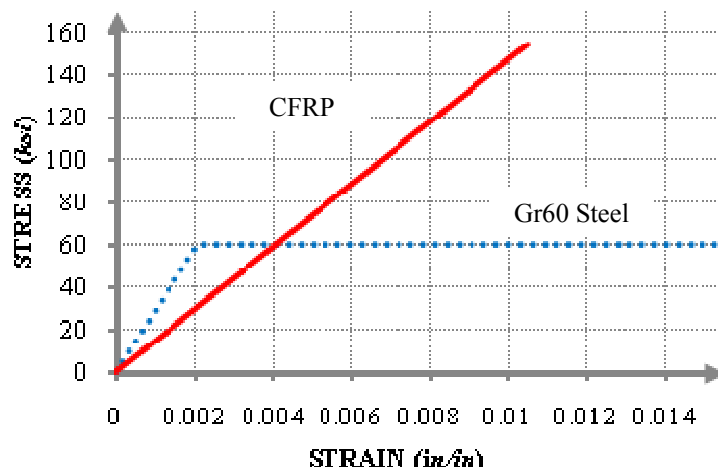
Figure 2-1 Material properties between steel and CFRP

These characteristics complicate the behavior of RC members strengthened with CFRP when used for shear strengthening. To utilize CFRP material capacity effectively, large strain must be developed. However larger strain may lead to serviceability problems Also damage to the concrete may occur before the full strength of CFRP material is

9

reached. For shear strengthening, wide cracks may occur, but would not be acceptable for serviceability.

2.1.3.2   Fiber properties vs. laminate properties

There are two different methods for determining material properties for design. One method uses the properties of the FRP composite (fiber and resin) which are calculated using the measured gross area of the FRP composite, the other method uses the properties of the fibers only, which are calculated using manufacturer-supplied area of the fibers in a dry sheet or fabric.

The fibers in manufactured laminates typically constitute 40 to 60% of the matrix. Therefore, laminates have different material properties from fibers. (See Table 2-1 and Table 2-2)

2.1.3.3   Manufacturer's specifications (ACI440.2R)

Manufacturer's specification sheets contain values of the ultimate design tensile strength which is defined as the mean tensile strength of a sample of test specimens minus three times the standard deviation ($f_{fu}^* = \overline{f_{fu}} - 3\sigma$) and, ultimate design rupture strain is defined similarly ($\varepsilon_{fu}^* = \overline{\varepsilon_{fu}} - 3\sigma$). This approach provides a 99.87% probability that the material will exceed these statistically-based design values for a standard sample distribution. In addition Young's modulus should be calculated as the chord modulus between 0.003 and 0.006 strain. A minimum number of 20 replicate test specimens should be used to determine these properties.

Based on this approach, the greater the standard deviation of the material strength, the lower would be the design strength compared to the mean value. Because the variation of FRP properties is greater than that of steel, the design efficiency of FRP will be lower. These characteristics are typical of brittle materials such as CFRP as will be discussed in Chapter 5.

2.2   EXTERNALLY BONDED FRP SYSTEMS

2.2.1   History of Externally Bonded FRP systems

The strengthening of existing concrete structures using FRP materials to resist higher design loads, correct strength loss due to deterioration, correct design or construction deficiencies, or increase ductility has been studies externally (ACI 440.2R). FRP is a viable alternative to traditional materials. The use of FRP wrapping for the confinement of concrete column subjected to lateral loads due to earthquakes was one of the early applications. Flexural strengthening with FRP materials has also been studied. Since the early 1990s, FRP shear strengthening of concrete members has been studied because of desire that flexure rather than shear governs behavior. Many researchers have studied the behavior of member strengthened in shear using FRP, but there is no unifying theory has been proposed to define this behavior.

2.2.2   Failure mode

Typical modes of failure in shear strengthened member include concrete crushing, FRP rupture and loss of bond between the FRP and the concrete surface. All their failure modes are brittle, but FRP rupture is the most desirable failure because the full capacity of FRP material can be utilized. The capacity determined by failure due to concrete crushing may provide a criterion for determining the strengthening limit. If the capacity is governed by concrete crushing, it is meaningless to apply additional FRP material. The most complicated failure mode is FRP debonding.

2.2.3   Debonding

Debonding is the loss of bond between FRP and substrates that complicate the behavior of FRP composite elements. Many studies have been conducted to evaluate the bond behavior between FRP and concrete substrates. Because many variables are involved, bond behavior still needs to be investigated. The bond stress between FRP and concrete substrates is important to determine the FRP contribution to shear capacity when

FRP debonding failure controls the FRP capacity. Because debonding occurred at considerably lower than ultimate stress, avoiding FRP debonding is a key to utilizing the full FRP material capacity. An improperly prepared surface is likely to accelerate debonding or delamination of the FRP system.

2.2.4   Surface Preparation Guideline from ACI 440.2R

2.2.4.1   Injection of crack

Cracks wider than 0.010 in. should be pressure injected with epoxy because those crack can affect the performance of the externally bonded FRP system through delamination or concrete crushing. Smaller cracks exposed to aggressive environments may require resin injection or sealing to prevent corrosion of existing steel reinforcement.

2.2.4.2   Bond-critical or contact-critical application

Surface preparation requirements should be based on the intended application of the FRP system, categorized as bond-critical or contact-critical. Bond-critical applications require an adhesive bond between the FRP system and the concrete, whereas contact-critical applications, such as confinement of columns, only require between the FRP system and the concrete in contact. Contact-critical applications do not require an adhesive bond between the FRP system and the concrete substrate.

2.2.4.3   Requirements for bond-critical applications

Where fibers wrap around the corners of rectangular cross sections, the corners should be rounded to a minimum 0.5 in. radius to prevent stress concentrations in the FRP system and voids between the FRP system and the concrete. Localized out-of-plane variations, including form lines, should not exceed 1/32 in. or the tolerances recommended by the FRP system manufacturer. Localized out-of-plane variations can be removed by grinding, before abrasive or water blasting, or can be smoothed over using resin-based putty if the variations are very small. Bug holes and voids should be filled with resin based putty.

2.2.5 Installation Process: Wet Lay-up and Dry Lay-up

There are two installation procedure including hand layup (wet-layup) and dry layup. Appendix A described the wet-layup process including CFRP anchor. In addition, the detail procedures of both layups were also described in the thesis of Quinn (2009) who was the person under same project. The capacity of CFRP strengthening is affected by quality of installation. Therefore, expertise of worker and quality control is also big issue to apply CFRP in practice. As a result, the certificate system for installers needs to be considered.

2.2.6 Strengthening Limit

The unstrengthened member without FRP reinforcement should have sufficient structural capacity to guard against collapse of the structure, or failure of FRP system. In ACI 440.2R, the beam before strengthening should satisfy following equation.

$$(\phi R_n)_{existing} \geq (1.1DL + 0.75LL)_{new} \tag{2-1}$$

2.2.7 Nature of Repair / Strengthening

Unlike the design of new members, the initial/residual conditions of the existing structure must be considered in the design of strengthened elements. Residual stresses might reduce the contribution of FRP to the member capacity. It is desirable to minimize initial stress conditions in practice. For this reason, the results from experimental studies in a laboratory should be considered in field application. For example, the accessible space for strengthening, expertise of workers and environmental conditions will affect the quality of application. An additional strength reduction factor may need to be considered under adverse field conditions. In this research, some tests were conducted with the damaged beams before strengthening with CFRP, but no sustained load was applied when the CFRP materials were installed. A beam in situ will be under some sustained load.

13

2.3   SHEAR STRENGTHENING

2.3.1   Shear Behavior

The general design concept for reinforced concrete member is that derived the overall behavior to be ductile rather than brittle. As a result, shear (brittle behavior) capacity of member is usually designed to be greater than the flexural (ductile behavior) capacity. It is generally known that the concrete shear contribution comes from (1) shear stress in the uncracked concrete; (2) aggregate interlocking; (3) dowel action of the longitudinal reinforcement; and (4) arch action. However, the shear behavior is still not clearly understood, so many researchers continue to study a various aspects of shear behavior.

Current ACI shear design is based on a plasticity mechanism. Steel stirrups across a critical crack will reach yield strain and maintain a stress equal to or greater than the nominal yield of the reinforcement. After yielding, a stirrup maintains a nearly constant stress as additional force is transferred to adjacent stirrups, so all stirrups across a critical crack can be assumed to reach yield at shear failure. An estimate of shear capacity depends on the number of stirrups contributing to the shear capacity as determined by the critical crack angle. Although the reported critical angle from many studies is usually less than 45 degrees, a 45 degree angle is assumed.

Modified compression field theory (MCFT) is adopted in AASHTO (2007) provision. This approach provides more detailed estimates of shear capacity, but it is quite complicated for design purpose.

2.3.2   Comparison between Flexure and Shear in FRP Strengthening

The lack of a compatibility condition for shear response makes evaluation of FRP strengthening more complicated. When a beam is governed by flexure, tension-control (yielding of reinforcement) or compression-control (crushing of concrete), the capacity is evaluated from compatibility of strains across the section. In addition, it is possible to

evaluate the FRP contribution to flexural strength because the strain information can be calculated.

To evaluate the shear behavior when CFRP is used, the following issues need to be considered. CFRP material behaves linearly up to failure, which means that there is no yield plateau or constant stress regardless of the strain level in FRP material. Therefore it is necessary to know the strain in the FRP reinforcement to estimate the FRP shear contribution. The force a CFRP strip carries is lost when rupture occurs and will be transferred to adjacent strips until they rupture. Therefore, a failure of the member may occur simultaneously when the first strip ruptures.

2.3.3   Previous Studies of Shear Strengthening

Shear capacity of members strengthened with FRP material continues to be studied because FRP strengthening in field application is becoming more common.

To date, there is no unique theory available to evaluate the shear behavior of FRP strengthened beams. Most researchers have defined the contribution of the FRP to the shear strength as the product between the effective stress in FRP, the area of the FRP, partial reduction factors that intend to take into account the quality of material and/or workmanship, and a geometrical factor depending on the type of strengthening system used, as well as fiber inclination with respect to the beam longitudinal axis. (Sas et al. 2009)

Triantafillou (1998) and Triantafillou and Antonopoulos (2000) developed a model based on regression analysis and truss analogy. They developed different effective FRP strain equations with respect to the type of strengthening schemes.

Triantafillou (1998) and Khalifa et al. (1998) modified the conventional shear equation with a modified effective strain, which is the product of a reduction factor and rupture strain. This reduction factor was applied to both fiber rupture and debonding the failure. Pellegrino and Modena (2006) continued to study this model and modified the reduction factor.

Chen and Teng (2001, 2003 a, b) developed a reduction factor for the FRP stress with using a truss model. The reduction factor was different for FRP rupture or FRP debonding. They stressed the importance of non-uniform strain distribution in the material. They will be discussed in more detail in Section 2.3.4.1.

Diniaud and Cheng (2001, 2004) used modified shear friction with different crack patterns for the flange and web of T-beams.

Zhang and Hsu (2005) proposed a shear bond model derived by curve fitting and different bond mechanisms. They concluded that debonding dominates over tensile rupture of CFRP laminates as they become thicker and stiffer, thus the effective strain needs to be consequently reduced.

Sas et al. (2009) studied existing shear models and compared computed values with an experimental database. They stated that the results of the comparison were not very promising and using a shear contribution for the FRP based on existing shear design equations should be questioned. However, it is adopted in present guidelines despite such inadequacy. More viable and reliable models continue to be needed. They stated that many studies have calibrated models with data from laboratory specimens that had unrealistic geometric conditions and stated that the following issues need to be addressed.

Is a rectangular beam compatible to T-beam?

Is size effect considered?

Is the laboratory condition consistent with field condition?

Is the quality of FRP monitored?

(application procedure or expertise of workers)

2.3.4 Parameters to Evaluate the Shear Contribution in the FRP

2.3.4.1 Strain distribution across the critical crack

The configuration of a critical shear crack is complicated. As the applied load increased, the location and orientation of shear crack might change. Although it is assumed that the critical crack at ultimate is the only concern, the crack width is not

constant along the crack. Furthermore, the critical crack orientation is not consistent and keeps changing along the crack. For this reason, the strains in the reinforcing elements, such as steel stirrup and CFRP sheet, are not uniform along the crack.

Many researchers have studied the non-uniform distribution of strains in FRP across the critical crack. Chen and Teng (2003, 2004) concluded that the stress distribution in the FRP along the crack plane is not uniform and proposed a model that takes into account fiber rupture and debonding. Carolin and Taljseten (2005) recommended 55 to 65% of the maximum measured strain value for engineering design based on non-uniform strain distribution.

Although the crack width can be measured, the angle between the crack and the reinforcing element also needs to be known because crack width in the direction of the fiber is important. In steel, bond between the steel stirrup and concrete is not uniform along the stirrup, which means the total stirrup length cannot be used when strain is calculated. However, once steel yields, the strain value is not important because the stress will be constant and the bond between steel and concrete also will be zero near the crack region.

Similarly, FRP debonding makes the strain evaluation in the CFRP difficult. The effective length (or stressed length) will be longer at the same strain level in the process of FRP debonding. Therefore, strains along the fiber direction may be constant during debonding even though the crack width increases.

In other words, there is no direct relationship between crack width and strain distribution. Furthermore, the strain values between steel and CFRP at the same location are not identical because the effective lengths of both steel and CFRP are not the same.

Finally, no strain compatibility condition can be derived. However, it is essential to evaluate the shear contribution of stirrup and FRP at certain levels of shear. For this reason, a simple strain distribution is assumed in this research. Therefore, a conservative approach can be accepted for design purpose as will be discussed in Chapter 5.

2.3.4.2 Amount of CFRP material

Many experimental results indicate that a linear relationship between the amount of CFRP material and shear contribution of FRP is not valid. The shear contribution is less than doubled when the material is doubled. Despite these test results, the shear capacity based on current guidelines is proportional to the FRP area. This may be unsafe when a large amount of CFRP material is used. The maximum strengthening ratio only controls excessive strengthening in current guideline. This characteristic is also observed in steel, but it is more significant in CFRP.

2.3.4.3 Interaction between steel stirrup and CFRP strip

Many studies indicate that evaluation of the CFRP shear contribution is related to the amount of existing steel stirrups. The shear contribution of FRP (i.e. V_f) tends to decrease with an increase in the stiffness ratio between the internal steel shear reinforcement and the external FRP shear reinforcement (Bousselham and Chaallal 2004; Pellegrino and Modena 2006). The maximum shear contributions of steel stirrups and FRP may not be reached simultaneously. The combined contribution may be less than the sum of the respective peak values of V_f and V_s. Chen at al. (2010) also stated that FRP shear contribution was reduced when a large amount of steel reinforcement was used in connection with FRP strips having a high axial stiffness.

Due to the brittleness of failure, the strains in some steel stirrups may be below their yield strain. Consequently, all steel stirrups intersected by the critical shear crack do not reach yielding at failure and may contribute less than what is predicted by existing shear strength models. Chen et al. (2010) also stated that as debonding occurs in a brittle manner at relatively small shear crack widths, some of the internal steel stirrups may not have reached yielding. For this reason, the yield strength of internal steel stirrups in such a strengthened RC bean cannot be fully used. Although many researchers have commented on this effect, there is no consideration for this interaction in design equation.

2.3.4.4 *Critical crack angle*

The critical crack is defined as the dominant diagonal crack that leads to failure and is used for evaluating the contribution of transverse reinforcement. The critical crack angle makes the evaluation of shear contribution in each material difficult because this angle cannot be specified when materials that have dramatically different properties are combined. Although experiments have shown that the crack inclination can vary between 30º to 60º, a 45 degree angle is used in most cases to be conservative. As applied load increases, the critical crack angle is likely to decrease. It is because the concrete itself finds the optimized load path at a cracked section. In other words, once cracked, a different load path may be more effective. More transverse reinforcement would be involved in the contribution to the system when critical crack angle decrease. Malek and Saadatmanesh (1998 a, b) studied the shear behavior with web-bonded FRP plates. Using an analytical approach, they concluded that the critical crack angle increased as more FRP material was applied.

Shear span to depth ratio is also a main parameter influencing the critical crack angle. For low shear span to depth ratios, compression in the direct strut is likely to affect the critical angle and most of the shear is transferred through a direct strut. The critical angle of a beam with low shear span to depth ratios will increase.

The shear contribution from direct strut makes up for the loss in steel contribution due to crack angle. Therefore, overall capacity can increase although the shear contribution of steel stirrups would be expected less due to steeper critical angle.

2.3.4.5 *Bond length*

Because the capacity of member strengthened with FRP is generally controlled by debonding failure, it is important to evaluate bond length. Usually, insufficient bond length accelerates the debonding process, whereas there is no additional benefit once bond length is greater than required length.

Effective Bond Length

- **—— 0.9999 Pu**
- —— 0.999 Pu
- — –· 0.96 Pu
- ········ 0.8 Pu
- — ·· 0.5 Pu
- ········ 0.2 Pu

Local bond stresses

Free end | Loaded end

Concrete

FRP

P

(a) Bond stress distribution

Effective Bond Length

- **—— 0.9999 Pu**
- —— 0.999 Pu
- — –· 0.96 Pu
- ········ 0.8 Pu
- — ·· 0.5 Pu
- ········ 0.2 Pu

Strain in FRP

Free end | Loaded end
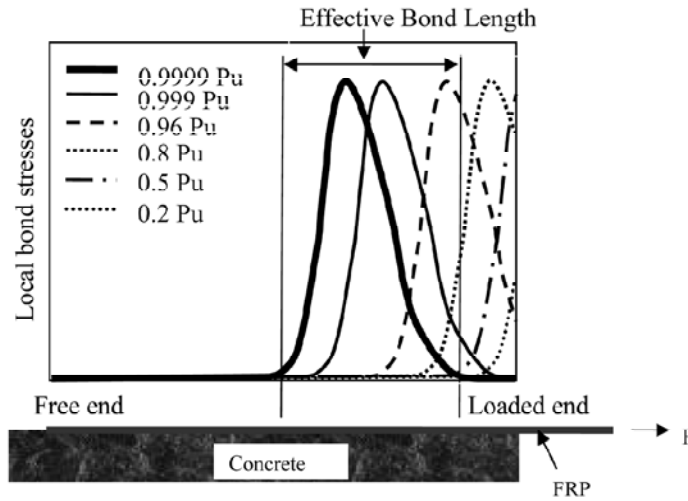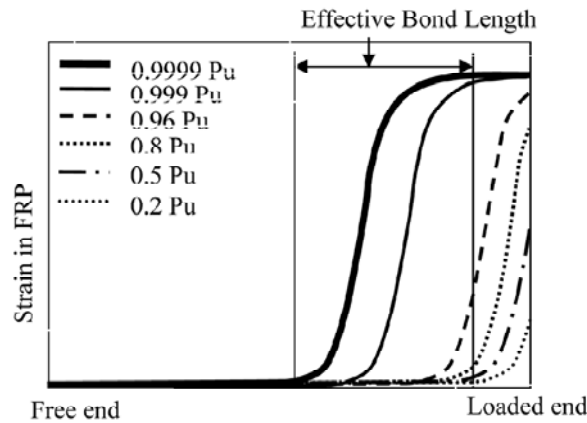
(b) Tensile strain (stress) distribution

Figure 2-2 Concept of the effective bond length (Ueda and Dai, 2005)

Debonding occurs first within the effective bond length (defined as a length over which the majority of the bond stress is maintained, see Figure 2-2) as a result of debonding of a very thin layer of concrete rather than debonding at the FRP-concrete interfaces. As shown in Figure 2-2, the shape of bond stress was changed and the tensile strain/stress was also affected by the bond stress as the applied load increased.

As shown in Figure 2-3, the effective length in one equation increases and the effective length using another equation decreases as the number of layers increases and indicates that bond behavior needs to be studied in more detail.

20
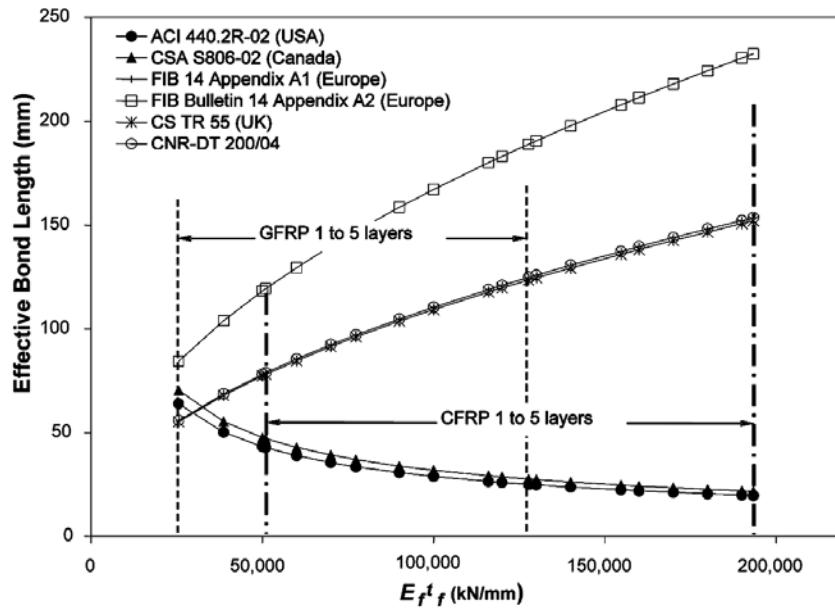
Figure 2-3 Bond length calculated by the current guidelines (Ouezdou et al. 2009)

The effective length proposed by Maeda (1997) was adopted in for the ACI 440. 2R shear equation developed by Khalifa (1998). In this equation, with the range 1 to 5 layer of CFRP, the effective bond length is less than 2 in. (50 mm) and the difference of these values is not much.

In shear behavior, there is no way for some FRP fibers to avoid bond failure at a diagonal crack except under fully wrapped condition. Therefore, most shear equations considering debonding failure include bond length as a parameter.

Most debonding failures in U-wrap can be avoided with anchorage systems. It is possible to remove bond length from parameters to determine the member capacity.

If service load is considered, the bond stress or debonded length is still important for evaluating the stiffness of FRP laminate. The strain in the FRP is usually limited to the debonded region. These strains along the debonded region are uniform and beyond debonded region the strain decrease dramatically due to bond between FRP and concrete. In other words, different strains develop even though crack width is the same. This fact makes it difficult to evaluate compatibility conditions between steel and CFRP reinforcement.

2.3.4.6 FRP sheet orientation

Ideally, it is best to place the FRP sheet perpendicular to the direction of the critical crack. However, there are several drawbacks. As the orientation of FRP sheet changes, the installation procedure becomes more difficult. In addition, the length of a strip normal to a crack will be longer than a vertical application, which means that more material is needed. With the same amount of material that is used in a diagonal application, a greater width of vertical strips can be applied.

2.3.4.7 Size effect

Size effect is still controversial in shear behavior even when FRP strengthening is not considered. In addition to this, size effect of FRP strengthening needs to be taken into acccount. Several studies showed that current design guidelines based on small beams are not valid for full- sized beam. (Chaallal et al., 2002)

In FRP shear strengthening, the size effect might be related to the depth of beam. The required bond length may be long compared with the depth of a short beam, but it may be less than the depth of a deep beam. Therefore, A shallow beam is more likely to develop end debonding. Even if anchors are used, the strain along a debonded region in a shallow beam will be greater than in a deep beam assuming the same width of crack, which means that a deep beam may exhibit lower stiffness. For these reasons, the equations derived from small specimens of experimental studies might not be applicable for practical beam sizes.

2.3.4.8 Other parameters

The effect of pre-existing cracks and negative moment on the performance of a strengthened beam is an interesting issue. According to the observations in NCHRP report 678 (2011), tests on beams with pre-existing cracks prior to strengthening showed that stirrups yield at a lower shear force than for beams without cracks. However, the existence of cracks seemed not to change the failure modes of the beams suggesting that the existence of cracks does not adversely influence the effectiveness of FRP shear

strengthening. In addition, beam continuity (negative moment) did not appear to influence the behavior of the beams strengthened with FRP (similar behavior to beams tested under positive moment conditions).

2.3.5 ACI 440.2R

ACI 440.2R is the most widely used guideline for externally bonded FRP systems. The design recommendations in ACI 440.2R-08 are based on limit-states design principles and are compatible with ACI 318-05. This approach sets acceptable levels of safety for the occurrence of both serviceability limit states (excessive deflections and cracking) and ultimate limit states (failure, stress rupture, and fatigue). FRP-related reduction factors were calibrated to produce reliability indexes typically above 3.5. Increasing the shear strength can also result in flexural failures, which are relatively more ductile in nature and more desirable than shear failures.

2.3.5.1 *Wrapping schemes*

Figure 2-4 shows three types of FRP wrapping schemes used to increase the shear strength. Completely wrapping the FRP system around the section on all four sides is the most efficient wrapping scheme and is most commonly used in column applications where access to all four sides of the column is usually available. In beam applications where an integral slab makes it impractical to completely wrap the member, the shear strength can be improved by wrapping the FRP system around three sides of the member (U-wrap) or bonding to two opposite sides of the member. The three-sided U-wrap is less efficient than a complete wrap and bonding to two sides is the least efficient scheme. (ACI 440.2R)

Completely wrapped   U-wrap 2-sides bonded

(a) Contact-critical application   (b) Bond-critical application

Figure 2-4 Wrapping schemes in shear applications
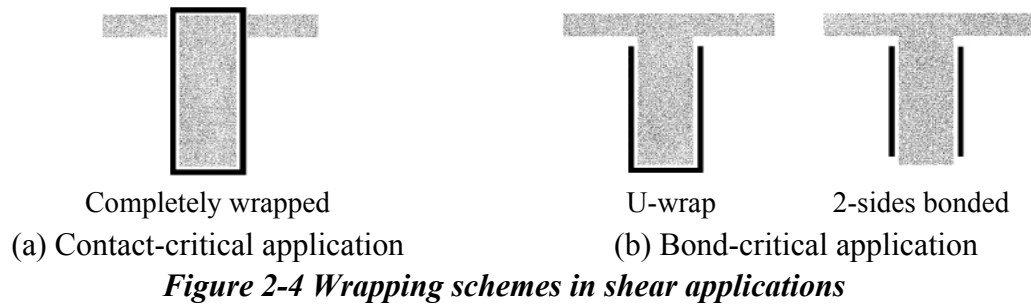
2.3.5.2 *Nominal shear strength*

Design equation for FRP shear strengthening (ACI 440.2R) is basically extended from ACI 318-05. The approach of evaluating FRP shear contribution is also same as steel except using an effective stress is used instead of yield stress.

Nominal strength can be evaluated by determining effective strain. Effective strain and additional strength reduction factor are different depending on the wrapping scheme. Basically, this equation includes the effect of debonding on the shear strength provided by the FRP in case where complete wrapping is not possible or utilized.

(a)   *(b)*   *(c)*
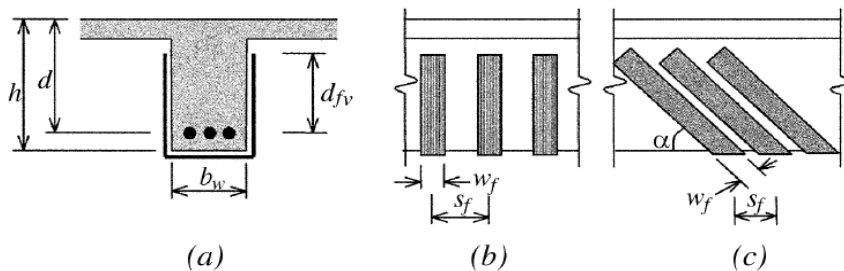
Figure 2-5 Description of the variables used in shear strengthening calculations for using FRP laminates

$$V_n = \phi(V_c + V_s + \psi_f V_f)$$

where

V_c, V_s, V_f = concrete, steel, and FRP shear contribution

ϕ = strength reduction factor

ψ_f = additional reduction factors for FRP shear reinforcement

$\begin{cases} 0.95\text{: completely wrapped member} \\ 0.85\text{: U-wrap and 2 sided schemes} \end{cases}$

$$V_f = \frac{A_{vf}f_{fe}(\sin\alpha + \cos\alpha)d_{fv}}{s_f} = \frac{A_{vf}f_{fe}d_{fv}}{s_f} \quad (\alpha=90°)$$

$$A_{vf} = 2nt_f w_f \, , \, f_{fe} = \varepsilon_{fe}E_f$$

where

h, d, b_w, d_{fv}, s_f, w_f, α are defined in Figure 2.5

n = number of plies of FRP reinforcement

w_f = width of FRP reinforcing plies (in.)

E_f = tensile modulus of elasticity of FRP

ε_{fe} = effective strain level in FRP reinforcement attained at failure

$\begin{cases} \varepsilon_{fe}= 0.004 \le 0.75\varepsilon_{fu} \quad \text{(completely wrapped members)} \\ \varepsilon_{fe}= \kappa_v\varepsilon_{fu} \le 0.004 \quad \text{(Bonded U-wraps or bonded face plies)} \end{cases}$

$$\kappa_v = \frac{k_1 k_2 L_e}{468\varepsilon_{fu}} \le 0.75$$

$$L_e = \frac{2500}{(n_f t_f E_f)^{0.58}} \, , \, k_1 = \left(\frac{f_c'}{4000}\right)^{2/3} , k_2 = \begin{cases} \dfrac{d_{fv}-L_e}{d_{fv}} \quad \text{(U-wraps)} \\ \dfrac{d_{fv}-2L_e}{d_{fv}} \quad \text{(2-sides bonded)} \end{cases}$$

where

L_e = active bond length (in.)

n_f = modular ratio of elasticity between FRP and concrete $(=E_f/E_c)$

t_f = nominal thickness of one ply of FRP reinforcement (in.)

f_c' = specified compressive strength of the concrete (psi)

d_{fv} = effective depth of FRP shear reinforcement (in.)

Figure 2-6 Shear calculation equations and procedures (ACI 440.2R)

2.3.5.3 Effective strain in FRP laminates

ACI 440.2R defines the effective strain, which is the maximum strain that can be achieved in the FRP system at nominal strength and is governed by the failure mode of the FRP system and of the strengthened reinforced concrete member. The following subsections provide guidance on determining this effective strain for different configurations of FRP laminates used for shear strengthening of reinforced concrete members.

Completely wrapped members—For reinforced concrete column and beam members completely wrapped by FRP, loss of aggregate interlock of the concrete has been observed to occur at fiber strains less than the ultimate fiber strain. To preclude this mode of failure, the maximum strain used for design should be limited to 0.004 for members that can be completely wrapped with FRP. This strain limitation is based on testing (Priestley et al.1996) and experience. Higher strains should not be used for FRP shear-strengthening applications.

Bonded U-wraps or bonded face plies—FRP systems that do not enclose the entire section (two-sided wraps and U-wraps) have been observed to delaminate from the concrete before the loss of aggregate interlock of the section. For this reason, bond stresses have been analyzed to determine the usefulness of these systems and the effective strain level that can be achieved (Triantafillou, 1998a). The effective strain is calculated using a bond-reduction coefficient (κ_v) applicable to shear. The bond-reduction coefficient is a function of the concrete strength (f_c'), the type of wrapping scheme used (k_2), and the stiffness of the laminate (L_e-active bond length). (Khalifa et al. 1998)

2.3.5.4 Reinforcement limits

The total shear strength provided by reinforcement should be taken as the sum of the contribution of the FRP shear reinforcement and the steel shear reinforcement. The sum of the shear strengths provided by the shear reinforcement should be limited based

on the criteria given for steel (ACI 440.2R-08 refers to ACI 318-05, Section 11.5.6.9). This limit is stated in Equation (2-2).

$$V_s + V_f \leq 8\sqrt{f'_c}\, b_w d \tag{2-2}$$

2.3.5.5 Mechanical anchorage

Mechanical anchorages can be used at termination points to develop larger tensile forces (Khalifa et al. 1999). The effectiveness of such mechanical anchorages, along with the level of tensile stress they can develop, should be substantiated through representative physical testing. In no case, however, should the effective strain in FRP laminates exceed 0.004.

Mechanical anchorages can be effective in increasing stress transfer (Khalifa et al. 1999), although their efficacy is believed to result from their ability to resist the tensile normal stresses rather than in enhancing the interfacial shear capacity (Quattlebaum et al. 2005). Limited data suggest a modest increase in FRP strain at debonding can be achieved with the provision of transverse anchoring FRP wraps (Reed et al. 2005). The performance of any anchorage system should be substantiated through testing.

2.3.5.6 Development length

The bond capacity of FRP is developed over a critical length (l_{df}). To develop the effective FRP stress at a section, the available anchorage length of FRP should exceed the value given by Equation (2-3) (Teng et al. 2001).

$$l_{df} = 0.057 \sqrt{\frac{nE_f t_f}{\sqrt{f'_c}}} \tag{2-3}$$

2.3.5.7 FRP strip spacing

For external FRP reinforcement in the form of discrete strips, the center-to-center spacing between the strips should not exceed the sum of $d/4$ plus the width of the strip. This limitation requires that a minimum number of FRP strips cross the critical section.

2.3.5.8 *Existing substrate strain*

ACI 440.2R has a limitation on existing substrate strain. Unless all loads on a member, including self-weight and any prestressing forces, are removed before installation of FRP reinforcement, the substrate to which the FRP is applied will be strained. These strains should be considered as initial strains and should be excluded from the strain in the FRP (Arduini and Nanni 1997; Nanni and Gold 1998). The initial strain level on the bonded substrate can be determined from an elastic analysis of the existing member, considering all loads that will be on the member during the installation of the FRP system. The elastic analysis of the existing member should be based on cracked section properties.

2.3.6 NCHRP Report 655 (2010)

This report summarizes the research conducted in NCHRP Project 10-73 to develop a recommended guide specification for the design of externally bonded FRP composite systems for repair and strengthening of reinforced and prestressed concrete highway bridge elements. This Guide Specification is presented in a format resembling that of the AASHTO LRFD Bridge Design Specifications, 4th Edition (2007) in order to facilitate their consideration and adoption by the AASHTO.

This project is focused on short- and medium-span bridges with spans ranging from 30 ft to 200 ft. Only dead load, live load, and dynamic load were considered in the reliability analysis on which the recommendations are based. Uncertainties due to inherent variability, modeling and prediction, and measurement should be also reflected. For FRP reinforcement, the strength depends on the engineering characteristics of the fibers, matrix and adhesive systems and on the workmanship in fabrication and installation.

It is meaningful that the anchorage system is included in the design guideline. The influence of the anchorage system is considered in two ways; the reliability of the shear capacity is increased and the effective strain of the FRP is also increased by preventing premature debonding failure.

2.3.6.1 Failure modes in shear strengthening

Four types of failure modes are categorized in NCHRP report 655.

1. Steel yielding followed by FRP debonding.
2. Steel yielding followed by FRP fracture.
3. Diagonal concrete crushing.
4. FRP debonding before steel yielding.

Depending on the amount of usable steel shear reinforcement in the structural element, FRP debonding can occur either before or after steel yielding. Diagonal concrete crushing in the direction perpendicular to the tension field can be suppressed by limiting the total amount of steel and FRP reinforcement.

Fracture of the FRP reinforcement is highly unlikely to occur because the strain when FRP debonds is substantially lower than that corresponding to the FRP fracture strength. However, fracture of FRP sheet is more likely when an anchorage system is used.

2.3.6.2 Introduction of jacketing combined with anchorage

In addition to side bonding, U-Jacketing and complete wrapping, a type of reinforcing scheme consisting of jacketing combined with anchorage is introduced. The effectiveness of FRP is increased by anchoring the fibers, preferably in the compression zone of the member. Properly designed anchors may allow the fibers to reach their tensile capacity, permitting the jacket to behave as if it were completely wrapped.

2.3.6.3 Nominal shear strength

The nominal strength is different depending on the reinforcing schemes. There are two stages in the determination of the shear strength. First, the nominal strength of U-jacketing combined with anchorages and complete wrapping is enhanced with regard to that compared of the side bonding and U-jacketing alone. A properly designed anchorage allows U-jacketing to be considered equivalent to complete wrapping. At the ultimate

limit state in shear (concrete diagonal tension), the FRP develops an effective strain in the principal material direction of approximately 0.004. This limiting strain is conservative compared with test results.

Next, the resistance factors of all reinforcing schemes are different depending on the reliability of the reinforcing scheme. Sufficient statistical data for determining reliability were available only for U-jacketing. The resistance factor for that case was found to be 0.55 and resistance factors for other methods of reinforcement were set by judgment. The resistance factor for U-jacketing combined with anchorage is 0.60, which is the resistance factor between U-jacketing (0.55) and complete wrapping (0.65). It means that the U-jacketing combined with anchorages is more reliable than U-jacketing only.

$$V_n = \phi(V_c + V_s + V_p) + \phi_{frp}V_{frp}$$

$$V_c + V_s \le 0.25 f_c' b_v d_v \text{ (AASHTO provision)}$$

$\phi = 0.9$ (defined as AASHTO)
ϕ_{frp} is a resistance factor, defined as follows:
  0.40 for side bonding shear reinforcement;
  0.55 for U-jacketing;
  0.60 for U-jacketing combined with anchorages;
  0.65 for complete wrapping.

$$V_{frp} = \frac{N_{frp}^e w_f (\sin \alpha + \cos \alpha) d_f}{s_f} = \frac{N_{frp}^e w_f d_f}{s_f} \quad (\alpha=90°)$$

* continuous FRP ($w_f = s_f$)

a) For side bonding and U-jacketing
$$N_{frp}^e = N_s$$

b) For u-jacketing combined with anchorage
$$N_{frp}^e = N_s + k_a \frac{1}{2}\left[N_{frp,w} - N_s\right]$$

c) For completely wrapping (closed jackets)
$$N_{frp}^e = N_s + \frac{1}{2}\left[N_{frp,w} - N_s\right]$$

N_{frp}^e = effective strength per unit width of the FRP reinforcement
N_s = FRP tensile strength /1-in width corresponding to a tensile strain of 0.004
$N_{frp,w}^e$ = the tensile strength of a closed(wrapped) jacket applied to a member of
  radius at the corners of the cross section not less than ½ in., defined as:

$$N_{frp,w}^e = 0.5N_{ut} \ge N_s$$

N_{ut} = nominal tensile strength of the FRP reinforcement;
k_a = 1 ; If the anchorage system is engineered in accordance with Articles D.3 and D.4
  of Appendix D in *ACI Standard 318-05;* Otherwise, $k_a = 0$

Figure 2-7 Shear calculation equations and procedures (NCHRP report 655)

2.3.7   NCHRP Report 678 (2011)

Recently, NCHRP report 678 "Design of FRP Systems for Strengthening Concrete Girders in Shear" was published. This report identified the parameters affecting the behavior of systems strengthened with FRP from a database of reported test results and presented design provisions for shear strengthening with externally bonded FRP systems. Existing models shear behavior were summarized and a statistical evaluation of the existing model was conducted using the database.

An experimental program was developed to further study parameters that were considered to have not been sufficiently investigated in earlier tests, including the effects of pre-cracking, continuity (negative moment), long-term conditioning (such as fatigue loading and corrosion of internal steel reinforcement), and prestressing. The experimental program included full-scale tests on RC T-beams and AASHTO type PC I-girders because most current design equations used in design specifications are based on small-scale test results.

2.3.7.1   Evaluation of existing design methods

The existing models have been divided into four groups based on their approaches as below.

1) Models relying on an empirically determined value of strain/stress associated with failure of the member for which the shear contribution of the FRP is determined.

2) Models based on the determination of an effective FRP strain.

3) Models focused on the non-uniformity of the strain distribution in externally bonded FRP reinforcements.

4) Models of mechanics-based theoretical approaches that do not rely on experimental results for regression or calibration.

An assessment of the existing design methods found significant differences in the magnitude of the FRP shear contribution calculated by various design methods. This

assessment revealed the deficiencies of the existing design methods in predicting the shear resistance of a wide range of girder and FRP reinforcement characteristics.

2.3.7.2   Statistical evaluation about the influence of FRP configurations

The frequency of occurrence of each mode of failure for different FRP configurations (side bonding, U-wrap, or complete wrap), as determined from examination of the database information, is illustrated in Figure 2-8. The figure indicates that (a) debonding is the dominant mode of failure for beams strengthened with FRP and bonded on the sides only, (b) FRP debonding almost never occurs in beams retrofitted with complete FRP wrap and U-wraps with anchorage systems, and (c) failure of beams retrofitted with U-wraps occurs by debonding (65%) or by other failure modes (35%), such as diagonal tension failure in the web, shear compression failure in the compression zone, and flexural failure.
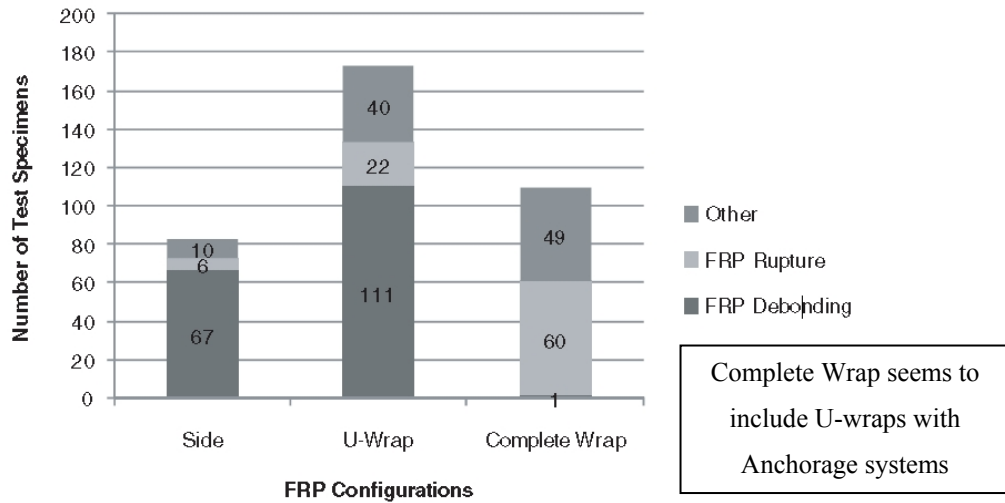
Figure 2-8 Frequency of occurrence of failure mode related to strengthening scheme
(NCHRP report 678 2011)

2.3.7.3 Proposed new design equation

New shear design equations for predicting the shear contribution of externally bonded FRP systems were developed and calibrated.

As shown in Figure 2-9, the effective FRP strain used in evaluating the FRP shear contribution can be expressed by two separate design expressions to consider the two predominant failure modes (i.e., debonding and FRP rupture). One expression is for members in which sufficient anchorage is provided (FRP rupture failure mode), and the other is for members in which insufficient anchorage is provided (FRP debonding failure mode).

$$V_f = \frac{A_f f_{fe} d_f}{s_f} \quad , \qquad f_{fe} = \varepsilon_{fe} E_f$$

1) FRP rupture "full-anchorage" : Complete Wrap or U-Wrap with Anchors

$$\varepsilon_{fe} = R \varepsilon_{fu} , \quad \varepsilon_{fu} = f_{fu}/E_f$$

$$R = 4(\rho_f E_f)^{-0.67}$$

2) FRP debonding or another mode of failure before FRP rupture

: Side bonding or U-Wrap

$$\varepsilon_{fe} = R\varepsilon_{fu} \leq 0.012$$

$$R = 3(\rho_f E_f)^{-0.67}$$

where $\rho_f E_f$ is in ksi units and limited to 300 ksi.

* Spacing requirement is the same as AASHTO 5.8.2.7

Figure 2-9 Proposed shear equations for evaluating FRP contribution in NCHRP 678

2.3.7.4 Suggestions for further research

1) An interaction exists between the internal transverse steel reinforcement and externally bonded FRP shear reinforcement, but there are insufficient data to quantify this interaction. Further investigations are needed to better quantify the mechanisms involved in this interaction and incorporate it into an enhanced model for the shear resistance of RC beams strengthened with externally-bonded FRP.

2) The use of mechanical anchorage involving discontinuous CFRP plates attached with steel concrete wedge anchors or bolts through the web was found to delay or, in some cases, prevent debonding of FRP. However, because these anchors and bolts are susceptible to corrosion, research is needed to explore alternative mechanical anchorage techniques that are not susceptible to such corrosion.

3) The cross-sectional geometry of PC girders influences the effectiveness of externally bonded FRP. Also thin web and stiff flange geometry reduce the effectiveness of the FRP shear strengthening. However, limited results are available to fully understand the mechanisms involved in such behavior. Further research is needed to examine the effect of cross sectional geometry of PC girders.

4) The effective strain concept was adopted for design guidelines and codes to provide a simple and practical method for estimating the shear contribution of FRP. Research is needed to investigate the effect of non-uniform FRP distribution and to develop more reliable design equations.

5) Research is needed to investigate the long-term fatigue performance of FRP systems for shear strengthening, particularly the effects of cracks on bond characteristics.

2.3.8   Other Guidelines discussed in NCHRP 678

In addition to ACI 440.2R and NCHRP report, other guidelines were also investigated.

In the Canadian Design and Construction of Building Composites with Fiber Reinforced Polymers (CAN/CSA S806 2002), the equations are based on the simplified method for shear design used in the concrete design code (CAN/CSA A23.3 1994), which is limited to the usual cases of shear reinforcement (including FRP) perpendicular to the longitudinal axis of beams. The ultimate strain is limited to 0.004 for failure due to FRP rupture and 0.002 for bond critical applications.

The British Concrete Society Technical Report 55, Design Guidelines on Strengthening Concrete Structures Using Fiber Composite Materials (Concrete Society 2004) is similar to fib-Bulletin 14 (fib-TG9.3 2001) in approach and scope; however it

addresses construction issues associated with the use of externally bonded FRP materials. Externally bonded FRP strips are treated using a 45 degree truss analogy. The strain in the FRP is limited to one half of the ultimate design strain for FRP rupture failure. For debonding failure, British Concrete Society Technical Report 55 adopts an equation proposed by Neubauer and Rostasy (1997); the strain is limited to 0.004 for all cases.

2.4 CFRP ANCHORS

2.4.1 General

To prevent premature failure by debonding, the introduction of anchorage systems is one of the most attractive solutions. To date, several anchorage systems have been developed and design guidelines for anchorage system also have been developed.

2.4.2 Previous Research of Anchorage Systems in Shear

2.4.2.1 Threaded rod

Deifalla and Ghobarah (2006) introduced an anchorage system using threaded anchor rods with steel plates. Although this system shown in Figure 2-10 prevented debonding, it might be difficult and unacceptable to install the rods that extend through the floor depending on the use of the structure.
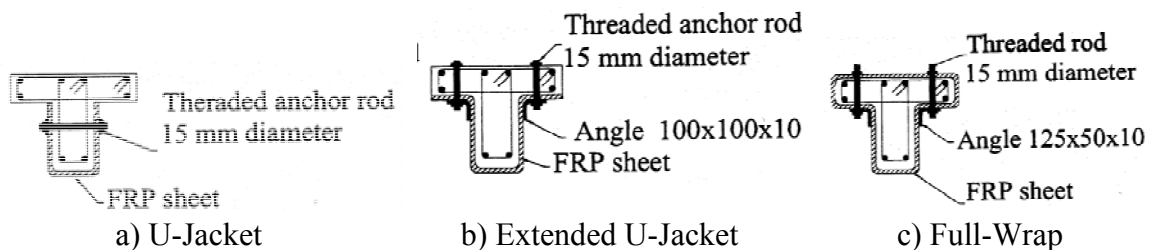
a) U-Jacket   b) Extended U-Jacket   c) Full-Wrap
Figure 2-10 Strengthening schemes for T-beams using rod (Deifalla & Ghobarah 2006)

2.4.2.2 CFRP straps

Hoult and Lees (2009) studied a system of CFRP straps to provide an external CFRP reinforcement similar to closed stirrups. In order to eliminate any protrusions into

the top of slab, two intersecting straight holes must be drilled in the concrete in order to tie the concrete compression zone to the concrete tension zone when anchoring CFRP strips. However, it is not easy to avoid the existing steel reinforcement locations when drilling into the concrete beam as shown in Figure 2-11.
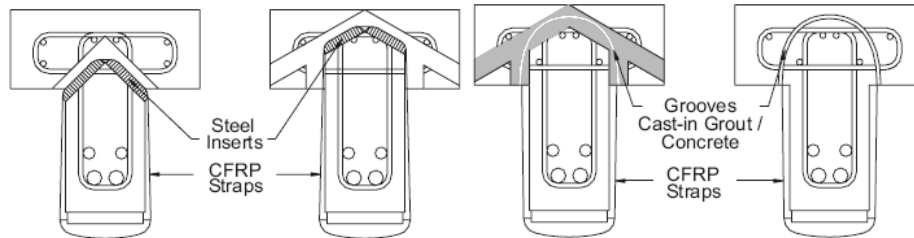
Figure 2-11 Cross section of the CFRP strap (Hoult & Lees 2009)

2.4.2.3 CFRP U-Anchors (using NSM)

Khalifa at al. (1999) developed a CFRP U-Anchor system. As shown in Figure 2-12, a groove is cut into the concrete element at the intersection between the web and flange to construct this anchorage system. The groove is coated with the adhesive epoxy material recommended by the manufacturer of the CFRP laminates. The CFRP sheet is then installed onto the surface of the beam and a glass FRP rod is used to insert the CFRP sheet into the preformed groove as seen in Figure 2-12.
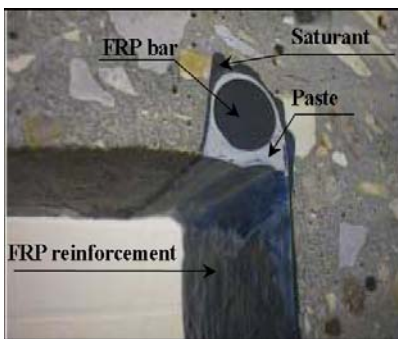
Figure 2-12 The CFRP U-Anchor system (Khalifa et al. 1999)

This rod also serves to anchor the sheet to the beam. Finally, an epoxy paste is used to cover the glass FRP rod and to fill the groove. One of the major benefits to this system is that it eliminates the need to drill into the concrete beam, removing any

37

possibility of damaging internal steel reinforcement. To construct the groove, two parallel saw cuts can be made at a predetermined depth. Then, the groove can be completed by chipping out the concrete between the two saw cuts (Khalifa et al. 1999). The groove can be cut into the concrete cover region to avoid any reinforcement. However, shear forces cannot be easily transferred to the concrete and surrounding internal steel reinforcement and pull-out failure might happen because the grove is not cut into the core of the beam.

2.4.2.4 Continuous and discontinuous CFRP plates

Ortega et al. (2009) introduced an anchorage system using CFRP plates and wedge anchors to prevent debonding of CFRP sheets. The use of CFRP plates eliminated the corrosion problem caused by the steel plates due to steel-carbon fiber contact (Khalifa et al. 1999). The use of continuous and discontinuous CFRP plates with anchorage bolts or bolts through the web delayed and in some cases, prevented debonding of the FRP, resulting in a greater increase of the ultimate shear resistance.

However, for PC girders with very thin webs, the embedment length of anchor bolts was sufficient to avoid premature failure and the anchor bolts pulled out and continuous CFRP plate buckled. In addition, slippage of the FRP sheet from beneath the discontinuous CFRP anchorage plate was observed as shown in Figure 2-13. To prevent this slippage, anchor details were modified with sandwich discontinuous mechanical anchorage as shown in Figure 2-14.

(a) Continuous CFRP plate (b) Bucking of continuous CFRP plate

(c) Discontinuous CFRP plate (d) Slippage of discontinuous CFRP plate

Figure 2-13 Anchorage system with continuous and discontinuous CFRP plate
(Ortega, et al, 2009)
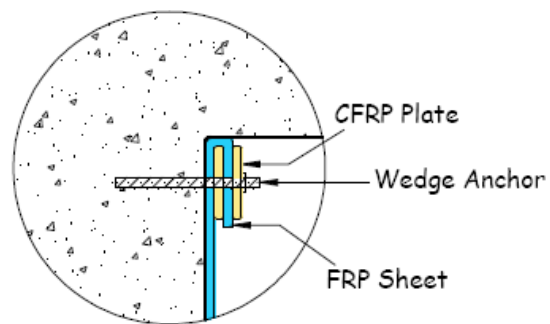
Figure 2-14 modified anchor bolt system (Ortega, et al, 2009)

2.4.3 History of CFRP Anchors

CFRP anchors developed by Kobayashi (2001) were used to provide continuity for CFRP wraps of columns in cases where concrete infill walls prevented the columns from bring completely wrapped with CFRP material. The CFRP anchors can be made of the same carbon fiber material used to strengthen the concrete member. They are inserted into predrilled holes and fanned out over the CFRP sheets to make a load path to transfer forces from the CFRP sheet into the concrete beam. A CFRP anchor in beam application can be subjected to different types of forces, including pull-out forces and shear forces by changing the direction of force.

Orton (2007) and Kim (2008) used CFRP sheet and CFRP anchors for providing continuity to prevent progressive collapse. They observed that the strains in the CFRP sheets with CFRP anchors were considerably higher than those of the CFRP sheets only. They observed that the CFRP sheets reached their full tensile strain capacity and eventually failed by CFRP rupture. In addition, they observed that the CFRP anchors could reach the ultimate tensile capacity of the CFRP sheets, regardless of the quality of surface preparation before installation. However, poor installation procedure might reduce the capacity of the CFRP anchors by up to 50% (Ozbakkaloglu & Saatcioglu, 2009). Therefore, expertise of the installers and quality control of the materials are essential.

2.4.4 CFRP Anchor Configurations

To install a CFRP anchor easily, a strip of CFRP fabric is folded in half as shown in Figure 2-15. Therefore the required length of the anchor must be doubled and the area of CFRP strip being anchored would be half of that required area for CFRP anchor.
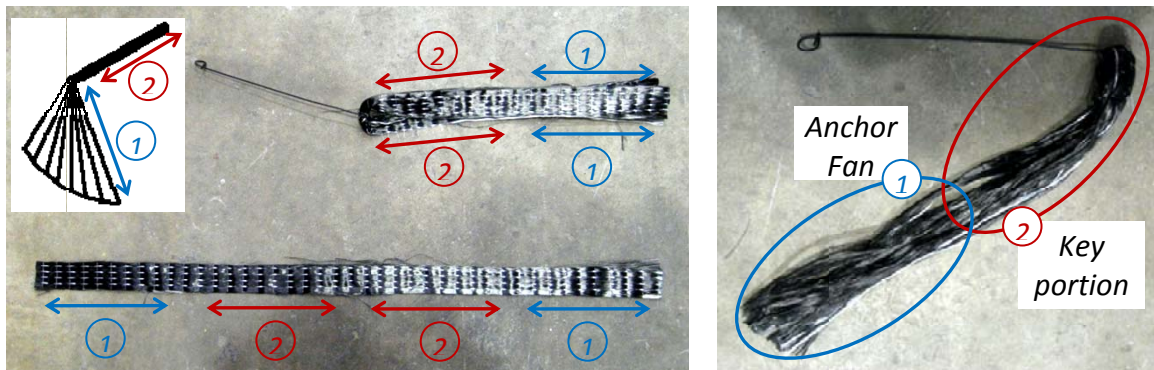
Figure 2-15 CFRP anchors

2.4.5 CFRP Anchor Detail

CFRP anchors were used to improve the performance of CFRP sheets. The following parameters have been found to influence the strength of anchor and sheet installation: 1) depth of hole, 2) hole chamfer radius, 3) amount of CFRP material in anchors, 4) diameter of hole, 5) fan length, 6) fan angle and 7) corner chamfer radius.
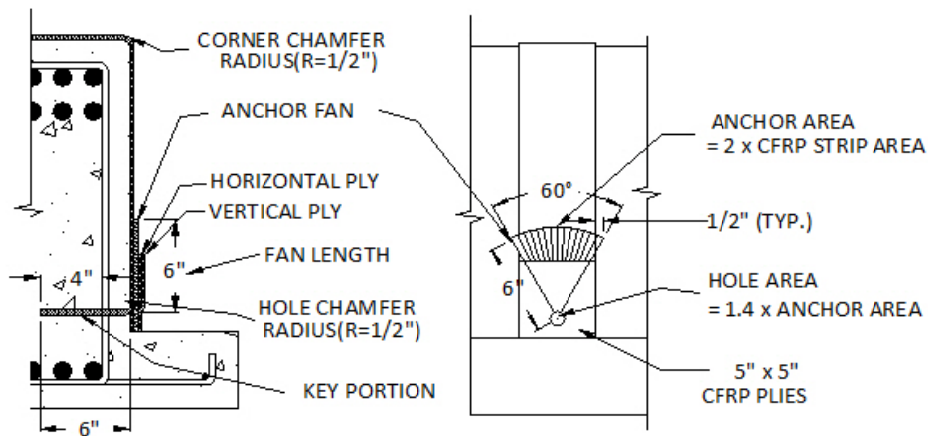
Figure 2-16 The CFRP anchor detail (used in this research)
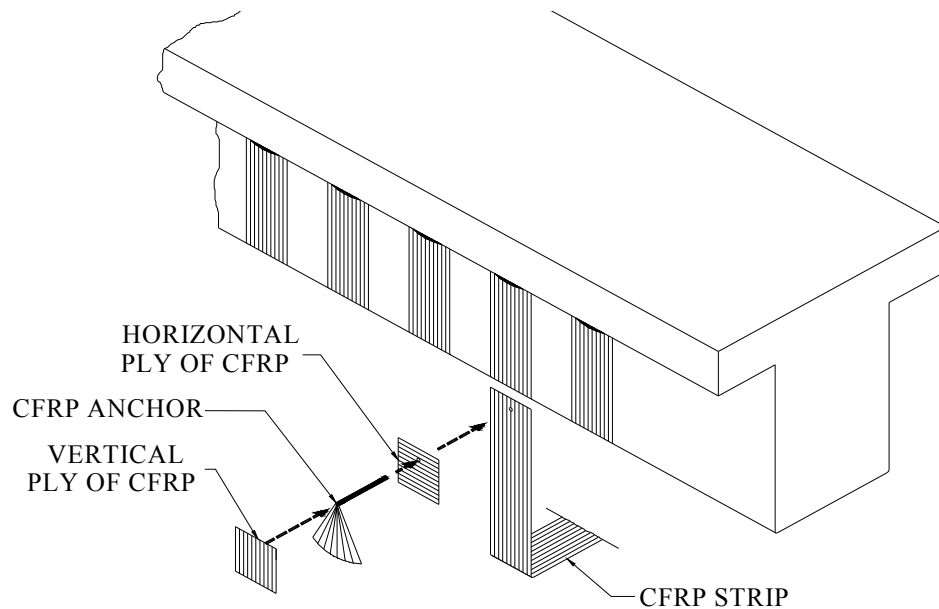
Figure 2-17 Isometric view of U-wrap with CFRP anchorage system

2.4.5.1 *Embedment length of anchor holes*

Anchors were inserted into holes drilled to a depth of 6-inch (including 2-inch of concrete cover) into the web of the T-beam specimen so that the anchor extended 4-inch past the reinforcement cage. Özdemir (2005) determined that there is a certain embedment depth of the CFRP anchors beyond which the capacity of the CFRP anchors no longer increases. As the embedment depth increases, the average bond strength along the surface of the drilled hole decreases. This implies that the stress distribution along the depth of the drilled hole is not uniform (Ozbakkaloglu & Saatcioglu 2009). Therefore, it is usually acceptable if embedment lenghth is beyond the required length so that the capacity of the CFRP anchor is not deminished. In addtion, this embedment depth ensures that failure does not occur by separation of the concrete cover (Orton, Jirsa, & Bayrak 2008).

Without the information of exact location of the steel reinforcement, it is possible for the reinforcement to interfere with the anchor hole. However, the hole can be angled

slightly to avoid the reinforcement without significant influence on the strength of the anchor in this case.

2.4.5.2 Hole chamfer radius, hole size and amount of material in CFRP anchors

Hole chamfer radius, hole size and the amount of material in CFRP anchors are correlated each other. The sharp or rough edge at the corner of the drilled hole can create stress concentrations in the anchor, which can cause the anchor to rupture prematurely and reduce the anchor capacity. Therefore proper rounding of the rough edge around the drilled anchor hole is needed when making a hole for CFRP anchors as seen in Figure 2-18. Kobayashi et al. (2001) recommended an anchor hole chamfer radius of ¾ in their study of CFRP anchors. ACI 440.2R-08 also recommends that all 90 degree corners be rounded to a radius of 0.5-in. However Morphy (1999) recommended that the radius of the bend located at the opening of the anchor hole be at least four times greater than the anchor diameter. Such a large bending radius is not practical. The Japan Society of Civil Engineers (JSCE, 1997) reported that the bend radius is crucial for preventing premature failure of anchors because CFRP strength is highly influenced by the bend and an equation was developed to evaluate the reduction in strength depending on the bend radius at the corner. Equation 2-4 can evaluate the strength reduction due to relationship between bend radius and diameter. This equation is also adopted in ACI 440.1R (Guide for the Design and Construction of Structural Concrete Reinforced with FRP Bars) equation (7-3), being used to determine the design tensile strength of FRP bars at a bend.

$$f_{fb} = (0.3 + 0.09 \frac{r_b}{d_b}) f_{fu} \qquad (2-4)$$

where
f_{fb} = design tensile strength of the bend of FRP bar, psi (MPa);
r_b = radius of the bend, in. (mm);
d_b = diameter of reinforcing bar, in. (mm); and
f_{fu} = design tensile strength of FRP, considering reductions for environment, psi (MPa).

Figure 2-18 CFRP anchor holes before and after making hole chamfer

Limited research on FRP hooks (Ehsani et al. 1995) indicates that the tensile force developed by the bent portion of a GFRP bar is mainly influenced by the ratio of the bend radius to the bar diameter r_b/d_b, the tail length, and, to a lesser extent, the concrete strength. (ACI440.1R). In fact, this equation is not intended to apply to the case of CFRP anchors. CFRP anchors tend to be under more stress concentration because the force in the strip is concentrated at the anchor hole by the anchor fan. There is a change in the direction of the stress, so a greater reduction in strength may be appropriate. FRP bars may have residual stresses which reduce the capacity if the FRP bars were bent from a straight bar. However, the installation of a CFRP anchor will not introduce residual stresses to the the anchor. When the CFRP strip and anchor are loaded, a relatively uniform stress is developed along the strip but the stress at the bend will not be uniform in either bent FRP bars or CFRP anchors. Therefore, this is not directly applicable to CFRP anchor, but is valuable for developing a new model.

According to this equation, the design tensile strength at the bend of a FRP bar will not be the same as the design tensile strength of the FRP material. Therefore, by increasing the amount of material in the CFRP anchor, the full strength of CFRP sheet can be transferred to the concrete.

In this experimental program, a hole diameter of 7/16 in. with a bend radius of ½ in. was used. From this equation, only 40 percent of full capacity of CFRP anchors can be mobilized. For this reason, the amount of FRP material for CFRP anchors was doubled.

However, the increase in material may still not be enough to develop the full strength of the CFRP sheet based on the equation (2-3) - 80% of full capacity was expected.
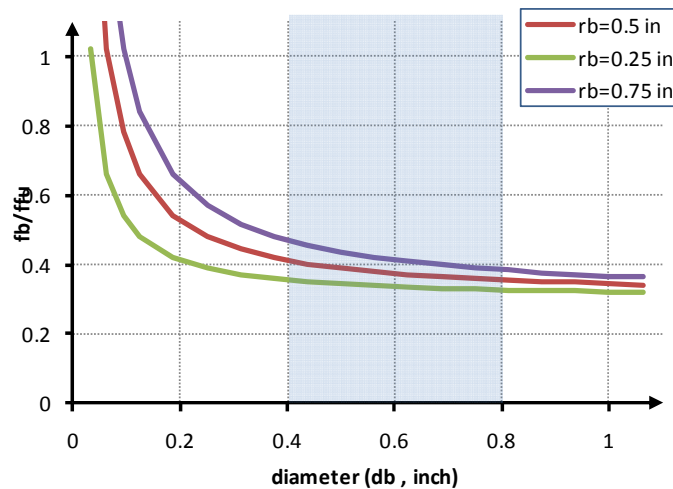
Figure 2-19 Reduction in capacity due to diameter and bend radius (Eq. (2-4))

As shown in Figure 2-19, this equation is less sensitive to bend radius as the diamenter of hole increased, which means that the strength variation due to change in bend radius is negligible under the same big diameter of hole. In addition, the strength variabtion under same bend radius according to diameter of hole, which is determined by the amount of FRP material in anchors is also negligible within the typical range of diameter of hole used in this study (shaded in Figure 2-19). That is the why the chamfer radius was kept constant regardless of the change in the amount of material. When the bend radius changed from 0.25 in to 0.5 in.,the bend strength of anchor was expected to be around 5% greater using the same amount of material. However, because all of these assumptions are based on equation (2-4), the values obtained from this equation need to be verified.

For design, the amount of material in a CFRP anchor can be determimed by the amount of CFRP material in the sheet. Kim (2008) and Orton (2007) recommended that the amount of material in the CFRP anchor be 1.5 and 2 times the amount of material in the CFRP sheet respectively. To accommodate the amount of FRP material in the anchor area, the area of hole was increased by 40% as recommended by Kim (2008). Too small

or too large a hole diameter would make installation of the anchor more difficult and would create quality control problems.

2.4.5.3 Fan length and fan angle

The total required length of a CFRP anchor is the sum of the embedment depth of the anchor and the fan length of the anchors. The calculation of embedment depth was already discussed in Section 2.4.5.1. The fan length depends on the required bond strength between the fan and the main sheet and on the fan angle. The maximum load resisted by the anchorage system increases as the length of the anchorage fan increases (Kobayashi et al, 2001). The CFRP anchor must be long enough to allow the fan to cover the width of CFRP sheet. The fan should extend 0.5 in. beyond the strip width as shown in Figure 2-16.

Kobayashi et al. (2001) recommended that the angle of the CFRP anchor fan be limited to less than 90 degrees. Because they only specified the extended distance of anchor beyond the width of sheet, if there is no limitation on the angle, the bond area between sheet and anchor and the fan length can not be controlled. In addition, the greater angle might be reduced the anchor capacity because the load transfer in outer fiber is not effective than the center fiber. Therefore, a fan angle of 60 degrees was used in this experimental study.
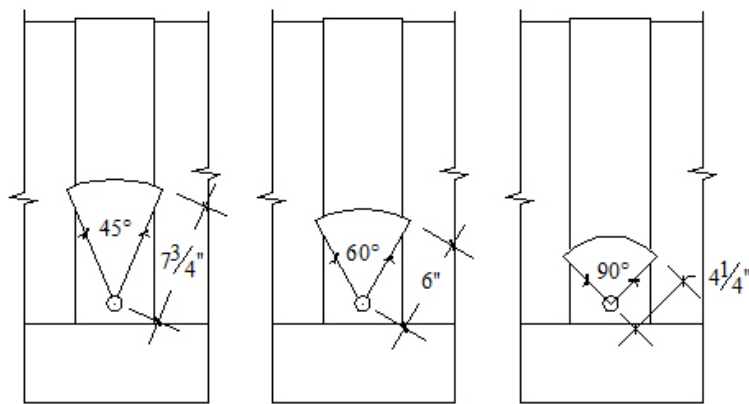
Figure 2-20 Anchor detail according to the different fan angles

2.4.5.4 Overlapping length

Kobayashi et al. (2001) recommended that the overlapping length of 4 in. (100-mm) or more between the anchorage fans of adjacent anchors to reduce stress concentrations in the center of the CFRP sheets and to increase the efficiency of CFRP anchors when multiple anchors installed on the same CFRP sheet. Kim (2008) also recommended that the overlaping length is at least 0.5 in. from each anchors.

2.4.5.5 Corner chemfer radius

As discussed in chapter 2.4.5.2, corner chemfer radius is the same concept as hole chamfer radius. The corner chemfer reduced the stress concentration caused by the change in the direction of stress in the CFRP sheet. ACI 440 also recommended the corner chemfer of 0.5 in. radius.

2.4.5.6 Number of CFRP anchors

The number of CFRP anchors per strip depends on the amount of material in the CFRP anchor. Orton et al. (2008) observed that the use a larger number of smaller anchors was more effective in developing the full tensile capacity of CFRP sheets under the same amount of total material because more redundancy are provided. However, a small number of CFRP anchors would be absolutely preferred in practice, so it should be compromised. Kobayashi et al. (2001) recommended the distance between anchors is less than 8 in. (200 mm). This recommendation also might limit and control the number of anchor.

2.4.5.7 Additional anchor patches

Two patches of CFRP material were applied. These patches helped to distribute anchor stresses across the width of the anchor and sheet more uniformly. The first patch was installed before installing CFRP anchors so that the carbon fibers were oriented transversely to the main CFRP strip. The second patch was then installed covering a portion of the anchorage fan oriented perpendicular to those of the first ply - parallel to

47

the CFRP sheet. Kobayashi et al. (2001) also recommends the use of a horizontal ply of fibers under the CFRP anchors. These patches were applied after several tests because some CFRP anchors failed before the CFRP sheet ruptured. The previous version of these patches was that both two patches covered the CFRP anchor, whereas the current application is that perpendicular patch is applied under CFRP anchor. The rupture of key portion in CFRP anchor was occurred under the previous application, so the risk might be reduced by changing the location of the perpendicular patch anchors.

2.4.5.8 Quality control

This research focused on the shear behavior of RC beam strengthened with CFRP sheet and CFRP anchors. Therefore, there was no additional consideration for the anchors if the capacity of anchors just had a greater than the capacity of the CFRP sheet. Because the application of CFRP anchors in shear strengthening still needs to be developed for reliable quality, the failure mode in some tests was rupture of anchors. However, the strain in CFRP sheet is greater than debonding strain although failed by rupture of anchors, which means that there is possibility to increase capacity if the failure mode can change from rupture of CFRP anchor to rupture of CFRP sheet. From this test program, it is difficult to evaluate the CFRP anchor detail in shear application because there is no direct relationship between parameter and anchor capacity. For example, the stress in CFRP anchor depends on the location and direction of crack and the crack profile cannot be anticipated. The stress levels between different CFRP sheets are not same. As the crack is located closer to the key portion of CFRP anchors, CFRP anchor is more likely to fail in rupture before develop the full capacity of CFRP sheet. The capacity at rupture of CFRP anchor is all summation of all components from concrete and stirrups and CFRP sheet across the critical crack. Therefore there is no direct way to evaluate the load fraction causing the rupture of CFRP anchor. Finally, to improve the CFRP anchor detail, separate experimental program - simple parametric study- needs to be considered.

CHAPTER 3

Experimental Program

To evaluate the shear contribution of CFRP sheets and to determine the effectiveness of CFRP anchors, 24 tests (16 tests: 24 in. depth and 8 tests: 48 in. depth) were conducted considering following parameters:

Beam dimensions

- Depth

- Shear span to depth ratio (a/d ratio)

- Transverse steel ratio

Strengthening - CFRP sheets

- Concrete surface condition (bond)

- CFRP material properties

- CFRP sheet layout

- Amount of CFRP material

- With / without anchors

- Anchor layout and detail

The beams were designed to simulate field conditions and to have a specimen that is controlled by shear failure. Most previous research has been focused on rectangular beams with fully wrapped FRP sheets for shear applications. However, in most bridge structures fully wrapping beams is not possible. Furthermore, the results from small-scale beams tested under laboratory conditions may not be applicable to large beams in practice. (Sas et al. 2009) Some researchers reported the capacity after strengthening was more than twice the capacity before strengthening, but these results were obtained using beams with little or no transverse steel. Current design codes generally require some

transverse reinforcement. For these reasons, full-scale T-beams with at least minimum transverse reinforcement are the focus of this research. To ensure failure in shear, the flexural strength was designed to exceed the expected shear capacity. CFRP design was based on ACI 440.2R guidelines and the CFRP anchor design was based on previous research conducted at Ferguson Structural Engineering Laboratory (Kim 2009, Orton 2008) with small modifications.
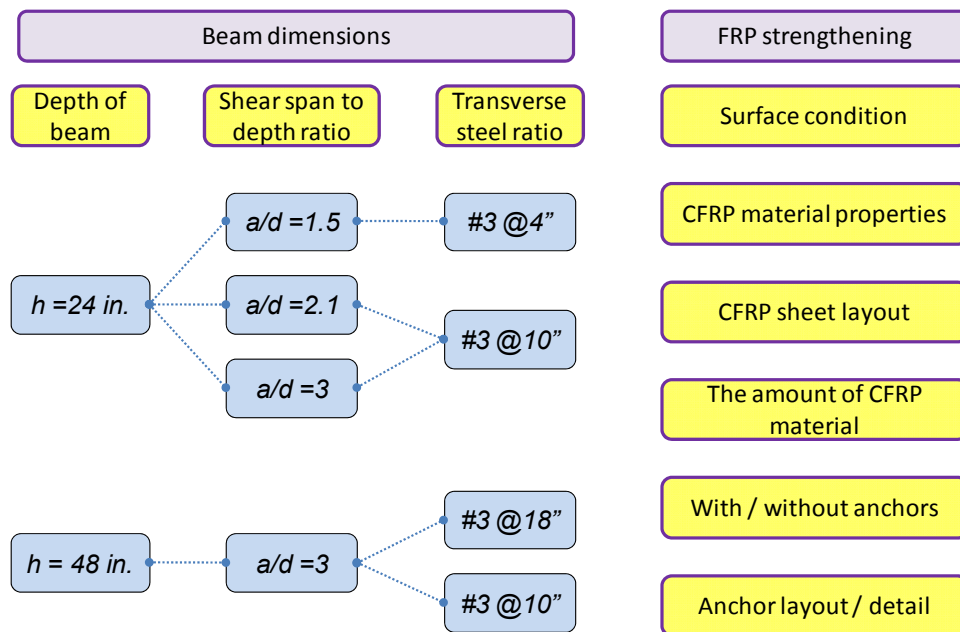
Figure 3-1 Experimental program with test parameters

All specimens were constructed and tested at the Ferguson Structural Engineering Laboratory at the University of Texas at Austin. Two tests were conducted from each beam. To keep the non-tested end from failing while one end was tested, a pre-stressing clamp system was used. Two different loading setups were used depending on the estimated capacity.

In this chapter, the specimen design considerations and material properties and loading setup and instrumentation are described. The construction process is described in Appendix A, including details of the reinforcing cages, formwork, concrete cast, and CFRP installation.

3.1 DESIGN CONSIDERATIONS

Specimen design was based on the American Association of State Highway and Transportation Officials (AASHTO) LRFD bridge design and American Concrete Institute (ACI) 318-08 minimum details for shear. ACI 440.2R was used for the CFRP transverse reinforcement design using procedures that are compatible with ACI 318. For this reason, ACI 318 requirements were selected when specimen are designed.

AASHTO LRFD shear provisions are similar to ACI 318. In AASHTO, a beam with shear span to depth ratio of less than two is defined as a deep beam. The maximum stirrup spacing in a deep beam is 0.4d, which is slightly different from the spacing of d/5 in ACI 318. The maximum spacing of other beams is generally 0.8d, whereas in ACI 318 the maximum spacing is d/2 (and d/4 for high shear demand location). For both cases, ACI 318 has stricter requirements for maximum stirrup spacing than AASHTO. Therefore, this research allows both design provisions to be evaluated.

3.1.1 T-Beam

A T-beam was selected to reflect typical bridge decks where the beam or girder is part of a monolithic floor or composite deck. In practice, a T-beam cannot be fully wrapped with CFRP laminates unless holes are made in the deck and traffic on the deck is controlled. In this situation, CFRP U-wrapping would be the only alternative and such wraps debond prematurely. CFRP anchors provide an alternate force transfer mechanism after debonding occurs. Test specimens were reinforced in shear by externally applying CFRP laminates in strips that were wrapped around the web and anchored using CFRP anchors just below the flange.

3.1.2 Shear Span to Depth Ratio

The current design guidelines (AASHTO 2007, ACI 318-08) define beams with a shear span to depth of two or less as deep beams. In deep beam, a direct strut from the loading point to the support provides most of the shear capacity. However, with a shear span to depth ratio greater than two, shear failures occur due to the formation of cracks

along an angle that is often assumed to be 45 degrees. Shear cracking is caused by tensile forces acting perpendicular to the inclination angle of the shear crack. Because the capacity of beams with a shear span to depth ratio of greater than five is generally controlled by flexure, these beams were excluded in this experimental program. Beams tested with small shear span to depth ratio exhibited a larger concrete shear contribution than beams with higher shear span to depth ratios.

Beams with 24 in. depth were tested with three different shear span to depth ratios: 1.5, 2.1 and 3.0. The effect of shear span to depth ratio on beam capacity will be evaluated from these tests.

3.1.3   Transverse Steel Ratio

Transverse reinforcement is a major factor influencing the shear strength of a reinforced concrete member. When CFRP materials are used to provide additional shear capacity, there is an interaction between the CFRP and the steel transverse reinforcement as the shear strength is mobilized. Ordinary shear reinforcement was included in the design of the specimens to provide a realistic representation of typical existing reinforced concrete members. In deep beams, the maximum allowable spacing of stirrups is $d/5$, whereas it is $d/2$ in other beams because deep beams have steeper diagonal crack. Therefore, the diameter and spacing of steel shear reinforcement was selected so that the shear capacity provided by the transverse reinforcement would meet minimum code requirements. Detailed calculations are presented in Appendix B.

3.1.4   Flexural Reinforcement

The flexural capacity of the test specimens was designed to exceed the expected shear capacity of the test specimens to force a shear mode of failure. In practice, the opposite is desired but the aim of the research was to determine the effectiveness of CFRP materials applied in shear. Although the nominal shear strength is usually assumed in conservative manner, shear failure are still possible because there is considerable uncertainty in shear calculation. To take into account of this uncertainty, the margin of

flexural to shear capacity was more than 1.5. Grade 75 flexural reinforcement was used in the tensile region of the member to provide a sufficient margin within limited space against flexural failure. Compressive reinforcement was included to preclude the possibility of a flexural failure due to crushing of the concrete.

3.1.5   CFRP Laminates

In ACI 440.2R, it is assumed that the applied CFRP system includes an unanchored U-wrap and therefore will have a tendency to fail by debonding before obtaining ultimate tensile strain. Based on this assumption, the effective strain in the CFRP is calculated, it is a function of "active bond length" defined in ACI 440.2R. In addition, this strain cannot exceed 0.004 in ACI 440.2R shear applications. It implies that the design guideline limits the maximum tensile strain value that can be reached in the CFRP to 40% of ultimate capacity (typical rupture strain is around 0.01). In addition, ACI 440 has a limitation on the strengthening ratio for maintenance purposes as discussed in section 2.1.6, Equation (2-1). Therefore, large increases in strength are not realistic in practice.

The use of CFRP anchors permits the development of high tensile strains in the CFRP sheets. Therefore, in all conceptual design calculations regarding the shear capacity of the CFRP materials, the 40% limit proposed by ACI 440.2R-08 was not considered. It was assumed that the full tensile capacity of the CFRP could be achieved before the CFRP ruptured. Detailed calculations are described in Appendix B.

3.1.6   CFRP Anchor

A conservative design for CFRP anchors was considered because the optimization of anchor detail was not the purpose of this research. Furthermore, the performance of CFRP anchors in shear applications has not been verified.

The configuration for CFRP anchors was based on research reported by Kobayashi (2001) and modified by Orton (2007) and Kim (2008). For this research program, Kim's recommendation was used for the CFRP anchor detail as discussed in

Section 2.4.5. However, in test of 24-3-3 (no bond between CFRP and concrete, poor installation of CFRP), the failure mode was fracture of CFRP anchors. For this reason, this anchor detail was modified as mentioned in Section 2.4.5.

In 48 in. beams, two CFRP anchors were installed in each 10 in. CFRP sheet. Two anchors provided a more uniform distribution of stress from the sheet to the anchor. However, more anchors increase labor cost which is a factor that must be considered in practice. Each anchor transfer tensile stress of a 5 in. wide CFRP strip, which is the same amount CFRP in the strips for 24 in. beams. Therefore, the size of anchor was identical to that used in the 24 in. beams.

(a) 1 anchor / strip   (b) 2 anchors / strip
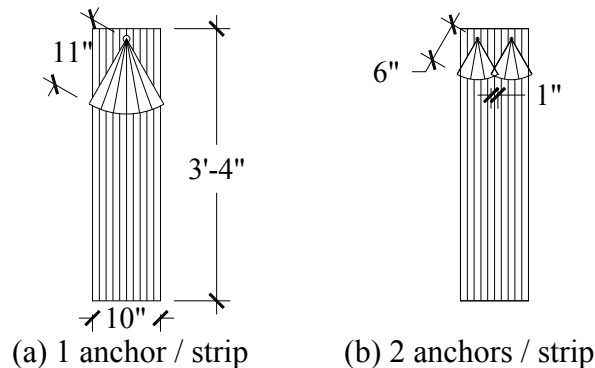
Figure 3-2 Alternatives of anchor details in 48 in. beams

Several different anchor details were used depending on the configurations of CFRP sheet such as two-layered CFRP strip, continuous layout, different CFRP material properties, diagonal application, intermediate anchors. However, the overall anchor design concept was the same and the detail of each case is described in the test results section and calculation procedure is described in Appendix C.

3.1.7   Initial Stress Condition

Stresses are present in the concrete and steel reinforcement at the time CFRP is applied in real structures. It is difficult to simulate such a condition in the laboratory and to evaluate the difference between existing structures and those that have been strengthened. In this program, CFRP strips were installed under two different initial

condition; pre-shear cracking and post-shear cracking. The sustained load at the time of the installation of CFRP was almost zero.

3.2   TEST CONFIGURATIONS

To evaluate the parameters affecting the shear contribution in the CFRP, 26 tests were conducted. Test parameters were sometimes modified depending on the results of previous tests.

3.2.1   24 in. Depth Beams

Sixteen tests were conducted with 24 in. beams. The test matrix is divided into three groups with a/d ratios of 1.5, 2.1 and 3. Shear span to depth ratio of 1.5 is classified as a deep beam, so different transverse ratio guidelines were applied. To investigate the effect of shear span to depth ratio, two tests with a/d ratio of 2.1 were conducted with the transverse steel ratio in these beams the same as that in the beams with a/d ratio of 3.

In each group, a control test with no strengthening was included to obtain an estimate of shear capacity. In some test programs reported in the literature, no control test was conducted, but the strength was calculated using design equation. However, design equations are generally conservative and the FRP contribution to shear might be over-estimated if strengthened beam is calculated.

Figure 3-3 shows the cross-section of 24 in. beams and the reinforcement layout for stirrups.
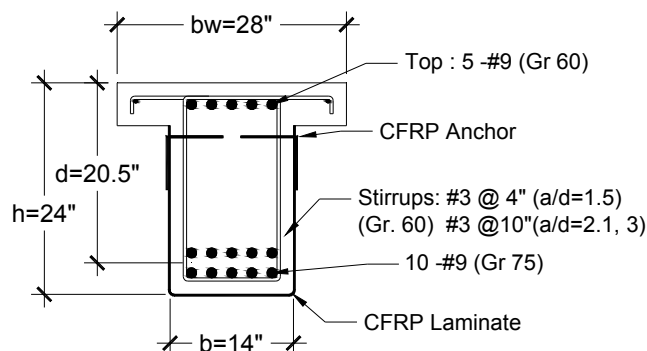
Figure 3-3 Cross-section of 24 in. beams

Ten tests were conducted in this group. All tests in this group have the same beam layout and a shear-span-to-depth ratio of 3. Test variables for this group are summarized in Table 3-1. Tests notation is as follows: the first value denotes the overall depth of the specimen in inches, the second value denotes the shear span to depth (a/d) ratio, and the third value denotes the sequential test number.

Table 3-1 Test Matrix in section shear beam (24-3-1 ~10)

Test	CFRP layout	Variables
24-3-1	No CFRP	(Pre-cracking)
24-3-1r	1 Layer, 5"@10"	Strengthening after initial loading
24-3-2	No CFRP	**Control**
24-3-3	1 Layer, 5"@10"	No bond (**poor application**)
24-3-4	1 Layer, 5"@10"	**No bond** (proper application / modified anchor)
24-3-5	1 Layer, 5"@10"	Laminate B: **low elastic modulus**
24-3-6	1 Layer, 5"@10"	Laminate C: dry layup, **high rupture strain**
24-3-7	1 Layer, **Continuous**	Different layout, compatible to 2 layers
24-3-8	**2 Layers,** 5"@10"	**The amount of material**
24-3-9	1 Layer, 5"@10"	**No CFRP anchor**
24-3-10	1 Layer, 5"@10"	**Inclined anchor**

The stirrup and CFRP layout are shown in Figure 3-4. No. 3 Grade 60 stirrups at 10 in. spacing on center are used. This spacing satisfies the maximum spacing of d/2 in ACI 318 guidelines. Five in. wide CFRP strips at 10 in. spacing were selected to compare with a continuous sheet and resulted in using half as much material. The maximum clear spacing (net spacing) in ACI 440 is d/4, which is 5 in. (20.5 in./4 = 5.1 in.) for this research.
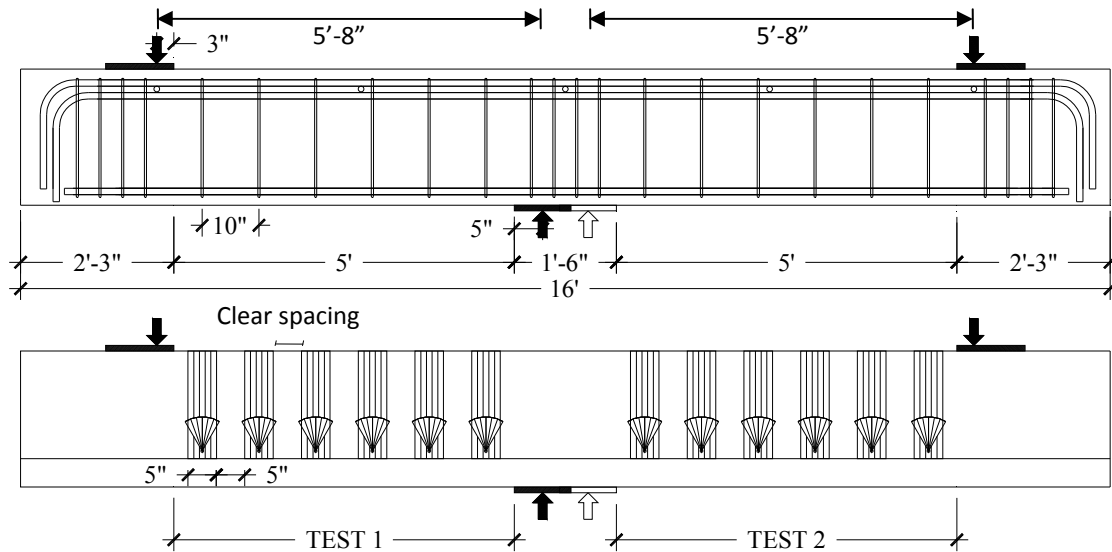
Figure 3-4 Reinforcing steel and CFRP layout for 24 in. beams with a/d=3

Test 24-3-1 was conducted to crack the beam and load to yielding of stirrups. Test 24-3-1r is a test of the same specimen after strengthening. To investigate the effect of a/d ratio, specimens with a/d ratio of 2.1 and 1.5 (24-2.1-1 and 24-1.5-4) having the same FRP layout as 24-3-1r were also tested.

In test 24-3-3 and 24-3-4, there was no bond between the CFRP strip and concrete surface. However, in 24-3-3, CFRP anchor installation was flawed due to a problem with the procedure used for eliminating bond as will be discussed in Section 4.4.1.3. Therefore, 24-3-4 was a repeated test with same unbonded condition, but with proper anchor installation.

In test 24-3-5 and 24-3-6, the CFRP was obtained from different suppliers to evaluate the effect of different material properties as will be discussed in Section 3.3.3. The CFRP sheets used in 24-3-5 have a lower stiffness compared with laminate A, so the thickness of one sheet is greater than that of laminate A to provide similar strength. The laminate C was applied using a dry layup procedure and has a high rupture strain. The estimated strength increase using laminate C was greater than laminates A and B, but would be developed at higher rupture strains.

In test 24-3-7 and 24-3-8, the amount of CFRP material was doubled and the layout was changed. A continuous sheet layout was applied in 24-3-7 whereas CFRP strips with two layers were applied in 24-3-8. Therefore, the CFRP anchor design was also changed. The number of CFRP anchors was doubled in 24-3-7, but in 24-3-8, the same number of CFRP anchors was used but the area was doubled.

Test 24-3-9 was conducted with no CFRP anchors. Many previous shear strengthening tests were conducted with no anchors. In some cases, a large increase in strength was reported using CFRP sheet without anchors. However, the strength increase depends on the existing conditions such as the transverse steel ratio and the beam configuration. Therefore, the efficiency of the CFRP anchor can be compared with 24-3-1r in this experimental program.

Test 24-3-10 was intended to evaluate the effect of the orientation of the CFRP anchor. In practice, it is hard to access the corner of web and slab in a T-beam, the anchor hole needs to be offset from the flange of a 90 degree hole is used. However, the area of concrete enclosed by CFRP sheet and CFRP anchors can be increased because it is possible to access to the corner by using inclined hole is drilled right at the corner between the web and flange.

(a) Typical CFRP anchor   (b) Anchor detail in 24-3-10
Figure 3-5 Comparisons of CFRP anchor detail between typical type and 24-3-10

3.2.1.2 Transitional beam (Tests 24-2.1-1 and -2)

Two basic tests including an unstrengthened control beam and a strengthened beam were conducted with shear-span-to-depth ratio of 2.1 to evaluate the effect of shear-span-to-depth ratio. As mentioned earlier, 10 in. stirrup spacing was used for No. 3 Grade 60 bar, which is the same as that for a/d ratio of 3.
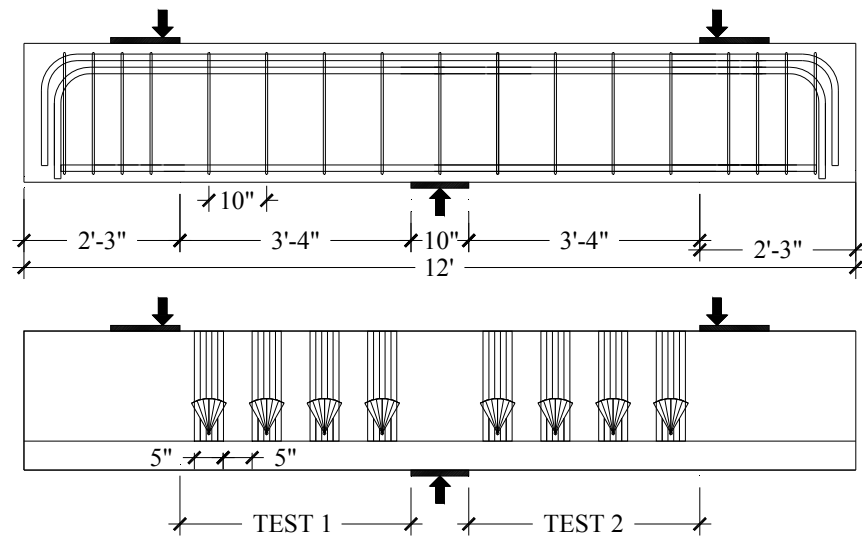
Figure 3-6 Reinforcing steel and CFRP layout for 24 in. beams with a/d=2.1

Table 3-2 Test Matrix in transitional beam (24-2.1-1 ~2)

Test	CFRP layout	Variables
24-2.1-1	1 Layer, 5"@10"	**a/d ratio**
24-2.1-2	No CFRP	**Control**

3.2.1.3   Deep beam (Tests 24-1.5-1 to -4)

Four tests were conducted with shear-span-to-depth ratio of 1.5. As shown in Figure 3-7, the stirrups were No.3 Grade 60 at 4 in. spacing on center, which satisfied the maximum spacing of d/5 for deep beams in ACI 318. The CFRP layout was the same as that of shear span to depth ratio of 3, but the number of CFRP strips was reduced from 6 to 3 due to the shorter span length. Table 3-3 shows the test matrix of test 24-1.5-1~4. Similar to tests 24-3-1 and 24-3-1r, test 24-1.5-1 intended to pre-crack and damaged beam for test 24-1.5-1r. Because test 24-1.5-1r did not fail due to reaching the capacity of loading setup, the beam was re-tested in a different setup as 24-1.5-1r2.

Test 24-1.5-2 was tested with CFRP strips without anchors and test 24-1.5-3 was tested without strengthening as a reference test. Finally, test 24-3-4 was tested with 1 layer of CFRP strips with anchors to compare with a similar beam, having a/d ratio of 3.
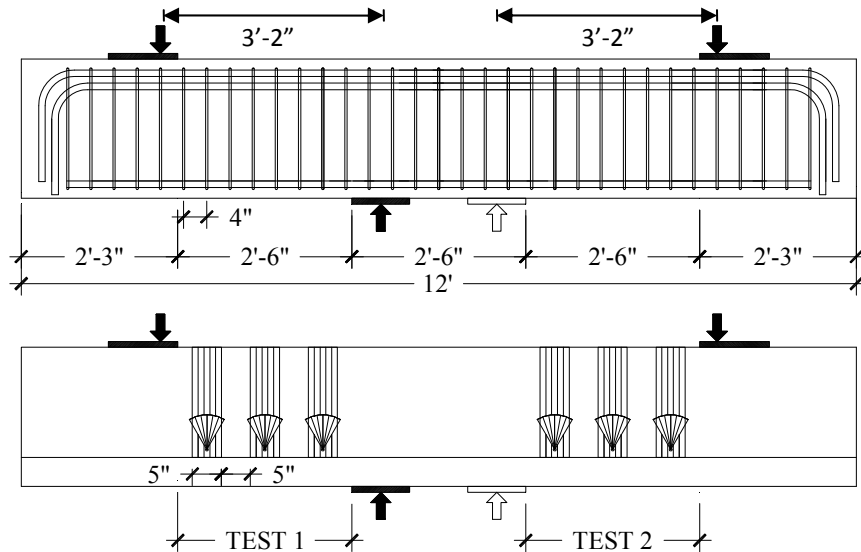
Figure 3-7 Reinforcing steel and CFRP layout for 24 in. beams with a/d=1.5

Table 3-3 Test Matrix in deep beam (24-1.5-1 ~4)

Test	CFRP layout	Variable
24-1.5-1	No CFRP	(Pre-cracking Load)
24-1.5-1R	2 Layers, 5"@10"	Strengthened, but load stopped due to setup capacity
24-1.5-1R2	2 Layers, 5"@10"	Strengthened, Reloaded as 24-1.5-1R
24-1.5-2	2 Layers, 5"@10"	**No CFRP Anchor**
24-1.5-3	No CFRP	**CONTROL**
24-1.5-4	1 Layer, 5"@10"	**a/d ratio**

3.2.2   48 in. Depth Beams

The effect of an increase in the effective depth of CFRP sheets was investigated by increasing beam depth to 48 in. In addition, this depth is more likely to reflect dimension of bridge elements. All 48 in. beam tests were conducted with a shear span to

depth ratio of 3 because the capacity of beams with a shear span to depth ratio of 2 or less were generally governed by a concrete strut failure that did not mobilize the steel stirrups or CFRP strips. Additionally, deep beams have high transverse steel ratio to satisfy minimum code provision and may not be suitable candidate for strengthening with CFRP.

Figure 3-8 shows a cross-section of the 48 in. beams and the reinforcement layout. The width (14 in.) was the same as in the 24 in. beam, so the cross-sectional area was doubled. Two spacing of stirrup reinforcement were used to evaluate the effect of transverse steel ratio. One group had No.3 stirrups at 18 in. spacing on center, which met the minimum steel requirement, whereas the maximum spacing controlled the stirrup layout in the 24 in. beams. The other had No.3 stirrups at 10 in. spacing on center, which was the same transverse steel ratio as 24 in. beams. Side bars were provided in the tensile zone as required in ACI 318 for beam depths greater than 36 in.
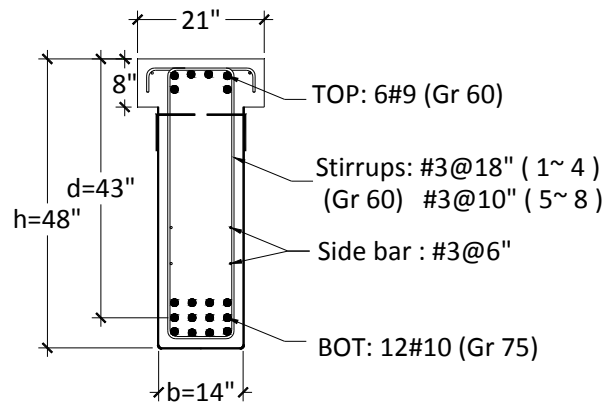
Figure 3-8 Reinforcement layout of 48 in. depth beams

3.2.2.1 *Minimum transverse steel ratio (Tests 48-3-1 to -4)*

Four tests were conducted with the minimum transverse steel ratio - No.3 Grade 60 stirrups at 18 in. spacing on center. The CFRP layout was 10 in. wide sheet at 20 in. spacing on center. The reinforcement and CFRP layout are shown in Figure 3-9. CFRP material ratio from this layout is the same as that in the 24 in. beams.
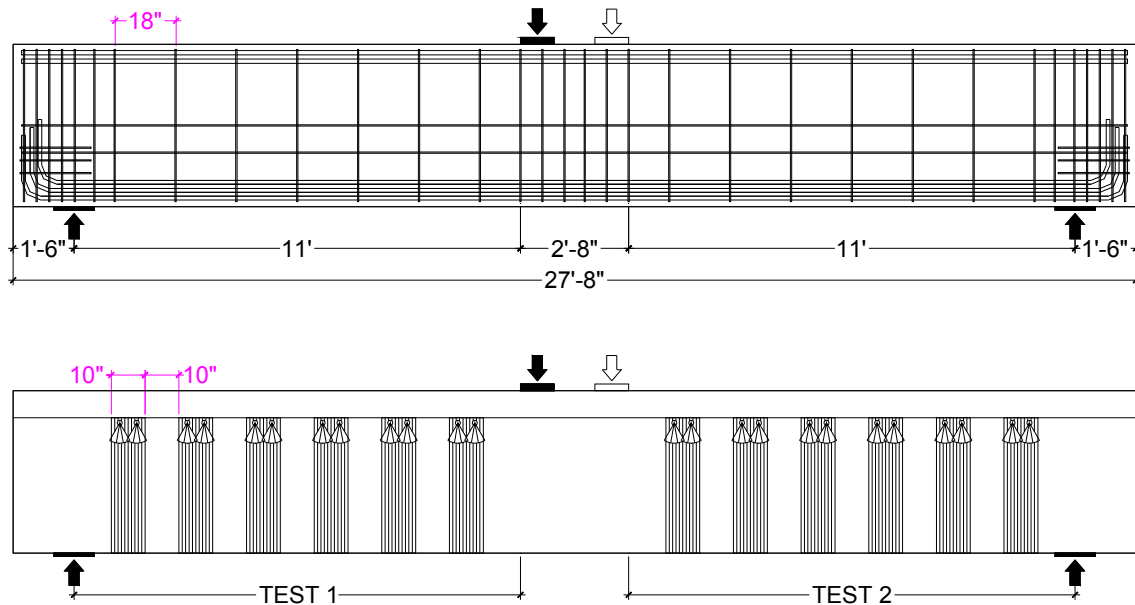
Figure 3-9 Typical Reinforcement layouts for test 1~4 in 48 in. beams

In Table 3-4, the test matrix of tests 48-3-1 to 48-3-4 is presented. Tests 48-3-1 and 48-3-2 were basic tests (control and strengthening). In test 48-3-3, the width of CFRP sheet is 14 in. instead of 10 in., but the same spacing between two sheets. This test intended to evaluate the effect of the amount of material and bonded area between CFRP sheet and concrete surface. In test 48-3-4, the diagonal CFRP strips were applied, but a continuous U-wrap with anchor is not possible. A strip was placed on each side of the web and the ends overlapped on the bottom of the beam.

Table 3-4 Test Matrix in minimum transverse steel ratio (48-3-1 ~4)

Test	CFRP layout	Variables
48-3-1	No CFRP	**Control**
48-3-2	1 Layer, 10"@20"	**Transverse reinforcement ratio**
48-3-3	1 Layer, 14"@20"	**Higher transverse reinforcement ratio**
48-3-4	1 Layer, 10"@20"	45 deg. **diagonal** strips

$$V_{f,48-3-4} = \frac{A_{vf}f_{fe}(\sin \alpha + \cos \alpha)d_{fv}}{s_f}$$

$$= \frac{A_{vf}f_{fe}(\sin 45° + \cos 45°)d_{fv}}{s_f}$$

$$= 1.4V_{f,48-3-1r}$$

$$V_{f,48-3-3} = \frac{A_{vf}^*f_{fe}(\sin \alpha + \cos \alpha)d_{fv}}{s_f}$$

$$= \frac{(1.4A_{vf})f_{fe}(\sin 90° + \cos 90°)d_{fv}}{s_f}$$

$$= 1.4V_{f,48-3-1r}$$
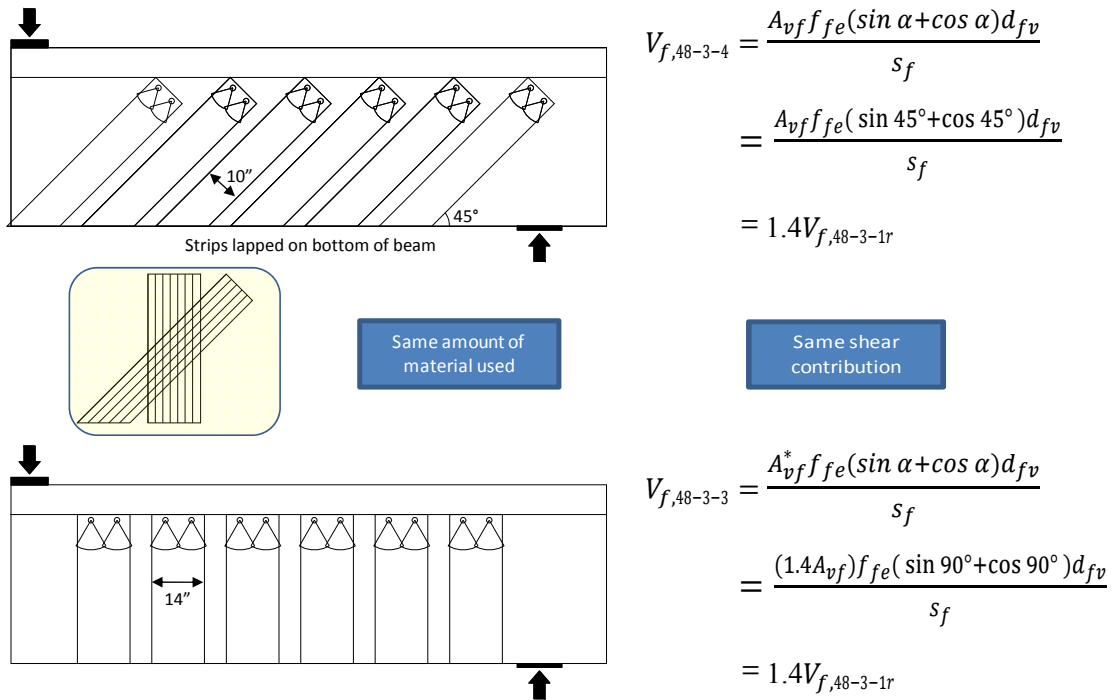
Figure 3-10 Conceptual design comparing 48-3-3 and 48-3-4

It is noted that the same amount of CFRP material is applied in tests 48-3-3 and 48-3-4. As shown in Figure 3-10, the length of strip is increased by changing the orientation of CFRP strip. The additional CFRP material used in 48-3-4 was replicated by increasing the width of CFRP strips in 48-3-3.

3.2.2.2 *Same transverse ratio with 24 in. beams (Tests 48-3-5 to -8)*

To evaluate the effect of the depth, tests 48-3-5~8 had the same transverse ratio as in the 24 in. beam. As shown in Figure 3-11, the stirrup layout is No.3 Grade 60 at 10 in. on center. Because the beam height is changed from 24 in. to 48 in. (effective depth: 20.5 in. → 43 in.), twice the number of stirrups cross the critical section would result in the same transverse ratio as in 24 in. beams. The CFRP layout was 10 in. wide strips at 20 in. centers, which was the same as that of the tests 48-3-1~4. Therefore, it is also possible to evaluate the effect of the transverse steel ratio by comparing with tests 48-3-1 and 48-3-2.
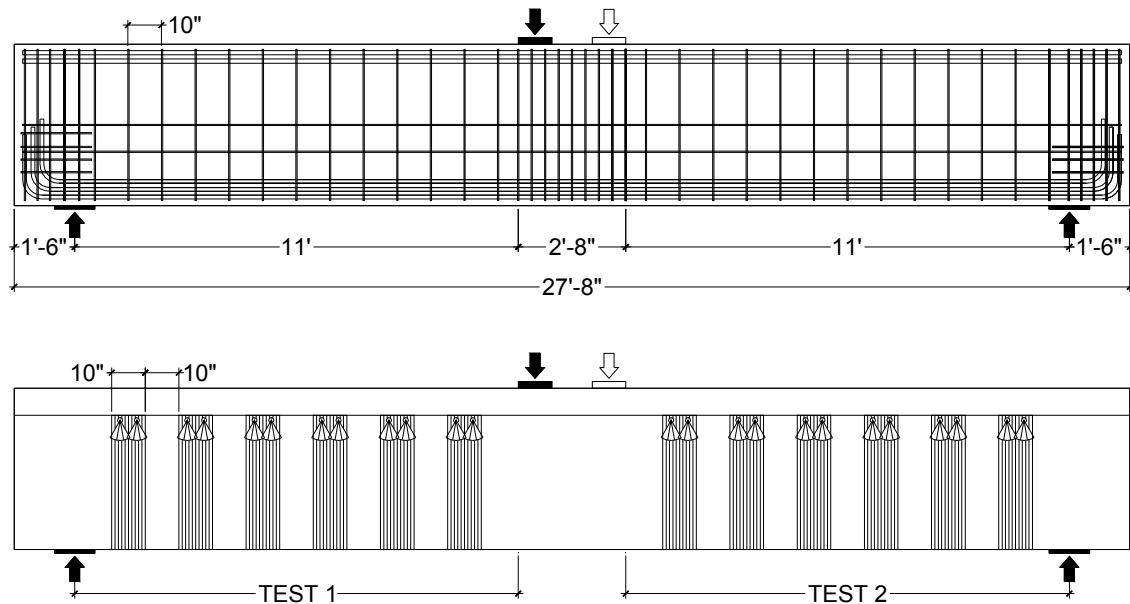
Figure 3-11 Typical reinforcement layouts of test 5 to 8 in 48 in. beams

After testing 48-3-6, epoxy injection and CFRP strengthening were applied to the same specimen and tested again as 48-3-6r. In test 48-3-7, effective length of the CFRP strips was changed by installing intermediate anchors. In test 48-3-8, the two layers of CFRP sheet applied and this test also compared with test 24-3-8 (2 layers).

Table 3-5 Test Matrix in same transverse steel ratio with 24 in. beams (48-3-5 ~8)

Test	CFRP layout	Variables
48-3-5	1 Layer, 10"@20"	**Depth** (compared w/ 24")
48-3-6	No CFRP	**Control**
48-3-6r	1 Layer, 10"@20"	Epoxy injection / **strengthening**
48-3-7	1 Layer, 10"@20"	**Intermediate** anchors
48-3-8	2 Layers, 10"@20"	**Double** area

3.3 MATERIAL PROPERTIES

To evaluate the material properties, several tests were conducted. Based on these material tests, the estimates of shear strength from design equation were modified using measured material strengths. More details including tables and graphs are listed in Appendix D.

3.3.1 Concrete

The design of the experimental T-beams was based on a low concrete compressive strength of 4000 psi. It is common in practice for the 28 day compressive strength to be higher than the specified nominal strength. For design, this additional strength is preferred, but in the case of research specimens, any additional strength might result in a different failure mode. Therefore, a 28 day compressive strength of 3000 psi was specified during construction so that the actual value of the compressive strength would be lower or around 4000 psi.

Measured concrete compressive strength at time of testing was 3300 ~ 3900 psi and the tensile strength from split tension test is 320 ~ 430 psi. These tensile strengths ranged between $5.97\sqrt{f'_c} \sim 6.26\sqrt{f'_c}$, and agreed well with theoretical relationships.

3.3.2 Steel

Two separate tension tests were conducted for the 24 in. and 48 in. beams.

For the 24 in. beams, ASTM A615 No. 9 Grade 75 bars were used for flexural tensile reinforcement, which had a measured yield stress of 81 ksi. No.10 Grade 75 bars were used for flexural reinforcement in 48 in. beams. The measure yield stress was about 80 ksi. Full flexural yielding in multi-layers was not expected, so it was desirable for the flexural steel to have greater strength than specified.

For transverse steel, ASTM A615 No.3 Grade 60 steel was used in both 24 in. beams and 48 in. beams. The measured yield stress of bars for 24 in. beams was 69 ksi. However, the variation between three tests was high, so the results were not reliable. Tension tests for 48 in. beams were conducted from coupons cut from stirrups because

the depth was long enough to extract a coupon for the tension test. The measured yield stress of bars for 48 in. beams was 61 ksi and the results were consistent.

3.3.3   CFRP

As noted in Appendix D, several coupon tests of the CFRP sheets were conducted. However, the CFRP coupon test results exhibited considerable variation. In NCHRP report 655 and ACI 440.2R, at least 20 tests are recommended to define the elastic modulus and ultimate strength. Based on this information, more coupon tests and more instrumentation were needed to obtain more reliable data meeting the procedure the ASTM D3039. Since designers are likely to use CFRP laminate properties provided in manufacturer's specifications, such data was used in this program.

The manufacturer's reported mechanical properties of three CFRP laminates are presented in Table 3-6. As discussed in Section 2.1.3.2, mechanical properties of the CFRP materials depended on the volume fraction of fiber and the amount of resin although the dry fiber properties of materials were identical. The test value is more appropriate when evaluating and constructing design equations because the design values are determined as mean values (test value) minus three times the standard deviation as discussed in Section 2.1.3.3. However the manufacturer's sheets for laminate B and Laminate C did not provide test values, so design values were used.

Table 3-6 CFRP laminate properties from manufacturer's specifications

CFRP Laminate	Thickness (in)	Elastic Modulus (ksi)		Ultimate Strain (in/in)		Ultimate Stress (ksi)	
		Test	Design	Test	Design	Test	Design
A	0.011	14800	12600	0.0105	0.0105	154	131
A-1[*1]	0.041	13900	11900	0.01	0.01	143	121
B	0.02	-	8200	-	0.01	-	105
C [*2]	0.0065	-	33000	-	0.0167	-	550

*1 material A-1 is used for CFRP anchor only because material A was too stiff to make anchor.
*2 The material properties of Material C are for fiber only because it is used for dry layup application.
*3 For evaluating shear estimates, typical tests value were used, but those of laminate B and C were not provided. Therefore, design values were used in laminate B and C

Laminate A was used for most tests. Laminate A-1 was provided by the same manufacturer of laminate A. Laminate A-1 was only used for CFRP anchors because laminate A was too stiff to fabricate anchors. The properties of the dry carbon fiber were presented in laminate C because it was installed using a dry lay-up procedure.

The stress-strain relation of laminate B is inconsistent because the elastic modulus times ultimate strain is not equal to the ultimate stress ((8200 × 0.01 =) 82ksi ≠ 105ksi). These properties were design value, not test value and the elastic modulus is evaluated from 0.003 to 0.006 strain, not from ultimate stress and strain and may explain why the relation between design properties was not consistent. The ultimate strength determined by elastic modulus and rupture strain were close to results from coupon tests, so these properties were used for evaluating shear contribution.

3.4 ESTIMATE OF BEAM CAPACITY

Prior to testing, the capacities of all the specimens were estimated using current code equations (ACI 440.2R and ACI 318) for shear. The contributions of the concrete (V_c), steel stirrups (V_s), and CFRP sheets (V_f) to the capacity of the beam were computed and are tabulated in Table 3-7. No strength reduction factor was applied in these calculations.

Table 3-7 Estimate of shear contribution using ACI provisions

		V_c	V_s	V_f	V_c+V_s (a)	$V_c+V_s+V_f$ (b)	Ratio (b)/(a)
24 in. beam	a/d =1.5 (#3@4")	36.3 k (V_c)	67.7 k (1.87V_c)	26.5 k (0.73V_c)	104 k (2.87V_c)	130.5 k (3.60V_c)	1.25
	a/d=2.1&3 (#3@10")	36.3 k (V_c)	27.1 k (0.75V_c)	26.5 k (0.73V_c)	63 k (1.75V_c)	89.9 k (2.48V_c)	1.42
48 in. beam (a/d=3)	1 ~ 4 (#3@18")	76.4 k (V_c)	31.6 k (0.41V_c)	59.9 k (0.78V_c)	108 k (1.41V_c)	167.9 k (2.20V_c)	1.55
	5 ~ 8 (#3@10")	76.4 k (V_c)	56.9 k (0.74V_c)	59.9 k (0.78V_c)	133 k (1.74V_c)	193.2 k (2.53V_c)	1.45

Note. *1) All calculations are based on the nominal material strength
2) V_f = one 5" wide sheet @10" (24 in. beams) / one 10" wide sheet @20" (48 in. beams)
3) Rupture strain of 0.01 is used for estimating V_f

Each shear contribution is also normalized in terms of the concrete contribution. The ACI 440 guideline limits the maximum strength to five times the concrete contribution because contributions greater than this value tend to provide failure by concrete crushing and there is no benefit from steel stirrups or CFRP in that case.

The two strengthening ratios for 48 in. beams were different although the same amount of CFRP was used. In addition, if there is no transverse reinforcement, the base capacity before strengthening is 76.4 k and the strengthened capacity is 136.3 k (76.4+59.9) in 48 in. beams. The strengthening ratio will be 1.78 (136.3/76.4), which is much greater than the ratio when transverse steel is provided. In general, as a larger amount of steel reinforcement is placed, a lower ratio of strength increase is expected.

3.5   TEST SETUP

To test 24 in. and 48 in. specimens, two separate test setups with different loading capacities were developed.

3.5.1   Loading Setup for 24 in. Beams

Test specimens were rotated 180 degrees for testing so that the load could be applied from the bottom as shown in Figure 3-12 and Figure 3-13. Load was applied upward at a single point along the beam. The loading system included a hydraulic loading ram, a load cell, and a spherical head. A load cell was used to monitor the load applied to the test specimens. A spherical head was also used to eliminate alignment differences between the concrete test specimen and the hydraulic ram.

Two tests were conducted on each T-beam specimen; one for each shear span. A clamping system using HSS $8 \times 8 \times 1/2$" sections was designed to provide external prestressing forces to prevent failure in the shear span not under consideration. With two pre-stressed rods, each external clamp was able to provide 60 k of clamping force to the test specimens. After the first shear span was loaded to failure, the same clamps were used to provide external reinforcement to the failed region of the beam so that the

untested (sound) end of the specimen could reach shear failure. Even with the external clamps applied, some minor cracking was observed within the larger shear span, but it did not impact the overall strength of the specimens.

Figure 3-12 Photo of loading setup for 24 in. depth beams
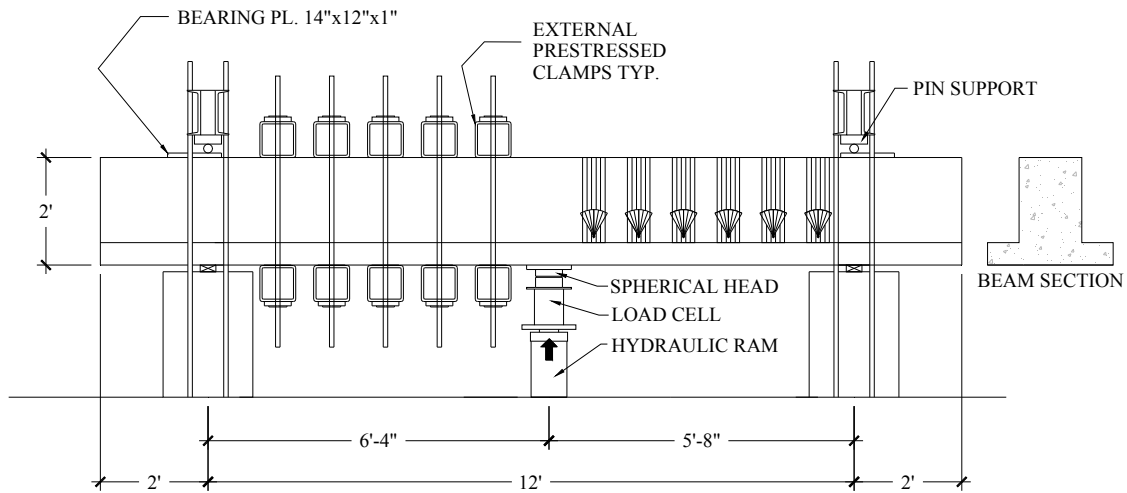
Figure 3-13 Loading setup for 24 in. beams

3.5.2 Loading Setup for 48 in. Beams

A W-section supported a loading ram which allowed the test specimens to be loaded in a downward direction and the beam did not have to be rotated. An elevation view of the high capacity test setup is shown in Figure 3-15. Similar to the loading setup of 24 in. beams, two tests were conducted with same clamping system.

69

Figure 3-14 Photo of loading setup for 48 in. depth beams
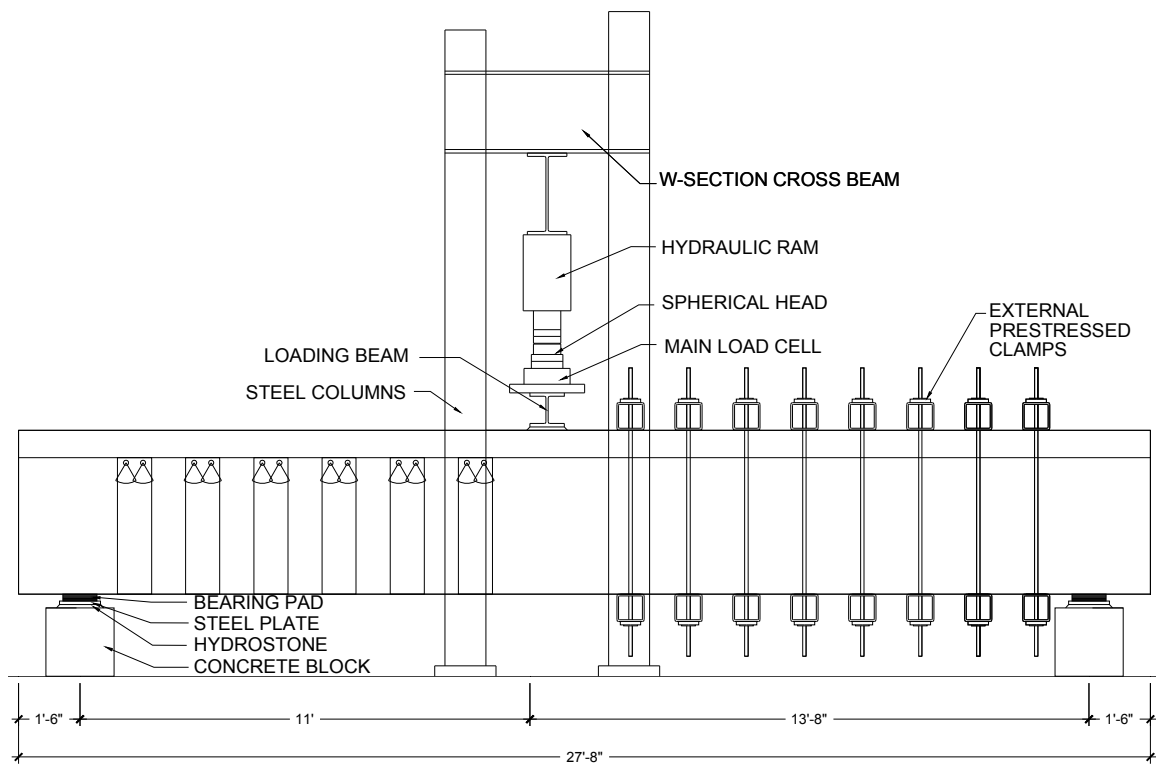
Figure 3-15 Loading setup for 48 in. beams

The bearing pads were used for both end reaction supports to stabilize the slender beams. Moreover, lateral rods were installed to monitor and resist unexpected lateral

beam movement caused by uneven loading. After testing one end, the specimen were turned around and placed so that the loading setup remained in place.

3.6 INSTRUMENTATIONS

To monitor strains in the stirrups and the CFRP sheet, beam displacement, and shear strain, several instrumentation devices were mounted. The strain gages were used to estimate the shear contribution of steel and CFRP. The beam displacement from Linear Variable Differential Transformers (LVDTs) was used for comparing overall behavior between the tests. Shear strain was calculated using three LVDTs within the critical section. The LVDTs were used to compare the member stiffness between the tests. It was difficult to set the location of the LVDTs for shear strain because the shear crack formed at different locations.

3.6.1 Steel Strain Gages

Most of strain gages were placed on the steel stirrups where the critical crack was likely to occur. Due to bond between the concrete and stirrup, strains along the stirrups were not uniform. If a gage was not located close to the crack, the data from this gage was not useful for evaluating the shear contribution. Therefore, multiple gages were mounted on the same stirrup to obtain more accurate data if the stirrup was likely to contribute to the shear capacity. In addition, some gages were also placed on the longitudinal steel to confirm that flexural failure did not occur.

To recognize the location of gages easily, a grid system was used as shown in Figure 3-16, Figure 3-17, and Figure 3-18. This grid system also allowed the flexibility of gage location between tests, so the gage location was modified to reflect the critical crack profile of previous tests. A few redundant gages were placed on the opposite side of the reinforcing cage because some gages may not function properly. Furthermore, redundant gages provide a check regarding symmetry of the specimen and point of load application.

71

(a) a/d =1.5   (b) a/d =2.1

(c) a/d =3
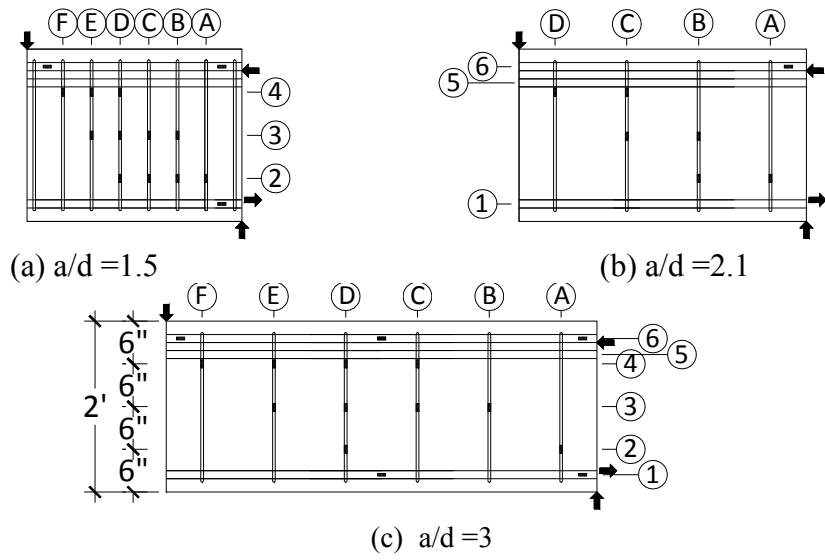
Figure 3-16 Grid system of strain gages in the steel stirrups (24 in. beams)
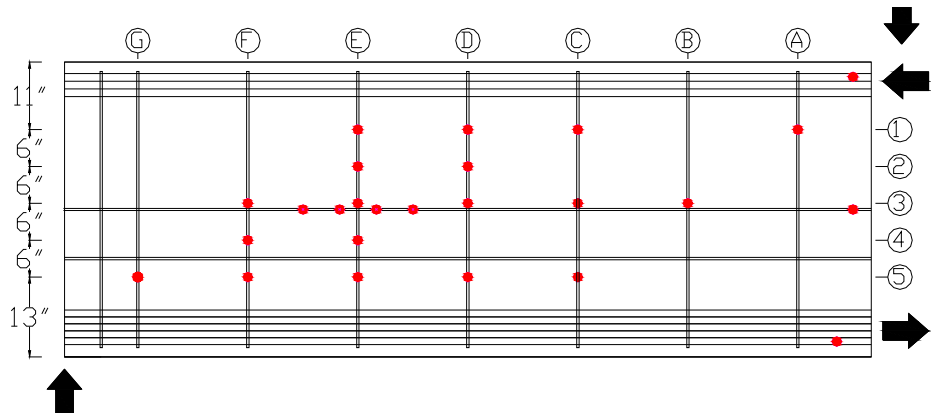
Figure 3-17 Grid system of strain gages in the stirrups (48-3-1 ~4 : #3@18")
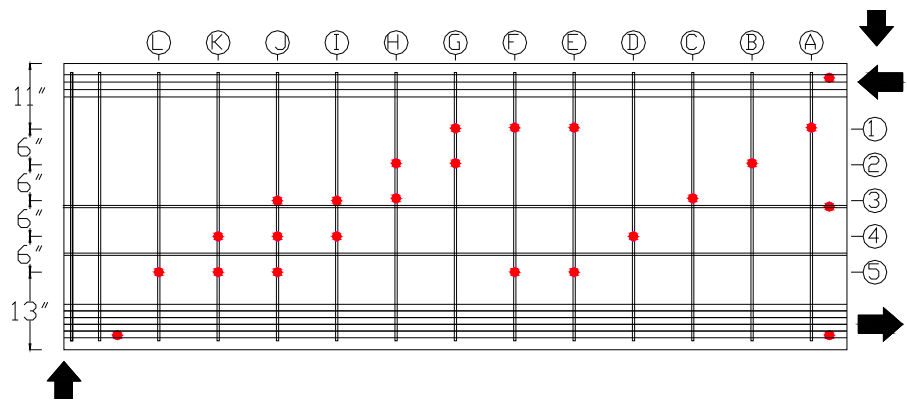
Figure 3-18 Grid system of strain gages in the stirrups (48-3-5 ~8 : #3@10")

72

In 48 in. beams, more gages were mounted at one stirrup to capture the strain at the critical section. In case of multiple gages along the stirrup, the spacing between two adjacent gages was 6 in. and this spacing was the same in 24 in. and 48 in. beams.

3.6.2 CFRP Strain Gages

To evaluate the CFRP shear contribution, several gages were also mounted on the surface of CFRP sheets. Because the strain range of CFRP is up to 0.01, much greater than that of steel, a different type of strain gage was used. No waterproofing treatment was needed because the CFRP gages were mounted on the surface of the CFRP sheets.

A separate grid system was developed for CFRP as shown in Figure 3-19 and Figure 3-20. Strain gages were placed at intersections of the grid lines which were likely to be near the critical crack. Similar to the steel gages, a few redundant CFRP gages were placed on the opposite side of the concrete specimen. The strain distribution in the CFRP strip was not uniform along the length of the strip, but also across the width. Therefore, multiple gages were also mounted across the width of some CFRP strips.

(a) a/d=1.5 (b) a/d=2.1

(c) a/d=3
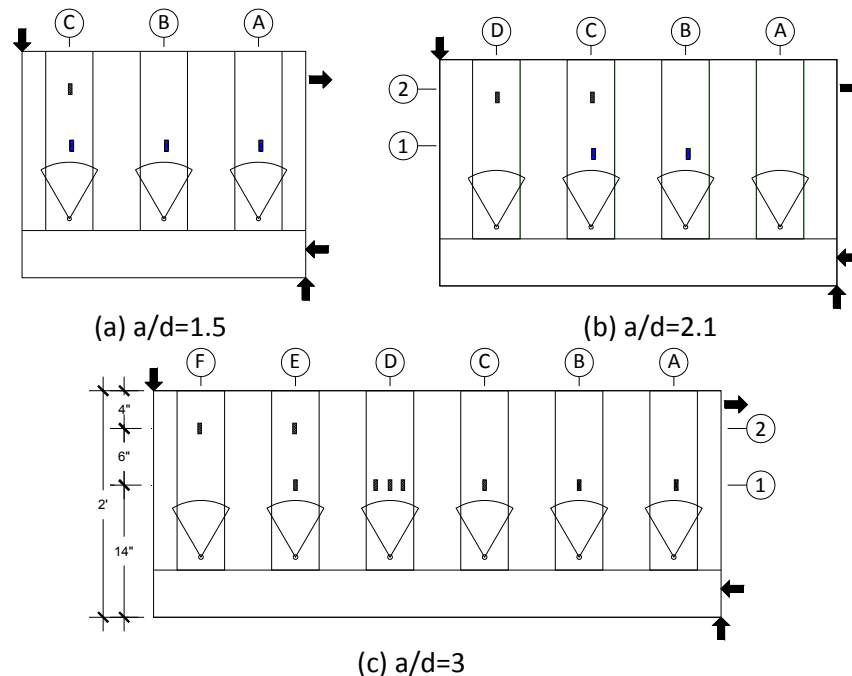
Figure 3-19 Grid system of strain gage in the CFRP (24 in. beams)
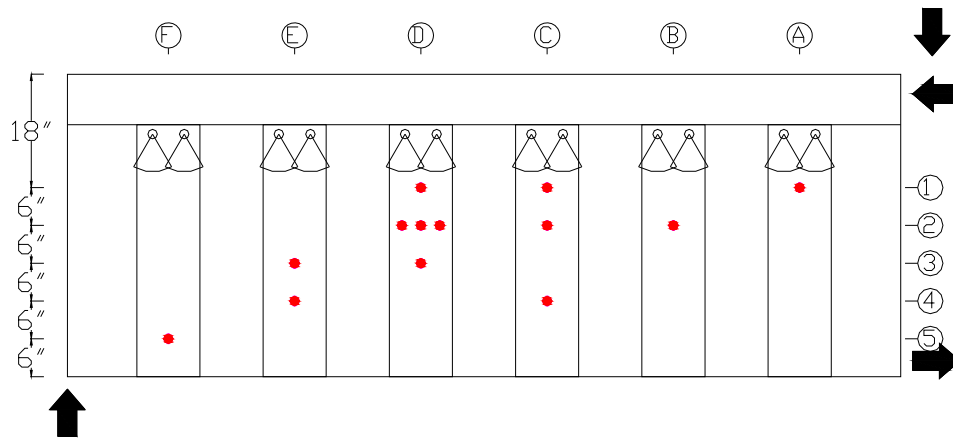
Figure 3-20 Grid system of strain gage in the CFRP (48 in. beams)

3.6.3 Linear Variable Differential Transformers (LVDTs)

Beam displacement and shear deformations were monitored by several linear variable differential transformers (LVDTs). According to the loading setup, different measurement schemes were used.

3.6.3.1 Monitoring displacement

In 24 in. beam tests, six LVDTs were used to monitor the beam displacements because the test specimens were restrained by steel rods which elongated during testing as described in Section 3.5.1. To remove the rigid body motion due to support elongation, the displacements of both supports as well as the displacement at loading point were measured. The elongations of both supports would not be same because elongation is proportional to the reaction force and the reaction forces of both ends are not the same. In addition, to monitor and adjust the possible uneven displacement between front and back side, LVDTs were mounted on both sides. The actual beam displacement could be calculated by subtracting the rigid body motion from the measured displacement at loading point.

74

Actual deformation   Total Deformation   Rigid Body Motion
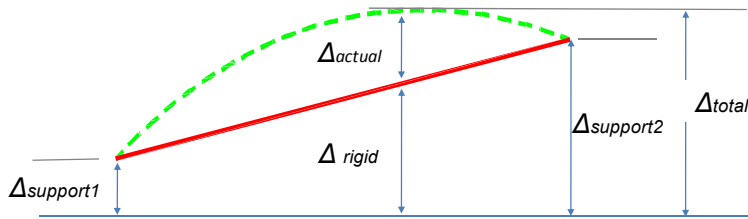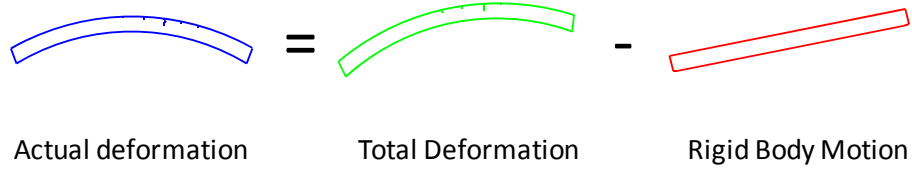
$$\Delta_{actual} = \Delta_{total} - \Delta_{rigid}, \quad (\Delta_{rigid} = \Delta_{support1} \times \frac{L-x}{L} + \Delta_{support2} \times \frac{x}{L})$$

Δ_{total}, $\Delta_{support}$, $\Delta_{support}$: data collected from LVDTs

Figure 3-21 Concept of determining beam displacement without rigid body motion

| (a) Loading point | (b) Reaction point |
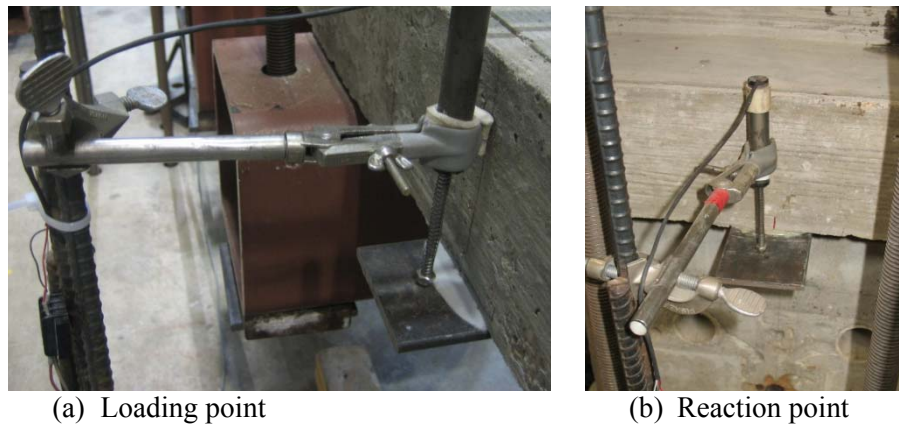
Figure 3-22 LVDTs configuration for beam displacement in 24 in. beam

In 48 in. beam tests, only two LVDTs were used to monitor the overall beam displacement at loading point because the supports displacement is negligible relative to beam displacement. Therefore the actual displacement was equal to the measured displacement at loading point assuming that there is no rigid body motion.

3.6.3.2 Monitoring shear deformation

In 24 in. beams, three LVDTs were used to monitor the shear deformation and were arranged in a triangular shape as shown in Figure 3-23. Because the data collected from LVDT's is not the strain value, each deformation value needs to be divided by the original length of between points from triangular to get the strain. Using Mohr's circle, the shear strain can be evaluated from these three strains and the angle of the diagonal leg.
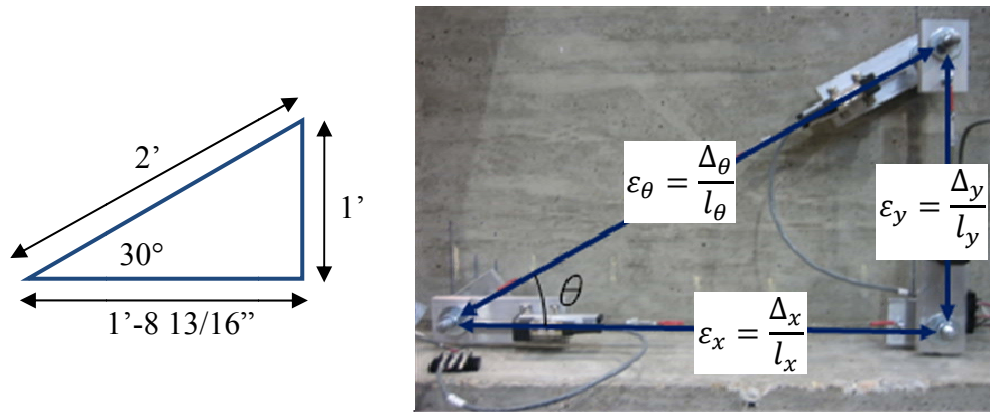
Figure 3-23 LVDTs configuration for shear strain in 24 in. beam

$$\gamma = \frac{\varepsilon_\theta - (\varepsilon_x \cos^2 \theta + \varepsilon_y \sin^2 \theta)}{\cos \theta \sin \theta}$$

However, it is noted that this value is obtained from the average strain between the two fixed points as shown in Figure 3-24, so triangular arrangement is not accurate when there is a variation of strain between the gage points. The diagonal displacement means the average strain at center point, but the two perpendicular displacements cannot present the average strain of x-direction and y-direction at center point. If the variation over the measured region can be assumed to be negligible, the shear strain values are useful for making comparison between tests. However, the strain variation in the x-direction is influenced by flexure. Therefore, the shear strain may be distorted by the differences between measured strain and averaged strain.
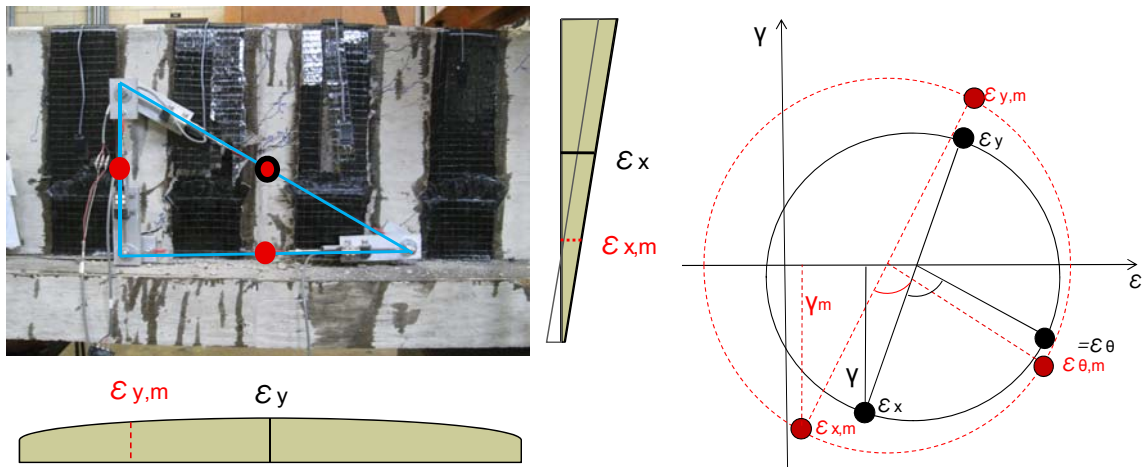
Figure 3-24 Differences in Mohr's circle's due to strain variations in 24 in. beams

This distortion would be greater as the depth of beam increases. To minimize this effect, additional LVDTs were placed in the 48 in. beams. To get the average strain at the center point, six LVDTs were arranged in a rectangular shape as shown in Figure 3-25. Two vertical displacements and two horizontal displacements were monitored to get the average strain at center point. In addition, another diagonal displacement - diagonal compression - was also measured to get the shear strain value from an additional set of triangularly arranged LVDTs. As a result, it is possible to get the shear strain in three different ways including (DT-V-H), (DC-V-H) and (DT-DC).

(DT: Diagonal Tension, DC: Diagonal Compression, V: Vertical, H: Horizontal)
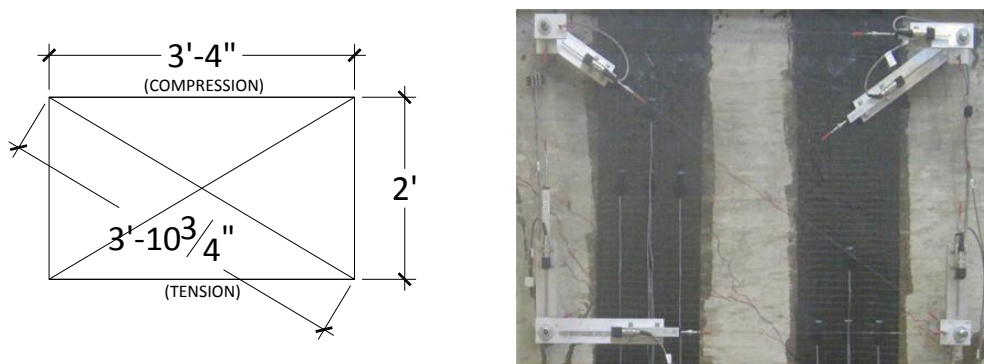
Figure 3-25 LVDTs configuration for shear strain in 48 in. beams

Nevertheless, it is impossible to evaluate the exact shear strain in the beam because concrete members cannot be taken as a homogeneous material. Therefore measured shear strains will be different depending on their location. Unfortunately, the exact location of the critical section cannot be predicted before loading. Therefore, the shear strain is not reliable if the critical crack did not pass through the instrumented region.

CHAPTER 4
Test Results

4.1 OVERVIEW OF TEST RESULTS

A total of 24 tests were conducted (16 tests with 24-in. depth beams and 8 tests with 48-in. depth beams). Table 3-1 summarizes all the test results. In 24-in. depth beams, the results are tabulated according to the shear span to depth (a/d) ratio (3, 2.1, 1.5) and in the 48-in. depth beams, the results are tabulated according to two different transverse steel ratios (Tests 1~4 : #3@18" ,Tests 5~8 : #3@10"). The a/d ratio of all 48-in. beams was 3. The shear capacities were compared with that of the reference test (control test) in the same group. The variables considered in each test are provided in the "description" column of Table 3-1. The failure mode is provided in the last column.

Some tests were stopped before failure to permit testing of the other end of the beam. If the end tested first was taken to failure, the damage would have been too great to prevent further testing of the beam.

General test observations are described in Section 4.2. In Section 4.3, the evaluation of the shear contribution from strain data is described. In Section 4.4 the overall response, observations of each test and shear contributions of each material are described.

Table 4-1 Summaries of Test results

Test	Description	Shear (kips)	Percent Increase	Failure mode
24-3-2	No CFRP, **CONTROL**	105	0%	Diagonal tension
24-3-1	No CFRP, (Precracking Load)	74	-	Only loaded to yield of stirrup
24-3-1r	1 Layer, 5"@10", Strengthening after initial loading	152	44%	Rupture of CFRP strip
24-3-3	1 Layer, 5"@10" No Bond (**poor application**)	118	12%	Rupture of CFRP anchor
24-3-4	1 Layer, 5"@10" **No Bond** (proper application)	152	44%	Rupture of CFRP strip
24-3-5	1 Layer, 5"@10" Laminate B	145	38%	Rupture of CFRP strip
24-3-6	1 Layer, 5"@10" Laminate C	134	27%	Rupture of CFRP strip
24-3-7	1 Layer, **continuous sheet,** (compatible to 2 layers)	165	56%[*1]	Rupture of CFRP strip
24-3-8	**2 Layers,** 5"@10" **The amount of material**	153	45%[*1]	Rupture of CFRP anchor
24-3-9	1 Layer, 5"@10" **No CFRP anchor**	109	4%	debonding
24-3-10	1 Layer, 5"@10" **Inclined anchor**	145	38%	Rupture of CFRP strip and CFRP anchor
24-2.1-2	No CFRP CONTROL	129	0%	Diagonal tension
24-2.1-1	1 Layer, 5"@10" a/d ratio	170	32%	Rupture of CFRP strip and CFRP anchor
24-1.5-3	No CFRP **CONTROL**	233	0%	Diagonal tension
24-1.5-1	No CFRP Pre-cracking Load	134	-	Only loaded to yield of stirrup
24-1.5-1r	2 Layers, 5"@10" Strengthening after initial loading	242	-	Loading stopped at capacity of setup
24-1.5-1r2	Retest with 24-1.5-1r	252[*2]	8%	Reloading to failure by concrete crushing
24-1.5-2	2 Layers, 5"@10" **No CFRP Anchor**	255	9%	Debonding
24-1.5-4	1 Layer, 5"@10" **a/d ratio**	264	13%	Rupture of CFRP strip

Table 4-2 Summaries of Test results (continued)

Test	Description	Shear (kips)	Percent Increase	Failure mode
48-3-1	No CFRP **CONTROL**	147	0%	Stopped loading
48-3-2	1 Layer, 10"@20" **transverse steel ratio**	226	54%	Rupture of CFRP strip
48-3-3	1 Layer, 14"@20" **width** of strip	239	63%	Stopped loading
48-3-4	1 Layer, 10"@20" 45 deg. **diagonal** strip	236	61%	Rupture of CFRP strip
48-3-6	No CFRP **CONTROL**	228	0%	Stopped loading
48-3-6r	1 Layer, 10"@20" epoxy injection / **repair**	327	43%	Rupture of CFRP strip and CFRP anchor
48-3-5	1 Layer, 10"@20" **depth** (compared w/ 24")	242	6%	Stopped loading
48-3-7	1 Layer, 10"@20" **intermediate** anchor	242	6%	Stopped loading
48-3-8	2 Layers, 10"@20" **double** area	255	12%	Rupture of CFRP anchor

*1. The amount of CRRP strip material is as twice much as the other test, which means the percent increase was expected to be 84%.

*2. The capacity of 24-1.5-1r2 might be reduced by concrete damage due to loading in 24-1.5-1r

*3. To conduct two tests from one specimen, loading was stopped before failure.

   It is likely that tests 48-3-1, 3, 5, 6, 7 would have exhibited additional capacity and would change the ratio

Three different approaches were used to evaluate the shear behavior of test with CFRP sheet and anchors as shown in Figure 4-1.

1. the evaluation of CFRP shear contribution based on computed strength vs. measured strength in Section 4.4

2. the evaluation of CFRP shear contribution based on test results with and without CFRP strengthening in Section 4.5

3. the comparison of measured strength at selected strain level compared with measured peak strength in Section 4.6

4.4 Computed strength vs. Measured strength

4.5 Control tests vs. Strengthened tests

4.6 Strength at Selected Strain. vs.Peak Strength

Proposed Design Equation
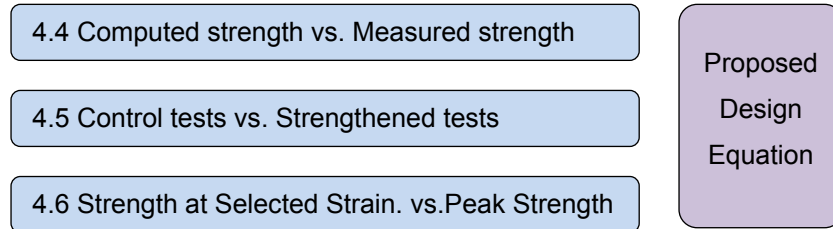
Figure 4-1 Three approaches to evaluate test data

4.2 TEST OBSERVATIONS

Estimation of shear contributions depends on the location of the critical crack and the location of strain gages. When a strain gage is not located at or close to the critical crack, the measured strain is under-estimated because some force is transferred by adhesive bond between the concrete crack and the gage location. In general, the installation of more strain gages along the length of steel stirrups or the CFRP strips could have improved estimates of the shear contribution of the steel or CFRP, but very close spacing would be impractical.

The steel stress is nearly constant once steel yields, but the CFRP stress is proportional to strain until the CFRP ruptures. As a result, steel contribution can be closely estimated regardless of gage location once strain value exceeds yield strain. However, the CFRP contribution is usually underestimated if the gage is not located at the point of maximum strain. The concrete contribution might be overestimated if the steel and CFRP contributions are underestimated because it is not measured directly but evaluated from subtracting the shear forces carried by the steel stirrups and the CFRP strips from the applied shear.

The determination of the critical crack angle is also essential for estimating the shear contribution of each material. Shear design equations are based on a 45 degree crack angle, but this angle changes as the applied load increases and a critical angle of less than 45 degrees is generally observed during the tests. A shallower critical crack angle enables more steel stirrups or CFRP strips to contribute to the shear capacity. As expected, the observed steel and CFRP contributions were usually greater than the

contributions estimated using design equations that were based on a 45 degree crack. For these reasons, the evaluation of the shear contribution from strain gages may vary depending on the gage location and critical crack angle. Therefore, engineering judgment was involved in determining critical crack angle and strain gages used to evaluate the shear contribution.

The beam displacement and shear strain were monitored to evaluate the overall shear behavior and to compare test results. All specimens were designed not to fail in flexure. The same amount of flexural reinforcement was placed in all specimens to keep the flexural stiffness the same. Therefore, the stiffness of specimens as indicated by a load-displacement graph did not vary much. On the other hand, the shear strain-applied shear response reflected the difference in shear stiffness between tests. However, shear strain also cannot be an absolute parameter of evaluating shear behavior if the critical crack does not occur in the location where shear measurements are being monitored.

4.2.1 Strain Response in the Steel Stirrup

In conventional reinforced beams, it is not important to monitor the stirrup strain because all stirrups crossing the critical section would likely reach yield strain and yield stress could be used regardless of strain value at ultimate. However, stress redistribution between stirrups might not be feasible under brittle failure due to CFRP rupture and some stirrups would not yield at failure. As a result, the strain value in the stirrups is important for evaluating steel contribution for this case. Furthermore, the strain value in the stirrup is also valuable for evaluating the interaction between the steel stirrups and the CFRP strips at any loading level.

At first, some of strain gage readings were not understood because the strain value increased dramatically and dropped to previous strain ranges after several cracks occurred. In addition, the strains between gages along the same stirrup were quite different depending on the relative distance from crack. There is no clear explanation, but it may be related to the bond stress between steel and concrete. Once a crack forms, a large increase in tensile strain occurs almost immediately, but a gage away from the crack

shows little change in strain as shown in Figure 4-2. Because gage D2 was located at the crack, the strain increased suddenly when cracking occurred. However, as the stirrups debonded, deformation due to the crack is distributed along a greater length of the stirrup, the strain of D2 and D3 were about the same.
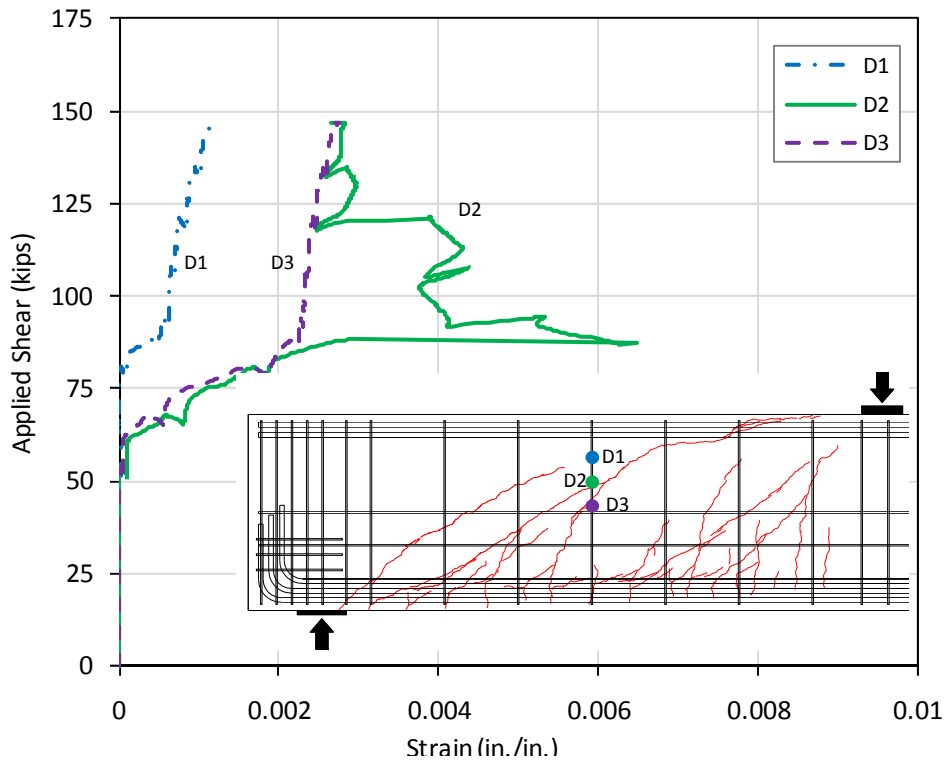
Figure 4-2 Comparison of strain response along the same stirrup

4.2.2   Strain Response in the CFRP

Because stress-strain relationship of CFRP material is linear up to rupture, CFRP strain should be monitored throughout the loading to evaluate CFRP stress. As mentioned before, the monitored strain is sensitive to the distance between crack and gage location. In addition, the critical crack angle is not aligned with CFRP fiber direction and the angle keeps changing over the span. Under this condition, the effective tensile strain in fiber direction would be different although the crack width is assumed same over the crack length.

84

As shown in Figure 4-3, the strain responses were different not only along the fiber direction because several cracks were across one CFRP strip. Strains across the width were varied because cracks crossed the CFRP strip at an angle. The strains at FD1 and FD2.2 increased abruptly at a shear of 100 k and the strain of FD3 increased suddenly at 160 k and finally at 200 k the strains of FD2, FD2.1 increased so that all of strains were similar. Based on these strain responses, a crack formed near gages of FD1 and FD2.2 and another crack occurred near FD3. As debonding occurred near the crack, all of strains were the same.

4.2.2.1   *Evaluation of CFRP contribution from strain gages*

From this case, several important points are illustrated. The load transfer pattern changed as load increased, which means that critical section was also changing and the gages for evaluating the shear contribution also need to be changed. In addition, if the strain difference between adjacent gages is significant, a single gage in a CFRP strip will not be enough to evaluate the CFRP contribution. The CFRP shear contribution may not be accurately determined if it is assumed that a gage located at critical crack reflects the strain across the strip because a strain variation across the strip width may still exist. In this case, the CFRP contribution will be over-estimated or under-estimated depending on the location of the gage relative to the crack development. Therefore, the shear contribution evaluated from strain gages was considered as an indicator of overall response, but, not an exact measurement. In addition, the critical crack and strain gages near the crack at ultimate capacity of the beam was used for evaluating shear contribution because the values of most interest were the contribution of concrete, stirrup and CFRP at ultimate.
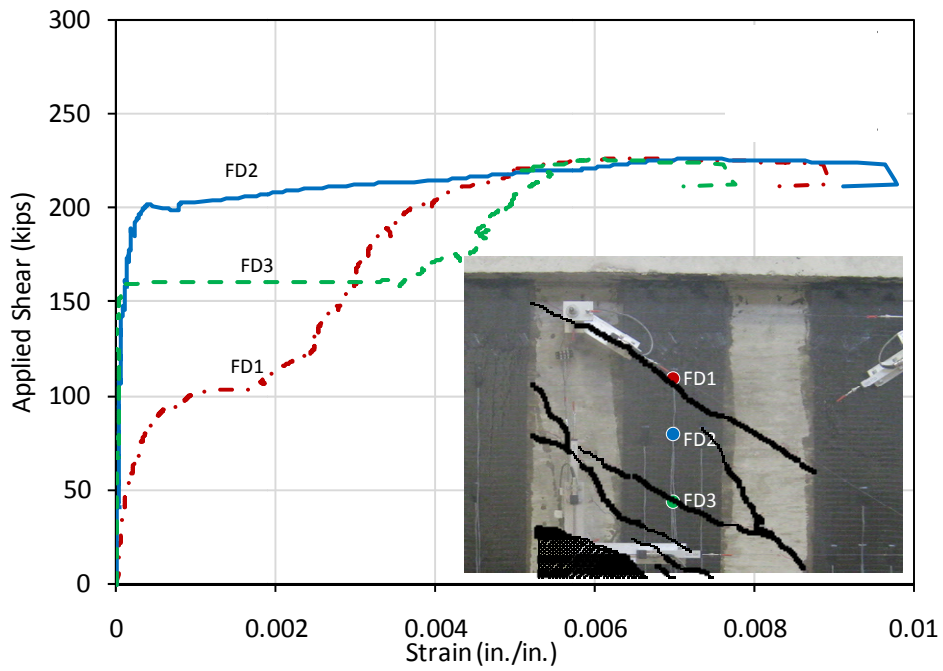
(a) Strain response along the strip direction
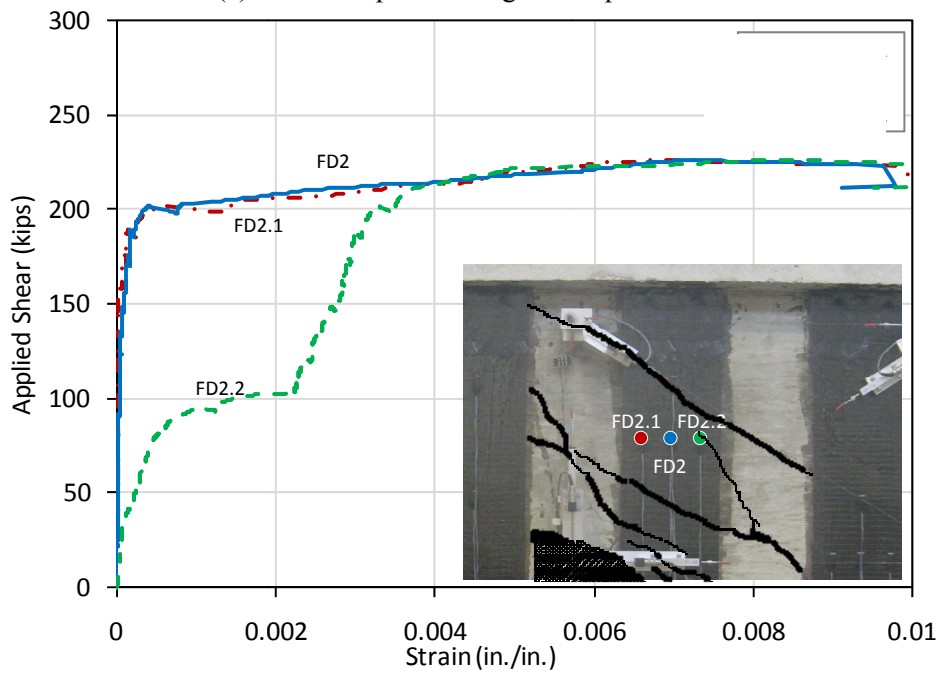
(b) Strain response across the width

Figure 4-3 Comparison of strain response in the same CFRP strip (48-3-2)

4.2.2.2 Debonding and effective length

Another issue is debonding, which complicates shear behavior of beam strengthened with CFRP. Bond stress transfers force from the beams into the CFRP strips. Before debonding occurs, there is virtually no strain in CFRP strip. However, once a crack forms, the CFRP strip starts debonding. As the debonded length increases, the CFRP strains may decrease under the loading on the beam. In addition, it was observed that the CFRP strain distribution in the test with unbonded CFRP (24-3-3 and 24-3-4) was nearly uniform as shown in Figure 4-4.

(a) Across the width   (b) Along the fiber direction
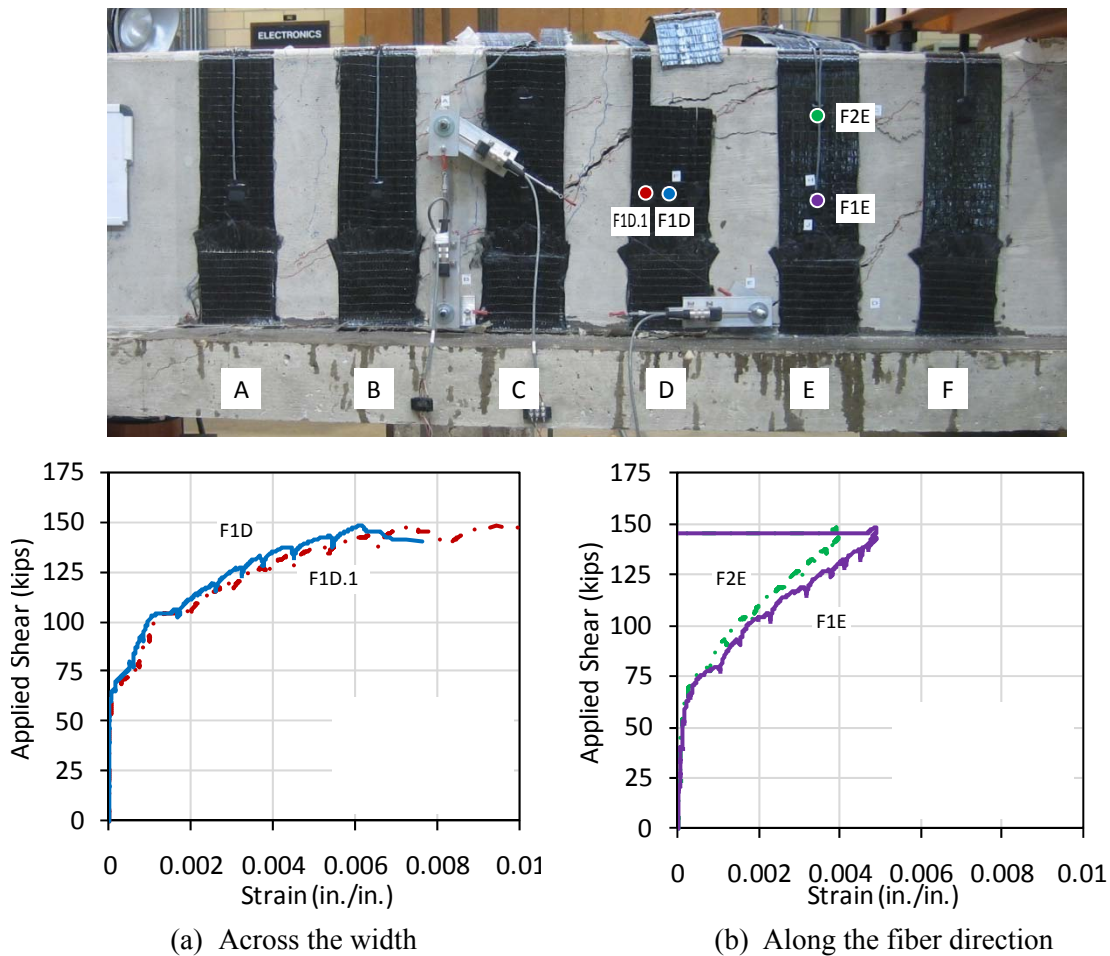
Figure 4-4 CFRP Strain responses of unbonded test (24-3-4)

Finally, there is no strain compatibility between the steel stirrup and the CFRP strip at the same location along the beam although the same crack passed through both materials because strain can be varied depending on the bond and the gages were not located at the crack. For this reason, all evaluations were the best estimate from monitored locations. Measured strains at critical crack were not uniform and all strips did not rupture at the same load. The rupture of one CFRP strip generally indicated that ultimate had been reached because the transfer of shear to the steel stirrups and other CFRP strips resulting in their rupture almost instantaneously. Therefore the shear contribution of the CFRP cannot be evaluated using the rupture strain and modulus of CFRP.

4.2.3   The Change in Critical Crack Angle (Load Path)

The critical crack angle is an essential parameter for evaluating the shear contribution of each material because the number of stirrups and strips are determined by this angle. Before cracking, the shear force is carried by the concrete, but once cracking occur, additional shear is carried by the reinforcement.

Depending on the amount of transverse reinforcement, the direction of the critical crack would change as shown in Figure 4-5 and Figure 4-6. In addition, this angle decreased as the applied load increased because more reinforcement was mobilized to carry the shear. Change in the crack angle is not important since the final critical angle at failure was used for evaluating the shear contribution of the transverse reinforcement. The number of steel stirrups and CFRP strips crossing the critical crack were used to determine the shear contributions. However, most design equations are based on depth/spacing ratio (d/s) to calculate the shear contributions. The difference in the crack angle and the critical section is a major reason for the measured shear contribution to be different from design shear contribution.
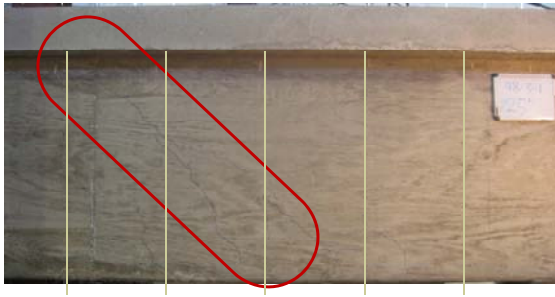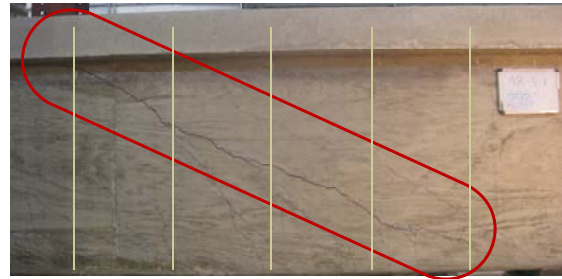
(a) Initial crack pattern (b) Final crack pattern

Figure 4-5 Crack patterns of different loading levels (48-3-1, no CFRP)
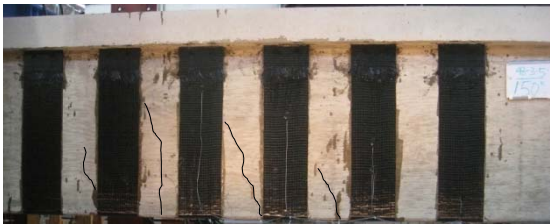
(a) Initial crack pattern (b) Final crack pattern

Figure 4-6 Crack patterns of different loading levels (48-3-5, CFRP)

4.2.4 Beam Displacement

The displacement at the loading point was monitored using LVDTs as described in Section 3.6.3.1. The responses from displacement showed no significant difference between tests because the failure modes were dominated by shear. As a result, up to failure deformations were small and caused by shear, not flexure.

4.2.5 Shear Strain

To evaluate shear strain, axial strains in three directions were measured in 24-in. depth beams. Because strain difference over the depth of the 48-in. with beam might distort the shear strain, more LVDTs were mounted to get the average strain at the middle of the 48-in. depth beam as described in Section 3.6.3.2. By using Mohr's circle, shear strain were calculated from three LVDTs. In addition, principal stresses and principal angle could be also calculated from Mohr's circle.

If the critical crack did not across the area where displacements were measured in Figure 4-7, the shear strain is not useful even though more LVDTs were used for

89

obtaining deformations. Nevertheless, in these beams where the critical crack pass through the instrumented region, shear strain were better indicators than beam displacements to represent overall response of beams failing in shear.
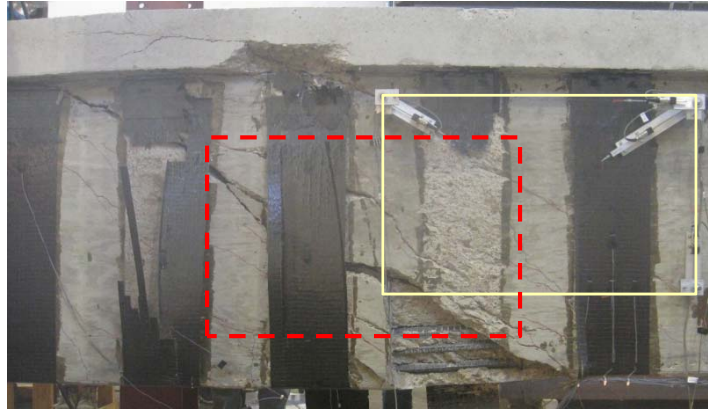
Figure 4-7 Relation between the location of shear measurement and critical crack

4.3   EVALUATION OF SHEAR CONTRIBUTION OF STIRRUPS, CFRP, AND CONCRETE

Monitored strains were used to estimate the shear forces resisted by steel stirrups, and CFRP strips that crossed the main shear crack. The critical crack angle of most tests was shallower than 45 degrees, which translated into more steel stirrups and CFRP strips contributing to shear resistance than estimated using ACI provisions.
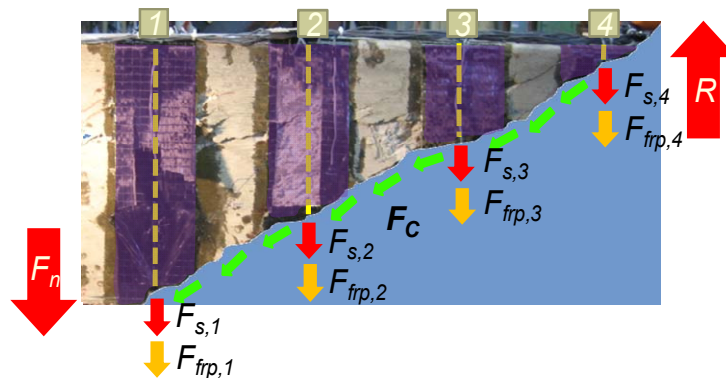
Figure 4-8 Concept for evaluating each shear contributions

As is common in RC elements, the strains in the stirrups varied depending on their distance from the shear crack. In this study, stirrup shear contribution was calculated from the gauge closest to the critical crack. Therefore, the estimate of stirrup shear contribution is likely to be lower than the actual contribution at lower load levels. A bi-linear stress-strain relationship with a flat yield plateau was assumed for the transverse steel. The estimated force in the transverse steel reinforcement crossing the critical shear section was calculated using Equation (4-1).

$$F_{s,i} = \begin{cases} A_s E_s \varepsilon_{s,i} & \varepsilon_{si} \leq \varepsilon_y \\ A_s f_y & \varepsilon_{si} > \varepsilon_y \end{cases} \tag{4-1}$$

where $F_{s,i}$ is the estimated force in the portion of reinforcement of interest, A_s is the cross sectional area of the transverse steel, E_s is the elastic modulus of steel, $\varepsilon_{s,i}$ is the measured strain and ε_y is the yield strain value of the transverse reinforcement.

For CFRP strips, a linear stress-strain relationship and a uniform strain distribution across the width of the CFRP strip assumed to simplify calculations. The estimated force in the CFRP crossing the critical shear section was calculated using Equation (4-2).

$$F_{f,i} = w_f \cdot t_f \cdot E_f \cdot \varepsilon_{f,i} \tag{4-2}$$

where $F_{f,i}$ is the estimated force in a portion of the CFRP, w_f is the width of the CFRP strip, t_f is the thickness of the CFRP strip, E_f is the elastic modulus of CFRP material and $\varepsilon_{f,i}$ is the strain determined from strain gauges attached to the CFRP strip.

The total estimated shear force resisted by the steel stirrups and CFRP strip can be calculated using Equations (4-3) and (4-4) where n is the number of stirrups or CFRP strips crossing the observed critical shear crack, respectively.

$$F_s = \sum_{i=1}^{n} F_{s,i} \tag{4-3}$$

$$F_f = \sum_{i=1}^{n} F_{f,i} \tag{4-4}$$

The total shear force resisted by the concrete can then be determined from equilibrium using Equation (4-5).

$$F_c = F - F_s - F_f \tag{4-5}$$

where F_c is the estimated shear force resisted by the concrete and F is the total shear force applied to the critical shear section.

Appendix E describes the detailed procedure and one example with specific values.
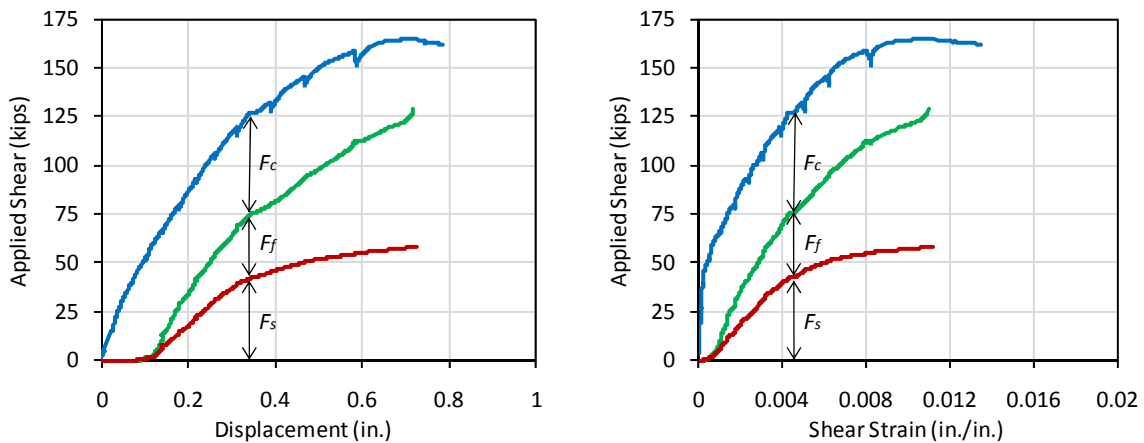
Figure 4-9 Typical response of steel, CFRP and concrete contributions to shear strength

Typical evaluations of material contributions to shear are plotted in Figure 4-9; (beam) displacement as discussed in Section 4.2.4 and shear strain as discussed in Section 4.2.5. The shear contribution of each material changed as loads increased. Before concrete cracking, most shear resistance came from concrete, but steel and CFRP contributions started to increase after concrete cracking.

Furthermore, the critical crack angle became shallower as the applied load increased. The points on the plot are based on the critical crack angle at failure by visual observation.

92

4.4 TEST RESULTS

4.4.1 24 in. Depth Beam Series I (a/d=3)

4.4.1.1 Test 24-3-2 (no CFRP, control)

Test 24-3-2 was conducted to determine the shear strength without CFRP. Failure occurred at a shear of 105 k and the mode of failure was yielding of stirrups. As seen in Figure 4-10, large shear cracks formed in the concrete member. The crack width was 0.03 in. at a shear of 84 k and over 0.05 in. at a shear of 90 k. As shown in Figure 4-11, after reaching a load of 90 k, shear strain increased dramatically.

(a) Front side

(b) Back side

Figure 4-10 Photos of both sides of test 24-3-2 after failure

93
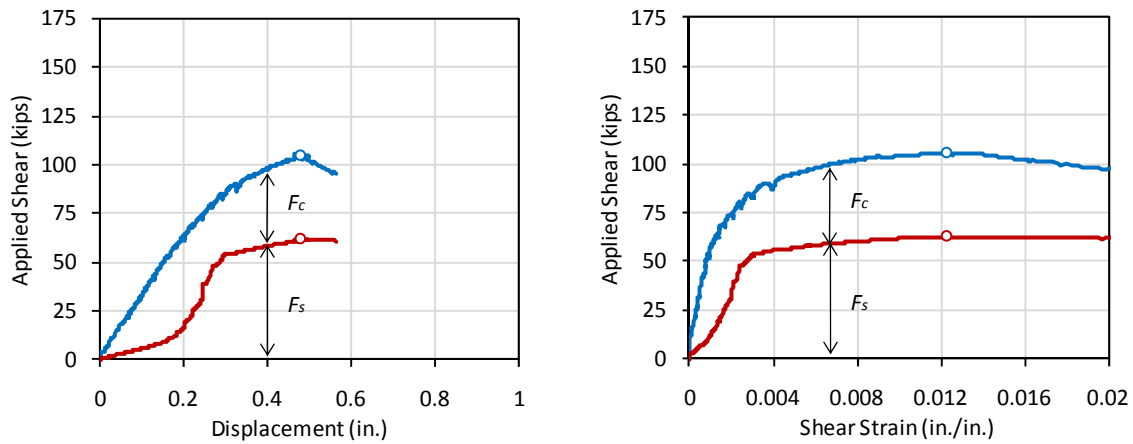
Figure 4-11 Component contribution to shear force vs. deformation response of 24-3-2

4.4.1.2 Test 24-3-1/1r (pre-cracked/strengthened)

The specimen was initially loaded to a shear of 74 k at which a stirrup yielded. Once yielding in the stirrups was observed, the specimen was unloaded and repaired with CFRP laminates.

Figure 4-12 shows the shear contributions of stirrups, CFRP and concrete plotted against beam displacement or shear strain. The calculations for evaluating shear contribution are described in Appendix E. The dotted lines show the response of test 24-3-1, i.e. response before strengthening.
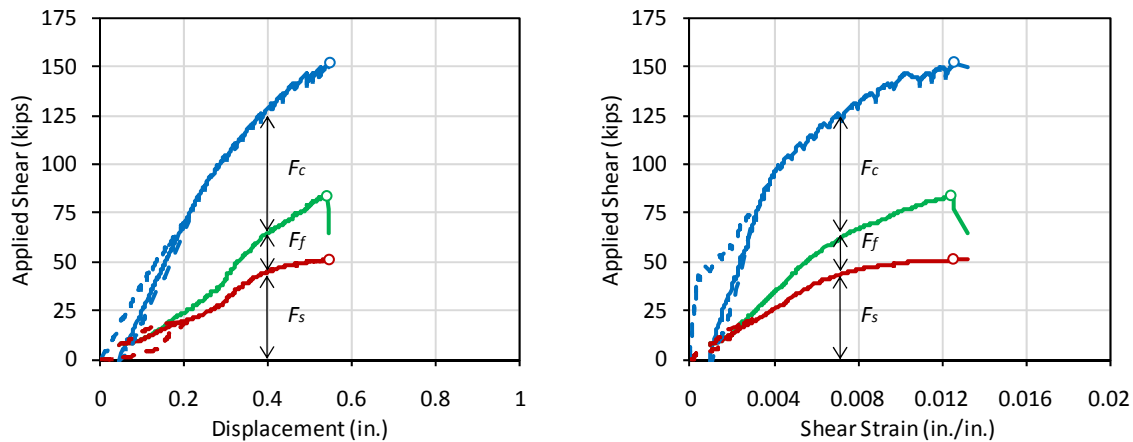
Figure 4-12 Component contribution to shear force vs. deformation response of 24-3-1/1r

94

The response of the beam displacement was nearly linear up to failure. At a shear of 50 k, the slope of the shear strain response changed, indicating that a shear crack formed. Prior to shear cracking, flexural cracks occurred near the loading point, but the change in slope of the displacement graph was insignificant. There were a small residual displacement and shear strain from the initial loading in Test 24-3-1. However, the unloading and reloading curves are almost identical until the same level of shear is load after strengthening with CFRP strips. After that loading level was increased, the shear contribution of CFRP increased. In addition, the shear contribution of CFRP continued to increase although the shear contribution of steel was nearly constant once all stirrups across the critical crack yielded.

As shown in Figure 4-13, failure of the specimen strengthened after cracking was initiated by a combination of rupture of the CFRP strips and the CFRP anchors.

(a) Front side
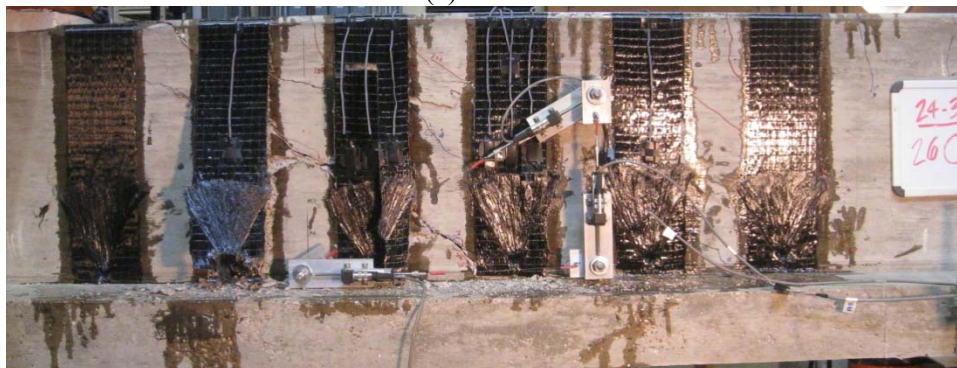
(b) Back side

Figure 4-13 Photos of both sides of test 24-3-1R at ultimate load

As the CFRP strips and some CFRP anchors ruptured, large cracks formed in the specimen, particularly in the flange of the concrete member. Shear failure occurred at a shear of 152 k. The maximum recorded CFRP strain was 0.0123 before the rupture of CFRP strip. This value was greater than the manufacturer's ultimate tensile strain value of 0.0105. The beam carried shear of 102 k immediately after rupture of the first strip.

Table 4-3 shows the comparison between experimental and calculated (ACI 440.2R-08) shear contributions. Shear strengths from test evaluation were higher for all tests than strengths estimated using ACI 440.2R-08, although the manufacturer's reported rupture strain of CFRP strips (0.01) was used in the calculations.

The shear contribution of CFRP at ultimate load was 33 k, which is 7 k greater than estimate. However, the ratio of 1.25 in CFRP shear contribution might be low because the ratios of concrete and steel shear contribution were 2 and 1.6 respectively.

Table 4-3 Comparison between shear estimates from equation and test in 24-3-1r

V (kips) from DESIGN EQ. (a)				F (kips) from TEST (b)				RATIO (b)/(a)			
V_c	V_s	V_f	V_n	F_c	F_s	F_f	F_n	F_c/V_c	F_s/V_s	F_f/V_f	F_n/V_n
33	31	27	**91**	68	51	33	**152**	2.0	1.6	1.3	**1.7**

4.4.1.3   Test 24-3-3 (no bond, poor installation)

Test 24-3-3 was conducted to determine the shear contribution of anchored CFRP strips when there is no bond between the CFRP and concrete substrate. A clear plastic wrap was used to prevent bond, but it was difficult to install CFRP strips and anchors under this condition. Because the clear plastic wrap did not adhere to the concrete, large gaps formed between the concrete substrate and plastic wrap as shown in Figure 4-14.

96

Figure 4-14 Poor application of CFRP strip and anchor due to plastic wrapping
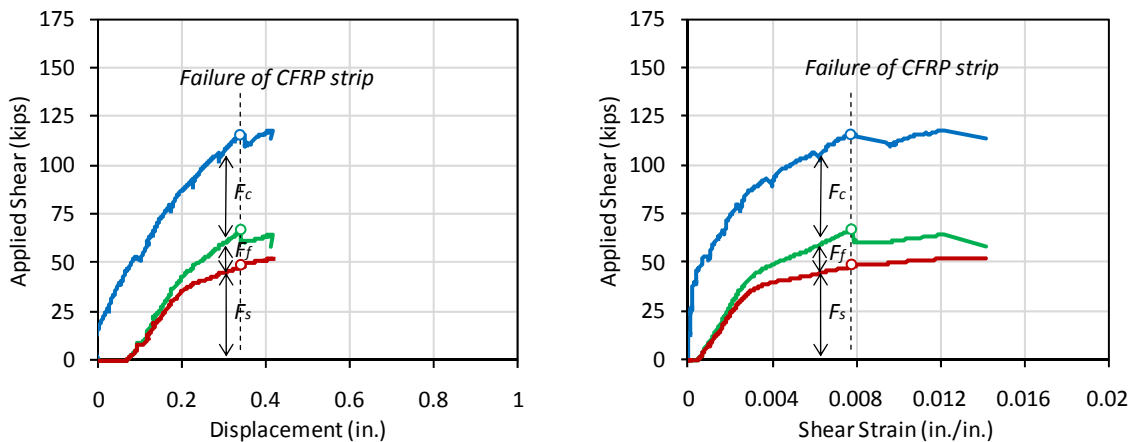
Figure 4-15 Component contribution to shear force vs. deformation response of 24-3-3

As shown in Figure 4-15, at the shear strain of 0.008, shear decreased from 115 k to 110 k and CFRP contribution also dropped from 19 k to 11 k. At that time, the maximum strain at F1D was 0.0087, which was the maximum measured CFRP strain during test 24-3-3. In addition, strains along and across the same CFRP strip decreased after gage F1D failed. It is clear that strip D lost some capacity at a shear of 115 k. However, failure occurred at a shear of 118 k due to fracture of the CFRP anchors in the strip D and E. After losing the capacity of strip D, most of the force in strip D was redistributed to strip E and the shear was dropped to 109 k at rupture of strip E. From this test, the poor installation of the CFRP strips with poorly placed (non-straight) CFRP

laminates and CFRP anchors resulted in the reduction in the overall capacity of the member.
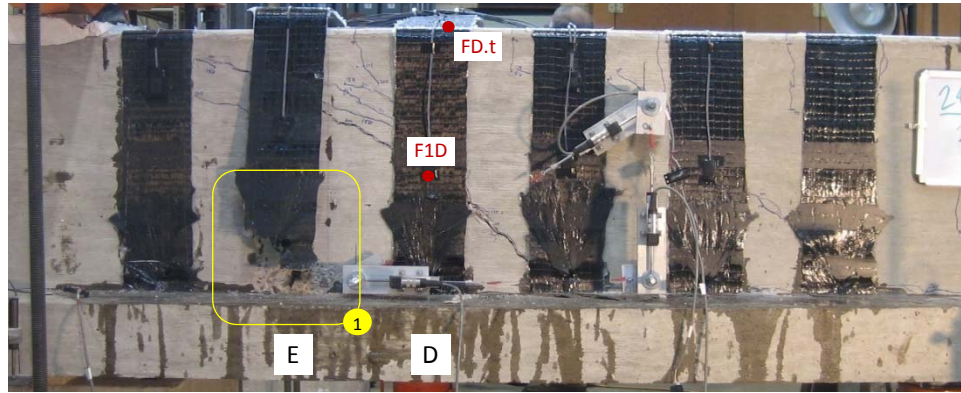
(a) Front side
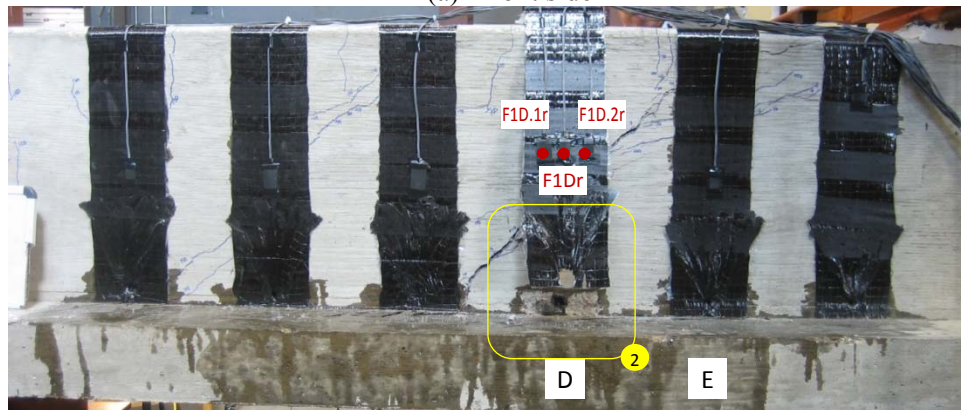
(b) Back side

Figure 4-16 Photos of both sides of test 24-3-3 at ultimate load
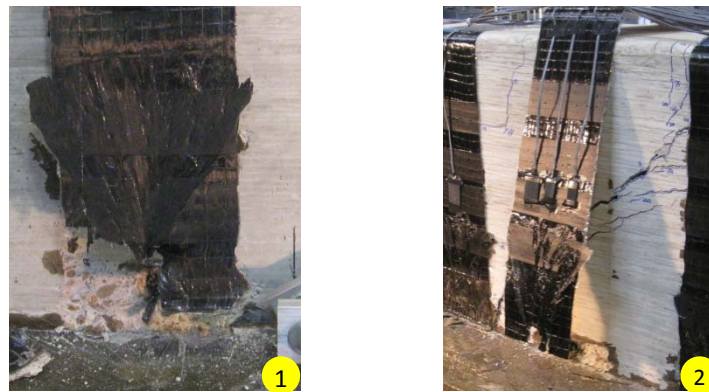
Figure 4-17 Fracture of CFRP Anchor in test 24-3-3

4.4.1.4   Test 24-3-4 (no bond, proper installation)

Because Test 24-3-3 failed by premature CFRP anchor fracture due to the poor installation, another test with the same parameters was conducted. Instead of plastic wrap, a clear plastic shelf liner with adhesive on one side was adhered to the surface of the concrete before installation of the CFRP for simulating the condition of no bond as shown in Figure 4-18.
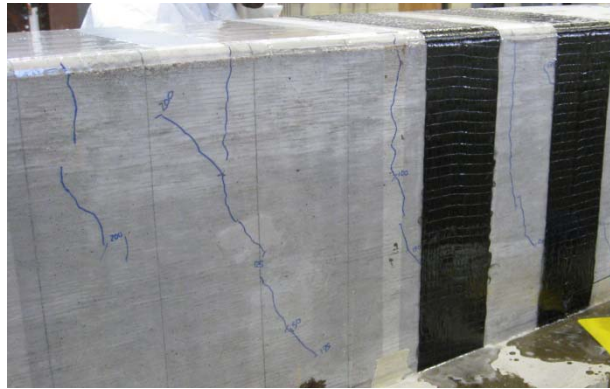
Figure 4-18 CFRP installation without bond using adhesive shelf liner

The CFRP anchor detail was modified and the modified detail was used for all tests except 24-3-1r, 24-3-3, 24-1.5-1r. The modifications of anchor details are as follows. 1) the area of CFRP anchor was changed from 1.5 to 2 times of the area of the CFRP strip, 2) two additional patches were attached over the CFRP anchors, 3) bend radius was increased from 0.25 in. to 0.5 in.
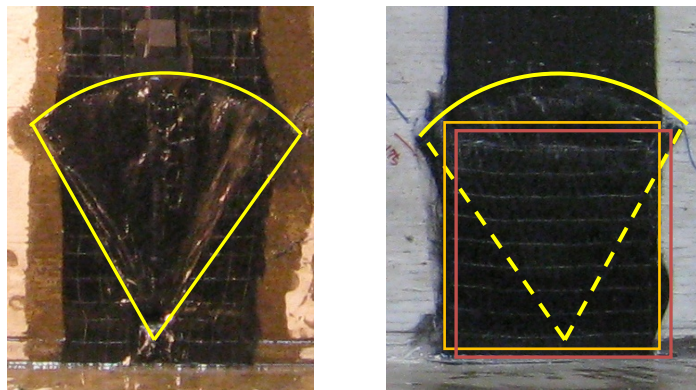
Figure 4-19 Photos of CFRP anchor detail before and after modification

Because the strain gage data from the CFRP strips was considered to be unreliable after the peak load was reached (Point 1 in Figure 4-20), the shear contributions of the steel, CFRP, and concrete were evaluated at Point 1 rather than Point 3. Strip E (Point 2) ruptured at a shear of 148 k and the shear dropped to 139 k. However, failure occurred at a shear of 152 k with rupture of additional CFRP strips (C & D). No CFRP anchors failed as shown in Figure 4-21.

The maximum reported CFRP strain was 0.0126. The maximum crack width was 0.05 in. at a shear of 94 k and was very large when peak load was reached and it was too dangerous to measure cracks at that point.
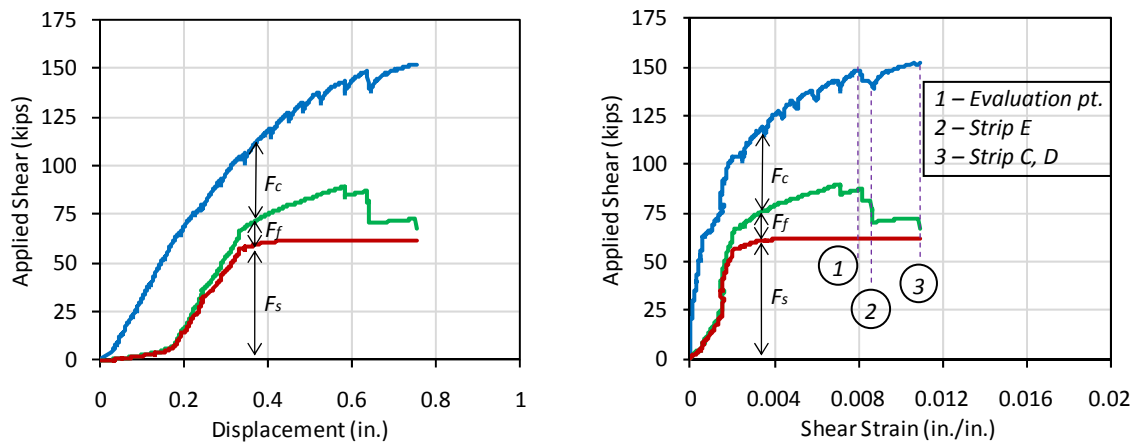
Figure 4-20 Component contribution to shear force vs. deformation response of 24-3-4
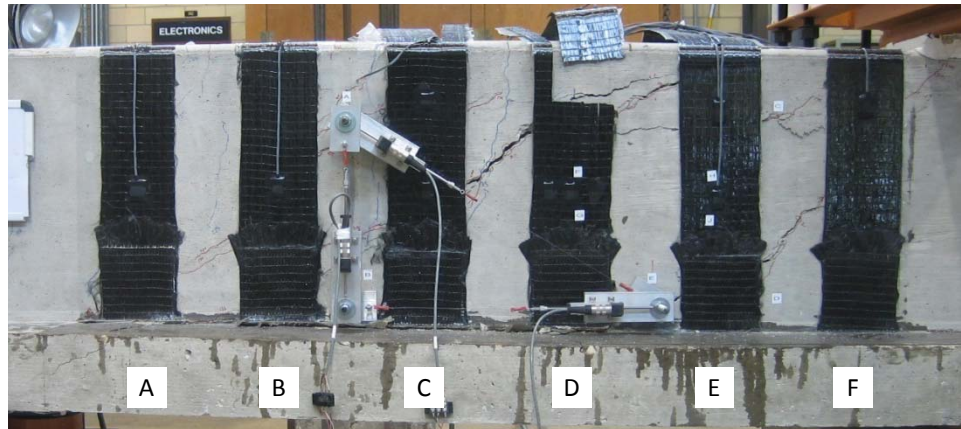
(a) Front side
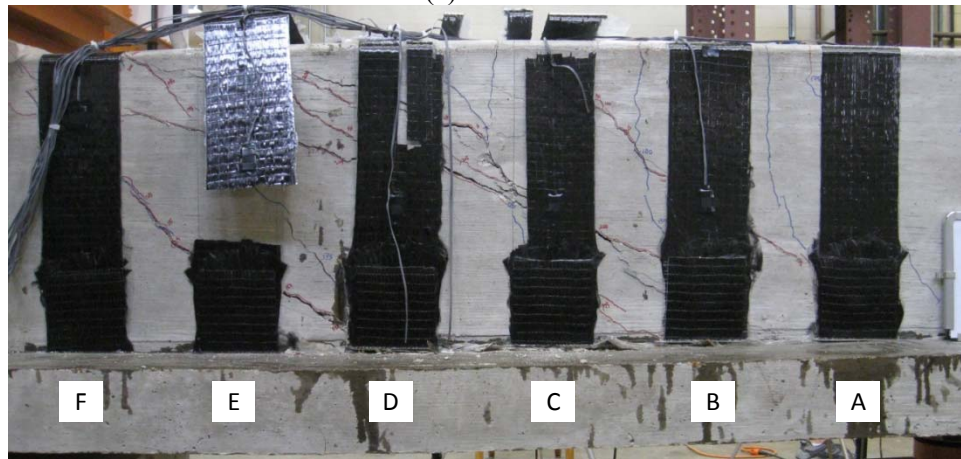
(b) Back side

Figure 4-21 Photos of both sides of test 24-3-4 at peak load

4.4.1.5 Test 24-3-5 (laminate B)

Test 24-3-5 and test 24-3-6 was conducted to evaluate the validity under various ranges of mechanical properties. Although the CFRP laminates were fabricated from carbon fibers that have similar properties, the properties of the carbon fibers and the polymer binder together would differ according to the volume fraction of fiber. Although there is significant difference in elastic modulus, ultimate tensile strain and thickness of laminate A, B and C, the stiffness and capacity of the two laminates were close each other as shown in Table 4-4. However, the anchor hole area was changed to accommodate the thickness of laminate B.

Table 4-4 CFRP properties of laminates A and B

	Laminate level			Strip level	
	A (in^2)	E (ksi)	ε_{fu}	k (k/in) (=EA/L)	P (kips) (= $EA\varepsilon_{fu}$)
Laminate A	0.011	14800	0.0105	162.8	1.71
Laminate B	0.02	8200	0.01	164	1.64

$A = t \cdot w =$ (thickness) × (width) , w = 1 in., L=1 in. (assumed for evaluating k, P)
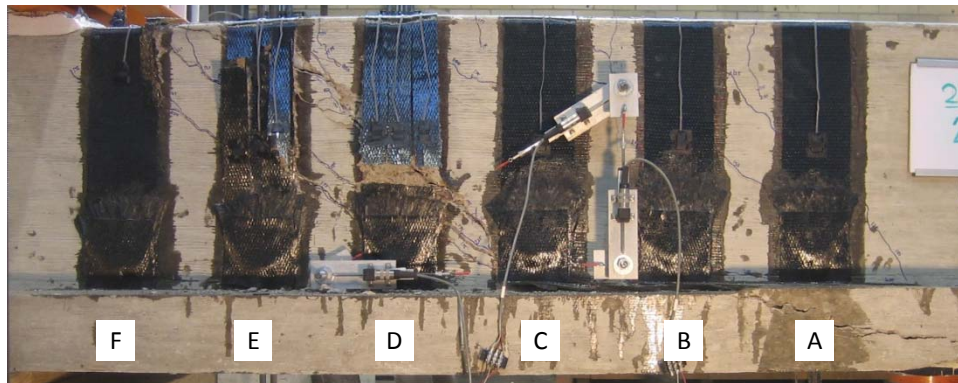
(a) Front side
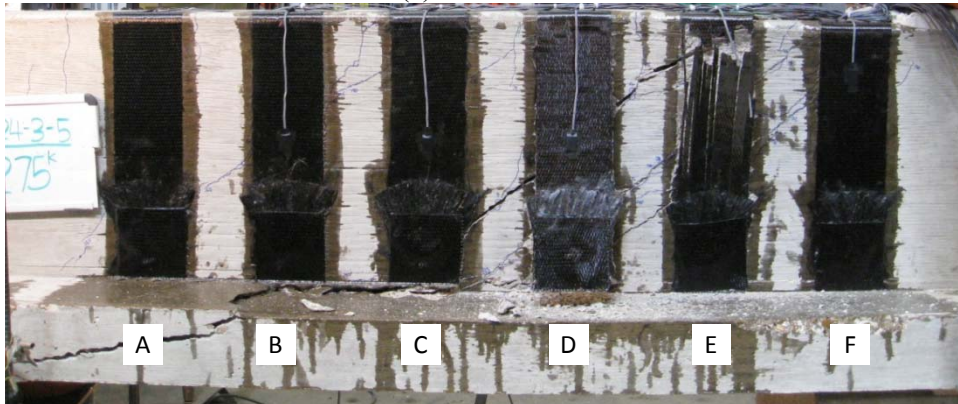
(b) Back side

Figure 4-22 Photos of both sides of test 24-3-5 at peak load

Figure 4-23 shows the overall response of 24-3-5. Failure occurred at a shear of 145 k when strips D and E ruptured.
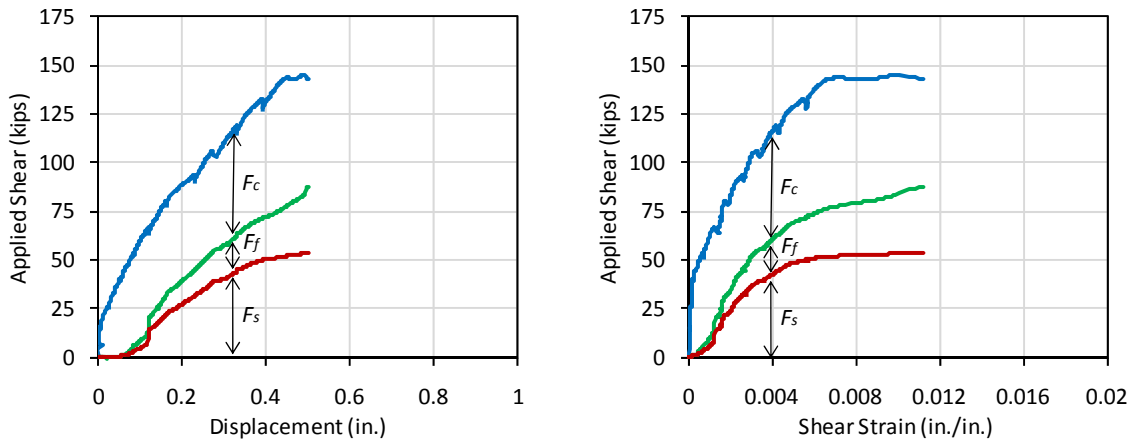
Figure 4-23 Component contribution to shear force vs. deformation response of 24-3-5
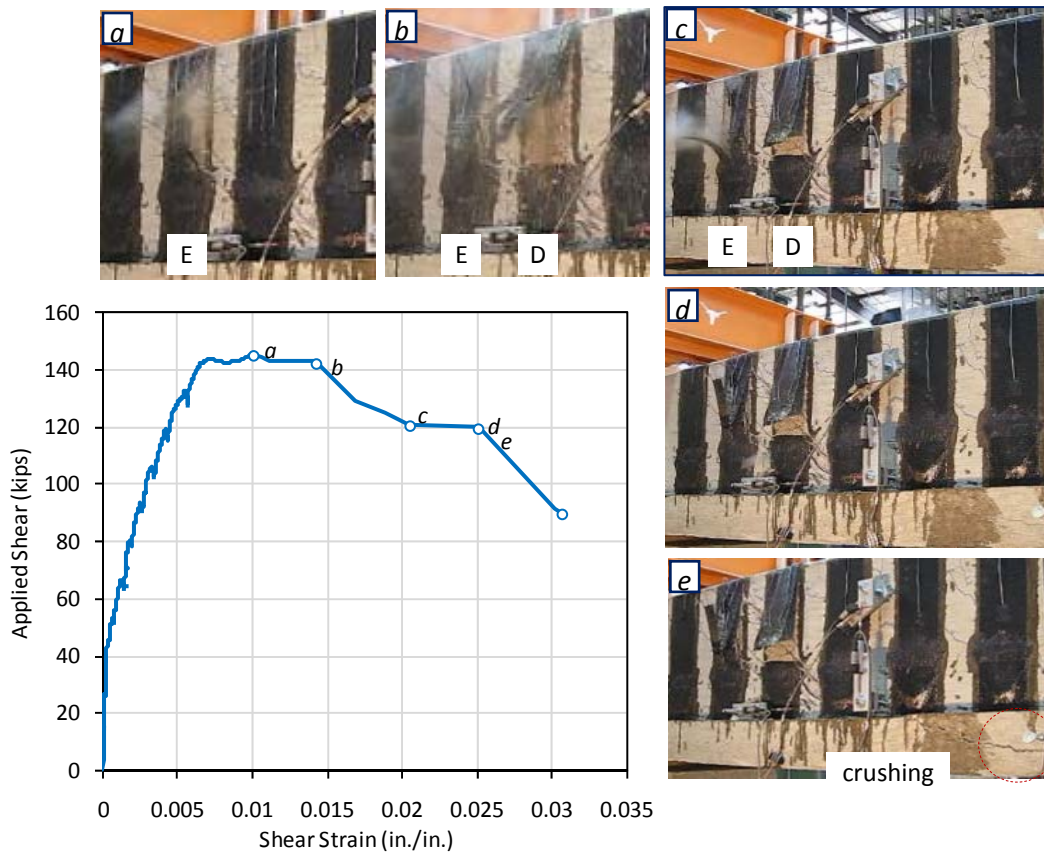
Figure 4-24 Failure sequence in test 24-3-5

Figure 4-24 shows the images captured from video at failure; (a) The front side of strip E partially ruptured and shear force decreased to 143 k. (b) Shear force was dropped to 134 k when strip D ruptured. (c) Strip E totally ruptured right after that. Finally, shear force was dropped to 90 k with (d) fracture of CFRP anchor in the back side of strip D and (e) concrete crushing. The time durations were 8 sec. for (a)-(b), 3 sec. for (b)-(c), 6 sec. for (c)-(d), and 1 sec. for (d)-(e). Although these time durations might depend on the loading rate, the relative duration between sequences still is meaningful. The maximum reported CFRP strain was 0.0115.

4.4.1.6 Test 24-3-6 (laminate C)

Test 24-3-6 was conducted with laminate C which was applied using dry layup procedure. (This procedure is described in Appendix A)

The manufacturer's sheet of laminate C included rupture strain and elastic modulus for the carbon fiber only. Based on this information, the stiffness and ultimate strength of laminate C were twice those of laminate A as shown in Table 4-5.

Table 4-5 Comparison of stiffness between laminate A and laminate C

	Laminate level			Strip level	
	A (in^2)	E (ksi)	ε_{fu}	k (k/in) ($=EA/L$)	P (kips) (= $EA\varepsilon_{fu}$)
Laminate A	0.011	14800	0.0105	162.8	1.71
Laminate C	0.0065	33000	0.0167	214.5	3.58

$A = t \cdot w =$ (thickness) × (width), w = 1 in., L=1 in. (assumed for evaluating k, P)
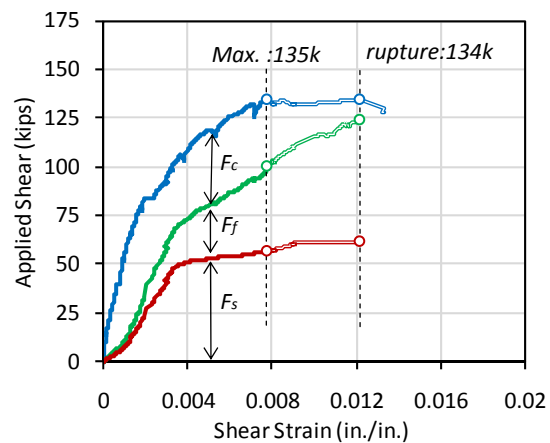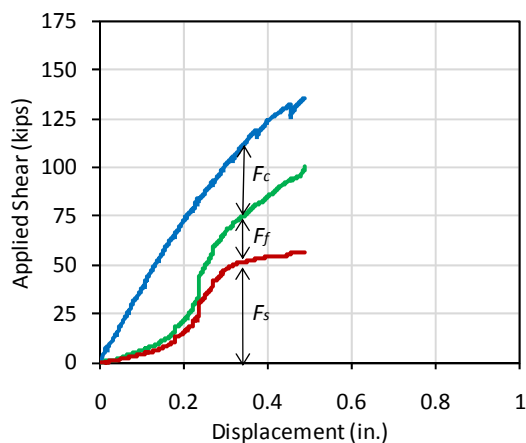
Figure 4-25 Component contribution to shear force vs. deformation response of 24-3-6

Shear failure was initiated by fracture of the CFRP anchors. After reaching the maximum shear of 135 k, a crack extended into the flange of the T-beam. The shear decreased to 132 k. Then shear increased slightly up to 134 k when CFRP anchor in the strip C ruptured and the load was dropped to 128 k. The difference in shear strain between shear at maximum and shear at failure was 0.0045 (= 0.0123−0.0078). After the explosive rupture of strip D as seen in Figure 4-27, the shear was dropped to 103 k.

CFRP shear contribution in this test was higher than those of others at same level of strain due to a higher elastic modulus or specified in manufacturer's sheet. The CFRP shear contribution continued to increase after reaching maximum capacity and accounts for the capacity being sustained as the concrete contribution decreases as the crack width increased. In other words, the CFRP shear contribution did not reach a peak when the beam reached the peak capacity. The maximum recorded strain in the CFRP was 0.0078 at the peak shear, whereas at fracture of CFRP anchor, the strain reached 0.0114. Therefore, the upper limit of strain in the CFRP in shear applications should be set to prevent over-estimation of the CFRP shear contribution.

The maximum capacity of 24-3-6 was 29 k less than the estimate using design equations. In addition, the shear contribution of each material was totally different between at maximum and at rupture. Steel and CFRP shear contribution increased while sustaining a load nearly equal to peak capacity. Test 24-3-6 is a good example of the maximum capacity of each material not being developed at the same time and allows that the maximum capacity is not the equal to the sum of the maximum capacity of each material.

Table 4-6 Comparison between shear estimates from equation and test in 24-3-1r

	V (k) from DESIGN EQ. (a)				F (k) from TEST (b)				RATIO (b)/(a)			
	V_c	V_s	V_f	V_n	F_c	F_s	F_f	F_n	F_c/V_c	F_s/V_s	F_f/V_f	F_n/V_n
24-3-1r	33	31	27	**91**	68	51	33	**152**	2.04	1.63	1.25	**1.67**
Max 24-3-6	34	31	56	**120**	57	42	37	**135**	1.69	1.35	0.66	**1.13**

Rupture					10	61.6	62.3	**134**	0.30	1.98	1.12	**1.11**
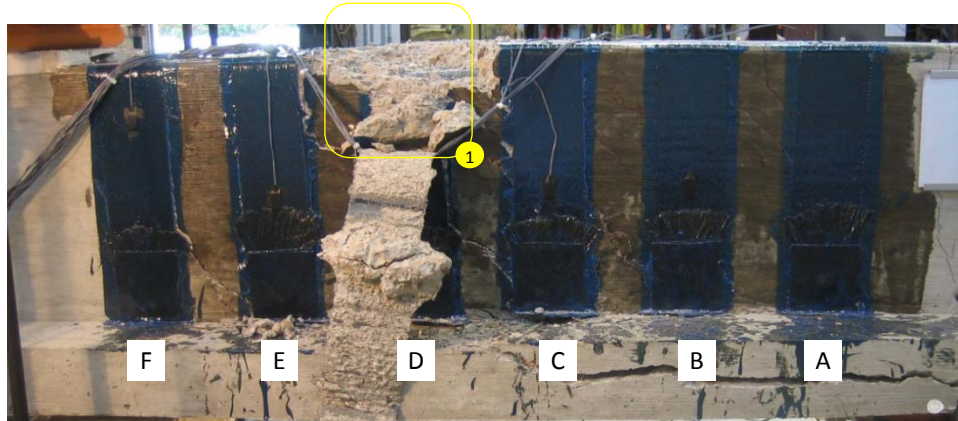
(a) Front side
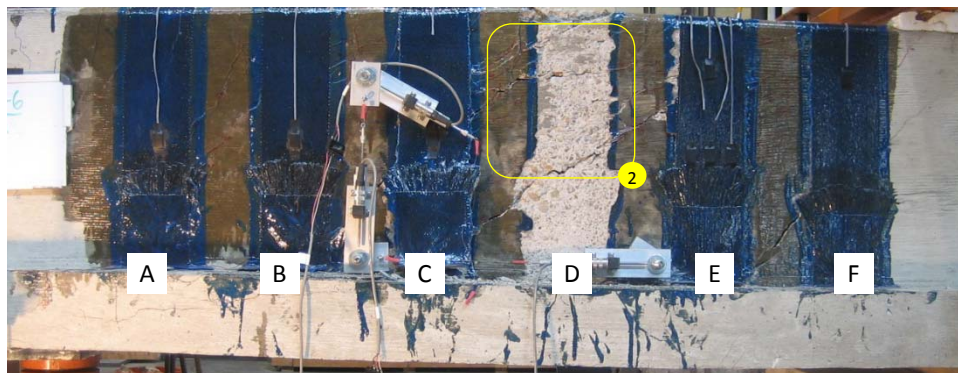
(a) Back side

Figure 4-26 Photos of both sides of test 24-3-6 at failure

Figure 4-27 Photos of explosive rupture of strip D

106

4.4.1.7   Test 24-3-7 (continuous sheet)

Test 24-3-7 was conducted with a continuous sheet resulting in twice the amount of material as in test 24-3-1r (same amount of material as test 24-3-8). As shown in Figure 4-28, the number of CFRP anchors also was doubled to transfer the stress in the CFRP strip because the typical CFRP anchor in 24-in. beams was designed for a 5-in. wide strip. Therefore, individual anchor dimension still remained same. The overlapping width between adjacent anchors was 1 in.

(a) Typical CFRP strip configuration   (b) Continuous CFRP sheets (24-3-7)
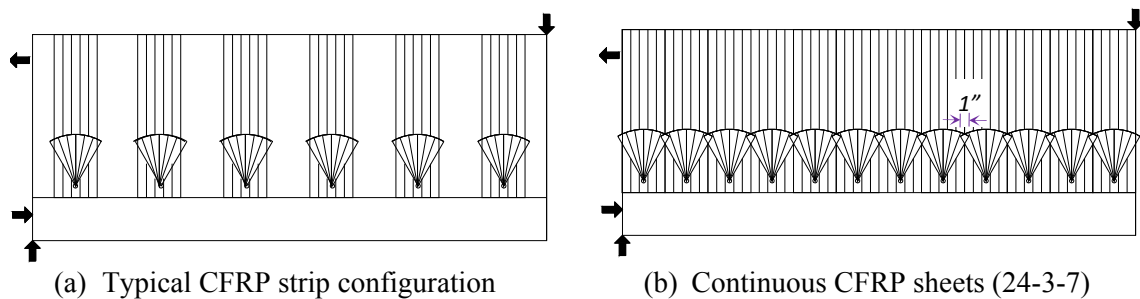
Figure 4-28 CFRP strip detail between continuous sheet and typical layout

Because the CFRP sheet covered all concrete surfaces, there is no way to observe cracking during the test. Therefore, an infra-red camera was used to monitor the crack pattern and the debonding of CFRP.

Failure occurred at a shear of 165 k and was initiated by partial rupture of the CFRP strip. This rupture was seen by visual inspection and in the image from the infra-red camera. As shown in Figure 4-30, a rupture of CFRP was higher temperatures than other locations and the location at debonding CFRP was lower temperature. The measured maximum CFRP strain was 0.014 from F1D.

After reaching maximum load, there was no sudden load drop and no additional ruptures in the CFRP, but load decreased slowly and steadily. A crack at the corner of web and flange where was the end of the CFRP sheet was seen and this crack extended into the flange of T-beam.

107
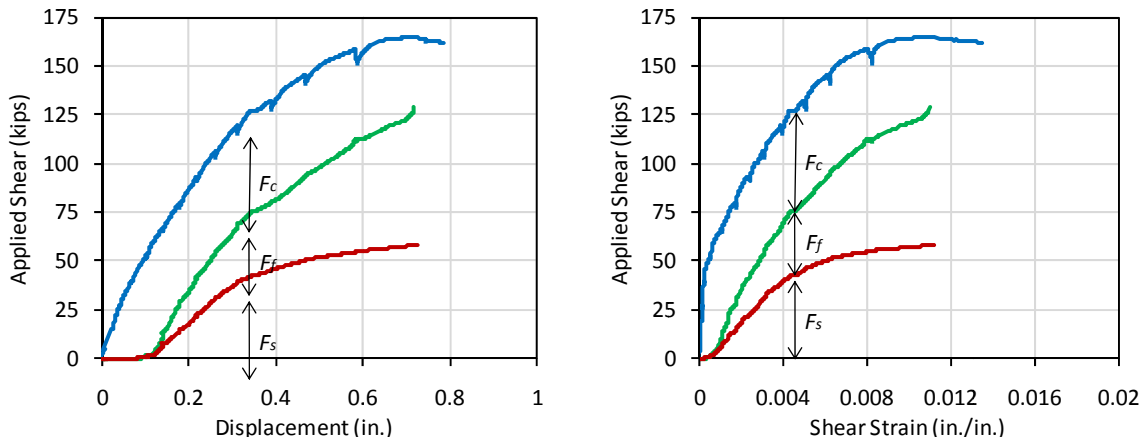
Figure 4-29 Component contribution to shear force vs. deformation response of 24-3-7
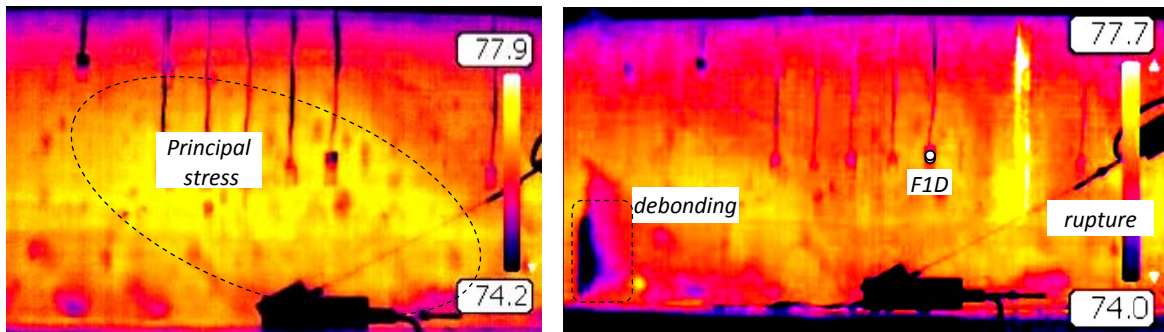
(a) At cracking load

(b) Maximum load

Figure 4-30 Images from infra-red camera in test 24-3-7 (front side)
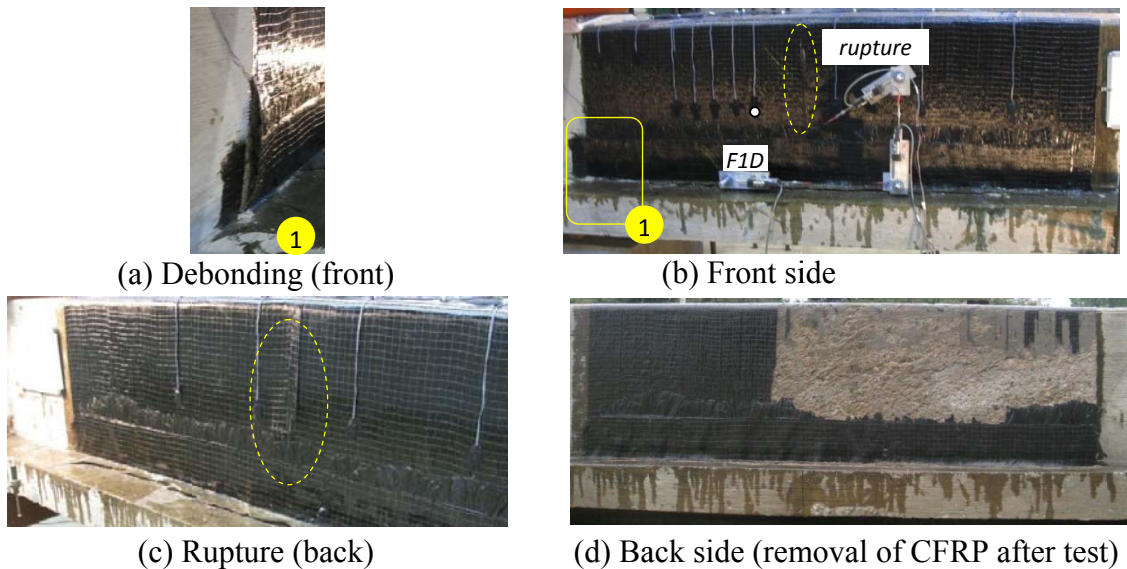
(a) Debonding (front)

(b) Front side

(c) Rupture (back)

(d) Back side (removal of CFRP after test)

Figure 4-31 Photos of both sides of test 24-3-7

4.4.1.8 Test 24-3-8 (2 layers)

Test 24-3-8 had two layers of CFRP strip to evaluate the CFRP shear contribution according to the amount of CFRP material. In addition, the effect of the CFRP layout with the same amount of material was examined same the amount of CFRP material in 24-3-8 was the same as that in 24-3-7. These comparisons will be discussed in Section 4.5.4 and 4.5.9.1.

The area of CFRP anchor was also doubled, so the number of CFRP anchor remained the same as that of specimens having strips with one layer of CFRP.
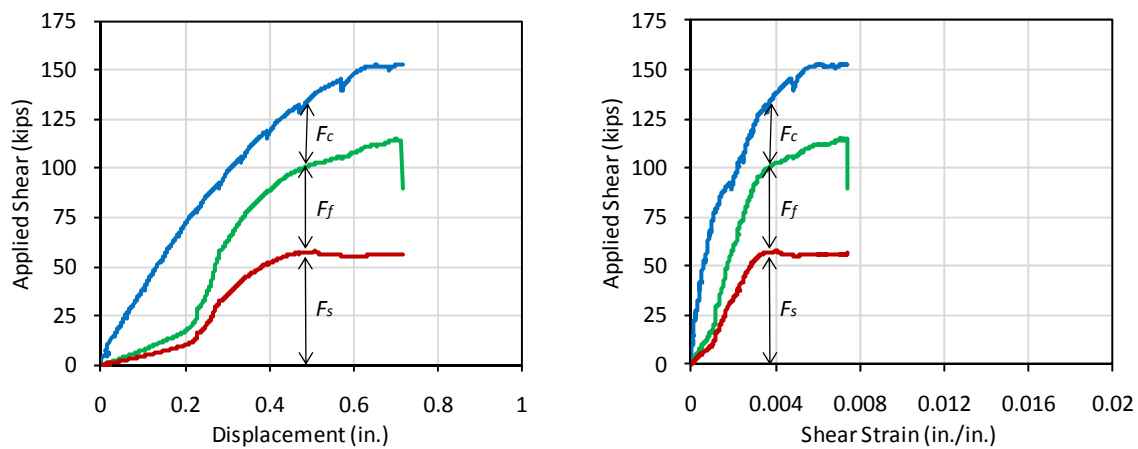
Figure 4-32 Component contribution to shear force vs. deformation response of 24-3-8

The maximum shear capacity of this test was 153 k, which is slightly greater than the capacity of test 24-3-1r (152 k). Failure mode in this test was fracture of a CFRP anchor in strip D that was located at a critical shear crack as shown in Figure 4-34. In addition, a large crack extended to the flange on front side where the CFRP anchor fractured. There was less damage on the back side. A shear of 133 k was remained after fracture of the CFRP anchor. The recorded maximum strain in the CFRP was 0.0072 (F1D.1) indicating that CFRP strips did not reach their maximum capacity. Improvements in CFRP anchor details for multi-layer strips will need to be considered and be discussed in Chapter 6.
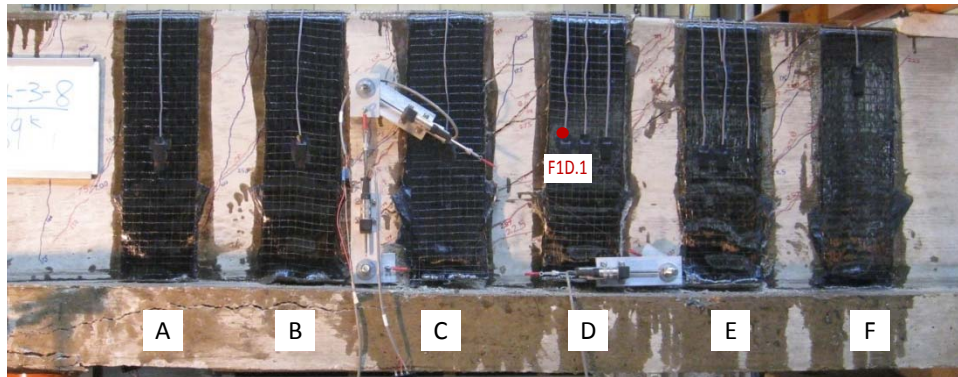
(a) Front side
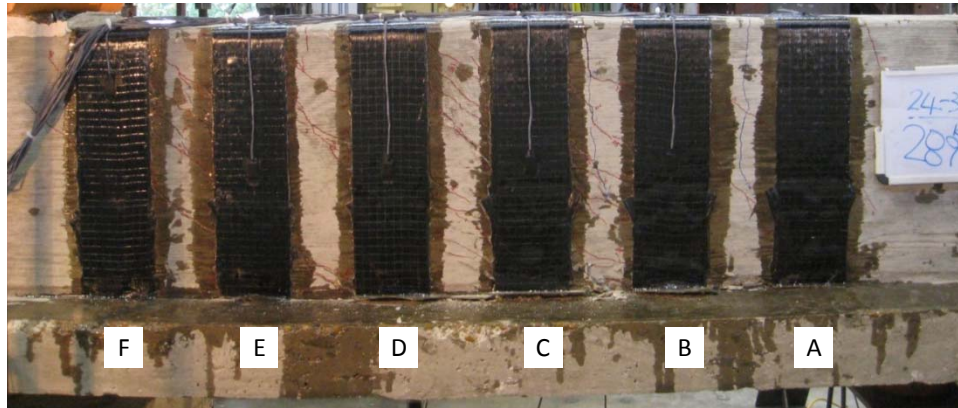
(b) Back side

Figure 4-33 Photos of both sides of test 24-3-8 at ultimate load

Figure 4-34 CFRP anchor failure of front side in 24-3-8

4.4.1.9 Test 24-3-9 (no anchor)

Test 24-3-9 was conducted to demonstrate the ineffectiveness of CFRP sheets with no CFRP anchors. All parameters except CFRP anchors were the same as that of 24-3-1r.

From this test, the debonding process could be easily observed. As shown in Figure 4-35, the maximum capacity occurred when was determined by de-bonding of the CFRP laminates. The maximum recorded strain in the CFRP was 0.0048 (F1E) at a shear of 101 k. The maximum shear capacity was 109 k; only 4 k greater than the capacity of the unstrengthened control test (24-3-2). The shear dropped to 99 k after debonding.

The sequence of crack formation was interesting. First, crack occurred between strip B and D. Another shear crack occurred between strip C and E. Finally, another crack occurred between strip C and F and formed the critical crack.
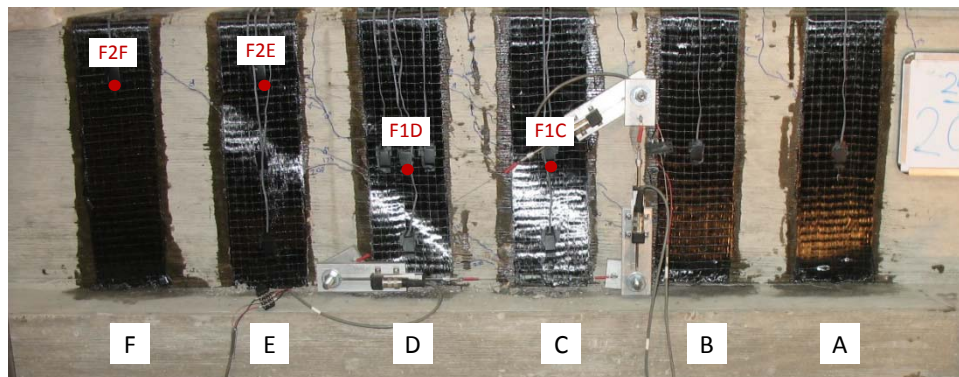
(a) Front side
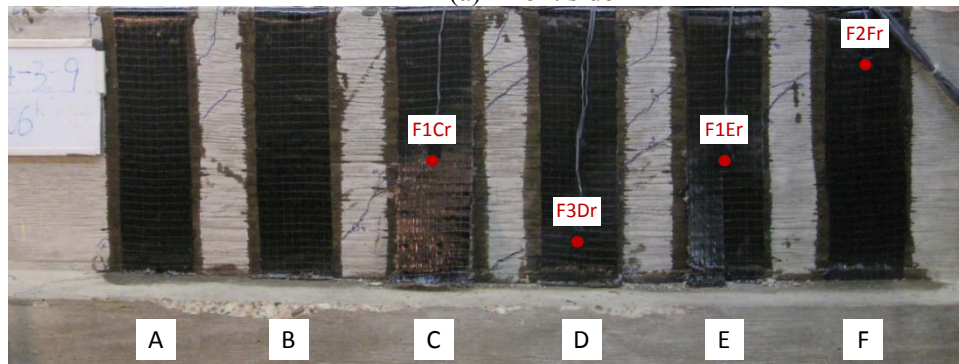
(b) Back side

Figure 4-35 Photos of both sides of test 24-3-9 at ultimate load

Because the CFRP strip with an end close to crack did not have enough bond length, this strip was vulnerable to early debonding. Therefore, some strips debonded and lost capacity before the beam reached maximum capacity.

As shown in Figure 4-36, the maximum CFRP contribution was 17 kips at a shear of 101 kip. In addition, CFRP shear contribution was 13 kips when reaching maximum shear on the beam. The steel contribution kept increasing after the composite member passed the peak load. It implied that the stirrups contributing to the shear capacity might not yield when the CFRP started to debond and reached its maximum capacity. Therefore, shear strengthening with CFRP without anchors could be effective until debonding, but the stirrup contribution might decrease because steel stress redistribution would not be expected until debonding. The maximum crack width was 0.05 in. at a shear of 105 k.

Figure 4-36 Component contribution to shear force vs. deformation response of 24-3-9

Figure 4-37 shows the strain response of each strip crossing the critical crack and a photo at the time of debonding. From the strain data and visual observation during the test, the debonding sequence can be evaluated; (a) First, the back side of strip D started to debond at a shear of 85.5 k based on gage F3Dr. (b) At a shear of 101 k, the front side of strip D was totally debonded from the crack to the end of the strip. The strains in the front side of strip D were different from each other until a shear of 85 k was reached. Strains were uniformly distributed until the strip D totally debonded. (Figure 4-37 (c), (d), (e), (f)) At maximum load, both sides of strip C and E debonded.
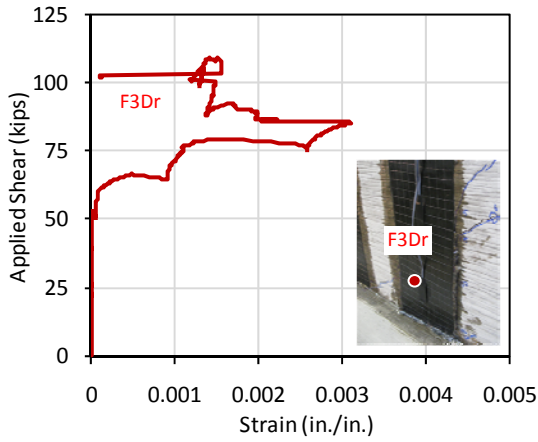
(a) Strip D on back side
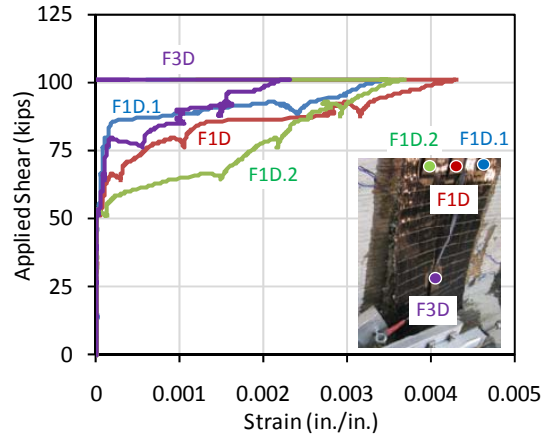
(b) Strip D on front side
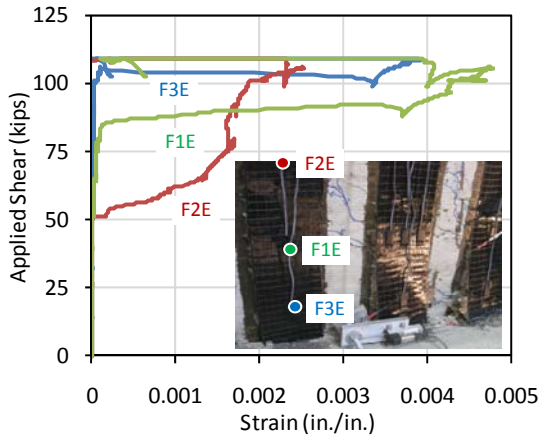
(c) Strip E on front side
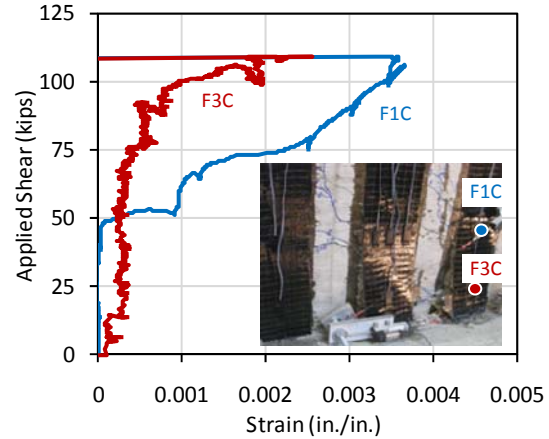
(d) Strip C on back side
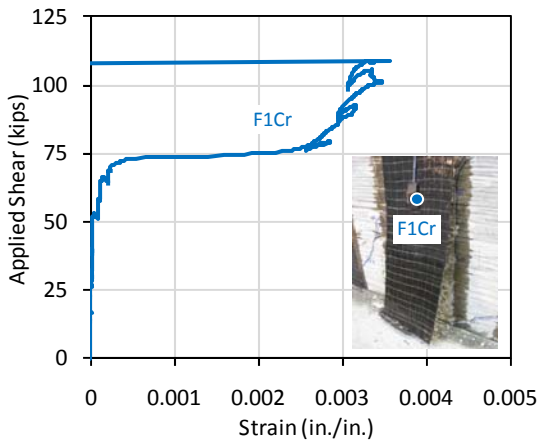
(e) Strip C on back side
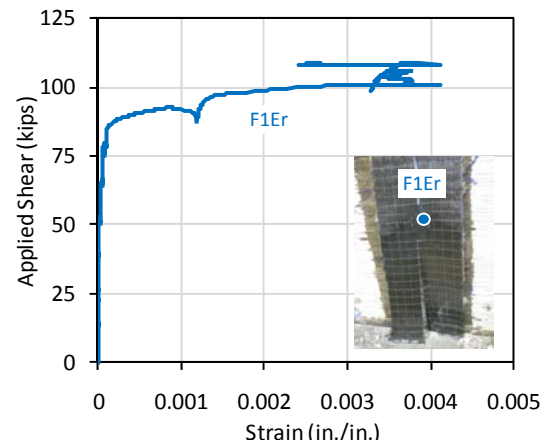
(f) Strip E on back side

Figure 4-37 Strain Response of critical CFRP strips (C, D and E)

113

Because the end of strip D was closer to the crack, the debonding process occurred earlier than the other strips. On the other hand, the critical crack were located at the middle of the strips C and E, so debonding started near the crack and extended into both directions. As the debonded region increased, the effective bond length in the direction of the strip end was insufficient. The strip then debonded suddenly. It is similar to the rubber band extension because the more the rubber is elongated, the more energy stored and the impact is more severe when it is released. It is noted that the dobonding at Strip C and strip E were not triggered from the same crack. Two parallel cracks were involved in the failure mechanism.
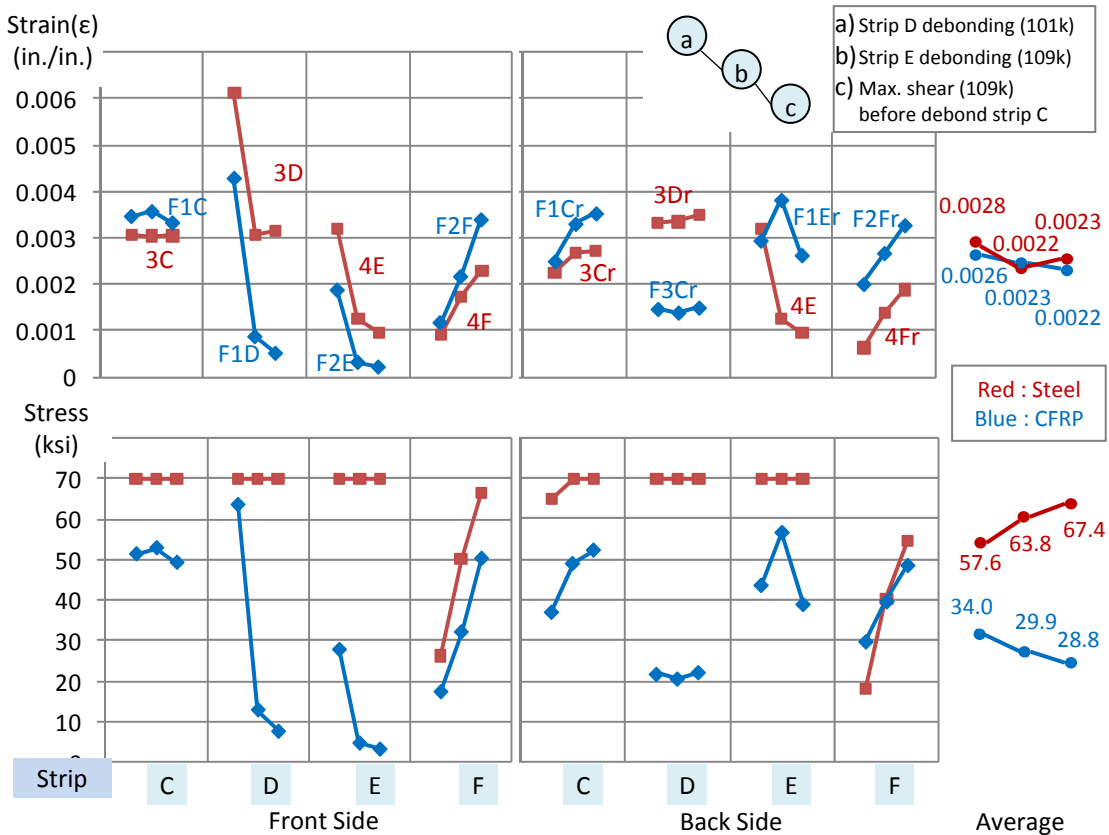
Note.
1) Three points in same strip are shown the variation according to the different loadings ((a)-(b)-(c)) shown in Figure 4-36
2) The strains are sensitive to the relative location from the crack locations.
3) The locations of FRP gages and stirrups gage are shown in Figure 4-35 and Figure 4-39 respectively.

Figure 4-38 Strain / stress of steel and CFRP across the critical crack at selected points

114
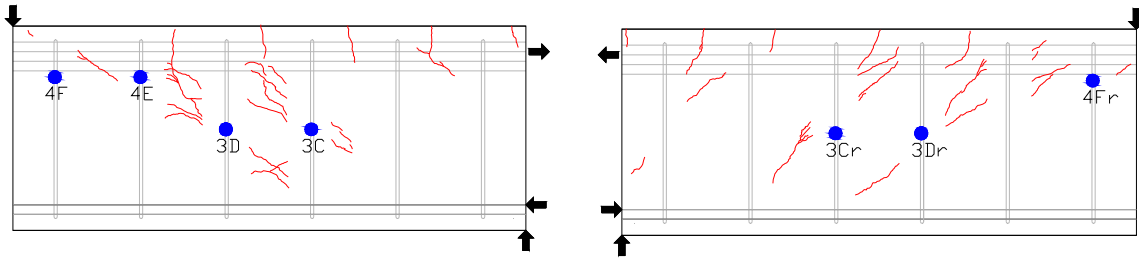
Figure 4-39 Crack pattern and the location of stirrup strain gages across critical crack

Figure 4-38 shows the strain and stress distribution in the stirrups and CFRP strip crossing the critical crack of both sides at three different loading stages. The average strain and stress in the stirrups CFRP strips are also shown. (The gage locations are shown in Figure 4-35 and Figure 4-39) The maximum CFRP contribution was at a shear of 101 k (point (a) in Figure 4-36). The strains in the stirrups across the critical crack ranged from 0.001 to 0.006 at that shear. The average strain in the stirrups was 0.0028, which is greater than yield strain. However this strain cannot be used to determine stresses in the stirrups because some stirrups have not yielded. After this point, the CFRP contribution kept decreasing whereas the steel contribution increased. The maximum contribution of each material did not occur at the same time, so the capacity of the composite member would be the less than the summation of each contribution to shear.

4.4.1.10 Test 24-3-10 (inclined anchor)

In test 24-3-10, the effect of the direction of CFRP anchors was studied. Due to inclining anchor, the anchor hole location could have been moved to the end of the strip. Therefore, it is expected that effective depth (d_f) and the confined concrete area enclosed by CFRP anchors were increased a little bit. As shown in Figure 4-40, the angle of CFRP anchor was less than 20 degrees to avoid interference with the compressive reinforcement.
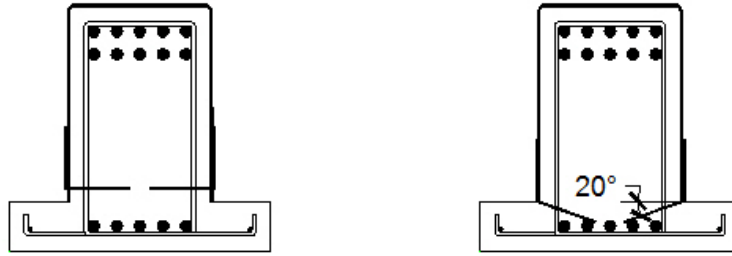
(a) Typical anchor detail   (b) Anchor detail in 24-3-10

Figure 4-40 Comparisons of typical CFRP anchor detail and that of 24-3-10

In Figure 4-41, the sequences of FRP rupture were investigated based on data from strain gages, load cells, and video at failure. The maximum capacity occurred when a shear of 145 k was reached and held for marking cracks and measuring crack width and observing damages. In the process of stabilizing the specimen, the shear capacity decreased to 139 k.
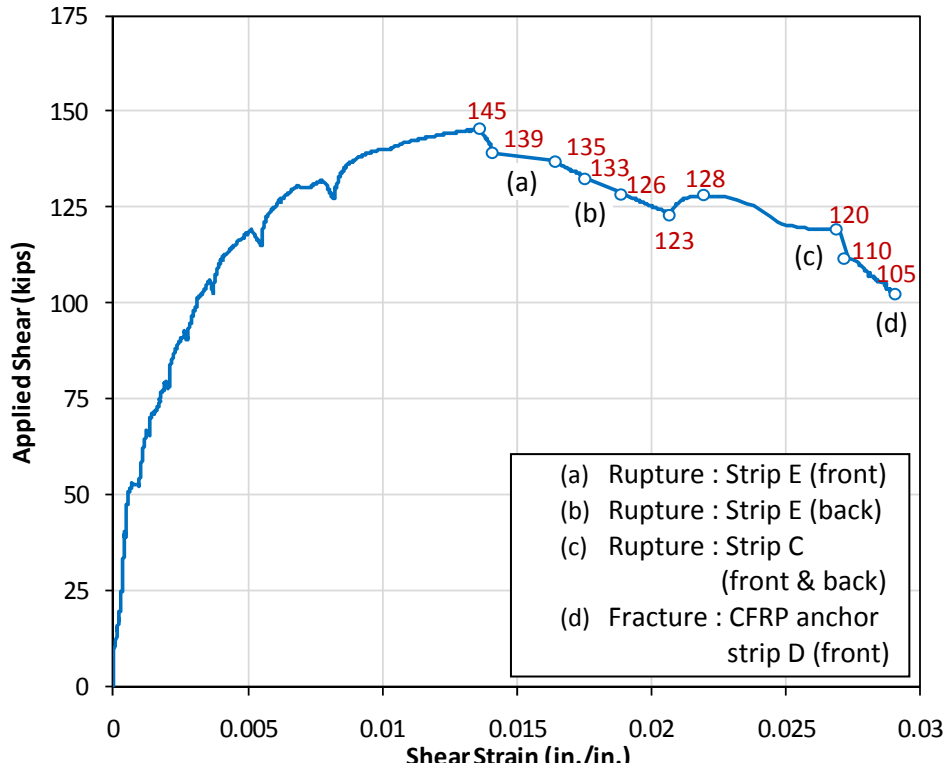
Figure 4-41 Failure sequences of test 24-3-10

With rupture of the strip E, the shear dropped to 135 k. In addition, the shear decreased slowly to 133 k at which the strip ruptured following. The shear was dropped to 126 k. When the shear kept holding 123 k, the additional load was applied to beam to observe stress redistribution. The shear capacity was increased by 5 k and decreased again. At a shear of 120 k, strip C ruptured and the shear was dropped to 110 k. At a shear of 105 k, the anchor in front side of strip D fractured, but there was no change in shear.

The increase in the effective length by inclining the key portion of the CFRP anchor in the T-beam did not increase shear capacity. However, the stress concentration at the reentrant corner of the web and flange in a T-beam may negate any advantage from increasing the effective depth.
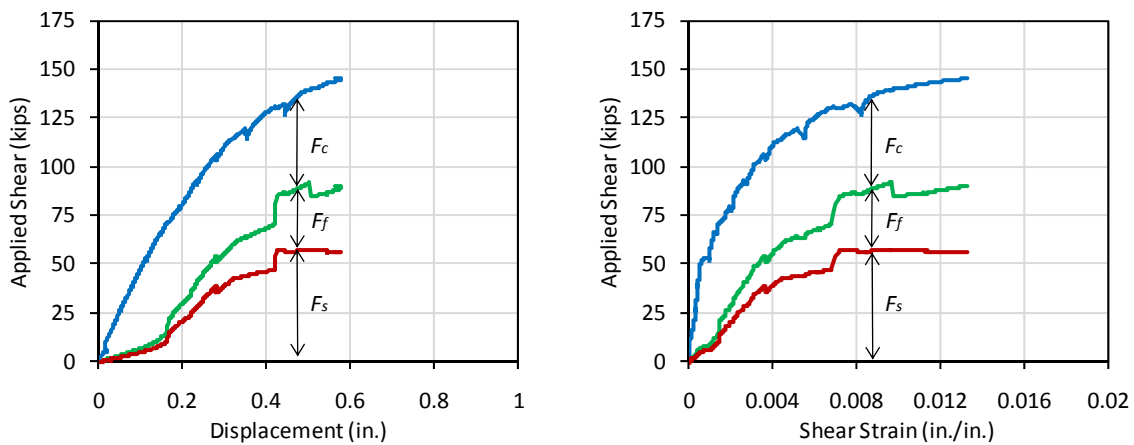
Figure 4-42 Component contribution to shear force vs. deformation response of 24-3-10
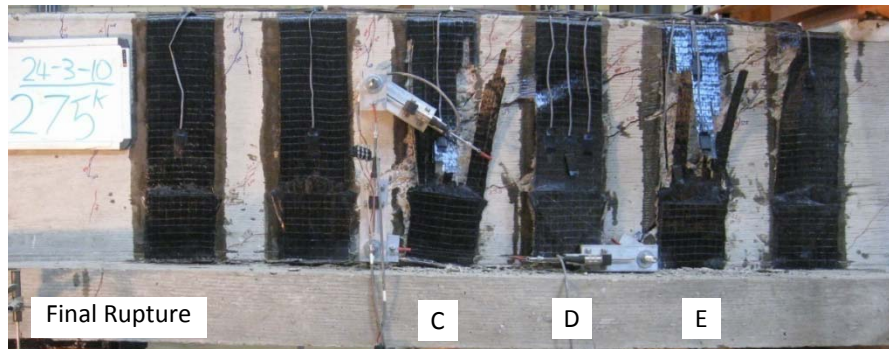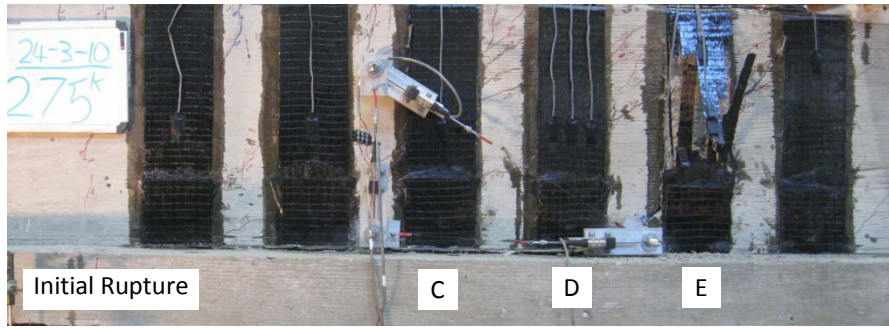
(a) Front side
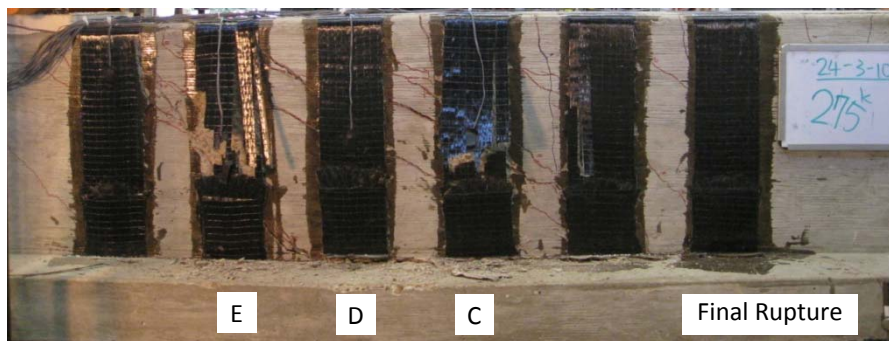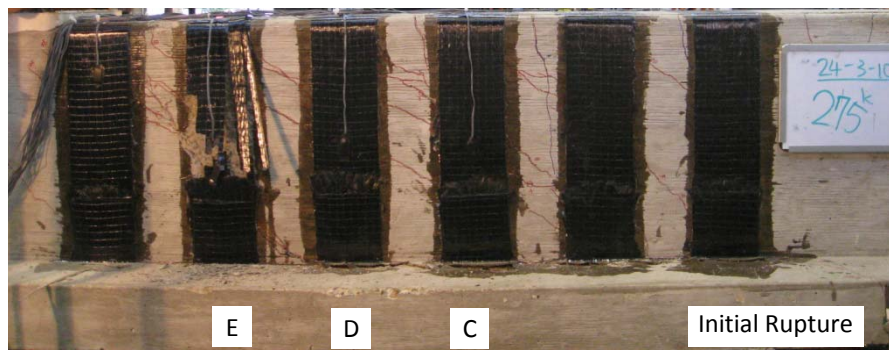
(b) Back side

Figure 4-43 Photos of both sides of test 24-3-10 at ultimate load

118

4.4.2   24 in. Depth Beam Series Ⅱ (a/d=2.1 and 1.5)

4.4.2.1   Test 24-2.1-2 (no CFRP, control)

      In these tests, the performance of beam with shear capacity of shear-span-to-depth ratio of 2.1 was investigated. In test 24-2.1-2, the base shear strength of beam with shear-span-to-depth ratio of 2.1 was evaluated. Most gages were lost in the process of drilling anchor holes, so the steel contribution was evaluated from just one gage. At the shear of 119 k, the maximum crack width exceeded 0.05 in. and kept increasing after that. Shear failure occurred at a shear of 129 k and failure mode was diagonal tension. After peak load, the shear capacity decreased slowly with large deformation.
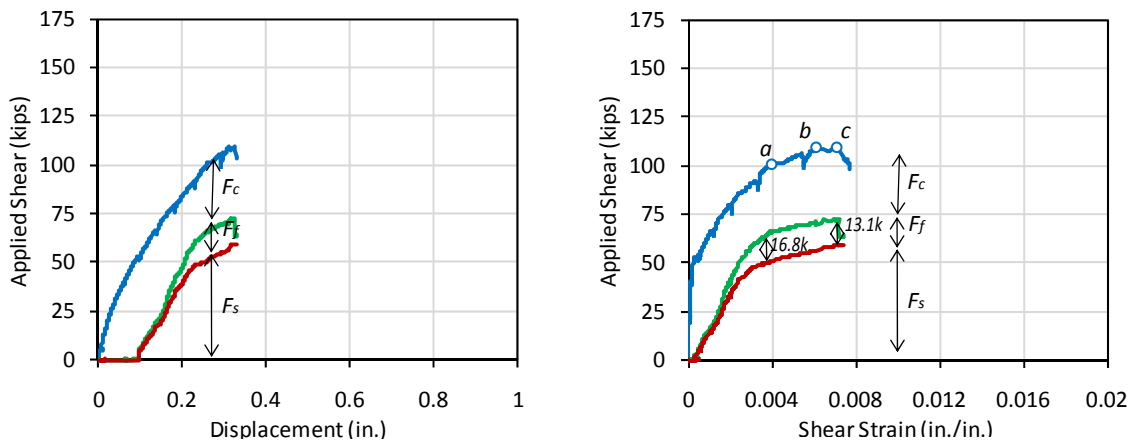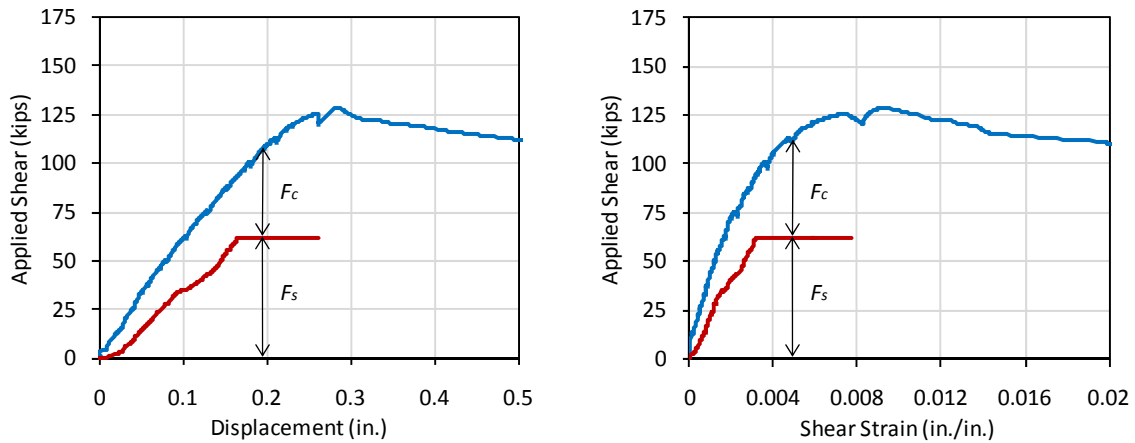

Figure 4-44 Component contribution to shear force vs. deformation response of 24-2.1-2

(a)   Front side   (b)   Back side

Figure 4-45 Photos of both sides of test 24-2.1-2 at ultimate load

4.4.2.2 Test 24-2.1-1(1 layer, strengthened)

The failure mode in test 24-2.1-1 was a combination of CFRP rupture and CFRP anchor failure. The maximum crack width exceeded 0.05 in. at a shear of 125 k and kept increasing up to failure. At a shear of 135 k, one strain at one location was greater than 0.01 and at a shear of 162 k, another location also exceeds 0.01, but there was no visual evidence of rupture. A high strain reading in one gage may over-estimate the FRP contribution in the strip because vary along the strip length and across the strip width as discussed in Section 4.2.2. Therefore, the FRP shear contribution was estimated with a range of value with the lower bound - strip based on rupture and upper bound - strip based on maintaining a strain of 0.01 without rupture.
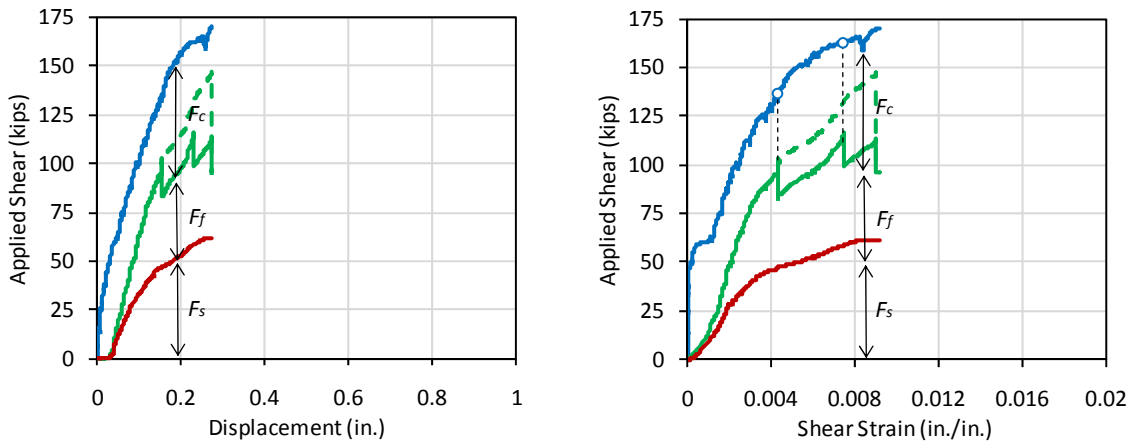
Figure 4-46 Component contribution to shear force vs. deformation response of 24-2.1-1
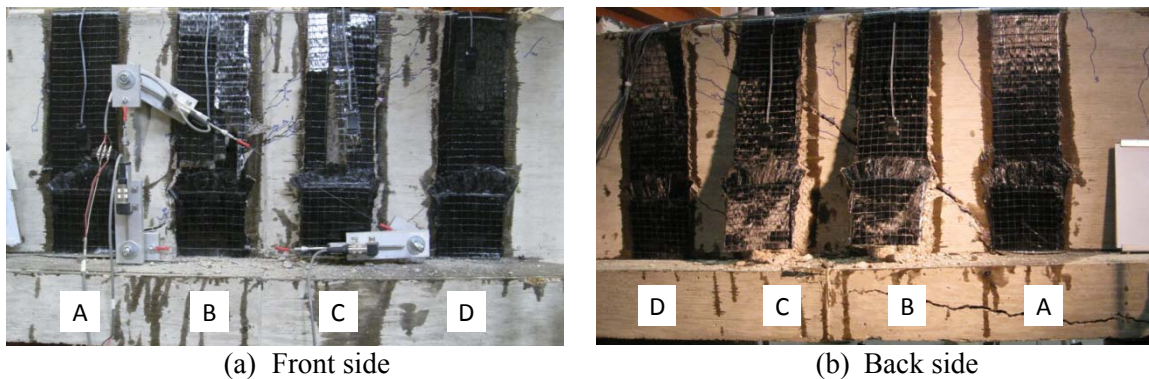
(a) Front side   (b) Back side
Figure 4-47 Photos of both sides of test 24-2.1-1 at ultimate load

120

This capacity was greater than that of 24-3-2. This increase in shear capacity was primarily due to shear-span-depth ratio because all other design parameters were identical. Therefore, the arch action by direct concrete strut might contribute to the shear capacity. The front side of strip C was partially ruptured at a shear of 162 k. Failure occurred at a shear of 170 k, which was 18 k greater than capacity of 24-3-1r. Comparing with 24-3-2, the shear capacity was 24 k greater. It implied that the strengthening in the lower shear-span-to-depth ratio was less efficient. More details about shear-span-to-depth ratio will be discussed in Section 4.5.2.

4.4.2.3 Test 24-1.5-3 (no CFRP, control)

A control test (24-1.5-3) was conducted to determine the base shear strength of the test specimen with a shear span-to-depth ratio equal to 1.5. No CFRP laminates were installed on the specimen. Failure mode was controlled by the crushing of the concrete strut at a shear of 233 k.

Figure 4-48 Component contribution to shear force vs. deformation response of 24-1.5-3

(a) Front side   (b) Back side

Figure 4-49 Photos of test 24-1.5-3 at failure

4.4.2.4 Test 24-1.5-4 (1 layers, strengthened)

Test 24-1.5-4 was conducted in the high-capacity loading setup because the applied shear from the experience of previous tests was expected to be greater than 240 k. After rupture of CFRP strip, the shear capacity at failure was 264 k. The capacities of all of tests in shear-span-to-depth ratio of 1.5 were close each other no matter how much CFRP material was used. It implied that CFRP strengthening is not likely to be efficient if the capacity is governed by compression failure of the concrete strut. This will be discussed in Section 4.5.2.

Figure 4-50 Component contribution to shear force vs. deformation response of 24-1.5-

4

122

<div style="text-align:center">(a) Front side   (b) Back side</div>

Figure 4-51 Photos of both sides of test 24-1.5-4 at ultimate load

4.4.2.5 Test 24-1.5-1/1r/1r2 (pre-cracking/strengthening/load to failure)

In test 24-1.5-1, the specimen was loaded to yield in the stirrups for simulating damaged beam and was unloaded. Yielding occurred at an applied shear load of 131 k (3ER) and the maximum crack width was 0.018 in.

In test 24-1.5-1r, the specimen was strengthened two layers of 5-in. wide strip at 10 in. spacing. The test was stopped at a shear of 240 k due to reaching the capacity of the loading setup.

The maximum concrete crack width observed during testing was 0.06 in. The CFRP strip started to debond and the maximum strain in the CFRP (F1C.1) was 0.0039.

<div style="text-align:center">(a) 24-1.5-1   (b) 24-1.5-1r</div>

Figure 4-52 Photos of test 24-1.5-1 and 24-1.5-1r at maximum load

In test 24-1.5-1r2, the specimen was moved to the high-capacity test setup and was loaded to failure. Failure occurred at a shear of 252 k and the failure mode was crushing of the concrete strut. None of the CFRP strips ruptured, but some of the anchors fractured near the anchorage holes as seen in Figure 4-53. The shear capacity was 19 k greater than that of 24-1.5-3.

(a) Concrete crushing   (b) Fracture at CFRP anchor
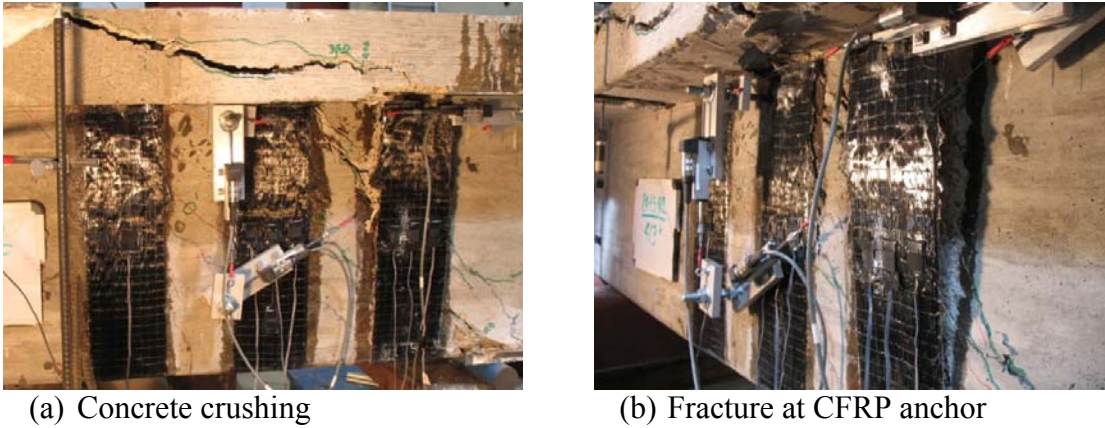
Figure 4-53 Photos of test 24-1.5-1r2 at failure

Figure 4-54 shows the shear contribution of 24-1.5-1 and 24-1.5-1r. Most gages in 24-1.5-1r2 were not functional due to loading and unloading before testing. However, the failure load of 24-1.5-1r2 was not much greater than when the first test was stopped, so the information in Figure 4-54 includes nearly the full range of loading. Most of shear capacity came from a direct concrete strut between the load point and the end reaction.
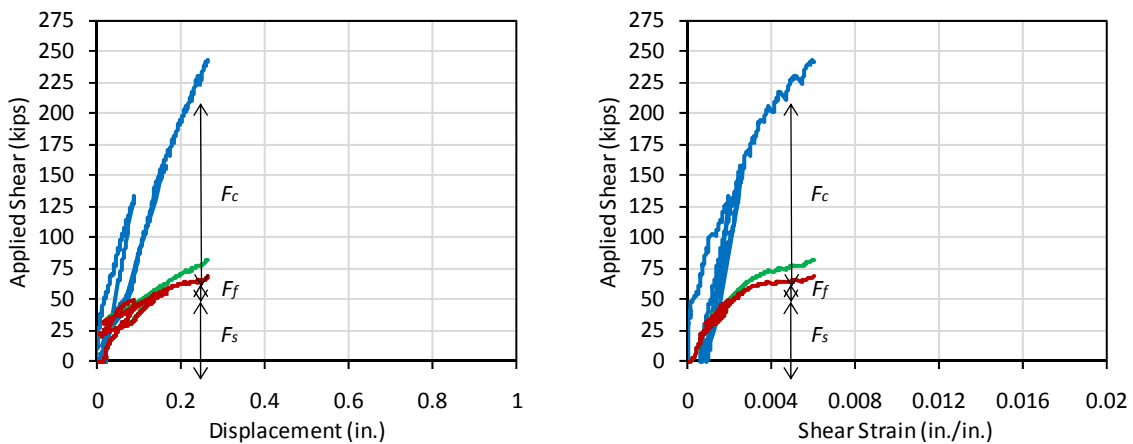
Figure 4-54 Component contribution to shear force vs. deformation response of 24-1.5-1/1r

4.4.2.6   Test 24-1.5-2 (no anchor)

Test 24-1.5-2 was conducted with same configuration as test 24-1.5-1r, but no CFRP anchors were used. Figure 4-55 and Figure 4-56 provide an indication of the performance. Failure occurred at a shear of 255 kips, which is nearly the same capacity of 24-1.5-1r2 and indicate that the CFRP strips had almost no influence on the capacity that was controlled by compression in the concrete strut. Failure in 24-1.5-2 was triggered by CFRP debonding. The maximum strain in the CFRP was 0.004. The overall behavior was close to 24-3-9 (no anchor test).
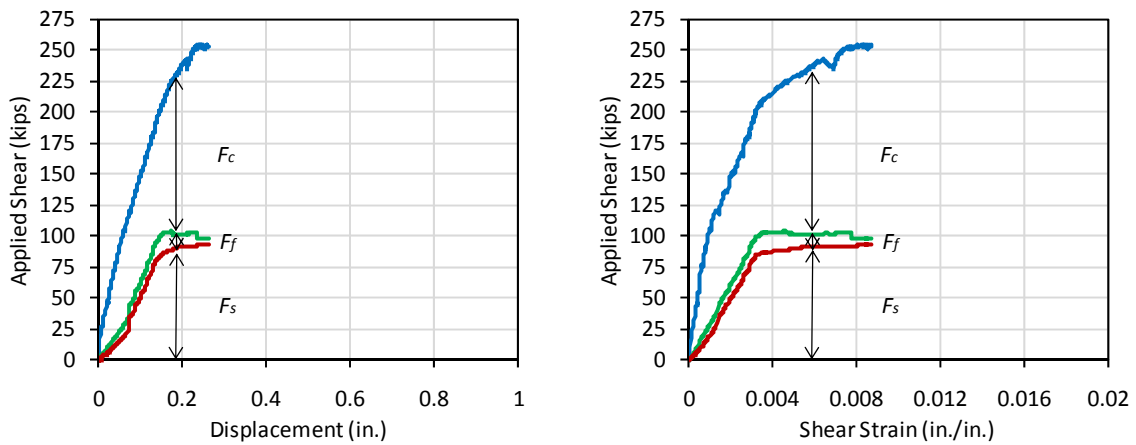
Figure 4-55 Component contribution to shear force vs. deformation response of 24-1.5-2

(a) Front side   (b) Back side
*Figure 4-56 Photos of test 24-1.5-2 at failure*

| (a) Strip-end debonding | (b) Intermediate crack debonding |

Figure 4-57 Debonding in test 24-1.5-2 at failure

4.4.3   48 in. Depth Beam Series I (18 in. stirrups spacing)

4.4.3.1   Test 48-3-1 (no CFRP, control for tests 1~4)

The estimated capacity of 48-3-1 was 108 k calculated using general design shear equations. A shear span to depth ratio of 3 is considered as the transition between deep beam and sectional beam behavior and the design equation is based on a lower bound to test data. Therefore, the expected load was greater than the estimated load. Based on the ratio of computed to observed strength of 1.66 for 24-3-2 (control), the capacity of this test was expected to be around 180 k. Loading was stopped at a shear of 147 k as shown in Figure 4-58.
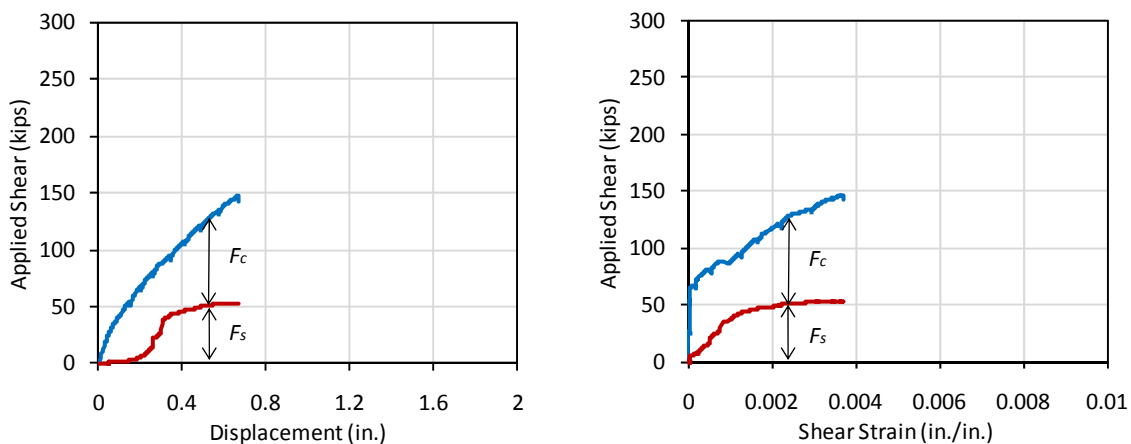
Figure 4-58 Component contribution to shear force vs. deformation response of 48-3-1

126

Around 30 k, the slope of load-displacement graph inclined slightly and several flexural cracks occurred at the loading point. At 67 k, one of the flexural cracks developed into a flexural-shear crack. From the shear strain-load response, the stiffness also changed at that load. In addition, strains in stirrup D (D2, D3 and D3r) were increased abruptly. At 81 k, the crack extended and was wider. The range of crack width was 0.007 ~ 0.016 in. Diagonal cracking extended across stirrups C to E. At 94 k, another shear crack formed across stirrup D to F occurred parallel to the previous shear crack. The crack width was 0.010 ~ 0.025 in., almost the same as the first crack. At 107 to 121 k, the existing cracks get wider. The shallow diagonal crack located across stirrups C to F was the dominant crack and extended to the flange region.

At 147 k, new shear crack across stirrup A to C occurred and the test was stopped to avoid damage that would prevent testing the other end of the beam. The maximum crack width is about 3/16 in. The maximum stirrup strain was 0.009 and all stirrups crossing the critical crack yielded.
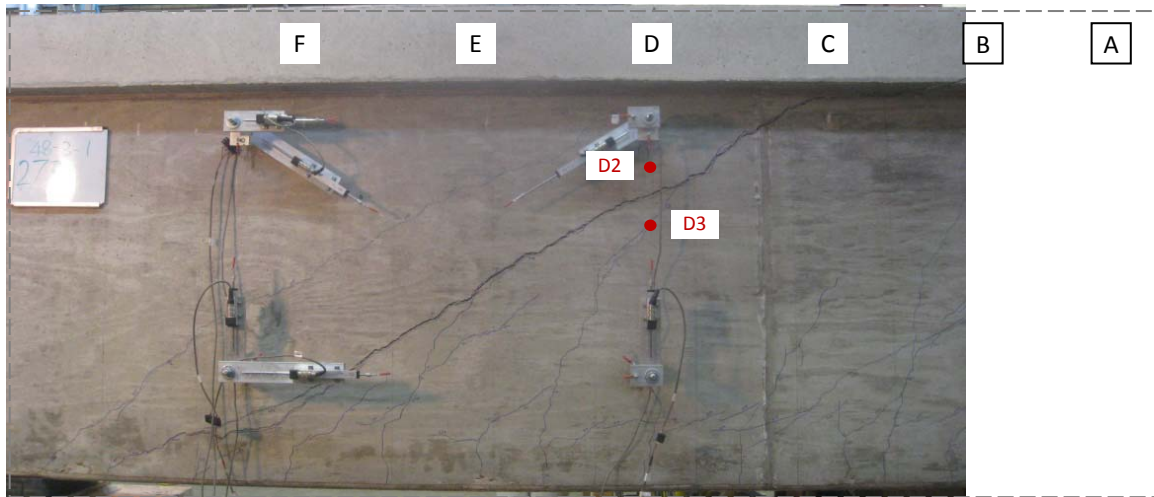
(a) Front side
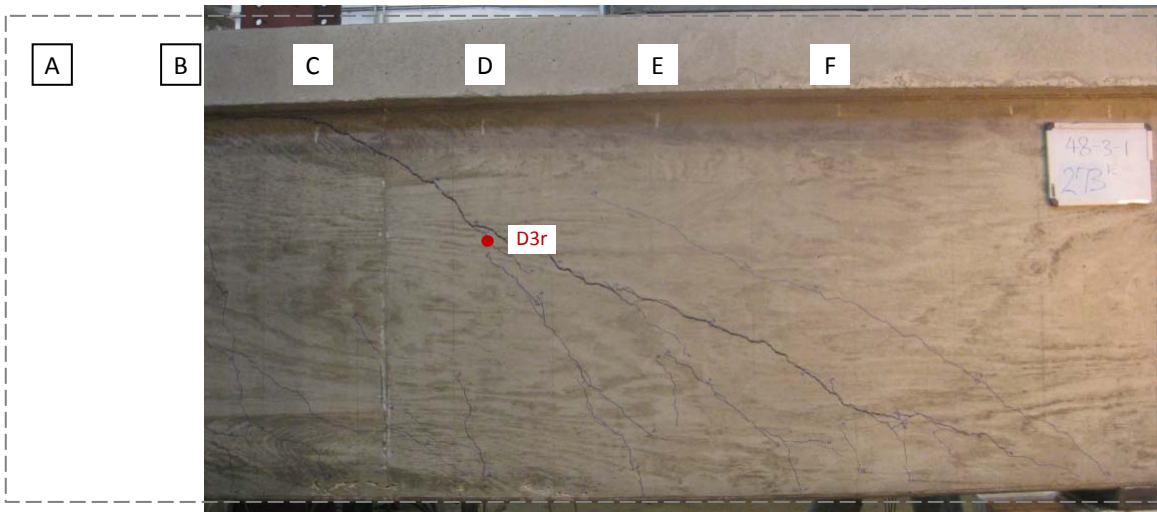
(b) Back side

Note. 1) Photos were not covered the entire test regions, but most shear cracks occurred at this area shown in these photos.

2) Labels in this figure indicate the location of steel stirrups (not CFRP)

Figure 4-59 Photos of both sides of test 48-3-1

4.4.3.2 Test 48-3-2 (10 in. wide strips)

Test 48-3-2 was strengthened with 10-in. wide CFRP strips at 20-in. spacing on center. Two CFRP anchors were installed for each CFRP strip. At 67 k and 94 k, a steep shear crack formed across strip B to D and strip A to C respectively (See Figure 4-61). At 107 k, a shallow shear crack formed across strip C to F. At 148 k, strip A started to

128

debond. At 175 k, maximum crack width was 0.06 in. After reaching the maximum shear capacity of 226 k, the load went down slowly to 223 k. Shear failure was initiated by an explosive rupture of several CFRP strips. Strip B ruptured first and the shear dropped to 209 k. Then strip C and D ruptured. Compared with the 24-in. beams, the failure was more explosive. As shown in Figure 4-62, one stirrup fractured after CFRP strips ruptured. The maximum strain in the CFRP was 0.0097 at peak load and over 0.0105 (manufacturer's rupture strain) at rupture.

Assuming that the CFRP strip was totally debonded, the total deformation over the strip length was roughly doubled at rupture because the length of the CFRP strips in 48-in. beams was twice of that of 24-in. beams. However, the deformation in steel stirrups occurred near the crack mostly regardless of the stirrups length. Therefore, at rupture of CFRP strip, the fracture of the stirrups was observed in tests with 48-in beams.
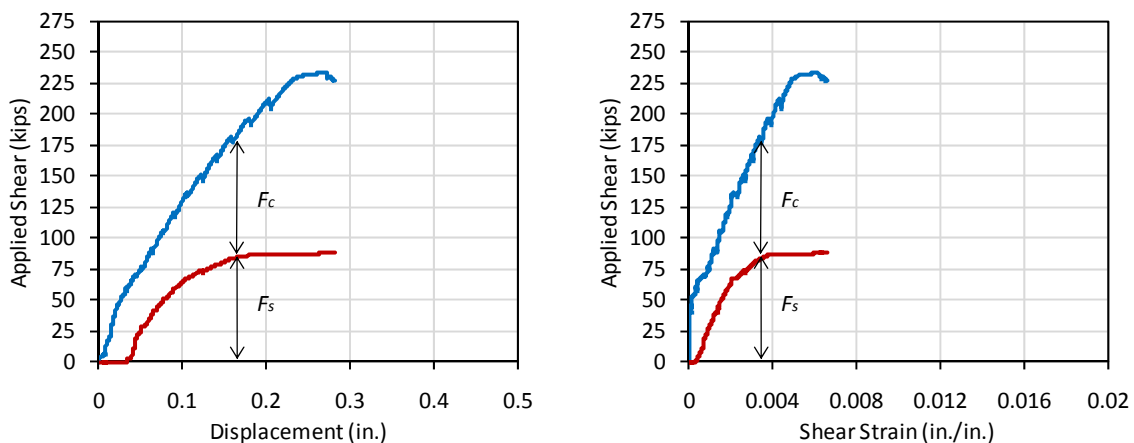

Figure 4-60 Component contribution to shear force vs. deformation response of 48-3-2
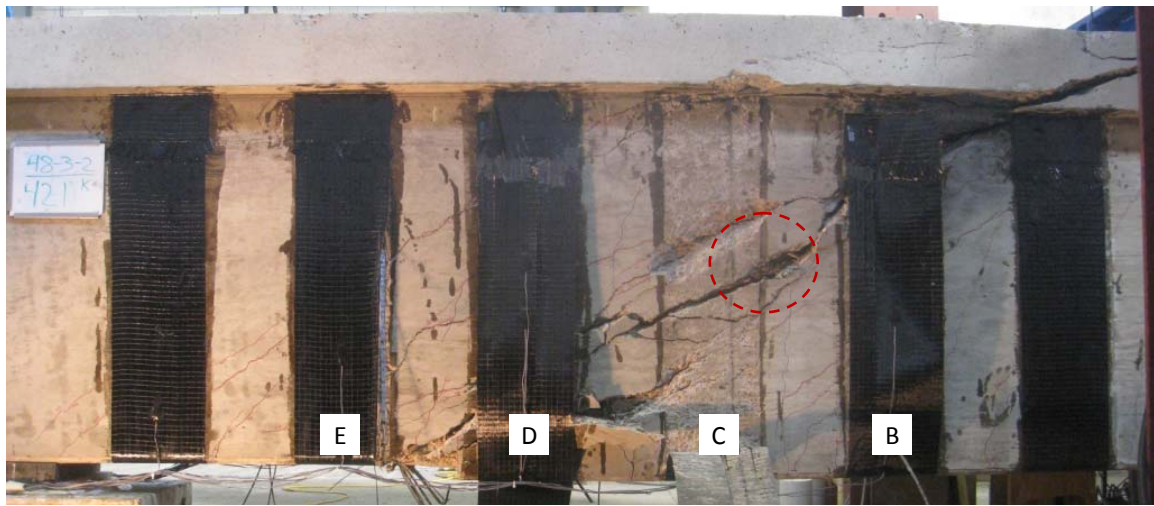
(a) Front side
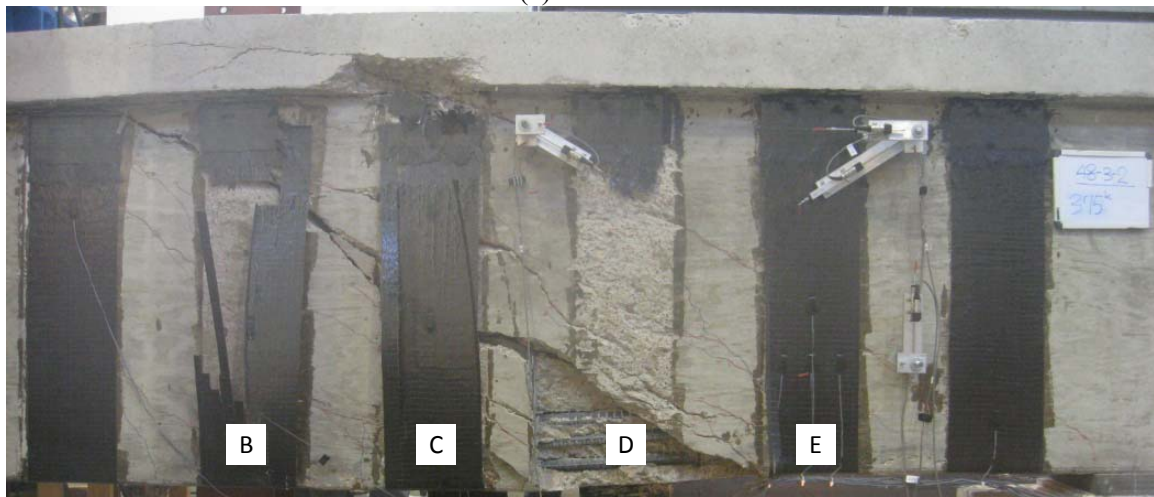
(b) Back side

Figure 4-61 Photos of both sides of test 48-3-2 at end of test
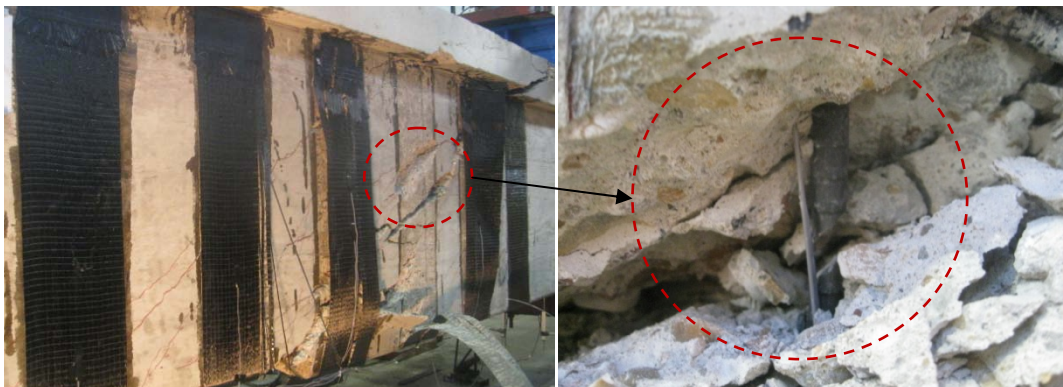
Figure 4-62 Photos of stirrup fracture after CFRP rupture

4.4.3.3 Test 48-3-3 (14-in. wide strips)

Test 48-3-3 was strengthened with 14-in. wide strips instead of 10-in wide strips at 20-in. spacing. From this test, the effect of the amount of material was investigated.

The response of 48-3-3 is shown in Figure 4-63. At 67 k, steep shear cracks formed between strip A to B and strip B to C as extension of a flexural crack that occurred at 54 k. A shallow shear crack then occurred between strips C to E at 107 k. The maximum strain was 0.001 in the stirrups and 0.0015 in the CFRP strips. At 121 k, another shear crack parallel to previous one occurred from strips D to F. At 148 k, a malfunction caused the load to drop but the beam was reloaded up to same level of shear and at 188 k, the CFRP strips began to debond. At 228 k, a small crack extended into the flange. When the test was stopped at 239 k, the CFRP strain was 0.009 at FD2.2 (FC1: 0.0083, FE4: 0.0072, FF5: 0.0048) and stirrup strain was over 0.01 at D2. The maximum crack width was 0.04. Based on the previous tests, the ultimate capacities were not much different from the capacity where the CFRP strain was 0.009. Therefore, the results can be considered at or very close to failure.
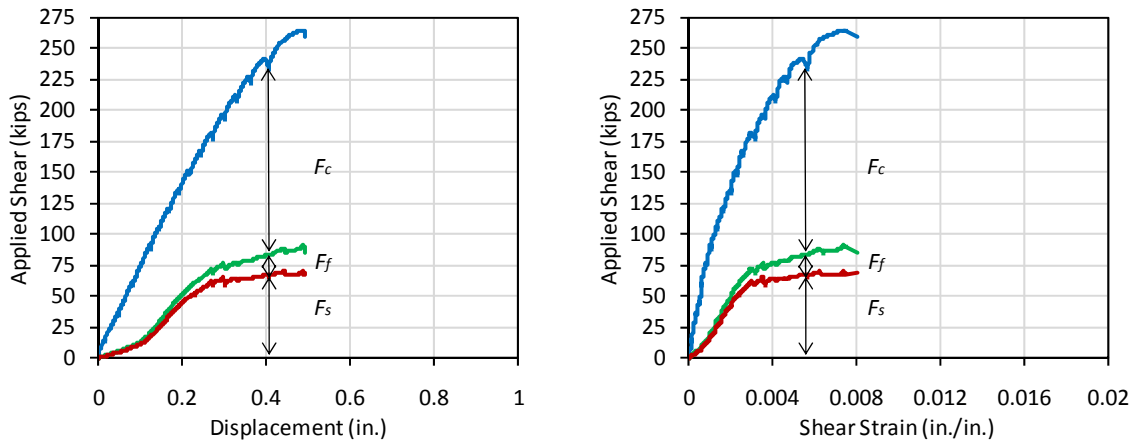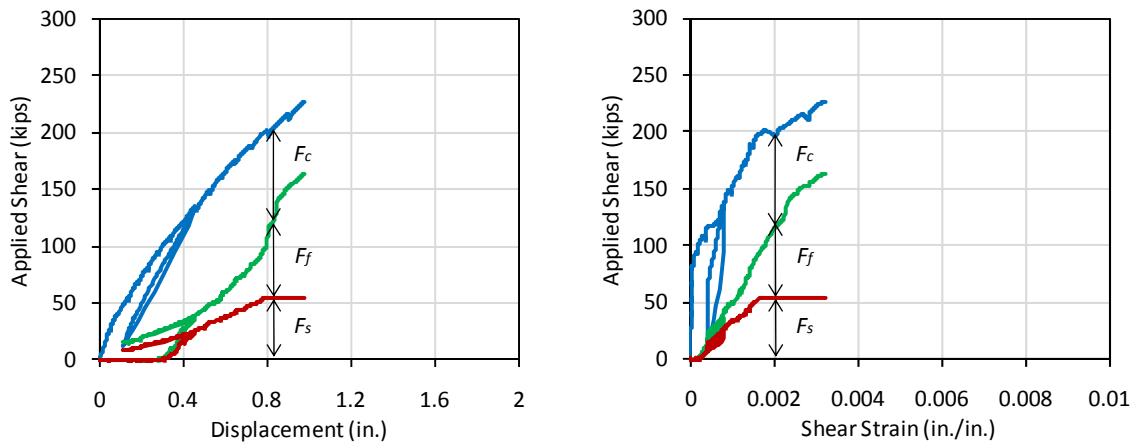

Figure 4-63 Component contribution to shear force vs. deformation response of 48-3-3
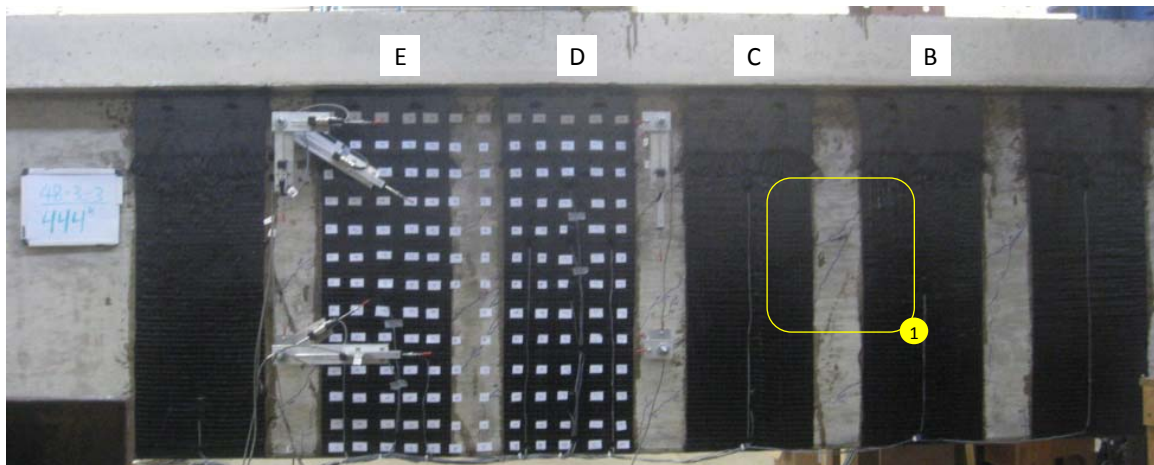
(a) Front side
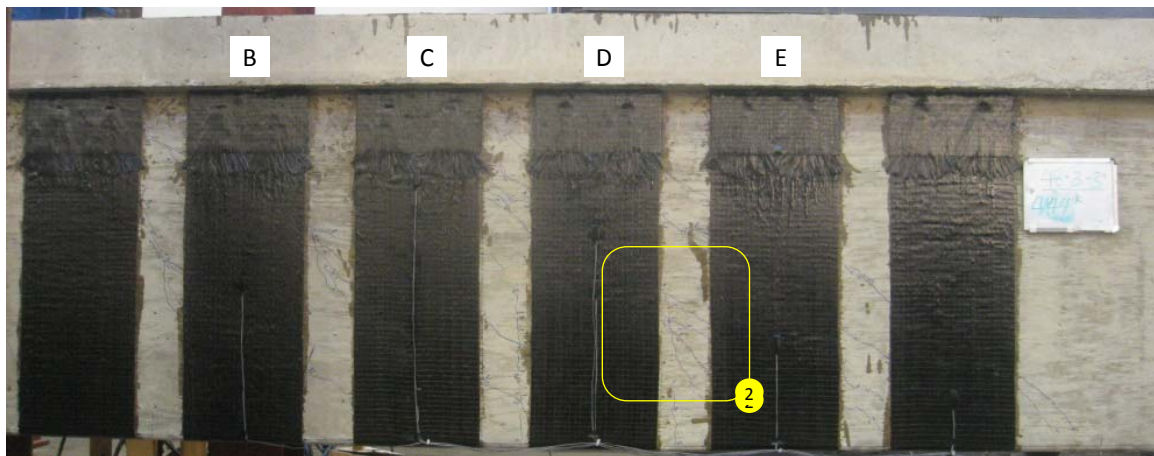
(b) Back side

Figure 4-64 Photos of both sides of test 48-3-3 at ultimate load
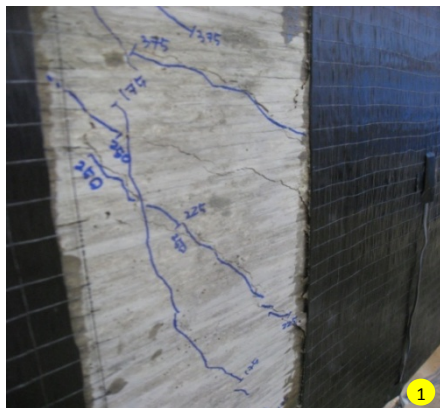
Figure 4-65 Debonding of CFRP strip of 48-3-3 at locations shown in Figure 4-64

132

4.4.3.4 Test 48-3-4 (diagonal strips)

Test 48-3-4 was strengthened using CFRP strips inclined at 45 degrees. By changing the orientation of strip, the length of the 10-in. strip was 41 percents longer. The intent was to orient the strips at an angle normal to the critical crack. Therefore, the total amount of CFRP material was increased and was equal to that of test 48-3-3 (14-in. wide vertical strips).

In addition, the CFRP strip could not be attached as a U-wrap. Two separate CFRP strips were used and overlapped at the bottom of the beam as shown in Figure 4-66. No debonding was observed in the overlapping areas during the test.
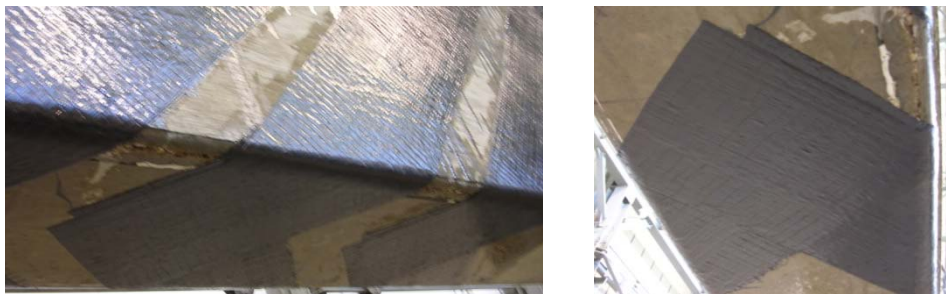
Figure 4-66 Overlapping of diagonal strips on bottom of beam

The maximum shear capacity was 236 k when partial rupture of strip B occurred and shear dropped to 193 k as shown in Figure 4-67. With the partial rupture of strip C and D, load was dropped to 186 k. Finally, strip B, C, D and E ruptured explosively and the beam lost nearly all shear capacity. The crack width was 0.05 in. at a shear of 228 k. No further crack measurements were made because of safety issues. The maximum strain in the CFRP strips was 0.008 at gage FD5 (in strip D) and the maximum strain in steel stirrups was 0.012 at D3 (in stirrup D). Unfortunately, the critical crack occurred at a location that was not heavily instrumented. Therefore, the shear strain and shear contribution from stirrups and CFRP strips will be underestimated. In Appendix E, the gage locations used to evaluate shear contribution are described. As can be seen in Figure 4-68, no anchor failure was observed. The strips were nearly perpendicular to the critical crack.

133

Figure 4-67 Component contribution to shear force vs. deformation response of 48-3-4
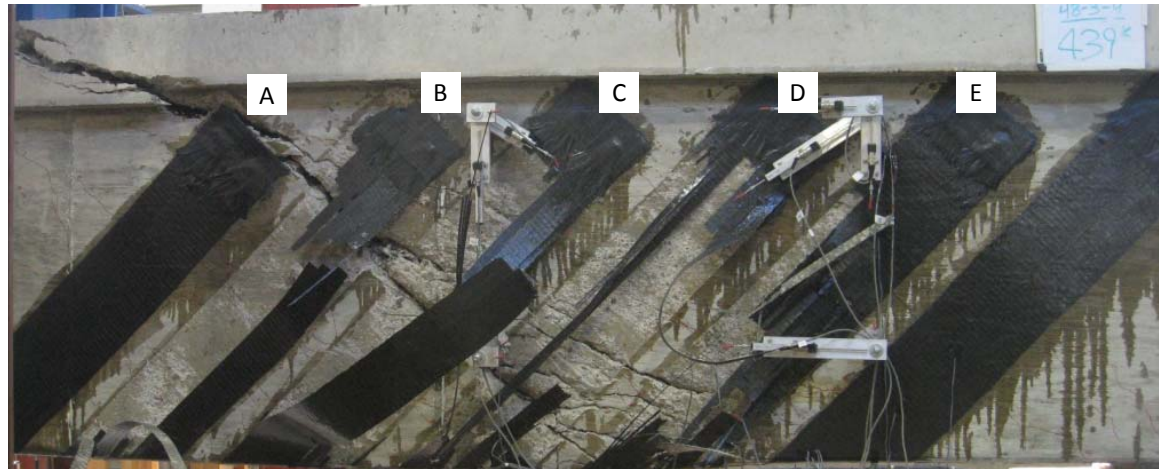
(a) Front side
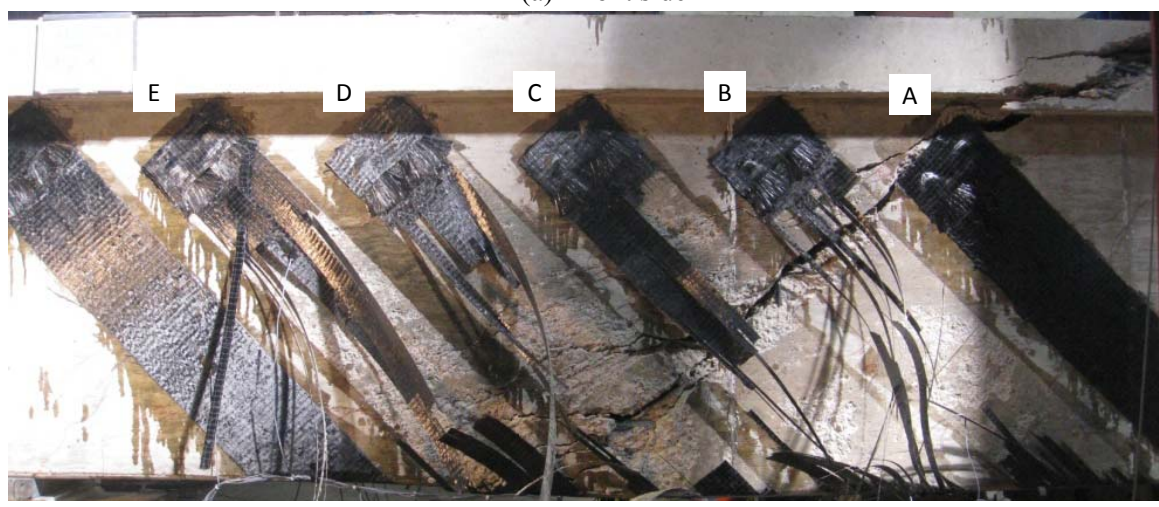
(b) Back side

Figure 4-68 Photos of both sides of test 48-3-4 at ultimate load

134

4.4.4   48 in. Depth Beam Series Ⅱ (10 in. stirrups spacing)

4.4.4.1   *Test 48-3-6 (no CFRP, control for test 5~8)*

      In test 48-3-6, another control test was conducted without CFRP because the stirrup spacing was reduced from 18 in. to 10 in. The loading was stopped (as shown in Figure 4-69) before reaching maximum capacity because strengthening test (48-3-6r) was planned using the same specimen. However, all stirrups crossing the critical crack yielded when load was stopped.

      At 134 k, a shallow shear crack occurred. A stirrup gage at J4 indicated strain to exceed yield strain at a shear of 155 k. At 161 k, a shallow shear crack parallel to previous crack occurred with a maximum crack width of 0.06 in. The shear crack extended into the flange when load was stopped at 228 k. The maximum crack width was 0.25 in. at 228 k and 0.06 in. after unloading.

Figure 4-69 Component contribution to shear force vs. deformation response of 48-3-6

(a) Front side

(b) Back side
Figure 4-70 Photos of both sides of test 48-3-6 when load stopped

4.4.4.2 Test 48-3-5 (strengthened)

Test 48-3-5 was conducted with 10 in. wide strip at 20 in. on center, which was same CFRP strengthening detail as 48-3-2 except that stirrups spacing was 10 in. instead of 18 in. This transverse reinforcement ratio was same as that of the 24 in. beams. Therefore, the effect of the beam depth and transverse reinforcement ratio will be discussed in Section 4.5.5.

The response of 48-3-5 is shown in Figure 4-71. At 94 k, a shallow web shear crack were observed from strip C to strip E. Several steep shear cracks formed earlier.

136

The crack width was 0.01 in. at 94 k. Steel strain at J3 was 0.0022, which indicated the yielding of stirrup. At 107 k, another shear crack parallel to the previous crack occurred from strip D to strip F. At 121 k, Strip D started to debond. The load was stopped at 242 k. All stirrups along the critical crack yielded and maximum recorded strain in the CFRP was 0.0088 at FC1. The maximum crack width was 1/8 in.
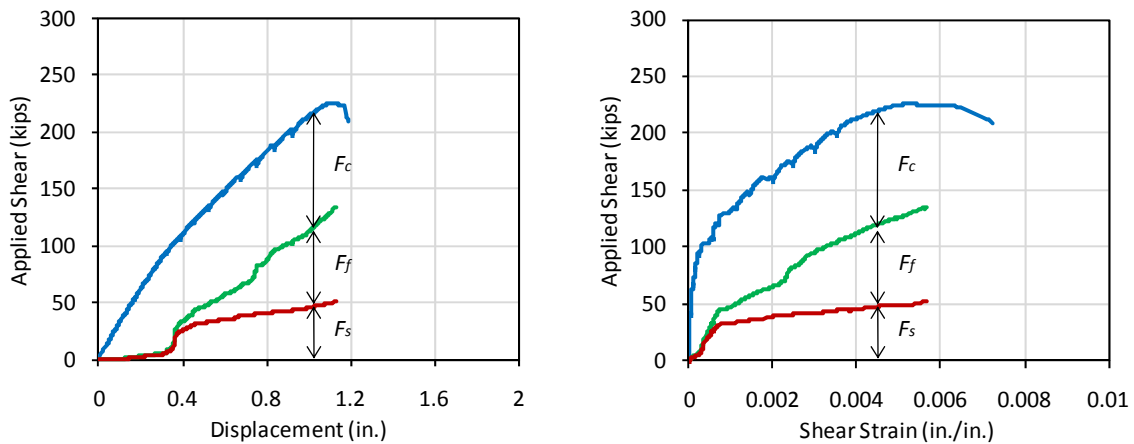

Figure 4-71 Component contribution to shear force vs. deformation response of 48-3-5
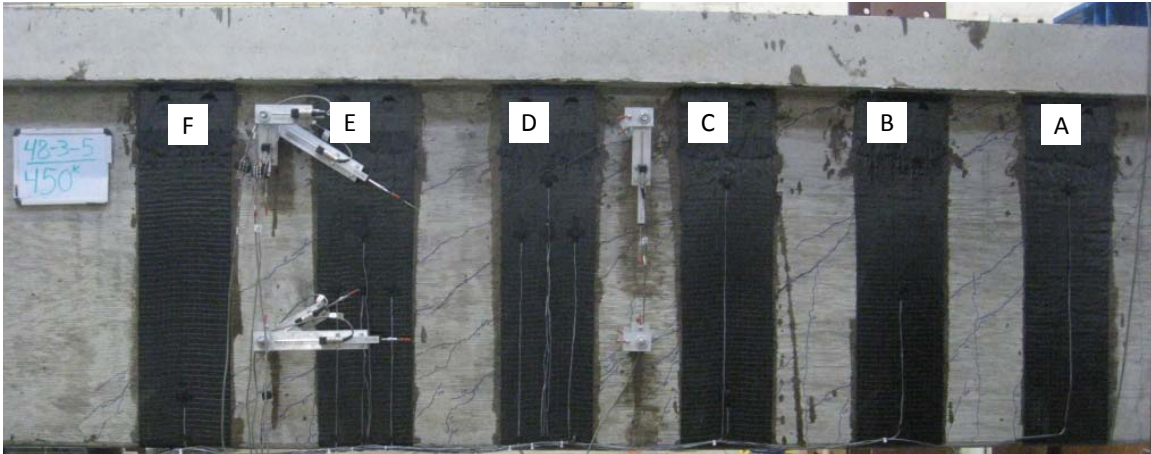
(a) Front side
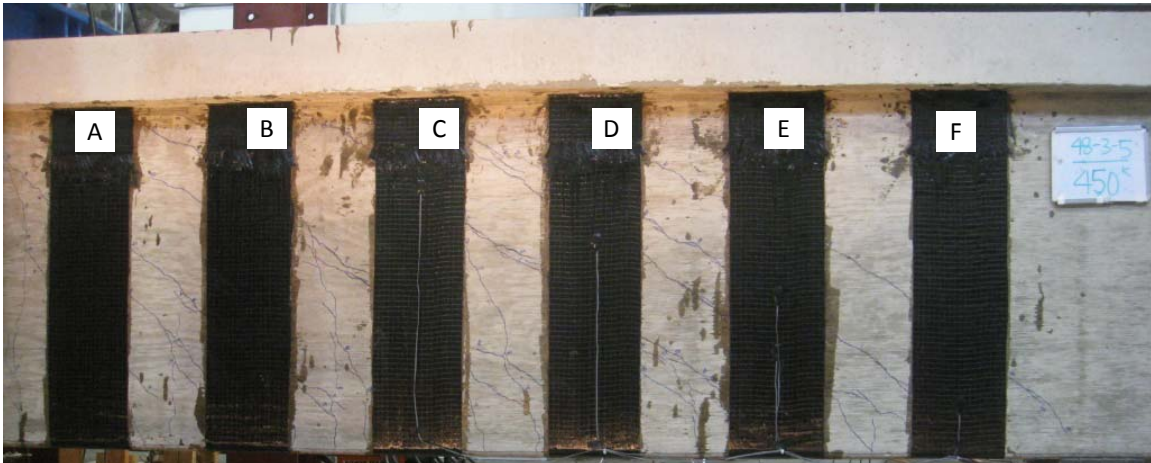
(b) Back side

Figure 4-72 Photos of both sides of test 48-3-5 at end of test
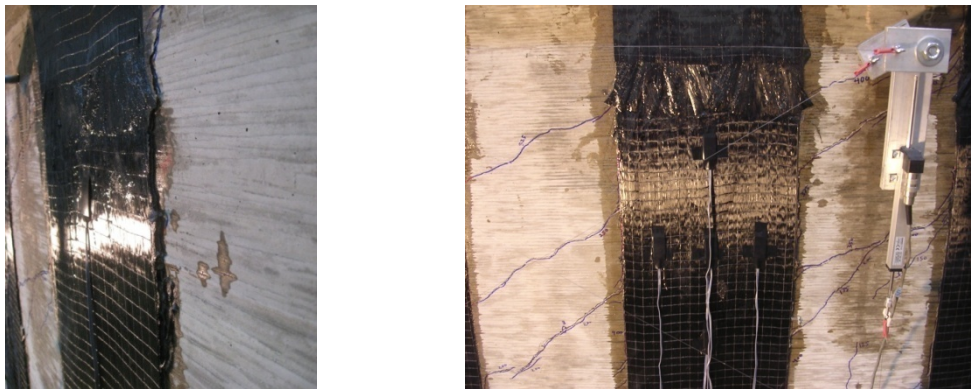
Figure 4-73 Photo of debonding of CFRP strip in test 48-3-5 at end of test

4.4.4.3 Test 48-3-6r (epoxy injection of cracks prior to strengthening)

After testing 46-3-6, the cracks in the specimen were epoxy-injected and the beam was strengthened with CFRP strips. The CFRP configuration was the same as test 48-3-5. After epoxy injection was completed, the concrete surface was prepared as shown in Figure 4-74 before applying CFRP.

(a) Epoxy injection

(b) Chipping

(c) Before grinding the surface

(d) After grinding the surface
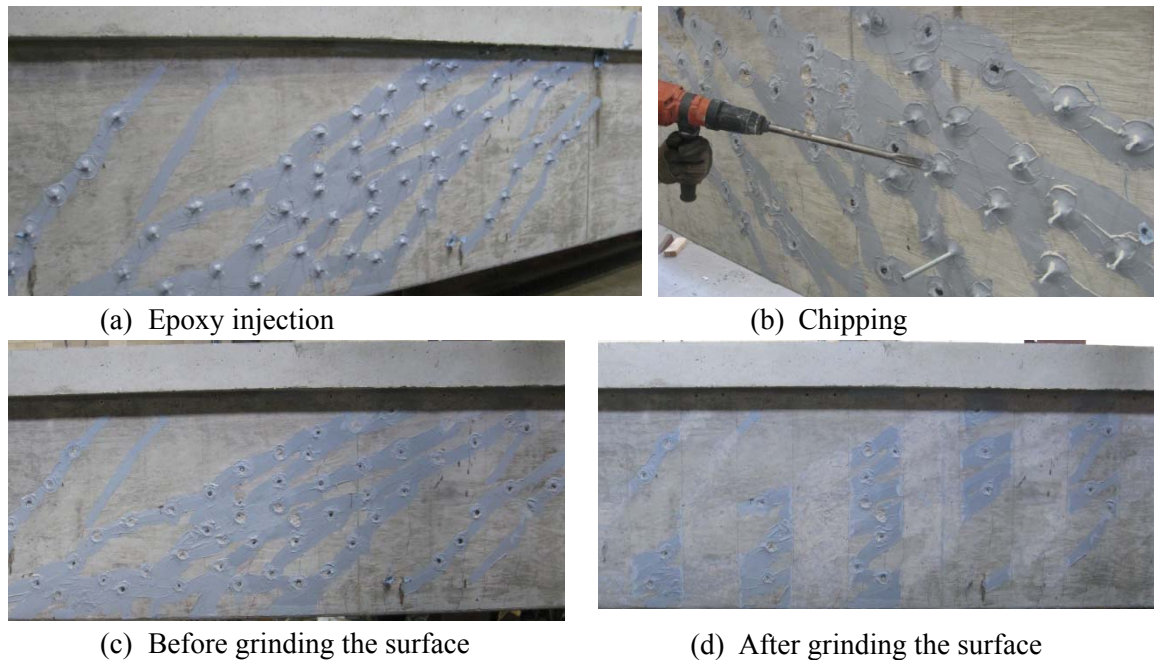
Figure 4-74 Epoxy injection and surface preparation

The response is shown in Figure 4-75. At 215 k, the maximum CFRP strain was 0.0037. At 228 k, cracks extended to the loading point and the CFRP strips started to debond. At 269 k, the maximum crack width was 0.04 in. At 327 k, flexural steel strain in the bottom layer of bars were as high as 0.0073. The tensile strains were high enough to produce strains near 0.003 in the concrete in compression indicating that the beam was near flexural capacity. At 293 k, an explosive rupture of CFRP strips occurred. The strain in the CFRP (FC2) was 0.009 at peak load and 0.012 at rupture. Although the beam reached flexural capacity, failure was triggered by loss of shear capacity when the CFRP strips ruptured.
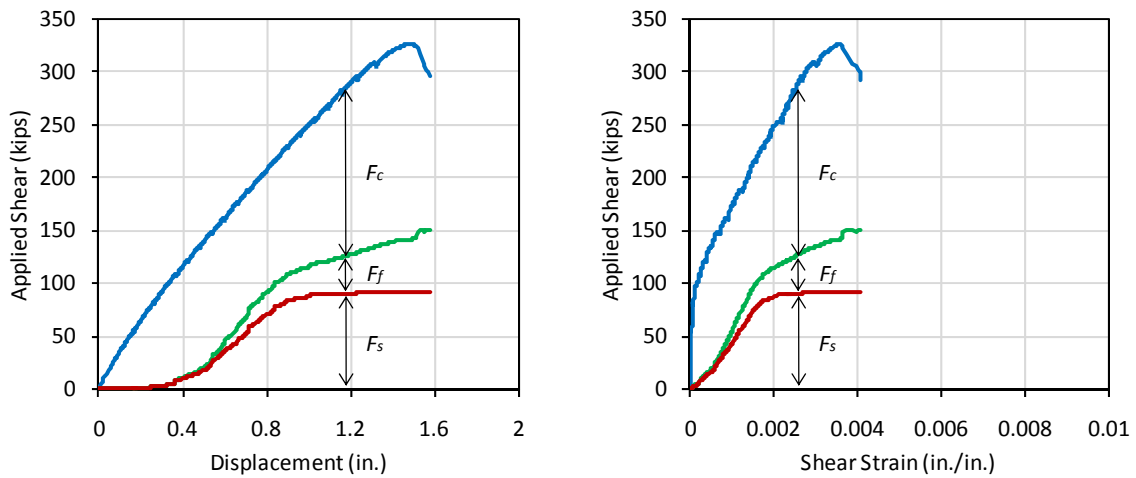
Figure 4-75 Component contribution to shear force vs. deformation response of 48-3-6r

The shear stiffness of 48-3-6r was much greater than that of similar beams, because critical crack occurred in a region outside of the points where shear measurements were determined as shown in Figure 4-76. As a result, the shear stiffness was over-estimated as discussed in Section 4.2.5
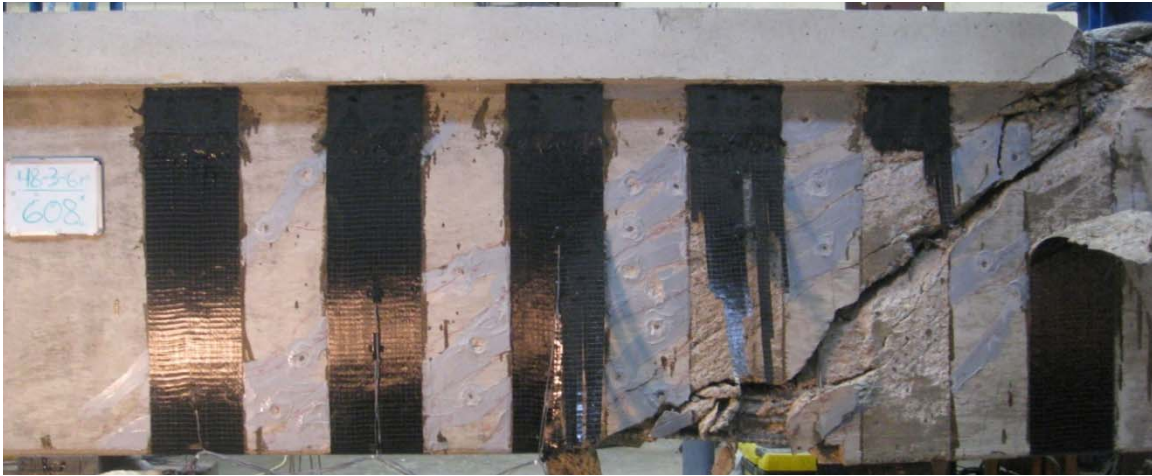
(a) Front side

(b) Back side

Figure 4-76 Photos of both sides of test 48-3-6r at ultimate

Figure 4-77 Photos of rupture of CFRP strip and anchor in test 48-3-6r

Most gages on the stirrups had residual strain from the previous test (48-3-6), but the effects of residual strain were not included in determining the steel contributions because most stirrups yielded and the stress-strain relationship was no longer linear and could not be monitored. When test 48-3-6 was unloaded, some stirrups might have been in compression because some cracks remained open. However, the residual stress could not be determined although residual strain was indicated by the strain readings as shown in Figure 4-78(a). Therefore, steel contribution in test 48-3-6r was evaluated without any adjustments for residual stress. Moreover, the critical cracks occurred away from gage locations, so it is likely that the steel shear contribution was under-estimated. The gage locations used to calculate the steel contribution are shown in Appendix E.

However, original stress-strain relationship might make steel contribution under-estimate because some additional stress would be obtained if the actual strain was large enough for strain hardening and the residual compression, if existed, might provide additional capacity (Figure 4-78 (b)). For these reasons, the maximum capacity of this test might not be compared with others.

(a) Residual strain from 48-3-6   (b) 48-3-6r
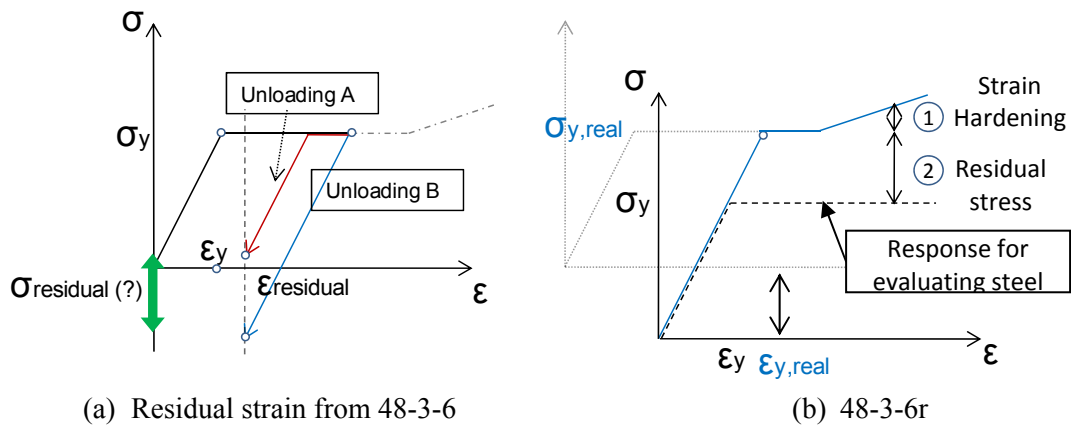
Figure 4-78 Conceptual approach of effect on residual strain from 48-3-6r

4.4.4.4 Test 48-3-7 (intermediate anchors)

Test 48-3-7 was identical to 48-3-5 except for the use of intermediate anchors. The purpose of immediate anchors was to increase stiffness and reduce cracking by reducing the effective length of the CFRP strips after debonding occurred. The strength of the specimen was not expected to increase because the amount of CFRP material did not change. As shown in Figure 4-80, the intermediate anchors were applied at the middle of the strip and fans were spread vertically in both directions. Therefore, it was difficult to monitor strain in the CFRP because no gage could be mounted at the anchor region.

The response of 48-3-7 is shown in Figure 4-79. At 94 k, a shallow shear crack occurred across strip D to E after several steep shear cracks occurred. At 121 k, the region around immediate anchors of strip D and strip E started to debond. At 134 k, stirrups started to yield. At 188 k, audible popping was heard due to debonding. At 215 k, the strain at FA1 was exceeded 0.01, but there was no evidence of rupture from visual observation. Therefore, FA1 was not considered as a reliable gage. The test was stopped at 242 k and the maximum CFRP strain (FD2r) was 0.0098 and the maximum crack width was 3/32 in.
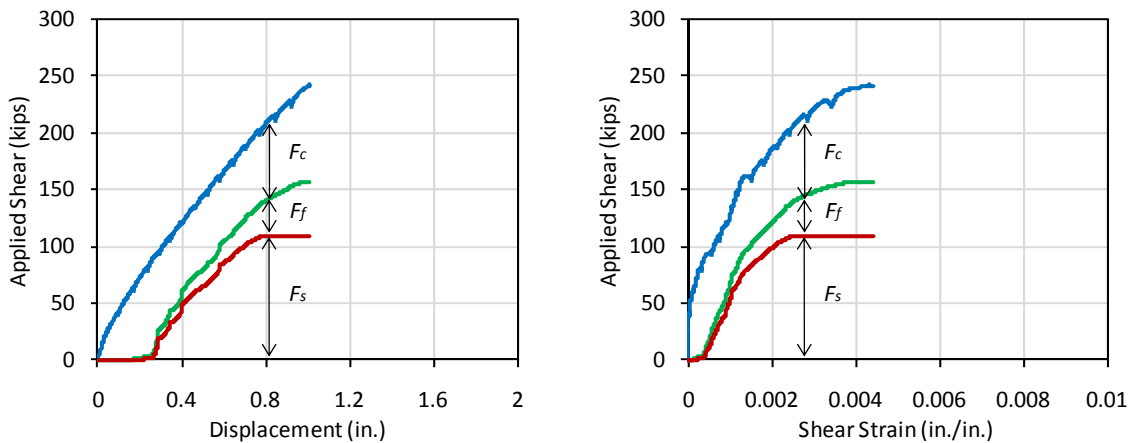
Figure 4-79 Component contribution to shear force vs. deformation response of 48-3-7

143
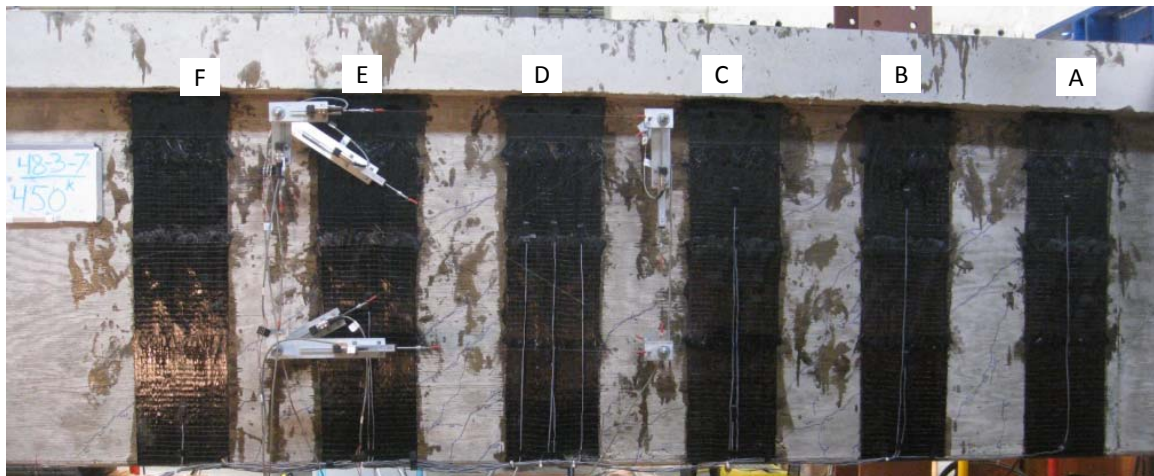
(a) Front side
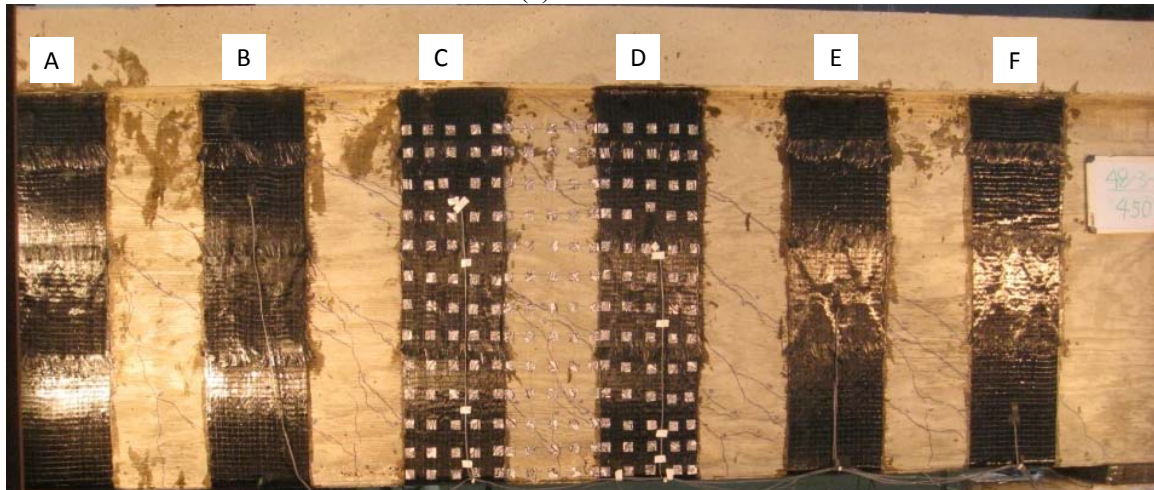
(b) Back side

***Figure 4-80 Photos of both sides of test 48-3-7 when load stopped***

debonding
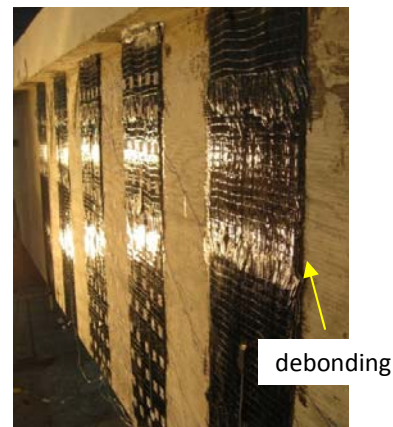
debonding

Figure 4-81 Photo of debonding of CFRP strip in test 48-3-7 when load stopped

144

4.4.4.5 Test 48-3-8 (2 layers)

Test 48-3-8 was conducted with two layers of CFRP strip in each to evaluate the effect of the amount of CFRP material.

The response of 48-3-8 is shown in Fig. 4-82. At 188 k, the steel strain at gage J4 was 0.0021, which indicated yielding of steel. The maximum CFRP strain was 0.0024 in gage FD2. At 228 k, strips B, C and D debonded and the maximum crack width was 0.05 in. The maximum shear in this test was 255 k and was maintained near that level as the beam displacement and shear strain increased. The shear dropped when several anchors fractured (Figure 4-84). No CFRP strip rupture was observed. Maximum recorded CFRP strain was 0.0079 (FE4) when the anchors fractured. The CFRP strain at maximum capacity was about 0.0048. The strain data indicates that after the steel stirrups yielded, the CFRP strips carried a higher portion of the total shear on the beam. (Figure 4-82)
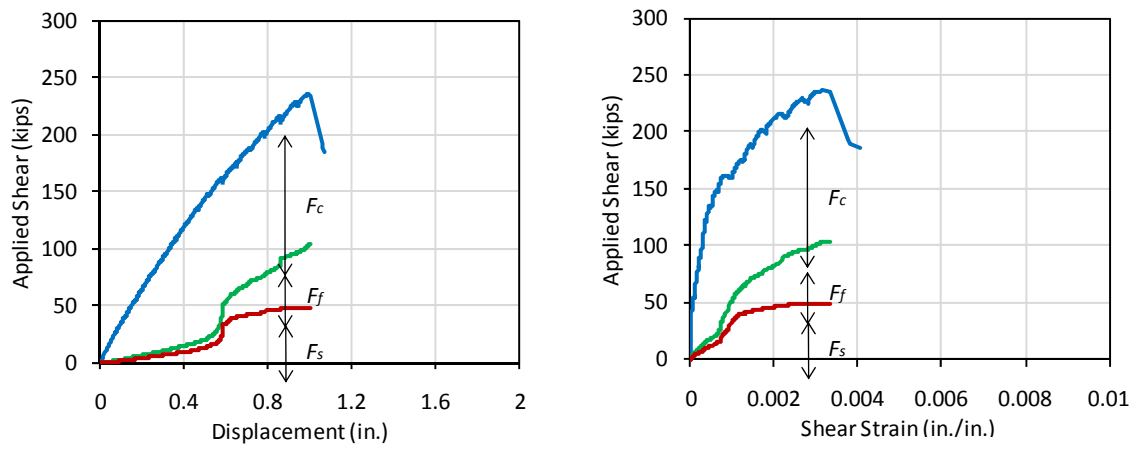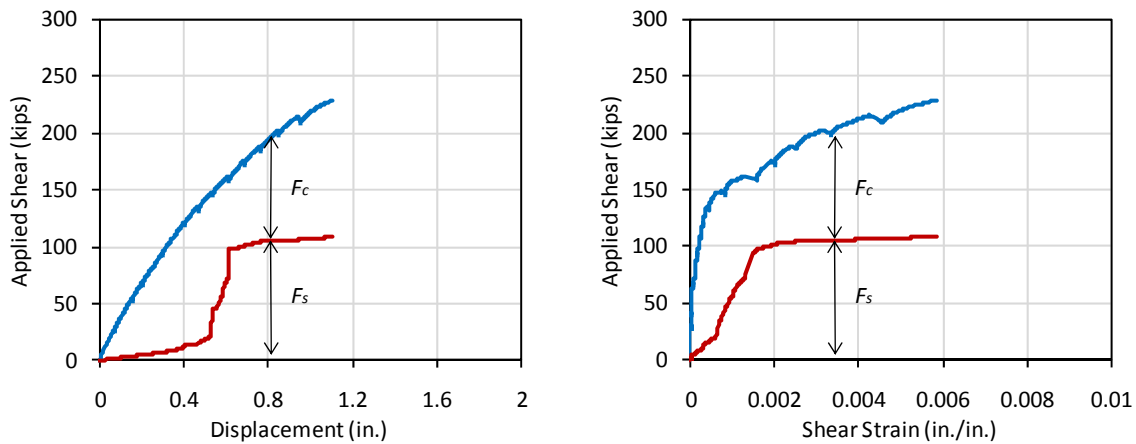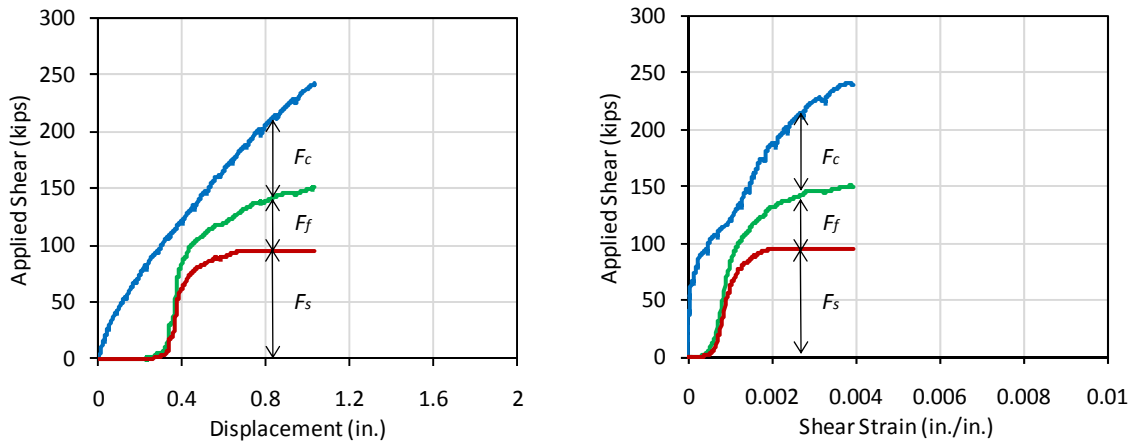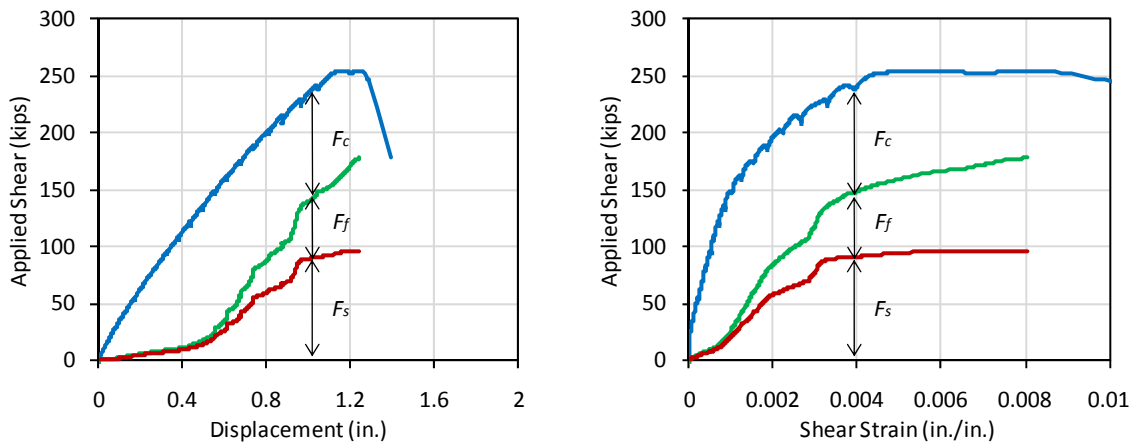

Figure 4-82 Component contribution to shear force vs. deformation response of 48-3-8
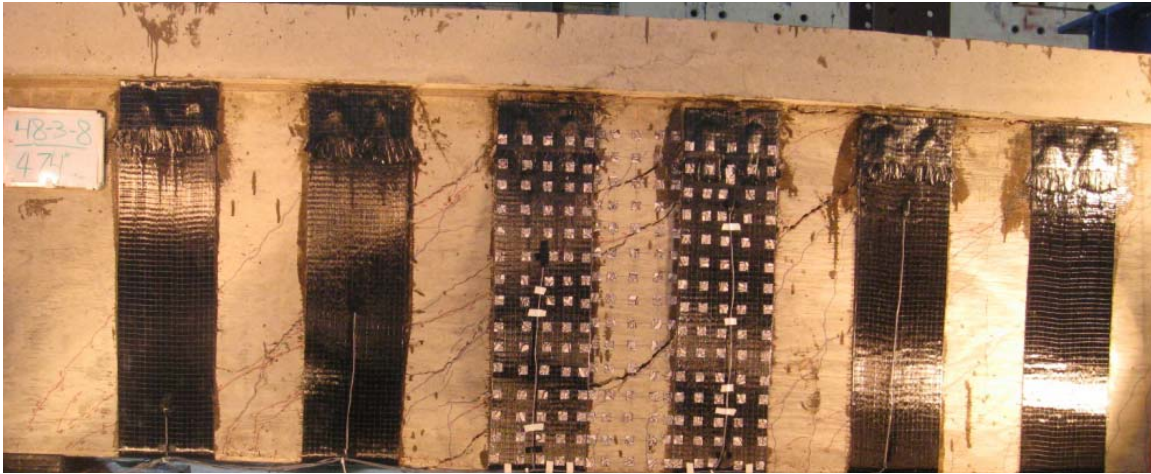
(a) Front side

(b) Back side

Figure 4-83 Photos of both sides of test 48-3-8 at ultimate load

Figure 4-84 Fracture of CFRP anchors

146

4.4.5 Shear Contribution of Each Material

The estimate of shear contribution of each material from calculated using design equations and from test measurements are presented in Table 4-7.

Table 4-7 Comparison between design estimate and test estimate

	V (k) from DESIGN EQ. (a)				F (k) from TEST (b)				RATIO (b) / (a)			
	V_c	V_s	V_f	V_n	F_c	F_s	F_f	F_n	F_c/V_c	F_s/V_s	F_f/V_f	F_n/V_n
24-3-1r	33	31	27	91	68	51	33	152	2.04	1.63	1.25	1.67
24-3-2	33	31		64	44	62		105	1.33	1.98		1.65
24-3-3	32	31	27	89	54	52	12	118	1.69	1.67	0.46	1.32
24-3-4	31	31	27	89	61	62	25	148*	1.99	1.98	0.96	1.68
24-3-5	31	31	25	91	60	54	31	145	1.76	1.72	1.23	1.60
24-3-6	34	31	56	120	57	42	37	135*	1.69	1.35	0.66	1.13
24-3-7	34	31	53	117	45	56	62	163*	1.40	1.81	1.16	1.40
24-3-8	32	31	53	118	38	56	59	153	1.14	1.80	1.10	1.30
24-3-9	34	31	10	74	37	59	13	109	1.12	1.91	1.30	1.48
24-3-10	33	31	27	89	55	57	34	146	1.77	1.82	1.27	1.64
24-2.1-1	35	31	27	92	84	51	35	170	2.42	1.65	1.31	1.84
24-2.1-2	34	31		66	67	62		129	1.95	1.98		1.96
24-1.5-1r	34	78	53	165	161	68	14	242	4.77	0.87	0.26	1.47
24-1.5-2	33	78	20	131	157	92	6	255	4.76	1.19	0.28	1.95
24-1.5-3	33	78		111	146	87		233	4.44	1.12		2.11
24-1.5-4	30	78	27	135	175	69	21	264	5.74	0.88	0.78	1.96
48-3-1	74	33		107	94	53		147	1.27	1.61		1.38
48-3-2	74	33	60	167	97	49	79	226	1.31	1.51	1.33	1.36
48-3-3	76	33	84	193	76	55	108	239	1.00	1.67	1.29	1.24
48-3-4	77	33	84	193	133	49	55*	236	1.72	1.48	0.66	1.22
48-3-5	75	59	60	194	91	96	55	242	1.21	1.62	0.92	1.25
48-3-6	75	59		134	120	109		228	1.59	1.85		1.70
48-3-6r	75	59	60	194	185	92	50	327	2.46	1.56	0.83	1.68
48-3-7	71	59	60	190	85	109	48	242	1.20	1.86	0.80	1.24
48-3-8	67	59	120	245	91	96	68	255	1.37	1.62	0.57	1.04

Note. Due to round-off error, total amount might not be the summation of each contribution.
  In test 24-3-4,6,7, the shear contribution were not evaluated from maximum shear, but close enough to maximum capacity and more representative the overall response.

In test 24-3-4, 24-3-6 and 24-3-7, the shear contributions were not evaluated from the maximum capacity. Test 24-3-4 reached the maximum capacity after rupture of one CFRP strip. In test 24-3-6 and test 24-3-7, the shear capacities remained the same value with increasing CFRP strain, so the concrete contribution decreased dramatically. Therefore, the evaluation was based on the point where the concrete contribution was reached. (Figure 4-85)

(a) 24-3-4   (b) 24-3-6
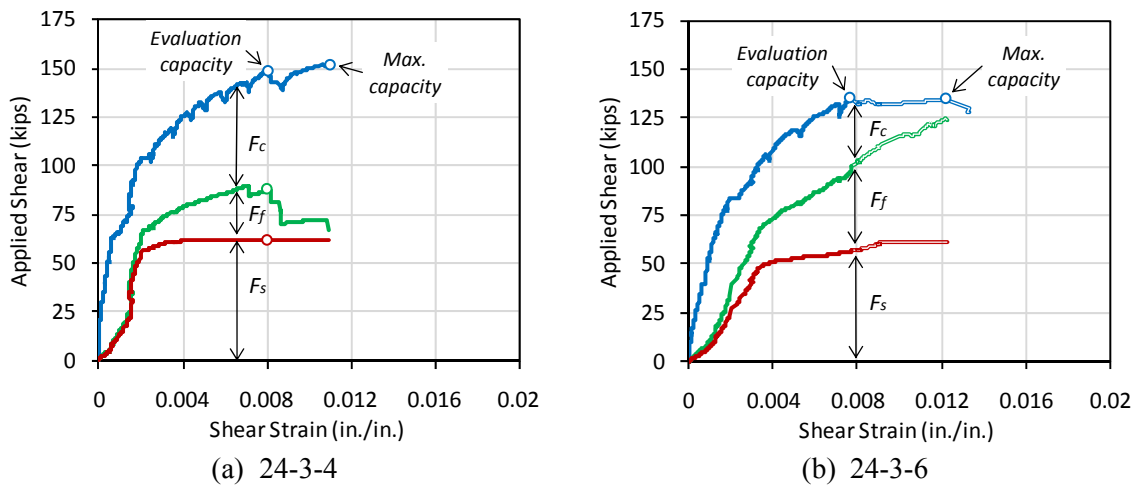
Figure 4-85 Cases in which the point of max. capacity was not used for evaluation

The CFRP shear contributions of tests with shear span to depth ratio of 1.5 were smaller than estimated and the concrete contributions were greater than estimated because the strength of deep beam was controlled by the concrete compressive strut additional capacity caused by arch action in the concrete strut. To remove the effect of the shear span to depth ratio, only the test results for shear-span-to depth ratio of 3 were included in the statistical summary shown in Table 4-8.

Table 4-8 Statistical summary of test results (a/d=3)

	24 in. (a/d=3) (10 tests)				48 in. (a/d=3) (8 tests)				All tests of a/d=3			
	F_c/V_c	F_s/V_s	F_f/V_f	F_n/V_n	F_c/V_c	F_s/V_s	F_f/V_f	F_n/V_n	F_c/V_c	F_s/V_s	F_f/V_f	F_n/V_n
Mean	1.43	2.03	1.04	1.49	1.41	1.70	0.91	1.34	1.42	1.87	0.99	1.42
Standard Deviation	0.29	0.22	0.30	0.19	0.44	0.14	0.30	0.23	0.36	0.25	0.29	0.22

All test capacities were greater than design estimates. CFRP shear contribution from test was close to design estimate in 24 in. beams and less than design value in 48 in. beams. It should be noted, however that mean value of capacity ratios in 48 in. beams was less than those of 24 in. beams because half of the 48 in. beams were not tested to failure.

The overall margin of safety came from conservative estimates of concrete and steel contributions rather than from the CFRP. For this reason, the design estimates of CFRP need to be more conservative to result in margins similar to those for the steel and concrete components of shear.

Test results in which failure mode was fracture of CFRP anchors were excluded. These includes tests 24-3-8 and 48-3-8 with two layers of CFRP strip, test 24-3-6 with dry lay-up failed at high rupture strain, and test 24-3-3 with poor application of CFRP. Due to improper gage location (48-3-4) and residual strain from previous test (48-3-6r), the shear contribution could not be evaluated properly. In addition, test 48-3-1, -3, -5, -6, and -7 were excluded because the loading was not taken to failure. The ratios from all other tests (filtered tests) are presented in Table 4-9 (a).

Compared with Table 4-8, the ratio of CFRP contribution increased because tests that failed by the fracture of CFRP anchor were excluded. Furthermore, the standard deviation of CFRP contribution decreased. Therefore, it is important to prevent fracture of CFRP anchor in order to get a more reliable design equation.

Table 4-9 Comparison between stopped tests and tests to failure (a/d=3)

	Tests to failure (24-3-1r,2,4,5,7,9,10, 48-3-2) (a)				Tests stopped before failure (48-3-1,3,5,6,7) (b)				(a) + (b)			
	F_c/V_c	F_s/V_s	F_c/V_c	F_c/V_c	F_c/V_c	F_c/V_c	F_f/V_f	F_n/V_n	F_c/V_c	F_s/V_s	F_f/V_f	F_n/V_n
Mean	1.54	1.80	1.20	1.53	1.22	1.78	1.00	1.36	1.43	1.79	1.15	1.47
Standard Deviation	0.35	0.16	0.12	0.15	0.21	0.12	0.25	0.20	0.34	0.14	0.18	0.18

The ratios evaluated from tests stopped before failure were presented in Table 4-9 (b) and compared with filtered tests. As expected, the mean of ratios were 12 percent less than that of filtered tests. It is evident from those ratios that the specimens were close to ultimate.

4.5 ANALYSIS OF RESULTS BY PARAMETERS

In Section 4.4, results were described for each test and shear contributions of concrete, steel and CFRP were evaluated from strain gages and compared with design estimates. However, the CFRP shear contribution cannot be taken independently without considering the role of CFRP in improving the concrete capacity by reducing crack widths. Furthermore, the presence of CFRP strips changes the steel shear contribution due to interaction between steel and CFRP. Therefore the shear contribution of CFRP was studied by comparing results with the control tests.

4.5.1 Control / Anchored

Each beam series included a control test which was not strengthened with CFRP in order to compare with strengthened tests.

Table 4-10 Comparison of design estimate and test capacity between control and strengthened tests

		V (k) from DESIGN EQ.			F (k) from TEST			RATIO		
		control test (a)	Strengthened (b)	**Increase due to CFRP** (c)	control test (d)	Strengthened (e)	**Increase due to CFRP** (f)	control test (a)/(d)	Strengthened (b)/(e)	**Effect of CFRP** (c)/(f)
24	a/d=1.5	110.1	136.6	**26.5**	233	264	**31** (13%)	2.1	1.9	**1.2**
	a/d=2.1	69.5	96	**26.5**	129	170	**41** (32%)	1.9	1.8	**1.6**
	a/d=3.0	69.5	96	**26.5**	105	152	**46** (44%)	1.5	1.6	**1.7**
48	#3@18"	120.7	180.6	**59.9**	147*	226	**79*** (54%)	1.2*	1.3	**1.3***
	#3@10"	146	205.9	**59.9**	228*	*242**	**14*** (6%)	1.6*	1.2*	**0.2***
	#3@10"(R)					327	**99*** (43%)		1.6	**1.7***

Note. 1) Estimates from design equation were based on the measured material properties.

2) To conduct two tests out of one beam, the applied load stopped before failure

150

Table 4-10 contains a summary of the shear estimated from design equations in ACI440.2R and compared with the estimates from test measurements and the corresponding responses of each case are shown in Figure 4-87. Some tests (48-3-3, 48-3-5, 48-3-7) were stopped when the monitored strain of CFRP was around 0.009 in order to conduct an additional test at the other end of the beam. As discussed before these tests might have had additional capacity, but it is likely that at least 90 percent of the ultimate strength was applied.

Test 24-3-1r was strengthened after cracking of specimen 24-3-1, the initial response is not appropriate due to residual deformation (Figure 4-12) that were not monitored. Test 24-3-9 was conducted without anchors, the response before debonding can be considered to represent the response of a strengthened beam with the same layout as 24-3-1r. The hybrid combination of these two responses is shown in Figure 4-86 and will be referred to 24-3-ref for comparison with other tests.
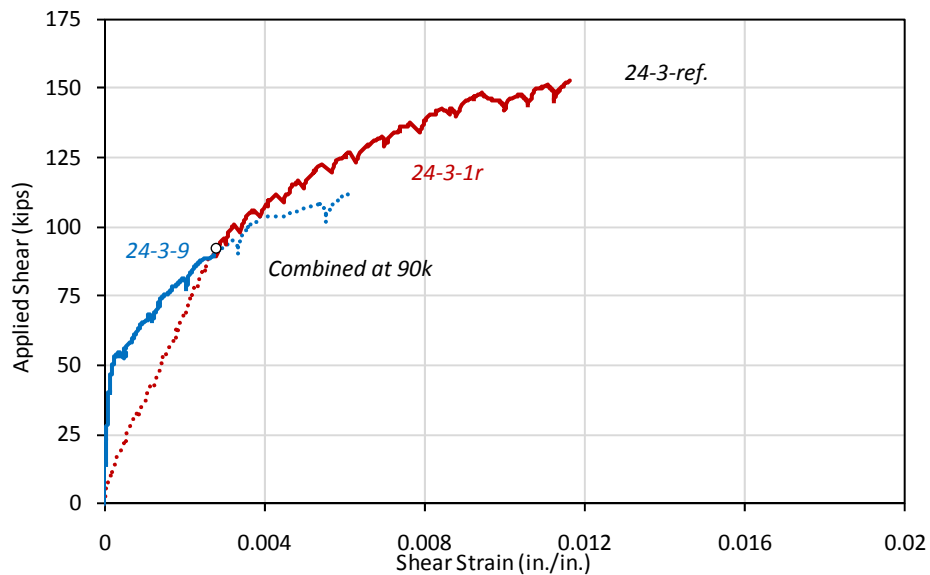
Figure 4-86 Response of 24-3-ref
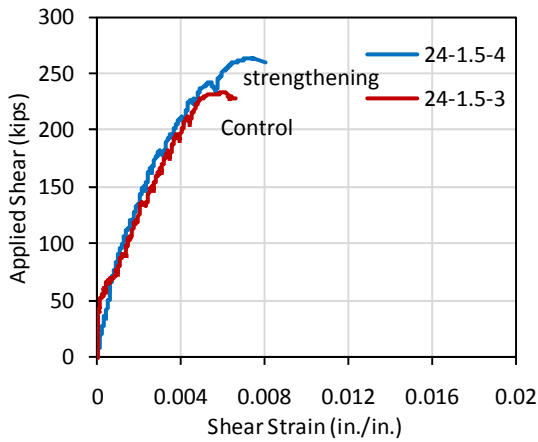
(a) a/d=1.5 (24 in. beam)
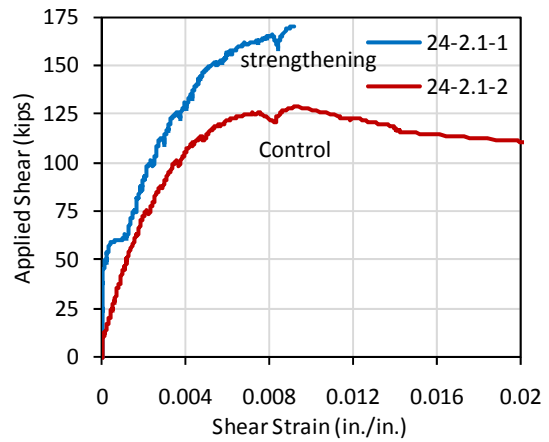
(b) a/d=2.1(24 in. beam)
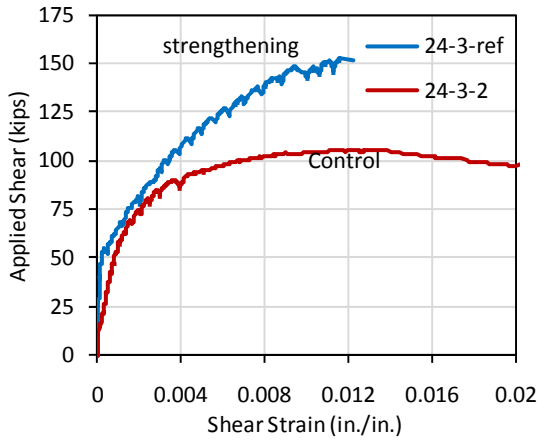
(c) a/d=3(24 in. beam)
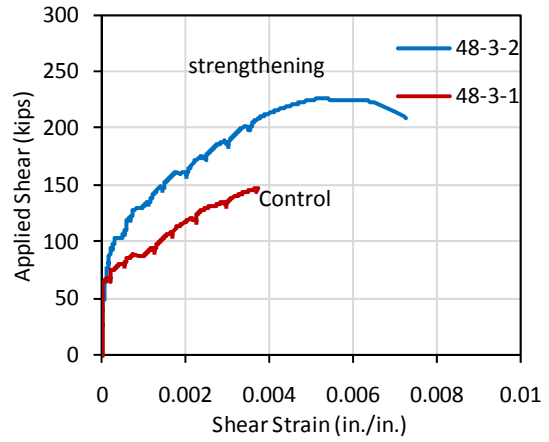
(d) #3@18" (48 in. beam)
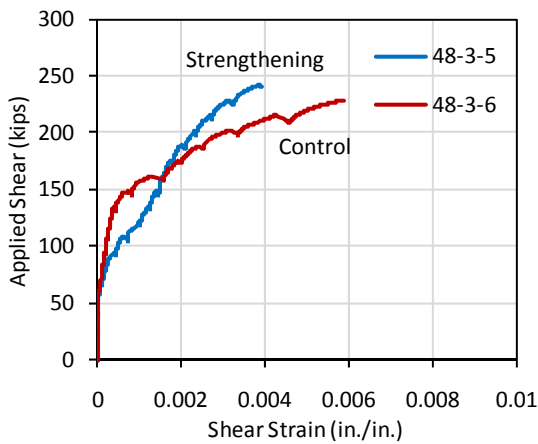
(e) #3@10" (48 in. beam)
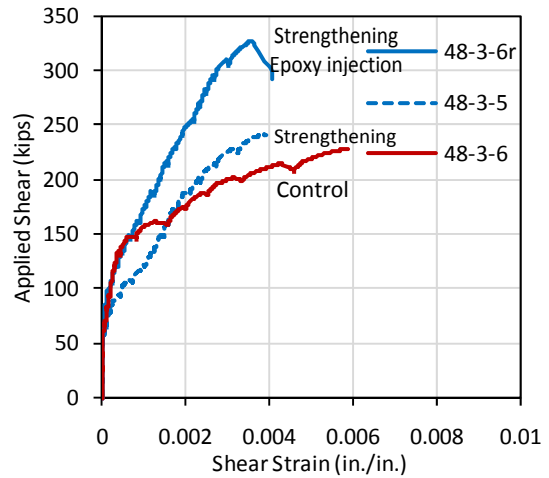
(f) #3@10" (epoxy injection)

Figure 4-87 Comparison of response between control test and strengthened test

152

The shear contributions of CFRP were greater than calculated using design equations except for 48-in. beams with a 10-in spacing of stirrups (test 48-3-5 and 6). However, the tests 48-3-5 and 48-3-6 were stopped before reaching maximum capacity. Therefore, any comparisons made using the values from these two tests are questionable. Although 48-3-6r was tested with the same FRP layout as 48-3-5, the capacity of 48-3-6r was 327 k, which is much greater than the capacity of 48-3-5. As discussed in Section 4.4.4.3, 48-3-6r was tested with residual stress and epoxy injection and the critical crack occurred at the region out of the shear measurements. Therefore, the unstrengthened and strengthened capacities of specimen having 10-in. spacing steel stirrups could not be evaluated directly. However, it is expected that the CFRP shear contribution ratio for a specimen having 10-in. spacing might be less than 1.3 because the ratios of specimens having 18-in. steel stirrup spacing was about 1.3 and with closer stirrup spacing, the control specimen would have additional capacity.
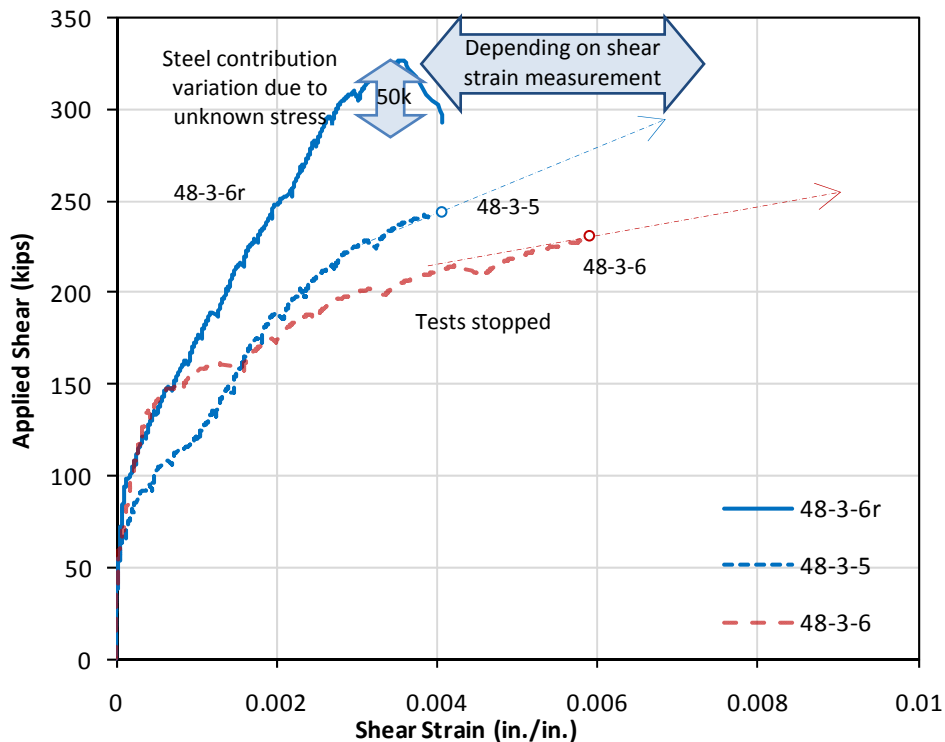
Figure 4-88 Estimates of responses in test 48-3-5, -6, and -6r

153

For the 24 in beams, the measured increase in load relative to the control test was greater than CFRP shear contribution determined from strain data as shown in Table 4-11. For the 48-in. beam tests, it is hard to compare between two values because some of the tests were stopped. In some cases, the location of the strain gage may not be at the point of maximum strain. Also it must be noted that the CFRP helps to increase the concrete shear capacity by controlling cracking and reducing the tensile strain of concrete.

Table 4-11 Comparison of CFRP shear contribution from measured strain gage and compared with difference in strength relative to control test

| | | CFRP shear contribution (k) | | (Test) |
		Compared with control test	From strain gage	
	a/d=1.5	31	21	24-1.5-4
24	a/d=2.1	41	35	24-2.1-1
	a/d=3	46	33	24-3-1r
	#3@18"	79*	79	48-3-2
48	#3@10"	14*	55	48-3-5
	#3@10"(R)	99*	50	48-3-6r

4.5.2 Shear Span to Depth Ratio

To evaluate the effect of shear span to depth ratio (a/d ratio) for shear strengthening, three different a/d ratios (1.5, 2.1 and 3.0) were used in 24-in. beams.

In Figure 4-89, the difference between strengthened and control beams with three different a/d ratios is shown. Test 24-1.5-3 (control) had much greater shear capacity and lower shear deformation capacity because the stirrup spacing was changed from 10 in. to 4 in. to satisfy deep beam code provision. However, the FRP shear contribution after strengthening is identical for three cases.
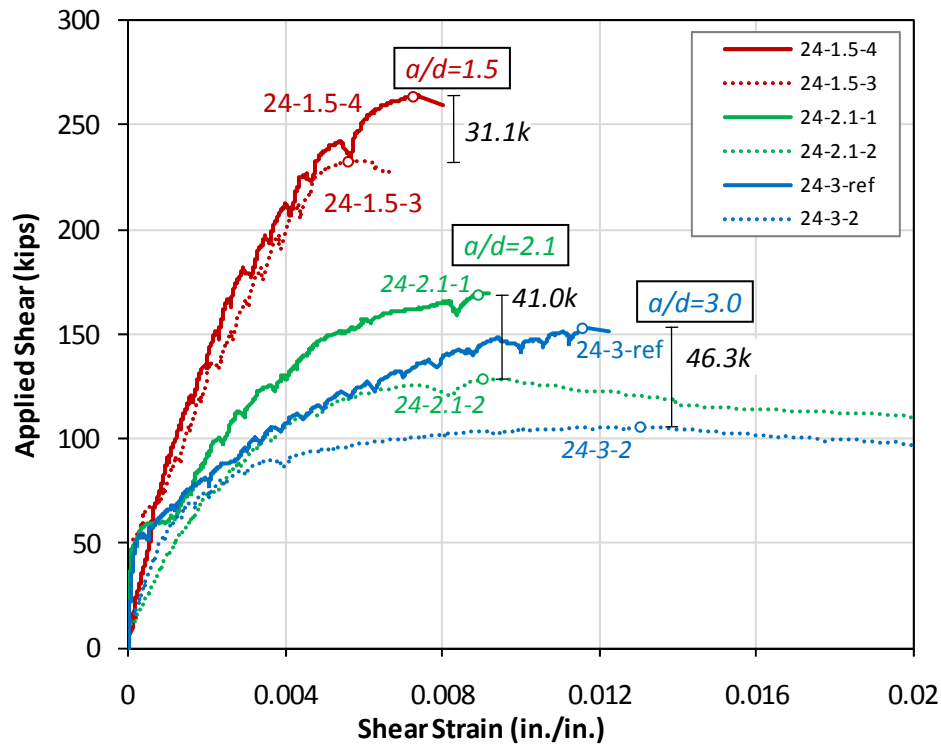
Figure 4-89 Comparison of response between control test and strengthened test according to shear span to depth ratio

In comparing 24-3-2 with 24-3-ref. and 24-2.1-2 with 24-2.1-1, the strengthened beams exhibited higher strength and failed at lower deformation. However, when comparing 24-1.5-3 with 24-1.5-4, there was little difference in stiffness and both beams failed at lower shear deformation capacity than the beams with higher a/d ratios. Therefore, the strengthening efficiency of beam with a/d ratio of 1.5 was less than others and the small increase in strength was due to increase in shear deformation at failure. It implied that strengthening efficiency depends on the geometry of beams to be repaired.

The shear efficiency of transverse reinforcement depends on the orientation of the critical crack, which means that beams with lower shear-span-to-depth-ratio have steeper critical angles and relatively less transverse reinforcement contributing to the shear capacity. Therefore, FRP shear contributions were 46 k (a/d=3), 41 k (a/d=2.1), and 31 k (a/d=1.5) although the estimates of FRP shear contribution were the same for all three cases.

155

Figure 4-90 shows the shear strain versus all tests with shear span to depth ratio of 1.5. Regardless of the CFRP strengthening, all responses are quite similar. The difference between them was that the capacity of strengthened beams was greater than that of control beam because ultimate shear strain was increased without changing stiffness much. This might be similar to the behavior of confined column, which means that most shear force was transferred by the direct concrete strut, not truss mechanism. In this case, the purpose of CFRP strengthening would be to decrease tensile strain perpendicular to principal strut and to increase concrete compression capacity by confining concrete strut. However, it is not clear that which parameter is more essential, shear-span-to-depth ratio or high transverse steel ratio. Therefore, further experimental studies will be needed for more accurate evaluation.
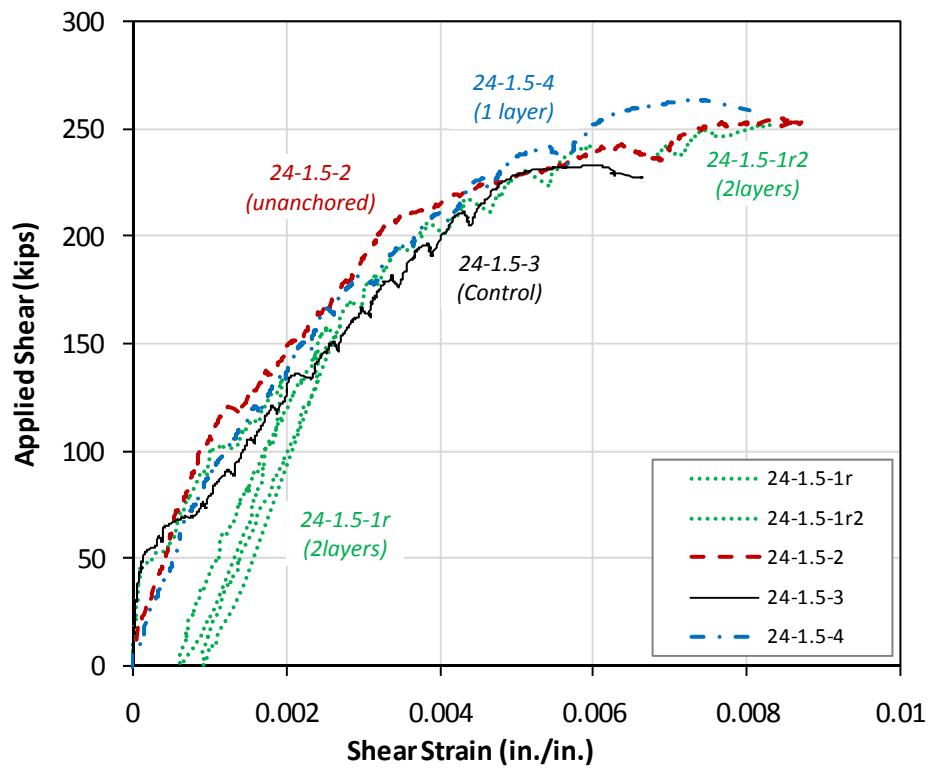
Figure 4-90 Comparison of response of shear-span-to-depth ratio of 1.5

4.5.3 Anchored / Un-Anchored

The main objective of this research was the evaluation of CFRP anchors. Many previous researchers have studied CFRP strengthening. Without anchorage, beams strengthened with CFRP were slightly stronger than unstrengthened beams, but they failed by premature debonding. In this program, 24-3-9 was tested without CFRP anchors and compared with 24-3-ref which was anchored test.
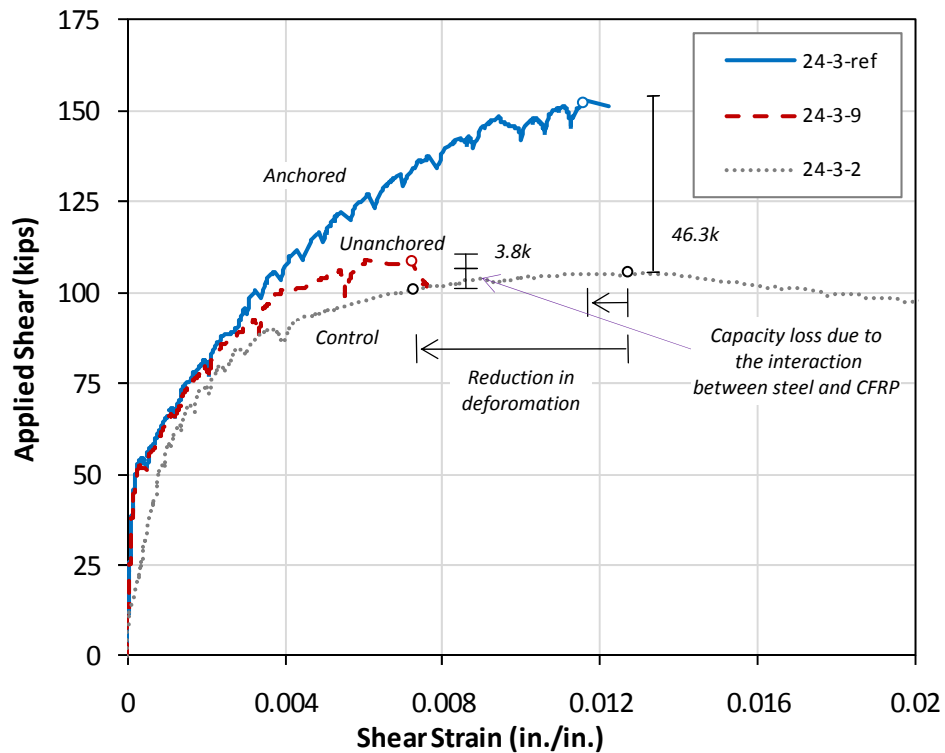
Figure 4-91 Comparison between with and without CFRP anchors

As shown in Figure 4-91, the initial response of an unanchored beam (24-3-2) was similar to the anchored beam (24-3-1r). However, when one strip started debonding, stiffness was reduced. The load dropped when a CFRP strip fully debonded from the concrete. The strain at debonding failure was around 0.004. The strength gain was 46.3 kips for anchored test and 3.8 kips for unanchored test. It is not only because un-anchored beam had a lower capacity, but it also deformed less at failure. The CFRP shear contribution at maximum capacity (shear strain =0.0072) of unanchored test (24-3-9) was

157

3.8 kips greater than that of unstrengthened test. Based on the effective strain of 0.004, the estimate was around 10 kips. In other words, maximum steel shear contribution was not obtained because the shear strain at maximum member capacity was reduced from 0.0132 to 0.0072. This situation is described in a simple and conceptual manner in Figure 4-92. In an unanchored test, some steel stirrups crossing the critical crack did not yield because the shear deformation at debonding was not sufficient to yield all stirrups when the FRP strips reached maximum capacity due to debonding. (Figure 4-92 (a)). However, it is likely that all steel stirrups crossing the critical crack will yield when FRP strips reach rupture strains. (Figure 4-92 (b))

(a) Unanchored   (b) Anchored
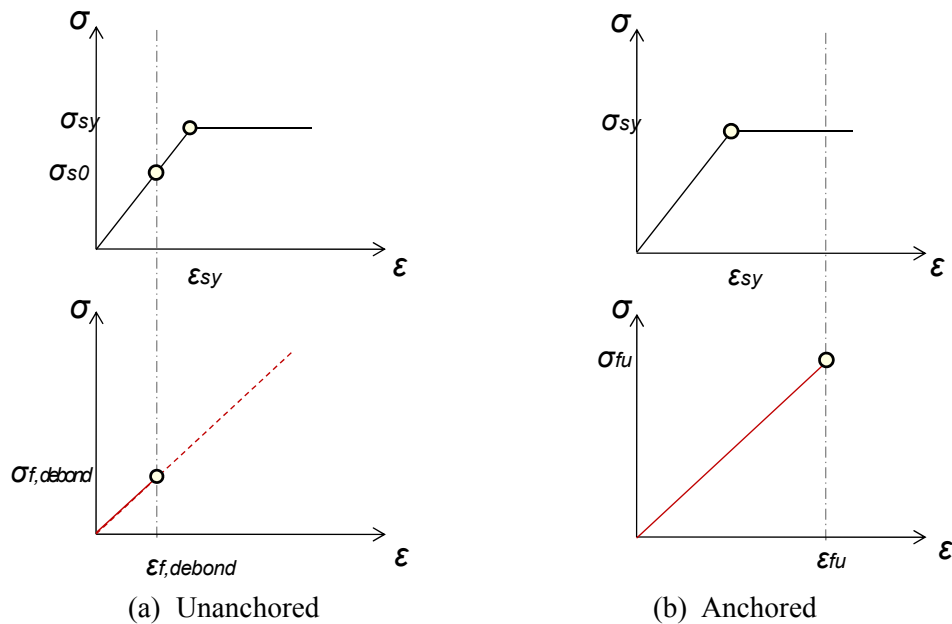
Figure 4-92 Influence of strain level in CFRP on steel contribution

Therefore, the shear deformation capacity after strengthening needs to be greater than the shear deformation at yielding of all stirrups for maximizing the steel contribution. It is also important to note that the shear contributions of steel and CFRP interact, so the steel and CFRP shear contribution cannot be superposed.

4.5.4 Amount of CFRP Material

Several tests were conducted to evaluate the effect of the amount of CFRP material on the CFRP shear contribution. Two layers of CFRP were applied in test 24-3-8 and 48-3-8. Unfortunately, these tests failed by fracture of CFRP anchors, not CFRP strips. However, it is still feasible to compare stiffness with other tests before failure. Test 48-3-3 had a 14-in. wide CFRP strip instead of a 10-in. wide strip. A continuous sheet was used in Test 24-3-7, which had double the amount of CFRP material and twice the number of CFRP anchors. This test failed by rupture of CFRP strip.

The responses between different amounts of CFRP material with same beam configuration are shown in Figure 4-93.
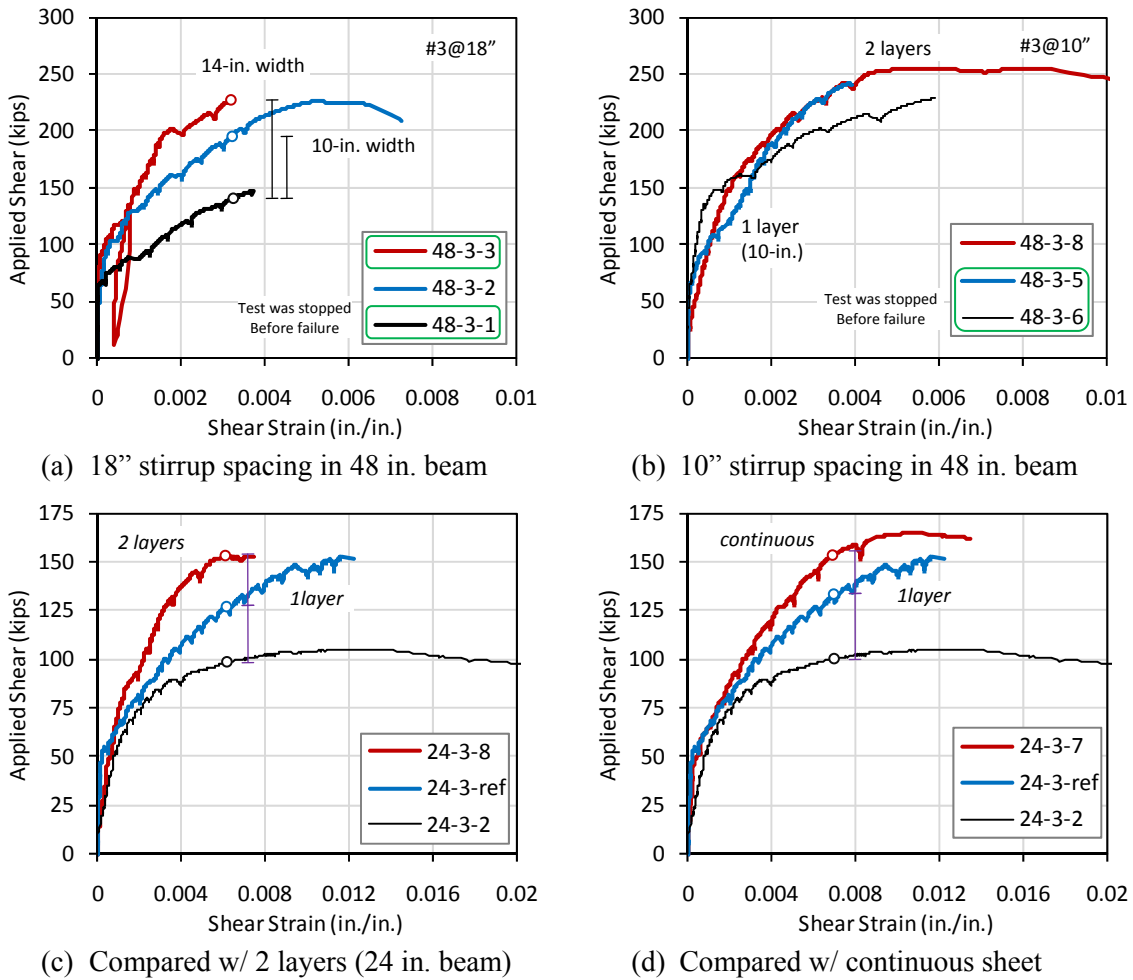
Figure 4-93 Comparison of the amount of CFRP material

159

The responses with different transverse ratio are shown in Figure 4-93 (a) and (b), but they could not be compared because the circled tests were stopped before failure. Furthermore, it seemed to be related to the transverse steel ratio because the effect of the amount of CFRP material was greater when the beam had lower transverse steel ratio.

As shown in Figure 4-93 (c) and (d), the CFRP shear contribution was not proportional to the amount of material because the shear strain at maximum capacity was decreased as the amount of material was increased. Compared with Figure 4-93 (c) and (d), the failure mode of continuous sheet was rupture of the sheet, whereas the failure mode of 2 layers was fracture of CFRP anchors. The difference between them was the number of anchor. Although the area of CFRP was doubled for 2 layers strip, stress concentration at the corner of CFRP anchors might be more than doubled. To develop the rupture of CFRP strip in multiple-layers, the CFRP anchor detail must be modified. The continuous sheet with more CFRP anchors had more redundancy and greater bond area between concrete and CFRP strip.

4.5.5   Different Transverse Steel Ratio

Many previous studies indicated that the transverse steel ratio influences CFRP shear contribution. As shown in Figure 4-94, the CFRP shear contribution of the beam with lower transverse steel ratio was greater although the same amount of CFRP material was used. Basically, CFRP strips have the same function as steel stirrups in a truss mechanism. Therefore, the shear force would be distributed according to the stiffness ratio of steel and CFRP. As a result, the shear force share of CFRP would be greater when a beam with low transverse steel ratio is strengthened. Furthermore, as transverse reinforcement ratio increased, the critical crack angle seems to be steeper and fewer FRP strips and steel stirrups contribute to the shear resistance. Therefore, the amount of steel transverse reinforcement is an important factor in evaluating CFRP shear contribution.
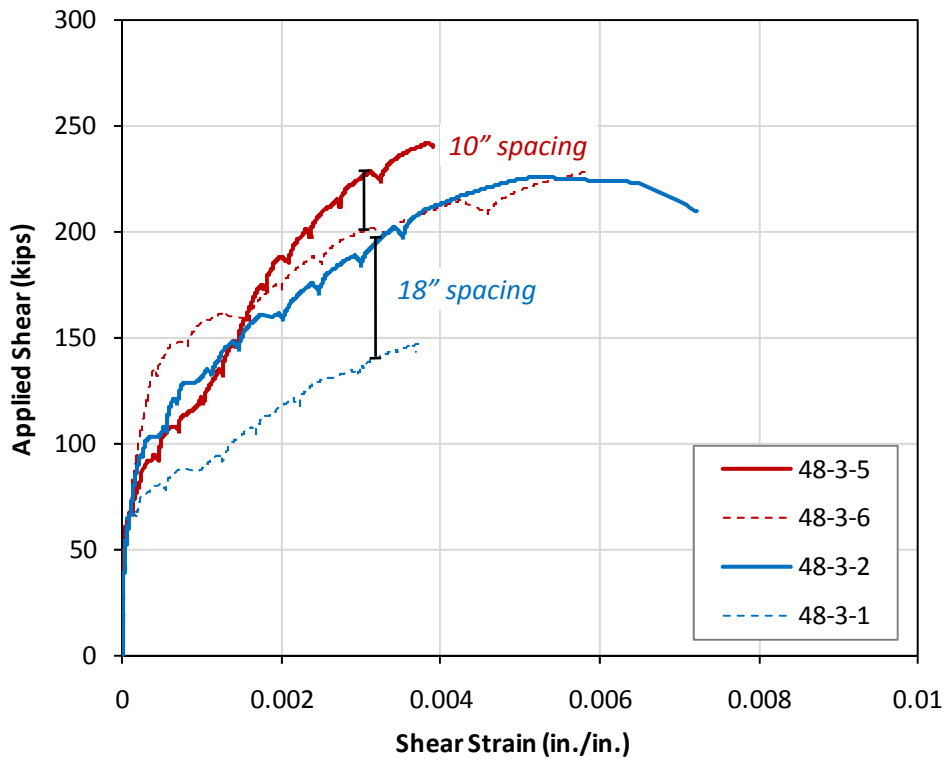
Figure 4-94 Comparison of test results according to different transverse steel ratio

4.5.6 Different CFRP Material Properties

To evaluate the performance of CFRP anchors with different material properties such as low stiffness and high rupture strain, test 24-3-5 and 24-3-6 were conducted.

Table 4-12 summarizes the design and test capacity of different laminates. The CFRP shear contribution of laminate C was less than the design estimate although the capacity of test 24-3-6 was greater than estimated. If a control test had not been conducted, the CFRP contribution might have been over-estimated.

Table 4-12 Comparison between estimate and test of different laminates

	EQUATION			TEST			RATIO TEST/EQUATION		
	control test	strengt hening	**CFRP**	control test	strengt hening	**CFRP**	control test	strengt hening	**CFRP**
24-3-1r (A)		89.9	26.5		151.6	46.3		1.69	1.75
24-3-5 (B)	63.4	88.8	25.4	105.3	145.1	39.8	1.66	1.63	1.57
24-3-6 (C)		118.9	55.5		133.8	28.5		1.13	0.51

161
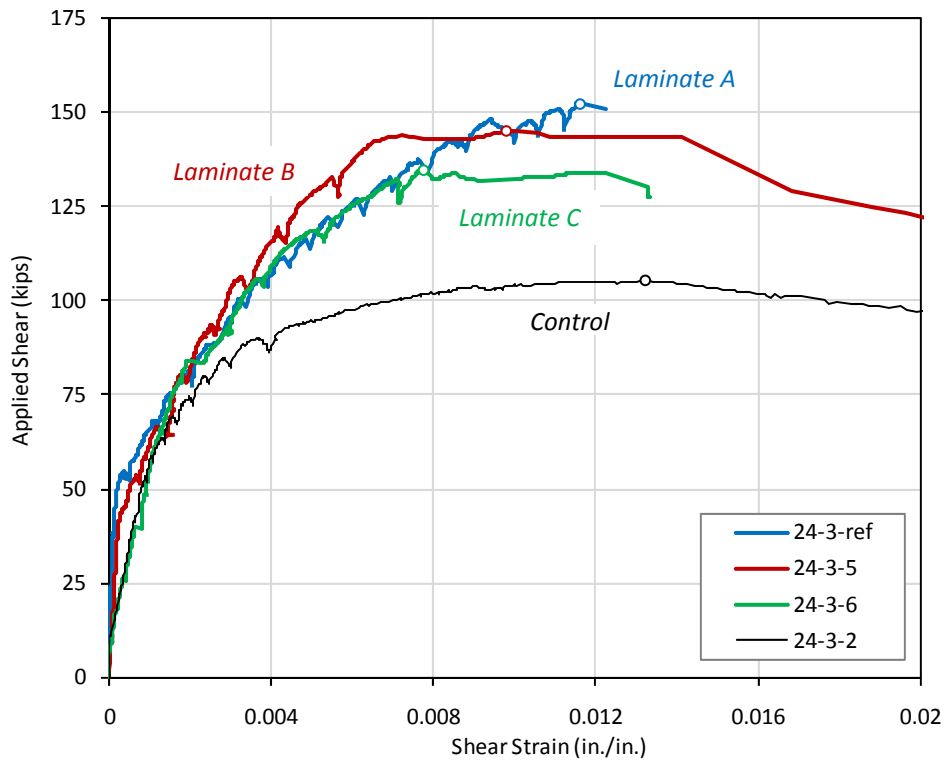
Figure 4-95 Comparison of test results of different laminates

Using the data from manufacturer's specifications, the estimated ultimate strength of laminate C was much greater than A and B because the rupture strain of laminate C was much greater. However, the responses of the three different laminates were similar because the stiffness of these laminates from tests was similar as shown in Figure 4-95. However, the shear capacity using laminate C was lower than others because its rupture strain was not reached when the member reached maximum capacity. As a result, the effective strain of laminate C was similar to or less than that of other laminates.

The CFRP anchors from three manufacturers performed well. By using the same material in the CFRP strip and the anchor, the design was simplified. However, if the laminates have high rupture strains, failure of the specimen may occur before the CFRP reaches its maximum capacity. Therefore, an upper limitation effective strain should be set.

4.5.7 Surface Condition
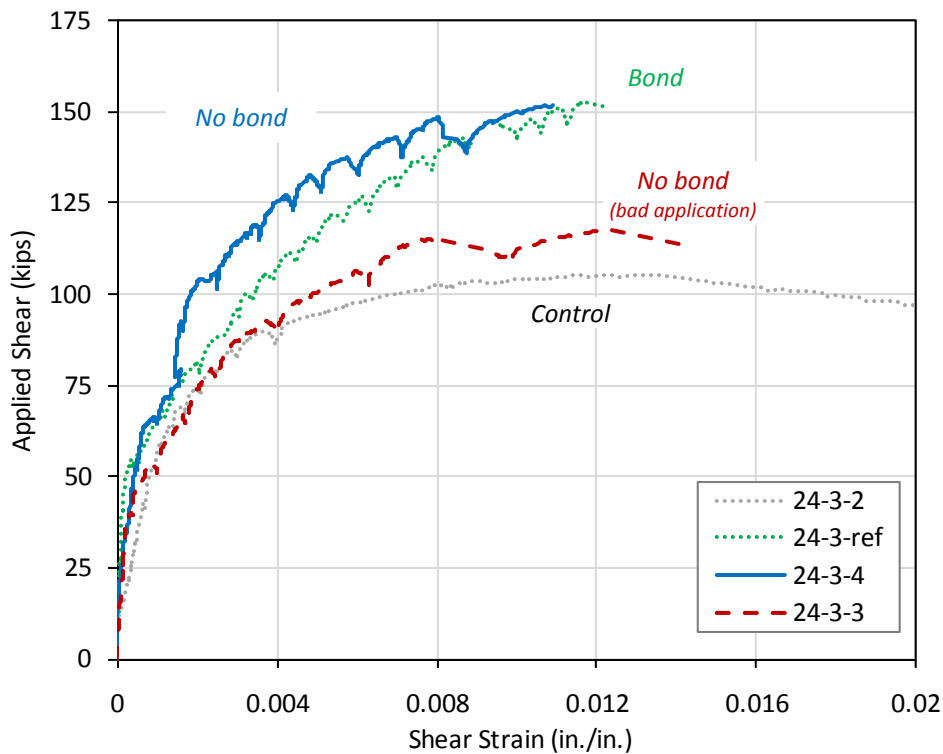
Figure 4-96 Comparison of test results with and without bond

As shown in Figure 4-96, the maximum capacity of 24-3-4(no bond) was the same as that of 24-3-ref. It implied that bond was not essential for strength. However, before debonding occurred the member with the bonded CFRP was stiffer than the member with the un-bonded CFRP. In a bonded strip, high strains were concentrated near the diagonal crack, whereas in an unbonded strip, strains were distributed over a longer distance. At early stages of loading, however, the shear stiffness was determined by the concrete with the CFRP strips, whether bonded or not, having little influence. In addition, the member with the un-bonded CFRP allows more CFRP strip to contribute to the capacity

In test 24-3-3, CFRP strips and anchors were not properly applied and the maximum capacity was less than 24-3-ref because failure was initiated by fracture of

CFRP anchors. However, it serves as demonstration of the importance of the quality control of application.

4.5.8 Size Effect / Depth of Beam

As the depth of beam was doubled and other parameters remained same, doubled shear capacity was expected in 48-in. beam. However, there was unfortunately no conclusion from this data because tests 48-3-5 and 48-3-6 were not conducted up to failure. From visual observation, 48 in. depth beams exhibited a more violent failure than 24 in. depth beams because of the higher released energy in the longer CFRP strips which was transferred to the steel stirrups causing them to fail almost immediately.
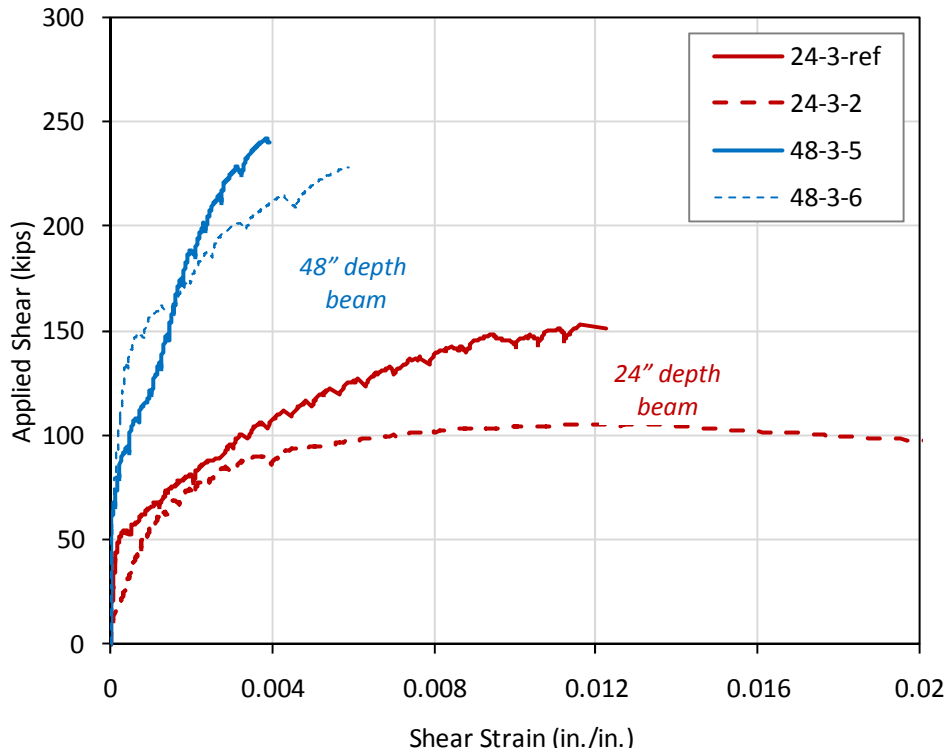
Figure 4-97 Comparison of test results between 24 in. beams and 48 in. beams

4.5.9 CFRP Strip Layout

Although the same amount of CFRP material is used to strengthen a beam, the shear capacity could be influenced by the CFRP layout. Because most tests were conducted with 5-in. strips with a 5-in. net spacing for 24-in. beams and 10-in. strips with

164

a 10-in. net spacing for 48 in. beams, the performance of other FRP strip layouts such continuous sheets and diagonal strips was evaluated. These tests were compared with the tests with vertical strips having the same amount of FRP material respectively.

4.5.9.1 Continuous sheet and multiple layer layout

Test 24-3-7 was conducted with continuous sheet and this test was also had the same amount of material as Test 24-3-8 (2 layers). Each test observations were described in Section 4.3.1.7 and 4.3.1.8. As shown in Figure 4-98, the capacity of the continuous sheet was higher, but the shear stiffness with two layers was higher. In the continuous sheet, the CFRP laminates were more uniform distributed and the number of anchor was doubled although the area of each anchor was half of that of 24-3-8. The continuous layout allowed more stress redistribution. The stress concentration at the CFRP anchor was smaller in the continuous layout. Although the failure mode in test 24-3-8 could have changed from fracture of CFRP anchor to rupture of CFRP strip, the maximum capacity would be expected to equal or less that of 24-3-7.
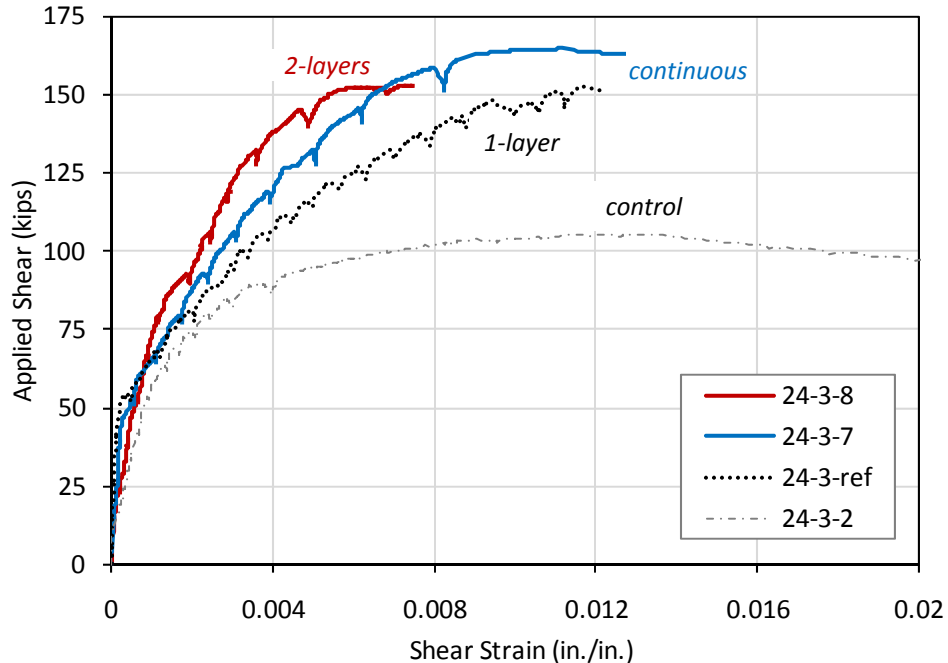
Figure 4-98 Comparison of test results between continuous sheet and multi-layers strip

4.5.9.2 Diagonal layout

If the crack location is known, the best direction of CFRP strip is basically perpendicular to the crack. For this reason, the shear design equation has an additional term to consider this effect based on 45 degree crack angle. Diagonal application would increase shear capacity. However, more material will be needed in diagonal application because the length of strip will be increased. In addition, the field application of diagonal strip will be more difficult than that of vertical strip because U-wrapping cannot be applied and the strips must be lapped.
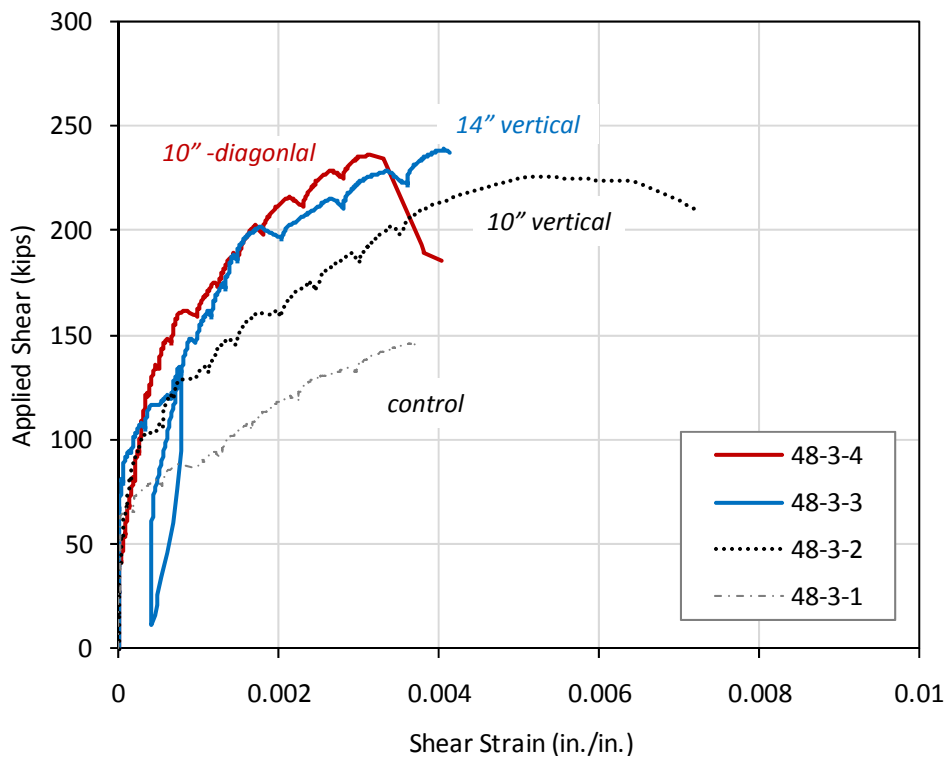
Figure 4-99 Comparison of test results for evaluating the feasibility of diagonal strips

Based on the shear equation (11-3) in ACI 440.2R, the CFRP shear contribution in this application should increase 41 percents from 60 k to 84 k by changing the direction of the CFRP strip. It implied that the shear capacity of 48-3-4 was expected to at least 24 k greater than that of 48-3-2. However, the maximum capacity was only 10 k greater than that of 48-3-2. Furthermore, this capacity was 6 k less than shear capacity of

48-3-3 although the capacity of 48-3-3 may have been greater, but the test was stopped. It cannot be concluded from just one comparison, but a wider strip in vertical application would be more feasible. As a result, diagonal application may not be a good solution for general beams.

4.5.10 CFRP Anchor Layout

This research focuses on the shear behavior of beam strengthened with CFRP, not CFRP anchor behavior. It is desirable to optimize the design, but it is not scope of this research. Therefore, although anchor design is not optimized, it does not matter if CFRP anchors work properly. The purpose of CFRP anchor is simply to develop the rupture of CFRP strip, which means that an over-designed CFRP anchor is acceptable. The large number of CFRP anchors with small cross-section area performed better, but it will require more labor and overall capacity will still be determined by the area of the CFRP strip. Therefore, tests shown below were intended to change other parameters. Inclined anchors could increase the effective depth by increasing enclosed concrete area and intermediate anchors could increase the stiffness of CFRP strip by reducing fully-debonded length.

4.5.10.1 Inclined anchors

Although the capacity of this test was expected to be greater than 24-3-1r because the effective depth of the strengthened web was slightly longer than that of 24-3-1r, the maximum capacity in test 24-3-10 was 7 k less than that of 24-3-1r (152 k) as shown in Figure 4-100. It was observed that the CFRP anchor was located in the middle of a crack as shown in Figure 4-101. The crack may have triggered failure. Because the anchor did not perform well enough to develop rupture of CFRP, the shear capacity decreased. Therefore, it is recommended that a simple parametric study needs to be conducted for evaluating CFRP inclined anchor performance only. In addition, if increase in effective length caused by inclining anchors is negligible, inclined CFRP anchor should not be considered.

167
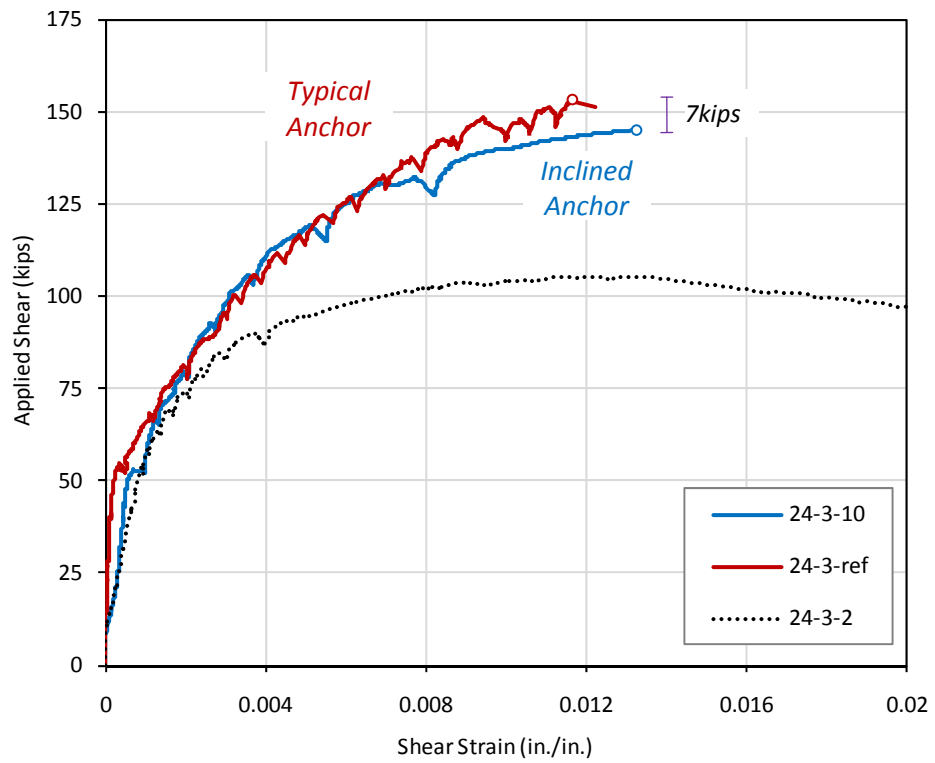
Figure 4-100 Comparison between inclined anchor and typical anchor

Figure 4-101 Anchor fracture in test 24-3-10

168

4.5.10.2 Intermediate anchors
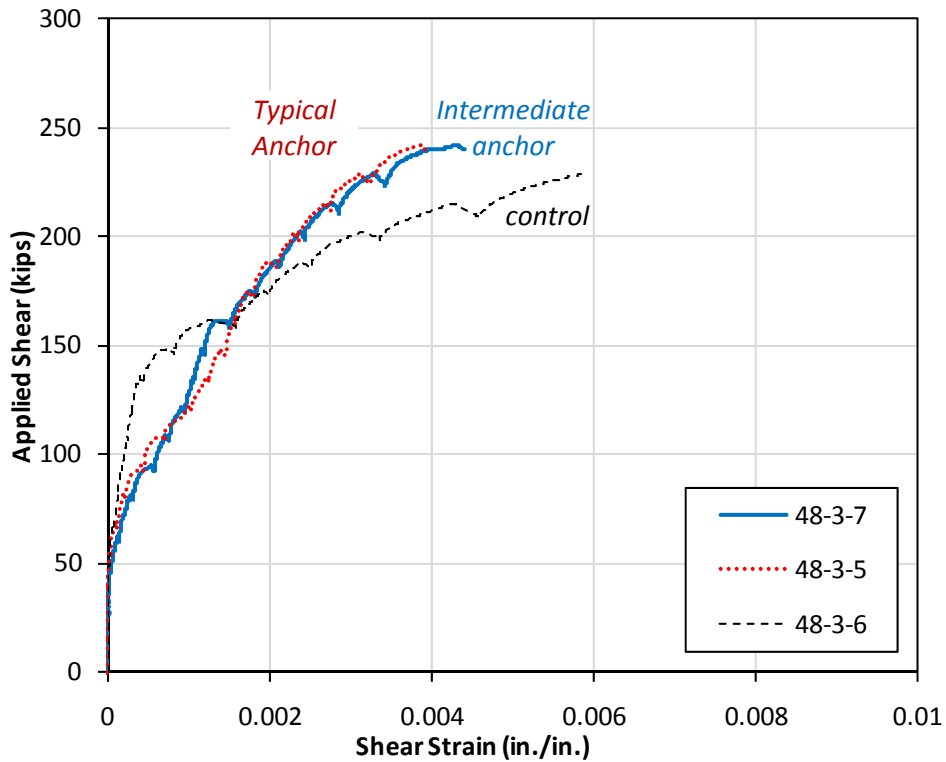
Figure 4-102 Comparison of behavior test with intermediate anchor

As seen in Figure 4-102, the response of test with intermediate anchors was not different from the response of test without intermediate anchors. It is not possible to compare capacity because all responses shown in this graph did not reach their maximum capacity. The location around an intermediate anchor is not appropriate for a strain gage because the local strain distribution might be varied within the small region. Therefore, to monitor the strain around intermediate anchor, strains were evaluated from camera images as shown in Figure 4-103. From this figure, it was also observed that the strain distributions both along the fiber and across the width are not uniform. It implies that the strain should be different depending on the location of gage. Furthermore, intermediate anchors decreased the debonded length and increased the stiffness of individual CFRP strips but overall stiffness was not much different.

169

The benefit of immediate anchors might reduce the risk due to explosive rupture of CFRP with large elongation. However, this benefit might not be attractive enough to add anchors at mid-height.
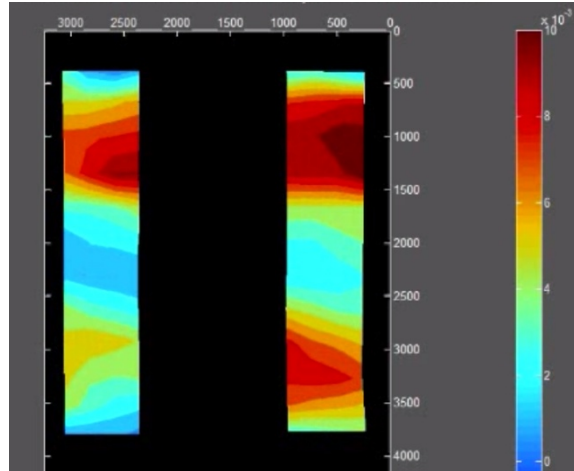
Figure 4-103 Strain distribution in the CFRP from camera image

4.6   SUMMARY OF TEST PERFORMANCE AT MAJOR EVENTS

The shear forces at several criteria listed below were collected and these forces were normalized with maximum capacity from the test.

1. Criteria based on steel stirrups

    1) first yielding of steel stirrup

    2) all stirrups crossing the critical section reach yield

2. Criteria based on CFRP strips

    1) maximum strain of 0.004 in the CFRP

    2) average strain of 0.004 in the CFRP

    3) maximum strain of 0.009 in the CFRP

These criteria were selected because they represent major events in the response of the specimens. The rate of increase in the steel shear contribution decreased after first yielding of a stirrup. As a result, the overall shear stiffness of the specimen decreased gradually, In addition, CFRP strips generally started to debond at a maximum strain in

the CFRP of 0.004. As the debonded length of the CFRP strip increased, the stiffness of the strip decreased dramatically.

Once all stirrups crossing the critical crack yielded, the steel shear contribution did not increase further. Next, a maximum strain of 0.009 in the CFRP indicates that the maximum capacity has nearly been reached. A strain of 0.009 is just 0.001 less than rupture strain (about 0.01) of the CFRP material used in this experimental program and it was observed that the strain increased dramatically with little increase in load after a strain of 0.009 was reached. Finally, the load at average strain in the CFRP of 0.004 is also important because a strain of 0.004 is the current limitation of ACI 440.2R for design of CFRP shear applications. The purpose of this limitation is mainly to prevent the loss of concrete capacity due to large tensile strain.

Figure 4-104 shows the normalized ratio of all tests with a/d ratio of 3. Test 48-3-1, 3, 5, 6, and 7 did not reach its maximum capacity, but the normalized values were not much different than those of other tests. For this reason, these tests were included in statistical analysis. Because the tests were conducted with a variety of test parameters, the points of normalized strength were scattered. In addition, the use of strains has a disadvantage in that the gage value represents only local strain.

In indicated in Figure 4-104 and Table 4-13, the loads at first yielding of a steel stirrup and maximum strain of 0.004 in the CFRP occurred at about 2/3 of maximum capacity. The displacements at these loads were 50% and 60% of displacement at max. capacity, respectively. The normalized shear strains were 27% and 40%, respectively. Most shear deformation occurred after these two events.

In addition, the standard deviation of the capacity ratio in loads at criteria (1), (2), and (3) were much less than that of in loads at criteria (4) and (5) and the standard deviation of the ratio at maximum CFRP strain of 0.009 was the lowest.

171
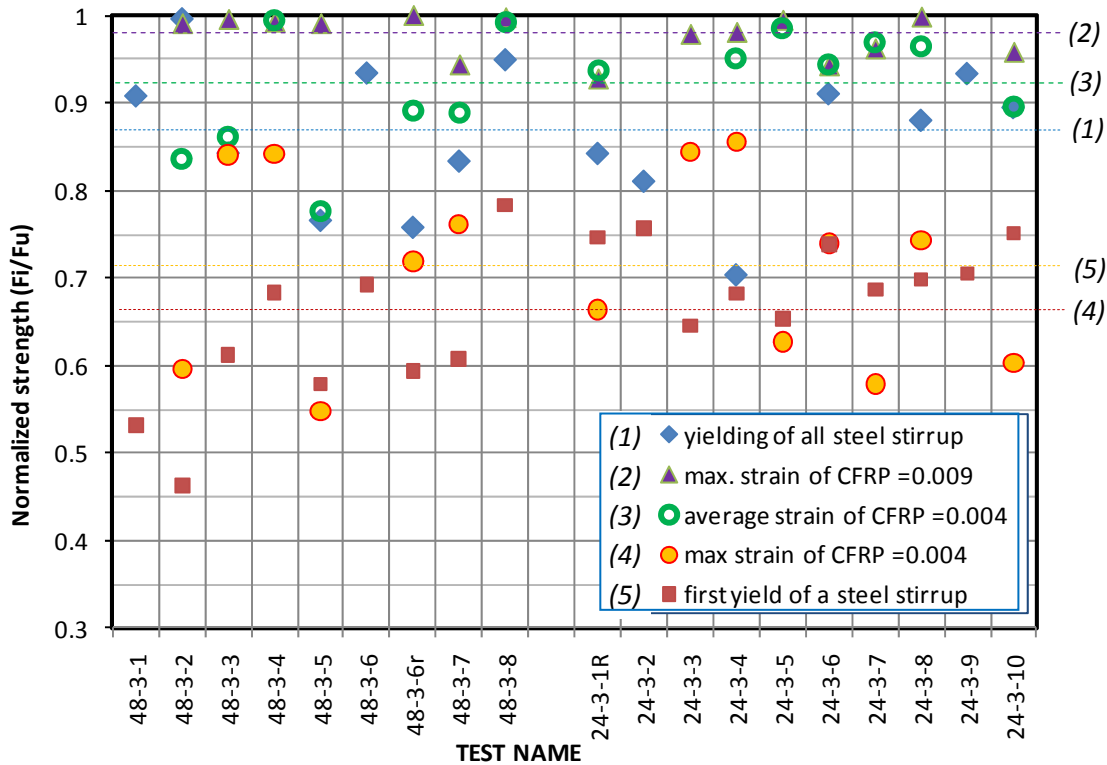
Figure 4-104 Normalized load ratio about maximum load of various loading levels

Table 4-13 Summary of load ratio at major events

	(1) Yielding of all stirrups	(2) $\varepsilon_{f,max} = 0.009$	(3) $\varepsilon_{f,avg} = 0.004$	(4) First yielding of a stirrup	(5) $\varepsilon_{f,max} = 0.004$
MEAN	0.87	0.98	0.92	0.66	0.71
STD.	0.081	0.024	0.065	0.083	0.109
COV.	9%	2%	7%	13%	15%

In the beginning of this research project, a rupture strain was considered to be an effective strain if CFRP rupture can be achieved through the use of CFRP anchors. However, all CFRP strips crossing critical crack did not rupture simultaneously Because CFRP shear contribution must be the summation of all CFRP strip contributions, the effective strain for design equation should be taken as the average strain of all strips crossing critical crack.

As shown in Figure 4-105, the average strain was monitored when the maximum CFRP strain reached 0.009. The mean of average strain in the CFRP was 0.0051 and this value was greater than 0.004 which is the strain limitation in ACI 440.2R shear applications. However, the standard variation of 0.0009 (COV.=17%) showed that average strains were inconsistent. Because average strain is different depending on strain distribution across the critical crack, it is not easy to determine the average strain as a single value for design.
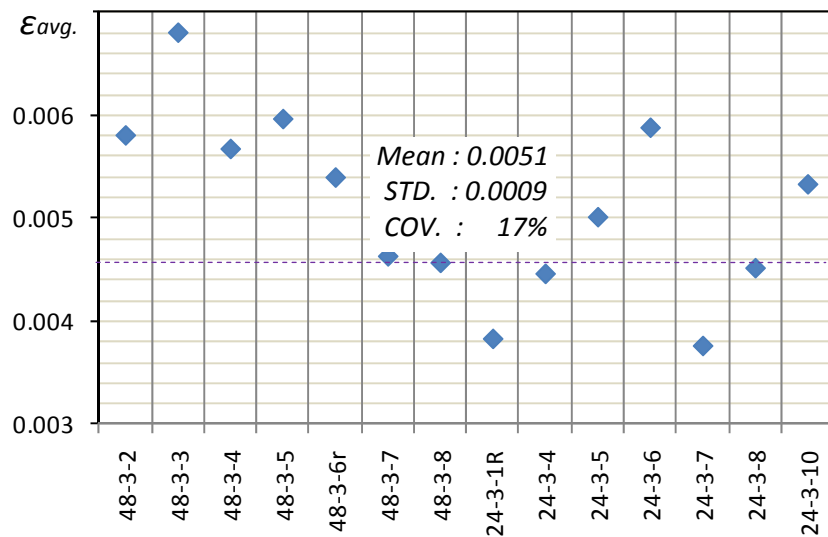
Figure 4-105 Average strain in the CFRP when the maximum strain of 0.009

The strain distribution in the steel stirrup was also not uniform. However, the stress distribution would be uniform regardless of non-uniform strain distribution if all stirrups across the critical section yield strain. For this reason, the steel shear contribution can be evaluated more easily than the CFRP shear contribution because the CFRP shear contribution changes depending on strain distribution. Therefore, a more conservative approach is needed for evaluating the CFRP contribution than for the steel contribution.

CHAPTER 5
Shear Behavior Model

To evaluate the shear behavior of the reinforced concrete beams strengthened with FRP, a simple behavioral model was developed. The main purpose of this model is to explain the different shear behaviors between brittle and ductile materials. As mentioned in Chapter 4, strain variation between strips and within strips makes the behavior of brittle materials complicated. In addition, the contribution of a brittle material to shear capacity can only be determined knowing material strain and it is difficult to estimate strains along the critical shear crack.

Given the complex interactions that are involved in reinforced concrete beams retrofitted with FRP, the behavior of brittle materials under axial tension is first investigated in Section 5.2. The bond behaviors of FRP and steel to concrete are then investigated in Section 5.3. Shear behavior of reinforced concrete sections strengthened with FRP neglecting bond behavior was subsequently studied in Section 5.5. Finally, all components are brought together to model the shear behavior of Reinforced concrete sections strengthened with FRP considering bond behavior in Section 5.6.

5.1 MOTIVATION FOR THE SHEAR BEHAVIOR MODEL

Reinforced concrete (RC) shear capacity is commonly evaluated as a sum of concrete capacity and steel capacity unless it is deep beam (ACI 318-08, AASHTO 2007, ACI 440.2R-08). While the concrete contribution to shear capacity cannot be evaluated exactly, a minimum guaranteed shear capacity for design can be derived from experiments. Such tests show that concrete shear capacity will decrease after reaching its maximum capacity although the deformation at maximum capacity is unknown. The transverse steel shear contribution will reach yield plateau when all stirrups yield. Tests

indicate that the critical crack angle will decrease (with respect to beam axis) as the applied load is increased due to stress re-distribution as individual stirrups reach yield. Assuming deformations are sufficient for all stirrups to reach yield and with an assumed constant critical crack angle of 45 degrees, the design shear capacity of the transverse steel can be estimated conservatively and is constant regardless of displacement.

In most cases, steel contribution to shear reaches its maximum prior to concrete reaching its maximum capacity. When strengthening with a brittle material like FRP, the maximum shear capacity is unlikely to be the sum of the maximum capacity of each component; except if the displacement at maximum concrete capacity and the displacement at maximum FRP capacity are identical. In general, the combined shear capacity will always be less than the sum of each material's maximum contribution. The most undesirable case is one in which FRP ruptured before steel and concrete reached their capacity. In such a case, the maximum capacity with FRP may not be much greater than that without FRP.

It can be concluded from this brief conceptual discussion that overall member shear capacity will likely increase with FRP strengthening, but that the total capacity would generally be less than the sum of each individual material's maximum capacity.

5.2   AXIAL TENSION

5.2.1   Axial Tension in Brittle Material

Axial stiffness is proportional to material modulus and cross-sectional area, and inversely proportional to member length. Often axial stresses are assumed uniform over a cross section when axial force is applied, but that is rarely the case. Such an assumption results in little error in ductile hardening materials in which stresses can redistribute and the yield stress can be developed across the entire section. Such an assumption however cannot be made with brittle materials. The maximum capacity of a section of brittle material will be less than the sum of the capacity of all elements because elements do not

usually rupture at the same strain due to differences in mechanical properties. Therefore the addition of each element capacity cannot be applied in brittle materials to obtain the maximum capacity of the whole.

To illustrate the differences between ductile and brittle materials loaded axially, consider three truss elements of same material, but with small variations in geometry due to fabrication errors; Figure 5-1 and Table 5-1. Although all elements possess the same young's modulus and yield or rupture strain, different element lengths generate different yield or rupture displacements, while different cross sectional areas generate different element strengths. The deformations of all three elements are assumed to be the same in this example.

E, A, L: the nominal elastic modulus, area, and length of the element
E_i, A_i, l_i: measured elastic modulus, area, and length of elements (i =1~3)
P: system force　　　　　　　T_i : element force
Δ : system deformation　　　Δ_i: deformation of elements

Figure 5-1 Axial behavior of truss members

Table 5-1 Truss element properties

	Nominal	Element 1	Element 2	Element 3
E_i *(ksi)*	10000	9500	10000	10500
ε_y or ε_{fu} (in./in.)	0.01	0.01	0.01	0.01
l_i (in.)	100	95	100	105
$\Delta_{y,i}$ or $\Delta_{fu,i}$ (in.)	1	0.95	1	1.05
A_i (in^2)	1	1	0.95	1.05
k_i (ksi)	100	105.3	95	100
T_i (k)	100	100	95	105

ε_y, Δ_y: yield strain and yield deformation of the ductile element
ε_{fu}, Δ_{fu}: rupture strain and rupture deformation of the brittle element

176

Consider the case where all three elements are made of ductile, elastic perfectly plastic material. The combined axial behavior exhibits different tangent stiffness as each element reaches its yield deformation as illustrated in Figure 5-2. Eventually the combined capacity reaches the summation of individual element capacities.

(a) Element response   (b) Combined response
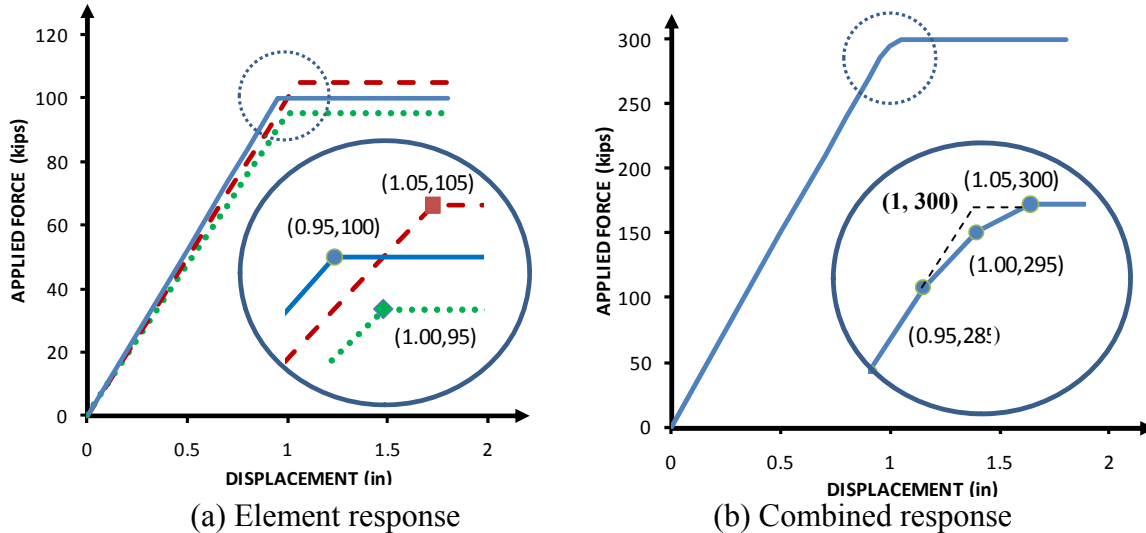
Figure 5-2 Axial force behavior of combined truss members in ductile material

If on the other hand all three truss elements are of a brittle material, a sudden drop in combined strength occurs when the first rupture occurs; Figure 5-3. In this case, the maximum capacity of the combined system is reached at first rupture and is less than the summation of all three element capacities.

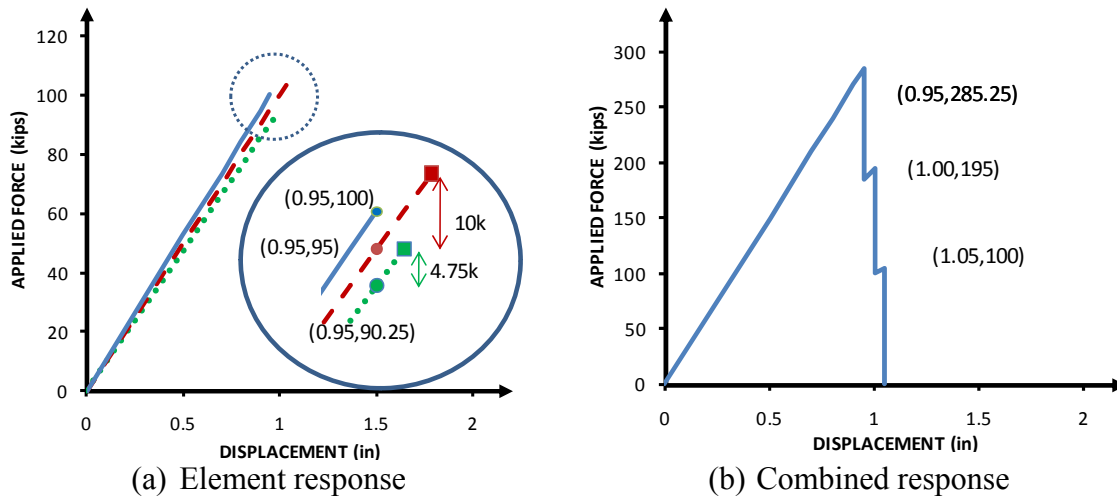(a) Element response   (b) Combined response

Figure 5-3 Axial force behavior of combined truss members in brittle material

177

A comparison of axial behavior between ductile and brittle material is summarized in Table 5-2. Two key observations can be made based on values listed in Table 5-2. First, the combined strength of ductile elements equals the sum of all element strengths. Second, the combined strength of brittle elements does not equal the sum of all element strengths, and will be lower than that sum. To calculate the combined capacity of brittle elements, one must know the displacement at first rupture that is needed to evaluate forces in all elements; in other words, it is not possible to evaluate element forces without displacement information.

Table 5-2 Comparison between systems with ductile material and brittle material

Combined system	Theoretical	Ductile	Brittle
E (ksi)	*10000*	*10000*	***10009***
ε_y or ε_{fu} (in./in.)	*0.01*	*0.01*	***0.095***
l_i (in.)	*100*	*100 (95~105)*	*100 (95~105)*
$\Delta_{y,i}$ or $\Delta_{fu,i}$ (in.)	***1***	***1 (0.95~1.05)***	*0.95*
A_i (in^2)	*3*	*3*	*3*
k_i (ksi)	*100*	*100 (100.09~95.24)*	*100.09*
T_i (k)	***300***	***300***	*285.25*

The strength of a system of brittle elements is likely to be governed by the element with lowest deformation capacity. However, if the remaining capacity at first rupture exceeds the lost capacity due to the first rupture, the overall capacity can be sustained and exceeded after partial rupture. In that case, the stiffness of the system will be lower after first rupture. Generalizing such behavior for a large number of elements (such as the number of fibers in FRP strips) suggests that the greater the number of elements, the lower the system strength normalized by the number of elements might be. Moreover, these observations imply that a linear relationship between the stiffness and cross sectional area may not be valid in brittle materials; particularly in systems where elements have drastically different geometries or different ultimate strains and stresses.

To further illustrate such behavior, the force-displacement responses to failure of two systems are presented.

1) System with elements of different lengths
2) System with elements of different cross-sectional areas

5.2.2 **Case 1: System with Elements of Different Lengths**

Deformations in transverse reinforcement can be concentrated over a limited length particularly around the crack. This example investigates an extreme case of variable element lengths by selecting the three-element system described previously, but taking the length of Element 3 to be one-fourth of what it is in Table 5-1. Such a system leads to axial strains in Element 3 that are approximately four times those of Elements 1 and 2 at the same displacement.

Systems with ductile and brittle elements are considered with differences between their behavior illustrated in Figure 5-4 and Figure 5-5. In both systems, the initial yield displacement or rupture displacement is reduced to one-quarter of that of the system detailed in Table 5-1. However, the stiffness of both systems is identical until first yield or rupture occurs. The tangent stiffness after first yielding of the ductile system is lower than the elastic stiffness of the original system. The maximum strength and corresponding displacement are close to those of the original model and thus the secant stiffness at maximum strength is the same as the previous one.

(a) Element response   (b) Combined response
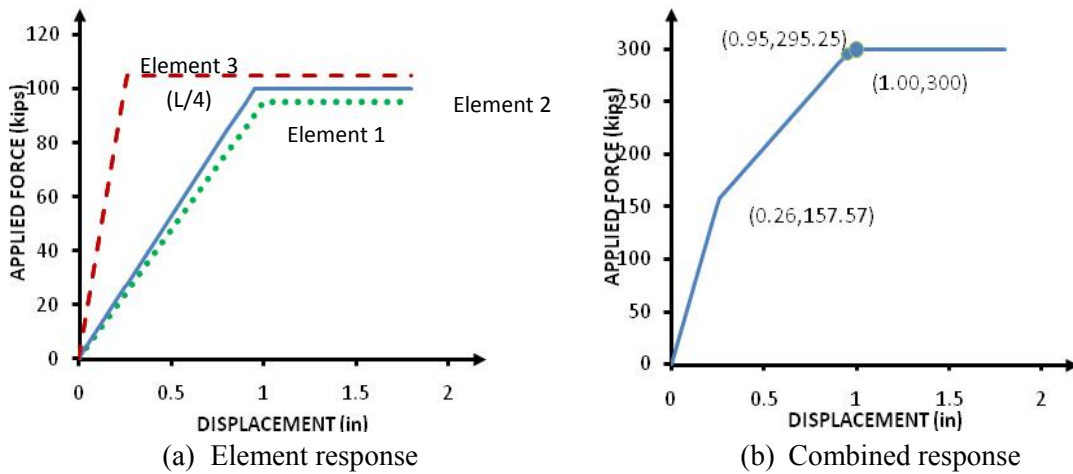
Figure 5-4 Axial behavior of ductile system (Case 1)

(a) Element response   (b) Combined response
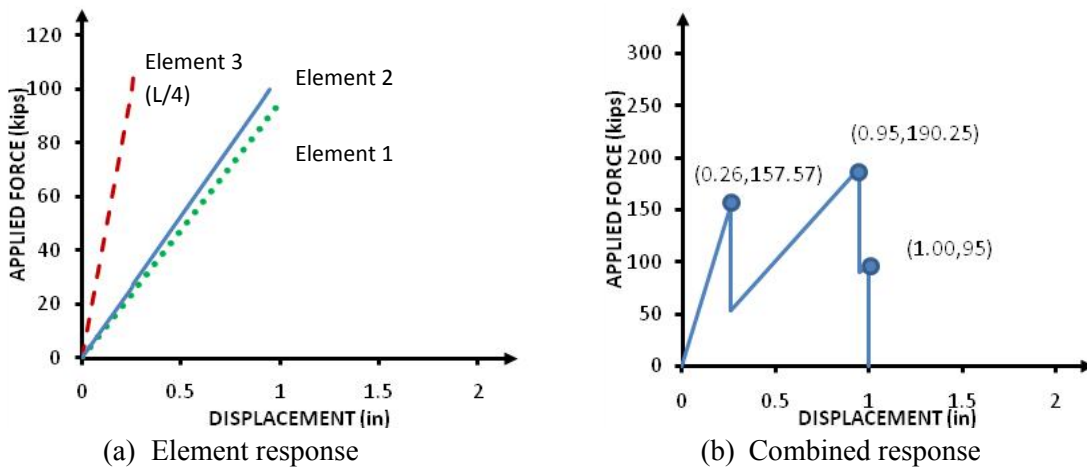
Figure 5-5 Axial behavior of brittle system (Case 1)

In the brittle system with reduced element length, the rupture of the short element reduces the force in the system at that displacement. However, the sum of the remaining element strengths exceeds the strength loss due to the ruptured element; allowing the system force to increase beyond the force at initial rupture but never to reach the sum of all three element strengths. Thus, the maximum strength of a system of brittle elements can depend on differences in element lengths. Compared with the previous example, the maximum strength was much less although the sum of strength of each element is identical in both cases.

In a system with lots of elements, the case where the remaining capacity at first rupture exceeds the strength loss would be common. Although this case is fairly

180

simplistic, as compared to FRP strips with many fibers, it highlights the need to consider the effects of differing element lengths on systems with brittle materials.

5.2.3   **Case 2: System with Elements of Different Cross-Sectional Area**

In Case 2, the cross-sectional area of Element 2 was increased from the original system. Here also both ductile and brittle materials were considered with their behaviors illustrated in Figure 5-6 and Figure 5-7.

As shown in Figure 5-6, the overall stiffness of the ductile system is close to that of element 2 whether the other elements yield or not. Furthermore, the maximum strength of the system is still the same as the sum of all element strengths. The brittle system will not rupture when the first element ruptures because the remaining strength is greater than the strength lost due to first rupture. As shown in Figure 5-7, if the ultimate stress is calculated from the area of all elements regardless of the loss of 'Element 1', the ultimate stress of the system may be perceived to be less than that of individual elements. Because the nominal area of a FRP strip is measured before testing and kept constant regardless of partial rupture, such lower ultimate stress may be observed when testing FRP strips in tension.

In conclusion, the system strength with ductile materials is not affected by its stiffness, but that of a system with brittle materials varies according to each element material properties. In brittle systems consisting of many elements (such as FRP strips), it may be impossible to evaluate the exact system strength.
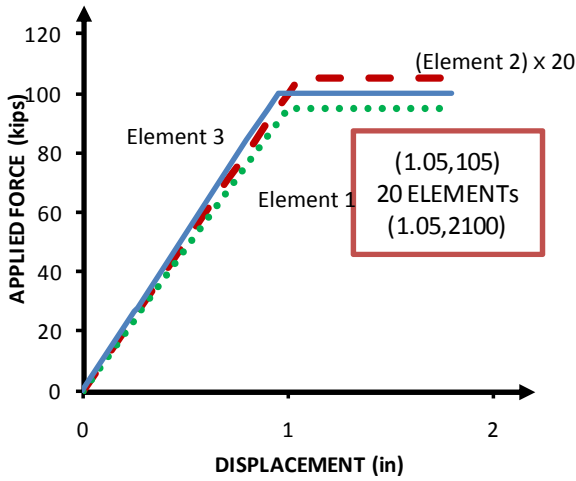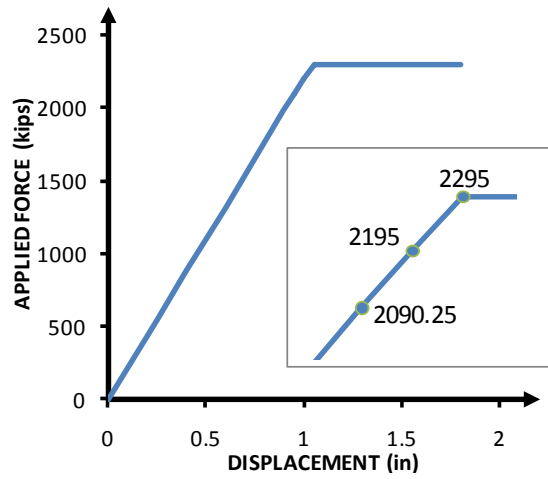
(a) Element response   (b) Combined response

Figure 5-6 Axial behaviors in ductile material (Case 2)
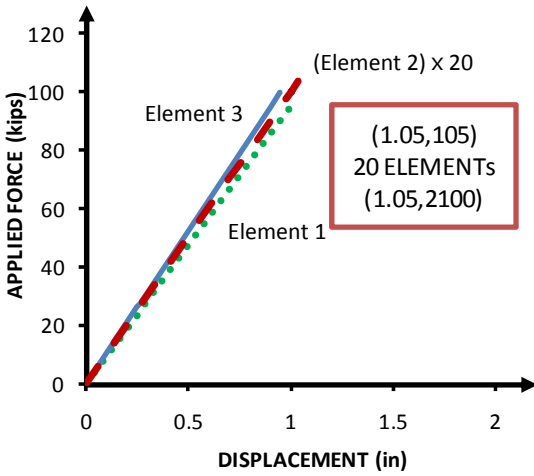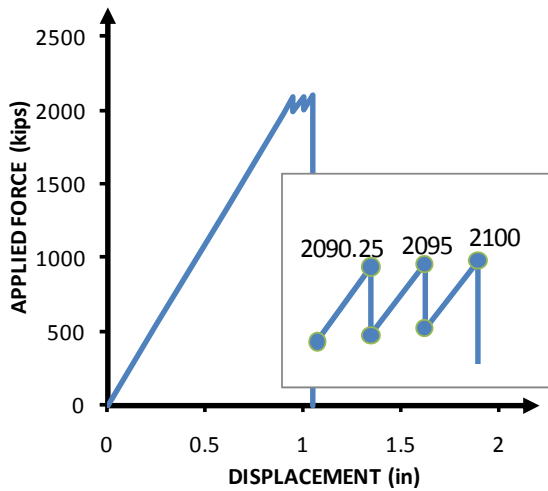
(a) Element response   (b) Combined response

Figure 5-7 Axial behaviors in brittle material (Case 2)

5.2.4 Tension Tests on Brittle Materials

Typically, the cross-sectional area, length, displacements, and applied load can be measured in a tension test. From those values, the strain (at yield or rupture) and Young's modulus are calculated. For ductile materials, small variations within a tested system having known values can be neglected and average values can be used for the system. In addition, the material properties derived from the test result can be extended to any other

system of the same material with little error. Variations in brittle elements on the other hand, alter the apparent material properties of the system, which will not possess the average properties of its elements. The force-displacement responses of the original system (detailed in Table 5-1) and cases 1 and 2 are compared in Figure 5-8. In all three systems, material and geometric properties were selected such that the initial tangent stiffness was the same for brittle and ductile systems. However, after the first element either yields or ruptures, the behaviors between ductile and brittle systems are significantly different as seen in Figure 5-8.

(a) Ductile material (b) Brittle material
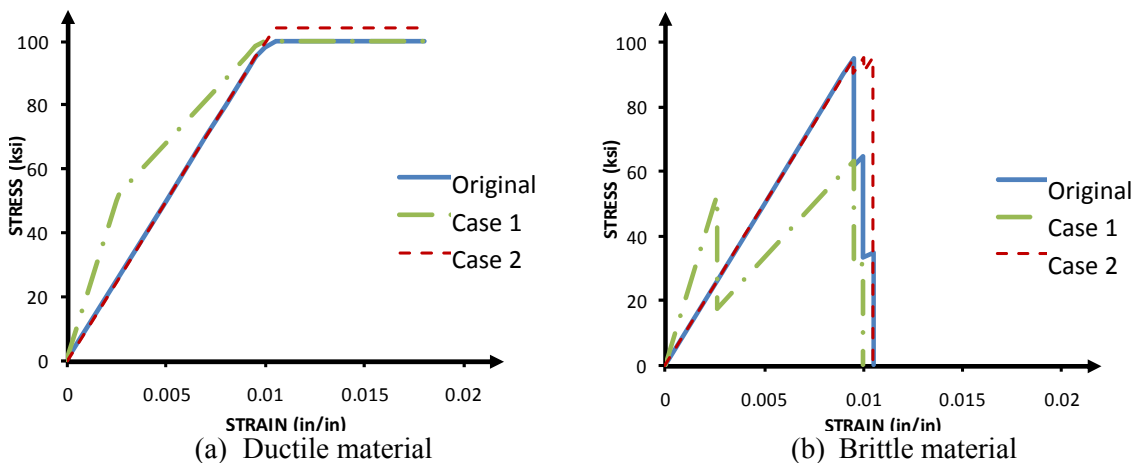
Figure 5-8 Stress-strain relationship derived from back-calculation

5.2.5 Probability Approach

As discussed in Section 2.1.3.3, the design of FRP strength is defined as the mean tensile strength of a sample of test specimens minus three times the standard deviation $(f_{fu}^* = \overline{f_{fu}} - 3\sigma)$. Any test value that is lower than the design value is not acceptable. Assuming that the yield or rupture strain distribution of a material follows a normal distribution, the strain distribution can be normalized by the mean and standard deviation values, giving a standard normal distribution as shown in Figure 5-9.

183
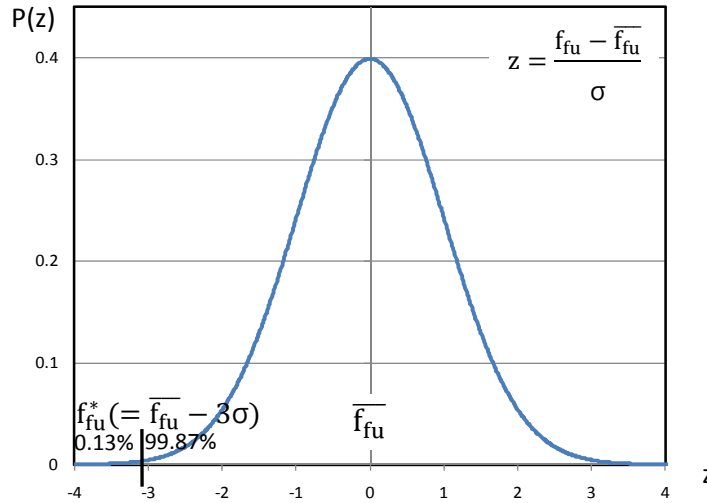
Figure 5-9 Standard normal distribution (mean:0, standard deviation:1)

If two elements are combined in a parallel system, the system distribution would be different depending on material type. Consider two elements taken from the same sample having mean value $(\overline{f_{fu}})$, and standard deviation (σ) that are combined in parallel.

It is assumed that the measured material ultimate strength of each element is $f_{fu}^1 (= \overline{f_{fu}} - 1\sigma)$ and $f_{fu}^2 (= \overline{f_{fu}} - 4\sigma)$ as shown in Figure 5-10. If these elements are of ductile material, the ultimate system strength would be $f_{fu}^{1+2} (= 2\overline{f_{fu}} - 5\sigma)$, which is greater than the design strength $(= 2\overline{f_{fu}} - 6\sigma)$. In this case, the strength of Element 2 is not acceptable, but the combined element is acceptable. However, if both elements are of brittle material, the ultimate system strength would be $2f_{fu}^2 (= 2\overline{f_{fu}} - 8\sigma)$ because the system strength is controlled by the element with lower strength. In this case, the combined element is not acceptable although the strength of Element 1 is acceptable.

Based on these observations, the unacceptable zones of probability distribution in both combined systems are shown in Figure 5-11. When brittle elements are used, the system probability distribution is obtained by summing the element normal distribution. System distribution would then be normal with mean ($\overline{f_{fu}^{1+2}} = 2\overline{f_{fu}}$) and standard deviation ($\sigma^{1+2} = \sqrt{2}\,\sigma$). Because the combined distribution in brittle material is evaluated from conditional probability, a Monte Carlo Simulation was performed.

184

$$z = \frac{f_{fu} - \overline{f_{fu}}}{\sigma}$$
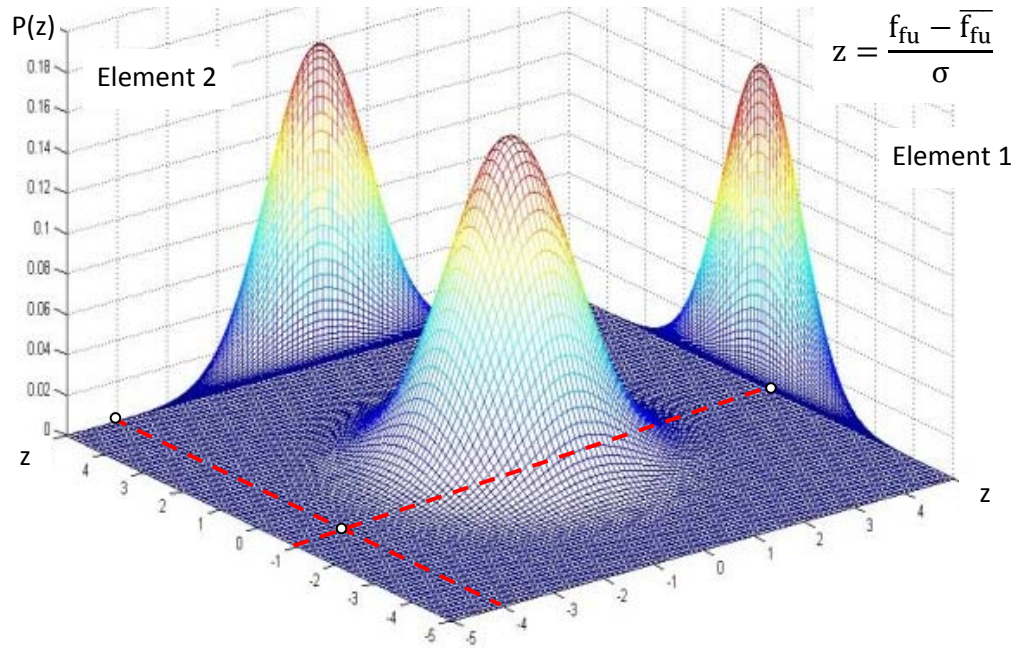
Figure 5-10 Joint probability density function

(a) Ductile material   (b) Brittle material
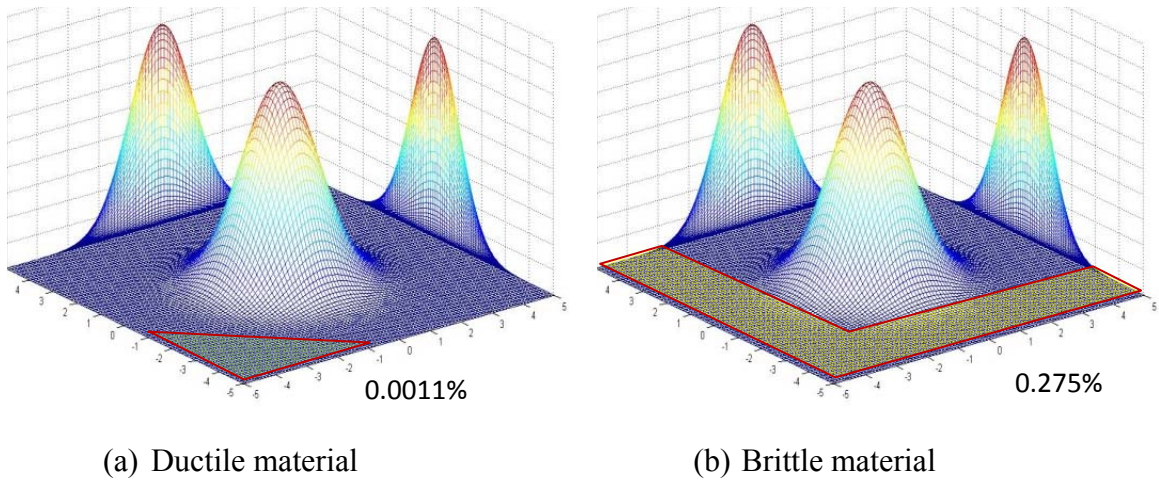
Figure 5-11 Unacceptable zone in joint probability density function

Given specified element design strengths that ensure 0.13% probability of failure at the element level, the system probability of failure using brittle elements is about twice

that at 0.275% (illustrated in Figure 5-11). For ductile elements, the system probability of failure is about hundred times smaller than the probability of failure at the element level.

Consider the combination of two elements with mean strength of 100 k and standard deviation of 1 k. The area of these elements is 1 in². As discussed, the design strength would be 97 k and also design stress is 97 ksi (or three standard deviations below sample mean).

When the elements are made of ductile material, the calculations and probability functions are shown in Figure 5-12 and Figure 5-13 respectively.

Element sample properties (Normal distribution)

  Mean value : P_m =100 k ,

  Standard deviation : $P_\sigma = 1$ k

  Design values : $P_n = P_m - 3 \times P_\sigma = 100 - 3 \times 1 = 97$ k

  $$f_n = \frac{P_n}{A} = \frac{97k}{1\text{in}^2} = 97\text{ksi}$$

Parallel system combing two elements (ductile material)

  Mean: $P_{m,sys} = 200$ k ($= 100+100$)

  Standard deviation: $P_{\sigma,sys} = 1.4$ k $= \sqrt{1^2 + 1^2}$

  System design strength for probability of failure $\leq 0.13\%$

  $P_{n,sys} = P_{m,sys} - 3 \times P_{\sigma,sys} = 200 - 3 \times 1.4 = 195.8$ k

  $$f_{n,sys} = \frac{P_{n,sys}}{A_{sys}} = \frac{195.8k}{2\text{in}^2} = 97.9\text{ksi} > 97 \text{ ksi} (\text{O.K.})$$

  → Element design strength can be relaxed to achieve the same probability of failure of 0.13% in the parallel system of ductile elements.
  Probability (system stress < design stress (97 k)) = 0.0011% (illustrated in Figure 5-14)

Figure 5-12 Calculations of combined strength in ductile material
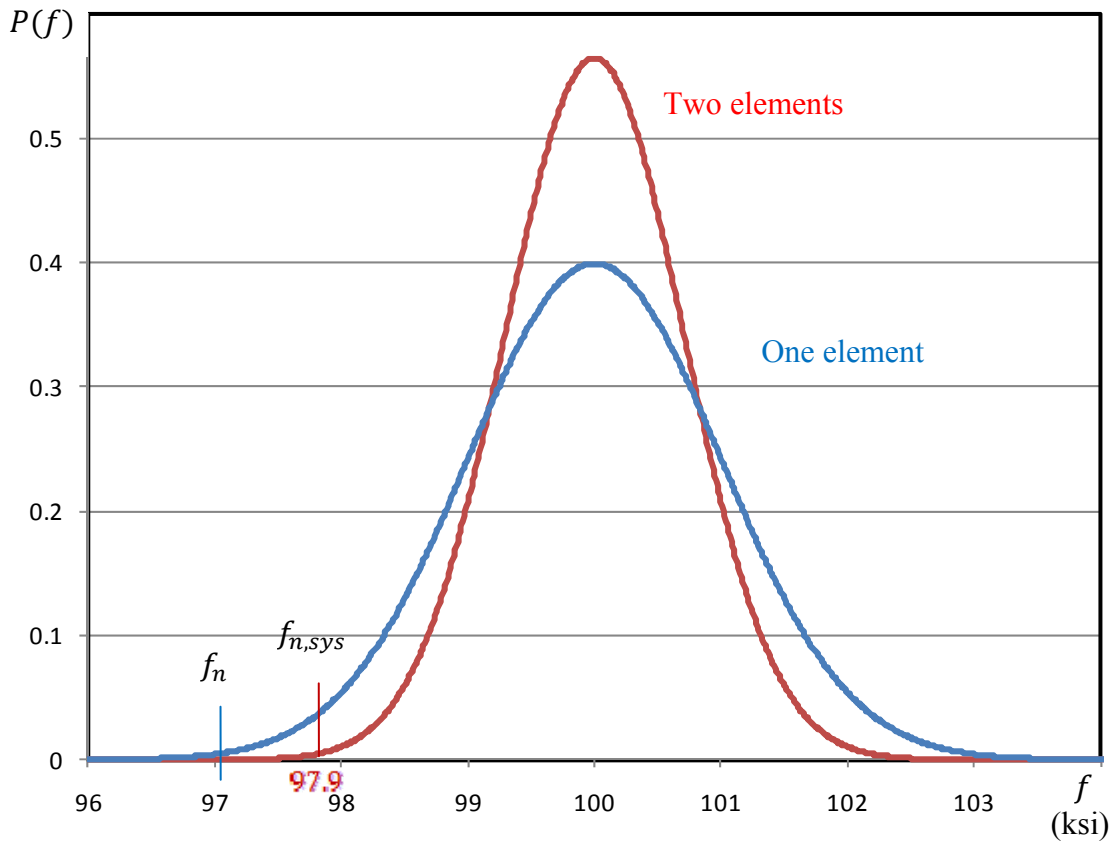
(a) Stress probability function
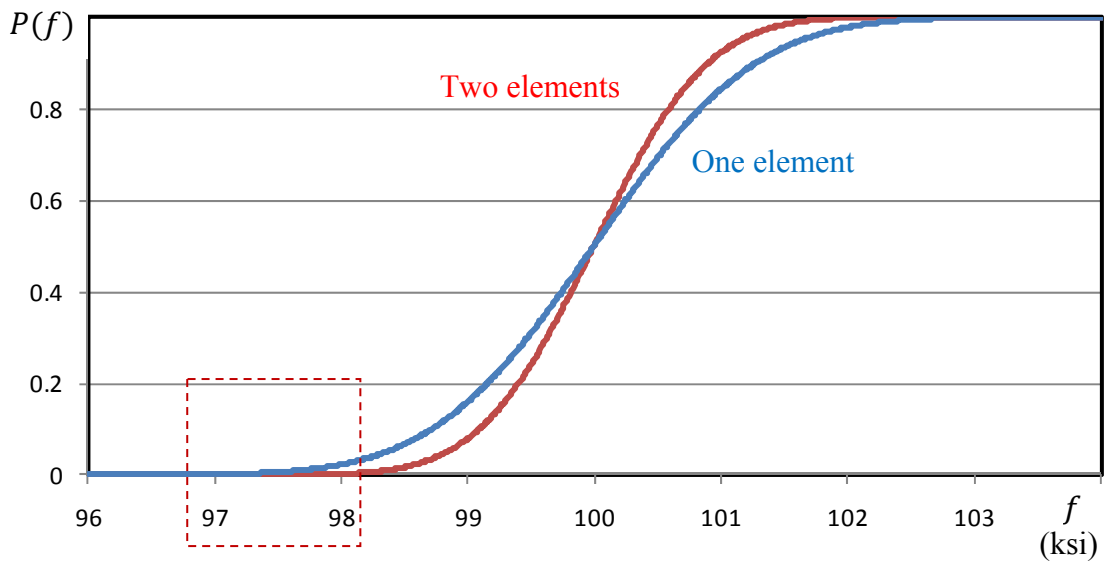
(b) Cumulative probability function for stress

Figure 5-13 Probability functions when ductile elements are combined

Figure 5-14 Probability functions at the range of design values

Because the combined distribution in a brittle material is evaluated from conditional probability, Monte Carlo Simulation was performed to obtain the system distribution. Using the same two material strengths and distributions as the previous example but with brittle materials, the probability density function and the cumulative probability function when two brittle elements are combined are shown in Figure 5-15.

The system design stress is evaluated from Monte Carlo simulation by finding the strength below which the probability of failure is (0.13%) as shown in Figure 5-16. For satisfactory system performance, the required system design stress was found to be 96.8 ksi, which is lower than the individual element design stress (97 ksi). The mean stress of the system with brittle material was evaluated as the stress at cumulative probability of 0.5 in the Monte Carlo simulation and was decreased from 100 ksi (for individual elements) to 99.45 ksi for the system. The results indicate that the mean stress and design stress would decrease as more elements are used in a brittle system.

188

(a) Stress probability per unit area

(b) Cumulated probability function

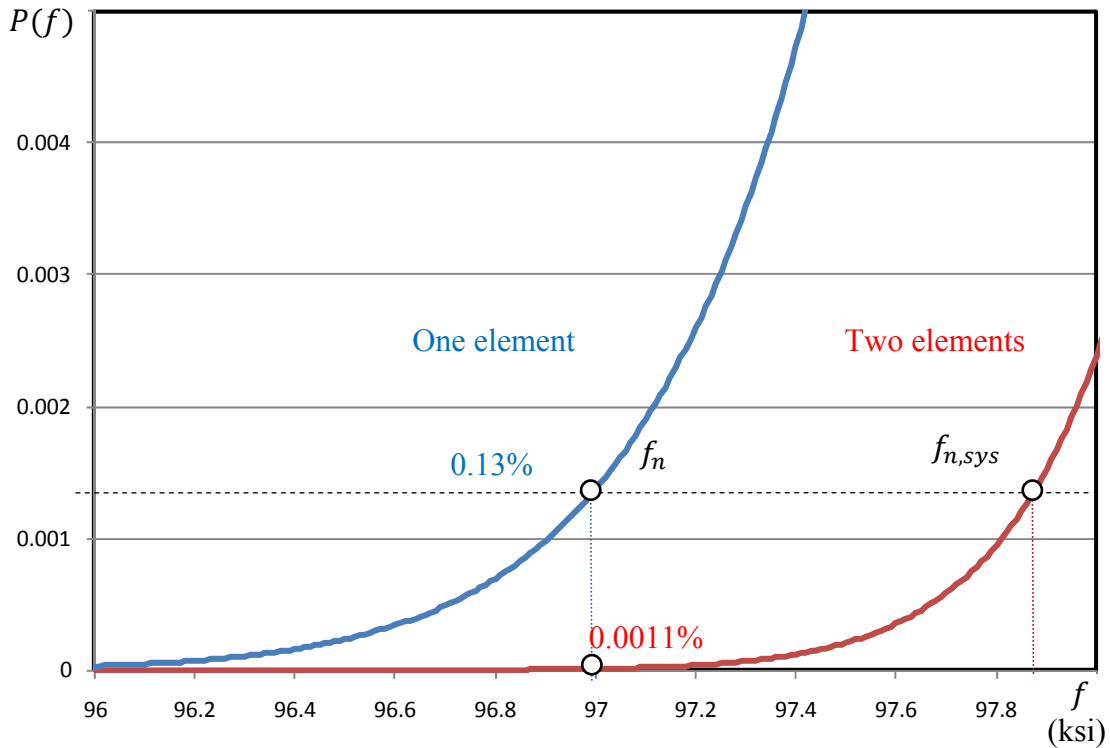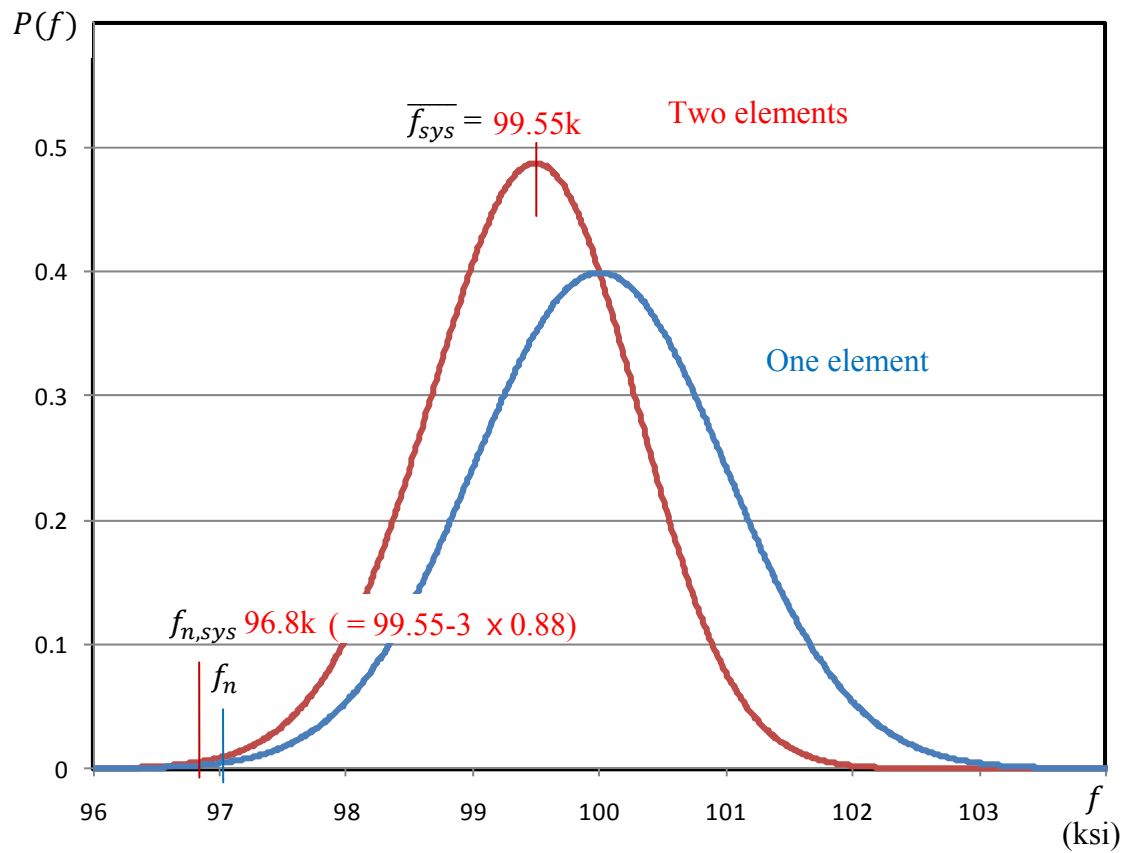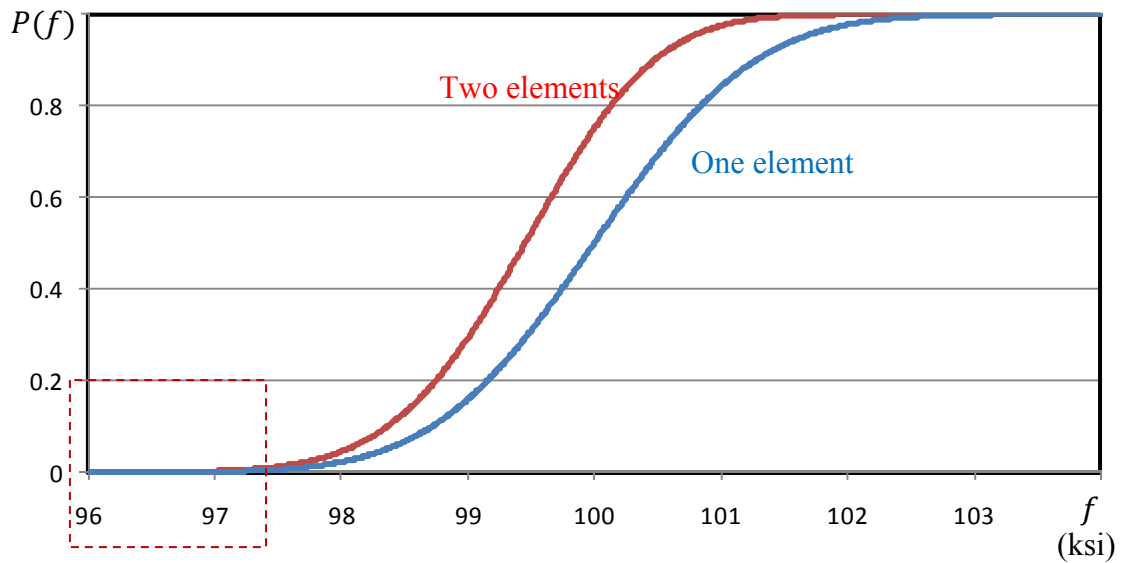***Figure 5-15 Probability functions when brittle elements are combined***

189
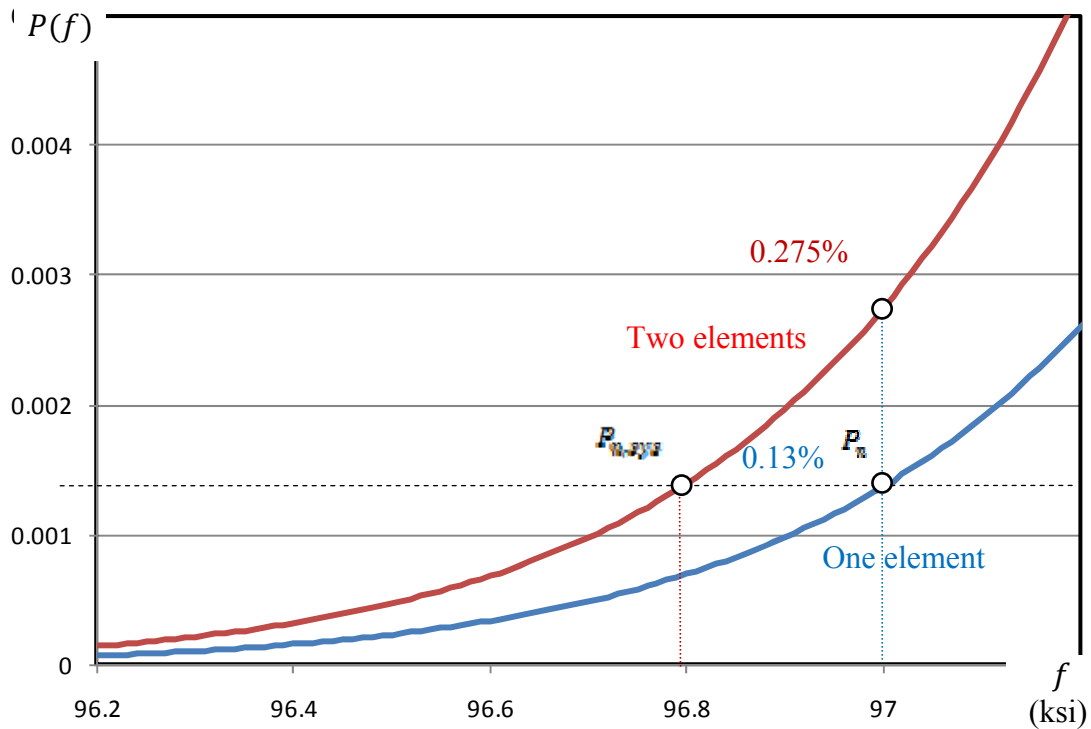
Figure 5-16 Cumulative probability functions at the range of design value (brittle)

The probability density distribution of a system of brittle elements is more concentrated at the mean value than element distribution as shown in Figure 5-15. The variance can be estimated assuming that the system is normally distributed, The standard deviation is thus evaluated at 0.88, which is lower than the standard deviation for individual elements ($= 1$) and greater than the standard deviation for two ductile elements ($= 0.7$).

The comparison of the distribution obtained from the simulation with a normal distribution of the same mean and with the estimated standard deviation is shown in Figure 5-17. It can be seen in the figure that the probability density from simulation is greater than that of the normal distribution near the mean value, while it is smaller at greater stresses than mean.

190
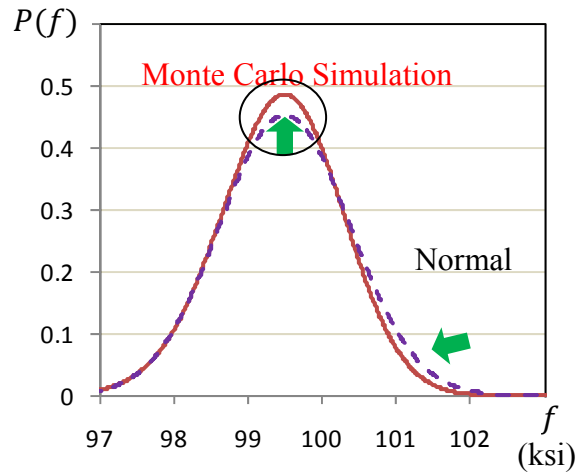
Figure 5-17 Probability distribution from Monte Carlo simulation

Using the same approach, four brittle elements were combined and the probability density distributions for the systems plotted in Figure 5-18. The simulation confirms that as the number of elements increases, design strength decreases. In Commentary C1.4 of the Guide Specifications of NCHRP report 655, a Weibull Distribution is used for modeling of the brittle materials.
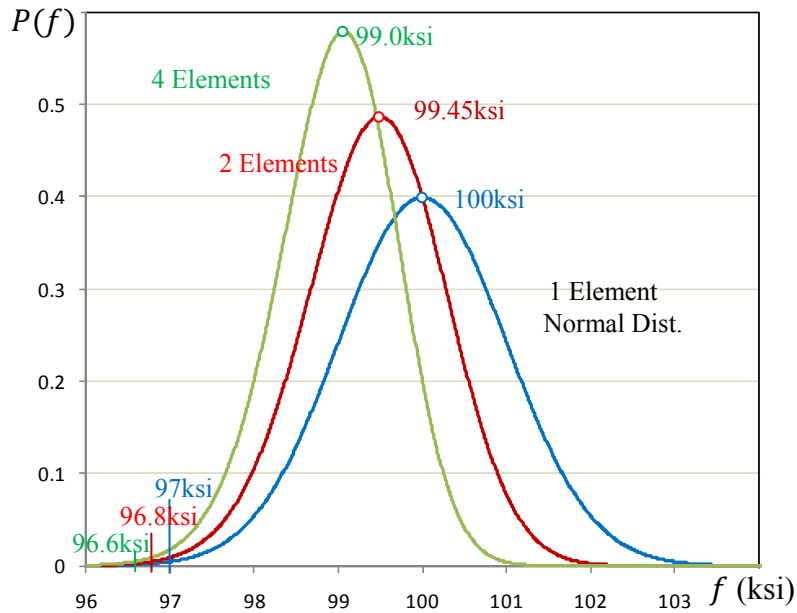
Figure 5-18 Comparison of probability density according to the number of brittle elements

191

Bank (2006) reported that ultimate strength of glass FRP bars as shown in Table 5-3. As the diameter (or area) increased, the guaranteed ultimate strength (design strength) decreased.

Table 5-3 Properties of glass FRP rebar produced in North America (Bank 2006)

Nominal Bar Size No.	Nominal Diameter (in.)	Nominal Area (in.^{2})	Reported Measured Area (in.^{2})	Guaranteed Longitudinal Strength (ksi)	Guaranteed Longitudinal Modulus (x 10^{3}ksi)
2	0.25	0.05	0.05	120-127	5.9-6.7
3	0.375	0.11	0.13	110-111	5.9-6.3
4	0.50	0.20	0.23	100-103	5.9-6.4
5	0.625	0.31	0.34	95-99	5.9-6.8
6	0.75	0.44	0.46	90-95	5.9-6.9
7	0.875	0.60	0.59	85	5.9
8	1.0	0.79	0.83	80-87	5.9-6.0
9	1.125	1.00	1.00	75	5.9
10	1.25	1.27	1.25	70	5.9

As shown in Table 5-4, the tensile modulus of laminate is about half of the modulus of dry fiber, but tensile strength is about one-quarter of the dry fiber. Although the volume fraction of the laminate is around half of dry fiber, reduction in tensile strength is high because the rupture strain decreases. In addition, the larger area has lower ultimate strength and rupture strain. These results from two tables comply with the observation from probability approach in brittle material discussed in this section.

Table 5-4 Comparison of the properties of CFFP laminates with different thickness

Thickness (in)	Ultimate tensile strength (ksi)		Elongation at break (in./in.)		Tensile modulus (x 10^3 ksi)	
	Test	Design	Test	Design	Test	Design
Dry fiber (0.0065)	555	-	0.017	-	33.4	-
0.011	154	131	0.0105	0.0105	14.8	12.6
0.04	143	121	0.01	0.085	13.9	11.9

One can therefore conclude that the design rupture stress of a brittle material (e.g., FRP) specified from coupons may not be applicable to the larger areas of bars or strips. The design properties from coupons with small areas would therefore need to be adjusted as a function of the cross-sectional area to obtain conservative estimates of material properties for larger areas.

5.3 BOND BEHAVIOR

Bond between steel or FRP and concrete is critical for reinforced concrete members to achieve composite action between all materials. In this section, the composite behavior of reinforced concrete members is investigated considering the effects of bond.

5.3.1 Effective length of strengthening elements

Member response considering bond cannot be determined exactly because it is difficult to evaluate the effective length of steel and FRP. One can, however, assume that the stiffness of a member with bond between elements would be greater than the stiffness without bond. Due to bond stresses, the strain distribution along the length of a FRP or steel elements is not uniform. Therefore, element deformation cannot be calculated based on total length and maximum strain.

Once cracking occurs in a concrete section, most deformation is concentrated near the crack region until debonding starts. As the debonded region around a crack lengthens, the stiffness of the element will decrease and its effective length will increase. Bond behavior between steel or FRP and concrete is assumed to generate a constant average bond stress along the bond length (l_{bond}). The resulting strain distribution is linear based causing the effective element length to be approximately the same as the bond length as shown in Figure 5-19. Bond stress in FRP is assumed for simplicity that to go to zero once the critical FRP debonding strain is reached.

The effective length of an embedded steel bar or FRP bonded to concrete surface is necessary to evaluate its strain, stress, and force under given displacement. The effective length ($l_{effective}$) is defined here as the length by which the strain at the crack is

multiplied to obtain the total deformation of the steel or FRP element. (illustrated in Figure 5-19).

(a) Steel   (b) FRP
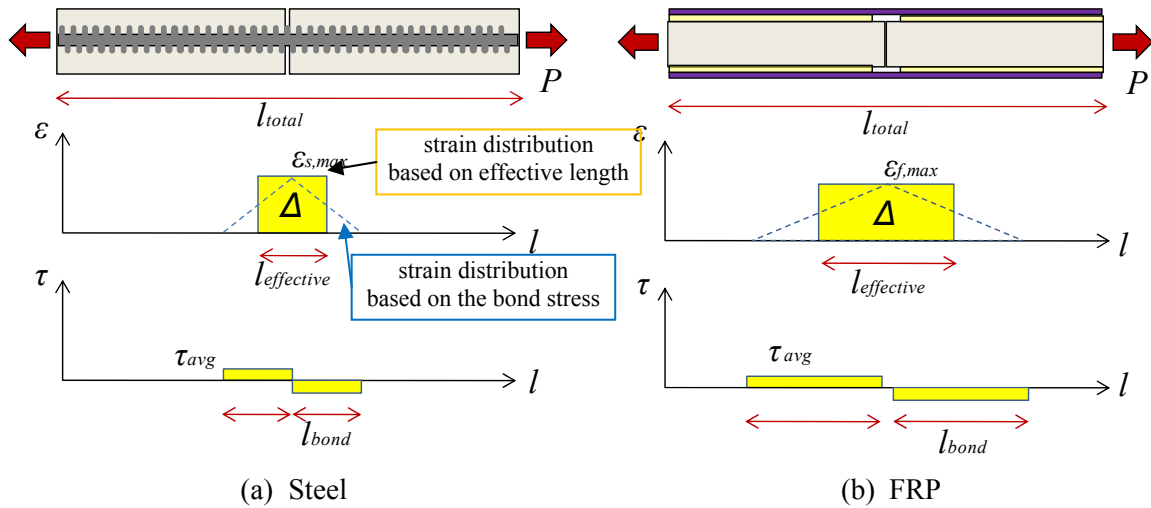
Figure 5-19 Concept of effective length

The force-deformation response of composite members using the effective length concept is shown in Figure 5-20.

The strain can be different if the effective length of two members is different although two members have the same displacement (points B and C). It is also possible that the displacement will be different even if both members reach the same maximum strain; if the effective length of two members is different (points A and C, points B and D). Assuming that bond stress is uniform and constant, the effective length of a member increases as the stress increases, while the stiffness decreases. Therefore the force deformation relation of a member can be represented by the curve from point D to point A.

194
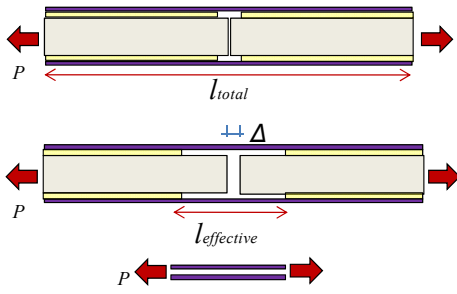
$$P = E \, \varepsilon_{f,max} A_f$$

$$\Delta = \int_0^{l_{total}} \varepsilon \, dl$$

$$= \varepsilon_{f,max} \, l_{effective}$$

(a) Definition of effective length
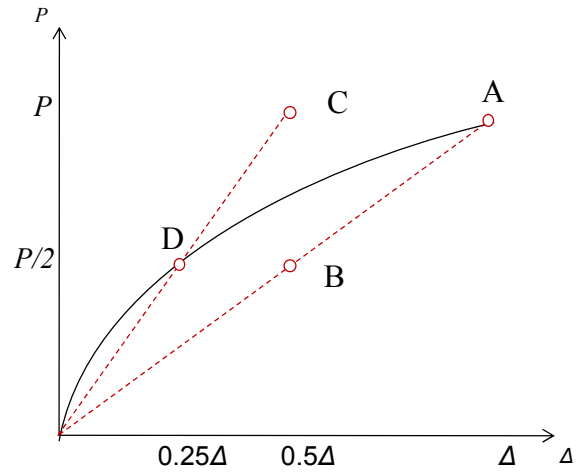
(b) Response considering bond
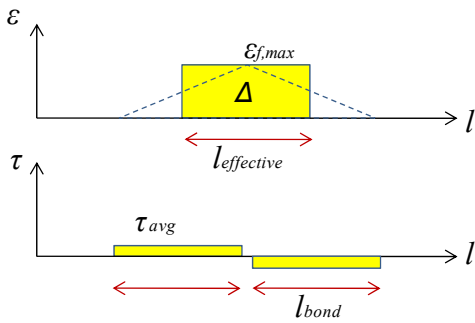
(c) Tensile strain and bond stress at A
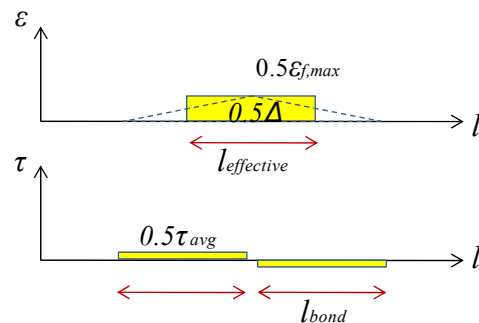
(d) Tensile strain and bond stress at B
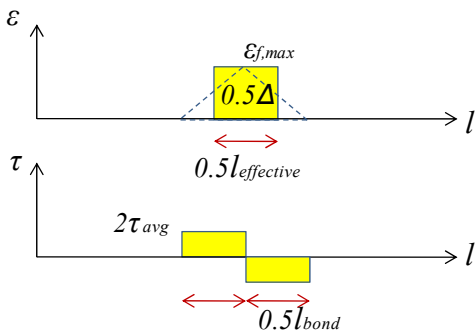
(e) Tensile strain and bond stress at C
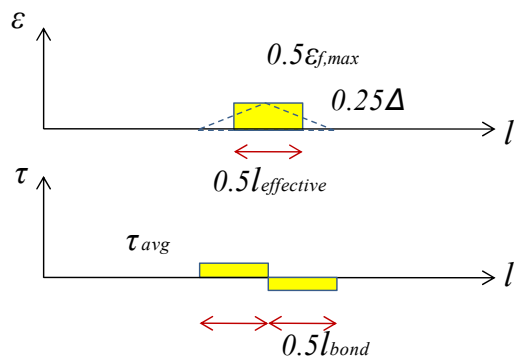
(f) Tensile strain and bond stress at D

$\varepsilon_{f,max}$, $l_{effective}$, l_{bond}, $\tau_{avg.}$, d are evaluated from load P at point A and these values at other points (B, C, D) are shown relative to values at point A.

Figure 5-20 Force-deformation response using effective length concept

5.3.2 Steel Embedded in Concrete

The force-deformation behavior of steel in reinforced concrete structures depends on the interaction between steel and concrete. Consider a simple system with one deformed steel bar embedded in a concrete element (Figure 5-21). It is assumed that a crack will form at some section along the member length. As a load is increased, the crack will widen. The resulting load vs. displacement response is illustrated in Figure 5-21. This concept can be applied to a steel stirrup in a beam depth of l_0. It is assumed that a critical shear crack will intersect the stirrup.

Bond forces between concrete and steel alter the apparent stiffness of the steel bar by reducing its effective length. Because debonding starts near the crack and extends in both directions, gradually, the effective length increases as load increases beyond point B in Figure 5-21.

(a) Cracking (A) then debonding (B) then yielding (C)

(b) Debonding simultaneously with concrete cracking

(c) Yielding prior to debonding

Figure 5-21 Bond behavior of steel embedded in concrete

196

When the concrete cracks, the tensile stiffness of the element is reduced significantly. Depending on the amount of steel, the st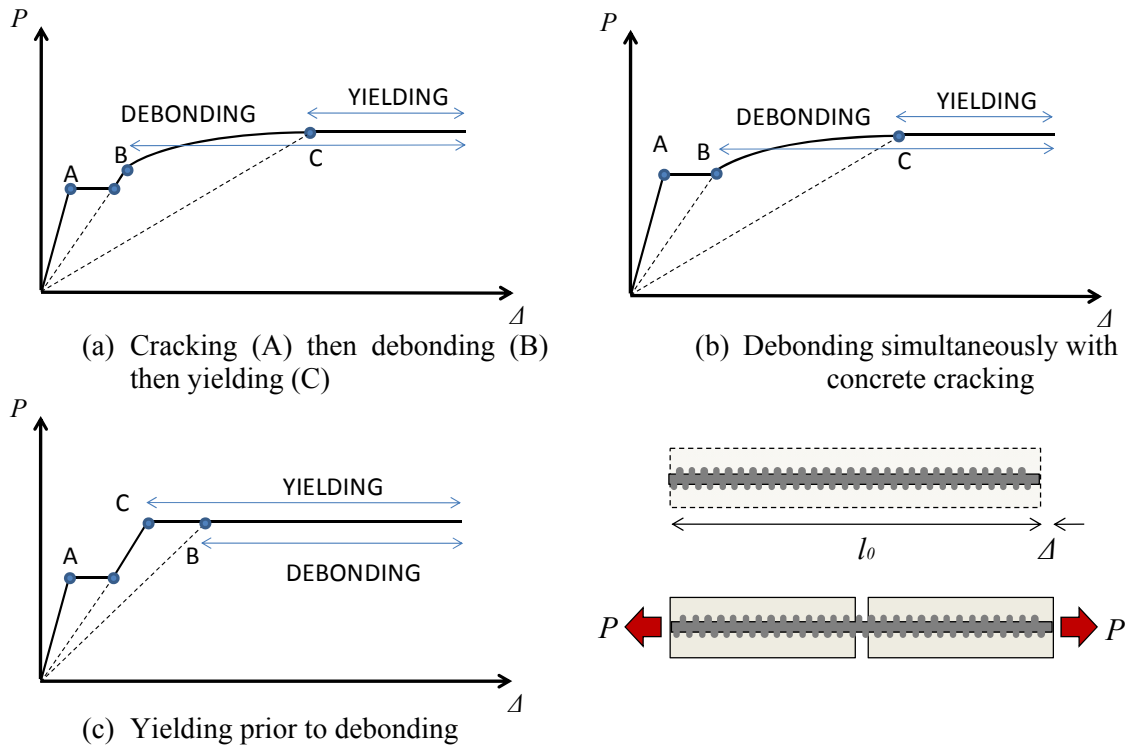eel may or may not yield at cracking. Debonding can also occur at concrete cracking if the bar force transferred through bond is less than the force in the concrete cracking. If the bond strength is not enough to develop the steel yield stress at the crack, debonding can occur before yielding (point B in Figure 5-21 – a, b).

After yielding of the steel, the element force remains constant in the yield plateau. The location of point B in Figure 5-21 cannot be estimated exactly because the stiffness of the composite element is difficult to evaluate. Often an effective element length is used to relate element forces with deformations through the secant stiffness of the element. If debonding occurs after yielding however, locating point B becomes immaterial (Figure 5-21 - c) because the capacity of the element is governed by the steel capacity regardless of loading history. Thus, deformation information is not required for evaluating the capacity of the element at large deformations.

5.3.3 FRP Bonded to Concrete Surface

FRP materials used for strengthening are typically applied externally. In such cases, bond stresses exist only at the interface between the concrete surface and the FRP. Consider a simple element comprised of concrete and externally applied FRP (Figure 5-22) that is loaded axially in tension and it is assumed that a single crack along the member length (l_0) occurs.
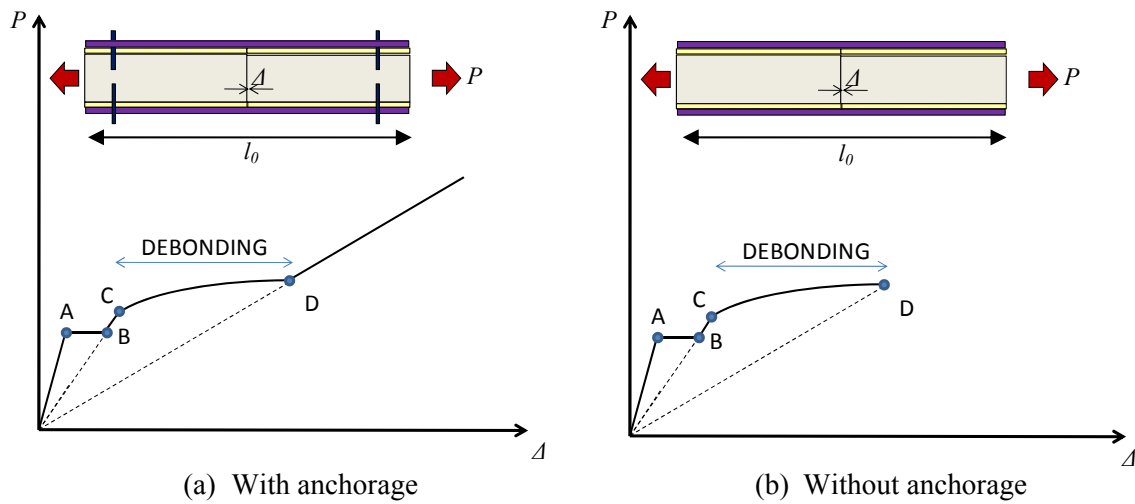
(a) With anchorage   (b) Without anchorage

Figure 5-22 Bond behavior of FRP attached to concrete surface

Before cracking, element axial stiffness is dominated by the concrete. At cracking, softening causes a sharp reduction in stiffness and an increase in deformations (from point A to point B in Figure 5-22). After cracking but before the debonding strain is reached, the effective element length remains nearly constant. However the effective length will increase and stiffness will decrease when debonding occurs. If proper anchorage of the FRP is not provided, complete debonding of the FRP will cause failure of the element (point D). With adequate anchorage, the overall element force could increase even beyond complete debonding. The effective length will then remain constant since element stiffness is determined by FRP properties and the length between adjacent anchorage points. At larger deformations either anchor failure or FRP sheet rupture can occur depending on relative capacities.

5.3.4 Summary

The differences between the bond behavior of elements comprised of steel bars embedded in concrete and those comprised of FRP applied to the surface of concrete were highlighted. Although global element displacement can be measured in these elements, strain distributions in steel and FRP are difficult to assess due to concrete cracking and bond slip. Thus relating element deformations to element forces is not

198

straightforward. The ultimate tensile capacity of a concrete element with embedded steel can be obtained from the yield capacity of the steel. Evaluating forces in the steel element is independent of deformations beyond yield. However, the capacity of the FRP element cannot be evaluated without knowledge of bond and anchorage capacities. Forces in the FRP element are always dependent on element deformations and the relation between force and deformation is difficult to evaluate because of concrete cracking and possible bond slip. At ultimate strength, if anchorage capacity exceeds the capacity of the FRP material, the element capacity is controlled by the capacity of the FRP material which can be easily estimated.

As bond strength increases, the stiffness of an element increases while its effective length decreases. If bond strength is ignored, the overall behavior would be less stiff giving larger deformation estimates.

5.4 SHEAR BEHAVIOR OF BEAMS STRENGTHENED WITH FRP

The location and direction of the critical shear crack and the strain distribution across the critical crack in RC beams strengthened with FRP cannot be evaluated exactly. Although we can measure the crack width at the surface of a member, it is not possible to evaluate material strain values from that crack width without knowledge of the effective length over which the strains are distributed. With similar reasoning, the measured strain from gages may not represent the force in the reinforcement even if the gage is located near the critical crack. Furthermore, the angle of a critical shear crack can change as the applied load increases (Figure 5-23). This angle is an essential parameter that is required to estimate the number of steel stirrups or FRP strips that cross the critical crack and the angle between the crack and the reinforcement; both of which are necessary for evaluating the contribution to shear strength of steel stirrups and FRP strips.
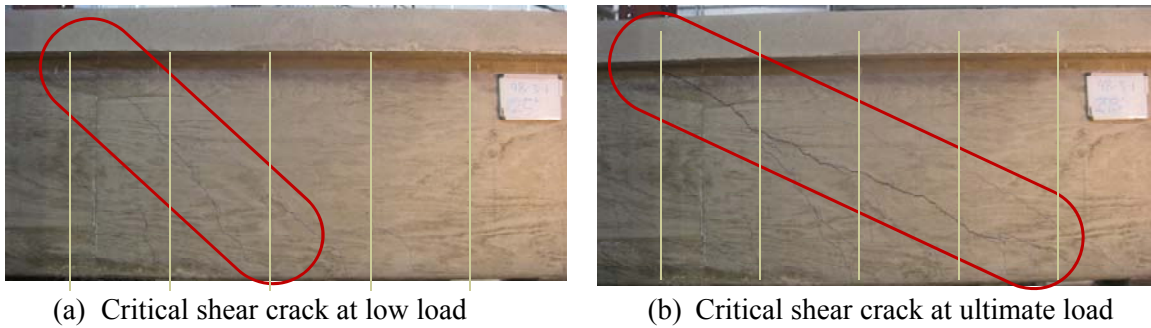
(a) Critical shear crack at low load   (b) Critical shear crack at ultimate load

Figure 5-23 Change in critical shear crack angle as applied load increases

In most design standards and guidelines, shear strength equations for RC beams are based on a plastic mechanism being achieved in the transverse reinforcement. Such a mechanism requires that all stirrups crossing the critical crack reach their plastic capacity at ultimate shear capacity. That assumption usually holds true in RC beams as the deformation along the critical crack is typically large enough to yield all stirrups across the crack, but compression failure is precluded because of the upper limit placed of steel shear contributions (V_s).

In contrast, the plastic mechanism assumption cannot be used in evaluating the shear strength of RC beams strengthened with FRP (brittle material). The FRP contribution to shear strength depends on the strain of the material that crosses the critical crack. One cannot assume a plastic strength in all FRP strips crossing a crack, and therefore, an average strain and the related stress needs to be estimated for FRP strips crossing the crack. Furthermore, in FRP reinforced beams, the interaction between transverse steel shear resistance and FRP shear resistance can affect the shear strength contribution of both materials. Due to difficulties in simulating the behavior of the different materials contribution to the shear capacity of a strengthened beam, a simple shear model was developed. In Section 5.5, the bond between concrete and reinforcements was not included in the model because the stiffness of the element would not influence the ultimate shear capacity in adequately anchored systems. In Section 5.6, bond is considered to compare the behavior of anchored FRP strips with the behavior of unanchored FRP strips, whose behavior is determined by bond.

5.5   S<small>HEAR</small> B<small>EHAVIOR</small> M<small>ODEL FOR</small> **FRP** R<small>EINFORCED</small> C<small>ONCRETE</small> B<small>EAMS</small>

In this section, bond strength is neglected to simplify the investigation of shear behavior. Neglecting bond results in conservative deformation and strength estimates, which is desirable for design purposes.

5.5.1   Background

In the experiments described in previous chapters, FRP sheets across the critical shear section did not rupture at the same time, which means that the strain distribution between adjacent sheets is not uniform at ultimate capacity. In other words, FRP shear contribution cannot be based on the material strength regardless of anchorage. In contrast, stresses in steel stirrups in reinforced concrete beams can be close to uniform at ultimate shear capacity, with all stirrups reaching yield stress in the critical region. Since stress in steel is independent of strain beyond yield, the strain distribution in stirrups across the critical region rarely matters at ultimate shear capacity. Therefore, the evaluation of the FRP shear strength contribution for a brittle material requires the use of strain levels and strain compatibility, which are not taken into account in current shear design equations (ACI440.2R-08, AASHTO 2007).

Chen and Teng (2003) stated that the average stress of FRP intersected by the shear crack is based on the assumption that the stress distribution in the FRP is not uniform. Graphs relating stress in FRP to distance from crack and the maximum achievable stress were introduced. Different shapes for a non-linear distribution of FRP strains over a crack are shown in Figure 5-24. The computational model of Chen et al. (2010) was derived for the widening process of a single major shear crack and is as follows:

$$w = w_{max} \times \begin{cases} \dfrac{1 - C\bar{z}}{1 - C}\bar{z} & 0 \le C < \dfrac{1}{2} \\[2ex] 4C\bar{z}(1 - C\bar{z}) & \dfrac{1}{2} \le C \le 1 \end{cases}$$

$$f_{FRP,e} = D_{FRP}\, f_{FRP}\,, \quad D_{FRP} = \frac{\int_0^{z_b} w\,dz}{w_{max}z_b}$$

where

w = crack width

w_{max}= maximum value of the crack width for a given crack (maximum crack width)

$\bar{z}$ = normalized vertical coordinate, $\bar{z} = z/z_b$ ($z_b = 0.9d$)

C = crack shape parameter

D_{FRP} = strain distribution factor, the ratio of the average strain to the maximum strain within the effective FRP length
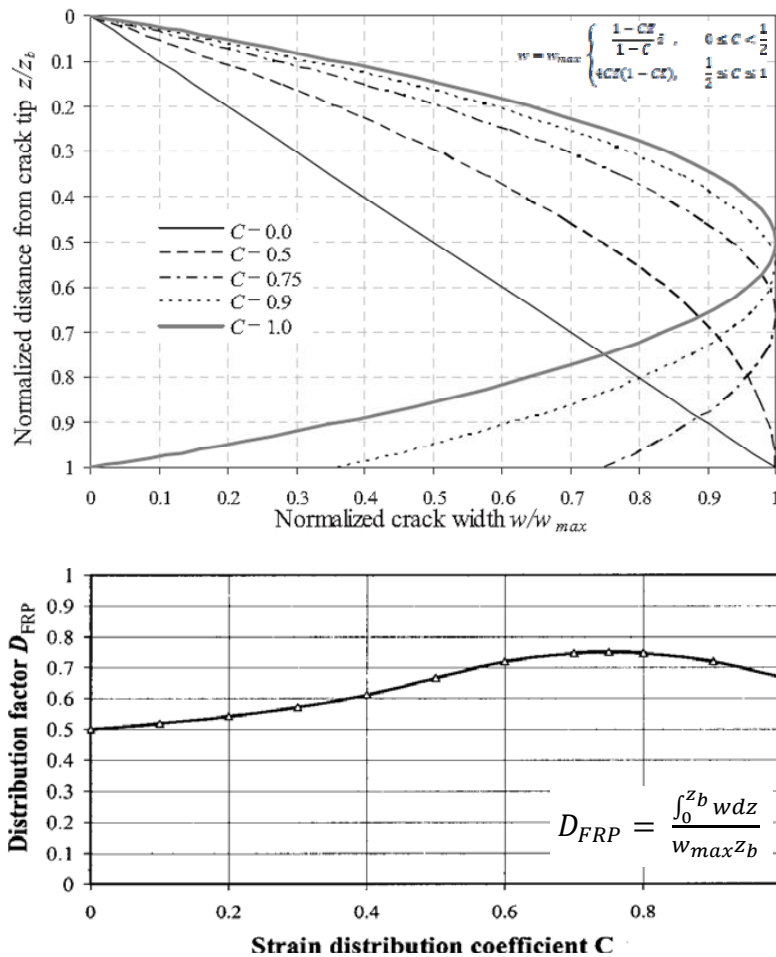

Figure 5-24 Crack shapes and distribution factor corresponding to different C values
(Chen 2003, 2010)

202

5.5.2 Model Assumptions

Although multiple shear cracks developed in reinforced concrete beams as shown in Figure 5-25, a single critical crack is assumed for the purpose of the proposed simple model. Furthermore, crack widths typically vary along their length. It is assumed that the variation of crack width can be presented with a simple function (e.g., multi-linear) in the model. Lastly, the angle between the critical crack and transverse reinforcement along the crack is assumed to be constant throughout loading.
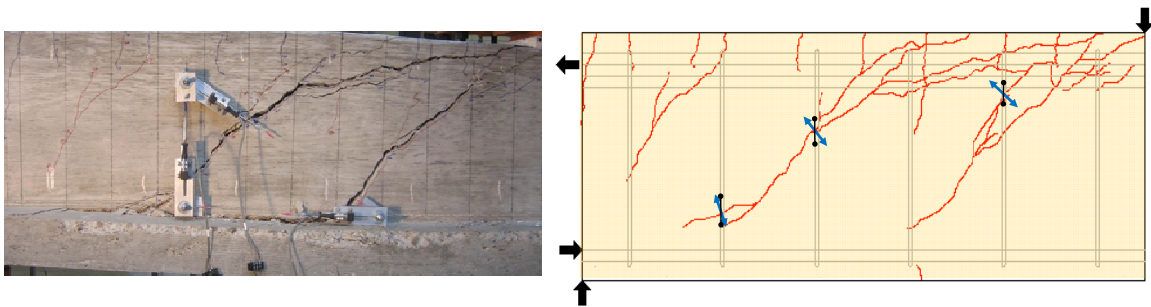

Figure 5-25 Crack patterns of RC beams (24-3-2)

Usually flexural cracks initiate at the bottom of a beam at the tension face and extend towards the compression region. Thus, flexural–shear cracks are typically wider at the tension face and get narrower toward the compressive region (Figure 5-26 (a)). The width of a web-shear crack will also be widest near mid-height (Figure 5-26 (b)); particularly in deeper beams. Real cracks typically have widths that vary in a hybrid fashion between the two extremes described, with mid-height widths being closer to the crack width at the tension face.
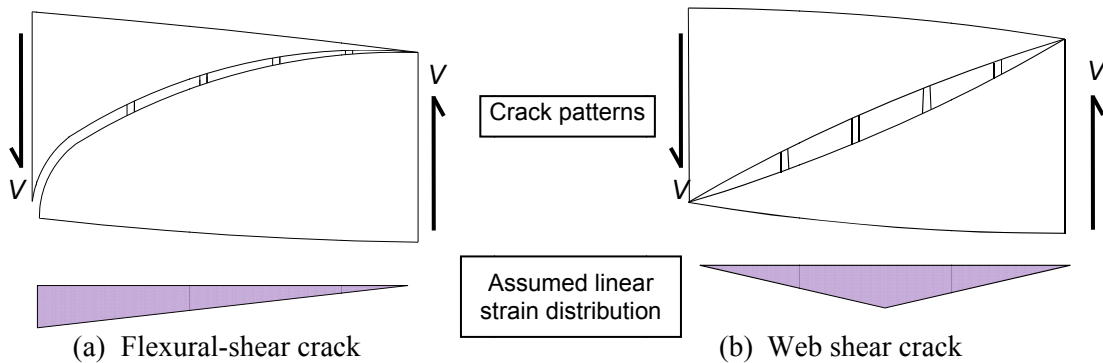

(a) Flexural-shear crack   (b) Web shear crack
Figure 5-26 Critical crack configurations for flexural shear and web shear

203

The critical crack width directly affects the strain distribution of the FRP along the crack and the FRP contribution to shear capacity. It is difficult to assess the strain distribution of FRP along a crack and a simple linear strain distribution is assumed for the proposed model. This simple strain distribution accounts for compatibility of deformation between adjacent steel stirrups and FRP strips.

The bond behavior between concrete and FRP is neglected in this proposed simple model, such that the stiffness of the shear reinforcement can simply be determined by the area of FRP and total vertical length of the strip. As shown in Figure 5-27, the simple approach is conservative because it under-estimates the force in this FRP element at a given displacement. Therefore, the shear contribution of the FRP before full debonding is under-estimated. Similarly, neglecting bond between steel stirrups and concrete will under-estimate the steel contribution to shear capacity before yielding occurs.
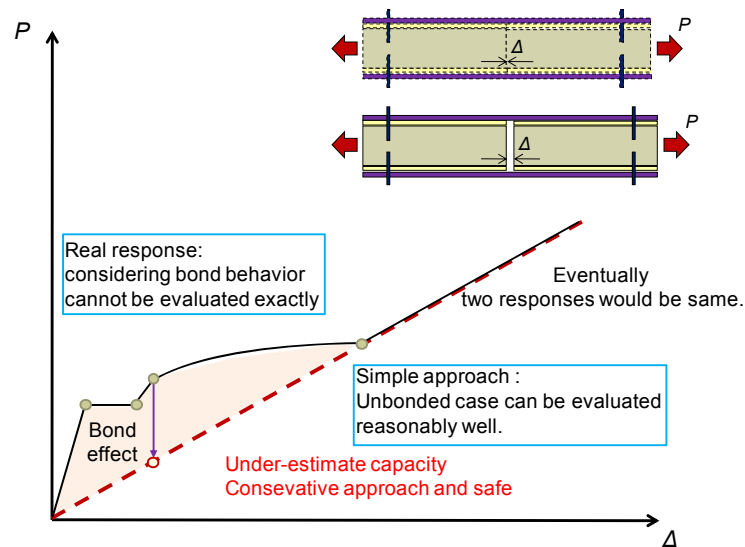

Figure 5-27 RC beam force deformation response from simple behavioral model

In summary, several simplifying assumptions are used in the shear model:

1. Single critical shear crack
2. Constant angle of critical crack
3. Strain distribution varies linearly across the critical crack
4. The strain along steel and FRP element lengths is constant because bond is not considered.
5. Concrete shear strength contribution is not considered.

5.5.3   Behavioral Model Configuration and Material Properties

To illustrate the model, a scenario similar in configuration and material properties to the test specimens is considered (Figure 5-28).
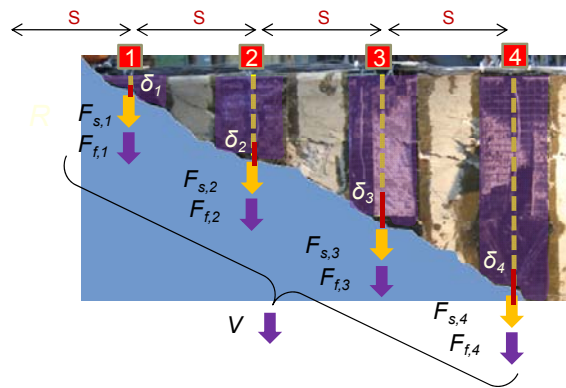
(a) Reinforcement layout across the critical crack
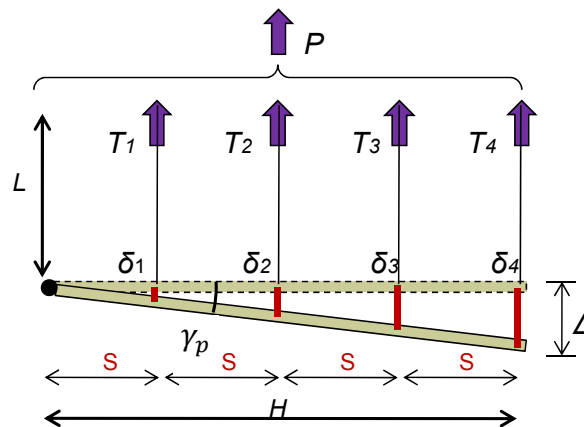
(b) Corresponding shear model

Figure 5-28 Illustration of Simple Shear Behavior Model

Four steel stirrups or four FRP sheets are assumed to cross the critical shear crack and therefore contribute to beam shear capacity. Assuming a linear crack width profile, the deformation of each steel or FRP element can be evaluated from pseudo-shear strain (γ_p) defined by the maximum deformation in the direction of the reinforcement divided by the length over the critical section. Pseudo-shear strain is not the same as the measured shear strain obtained in the experimental program, but it provides a means of comparing test observations with the model response.

As shown in Figure 5-29, linear distribution is a reasonable assumption because the shear contribution based on this distribution will be close of that based on any strain distribution.
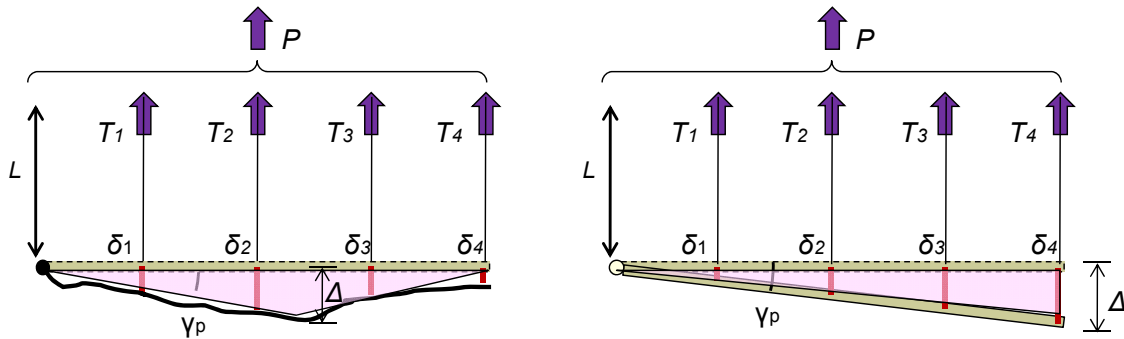

Figure 5-29 Illustration of Shear Behavior Model at arbitrary crack profiles

Dimensions and material properties used for the illustrative example are shown in Table 5-5, Figure 5-30, and Figure 5-31.

Table 5-5 Parameters of Simple Shear Behavior Model

Parameters		
The span length within critical crack	H	80 in.
Reinforcement length, effective length or height	L	40 in.
Reinforcement spacing	s	20 in.
2 leg #3 @20"	A_s	0.22 in.^{2}
0.011 in. thick., 10 in, wide @ 20" (both face)	A_f	0.22 in.^{2}

(a) stress- strain   (b) force-displacement of element

Figure 5-30 Properties of steel
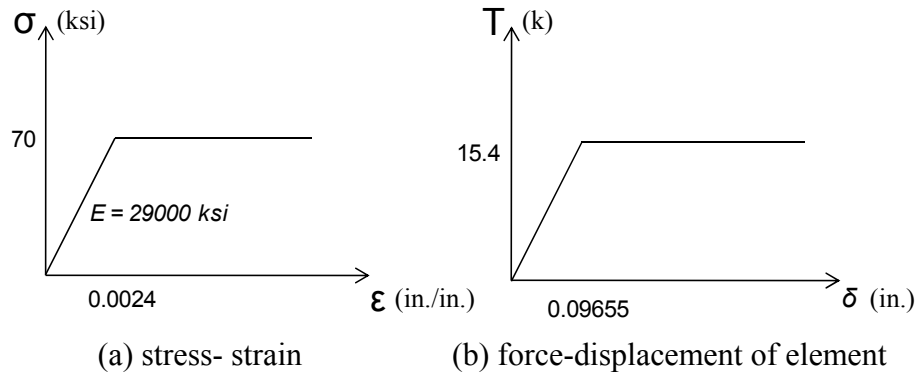

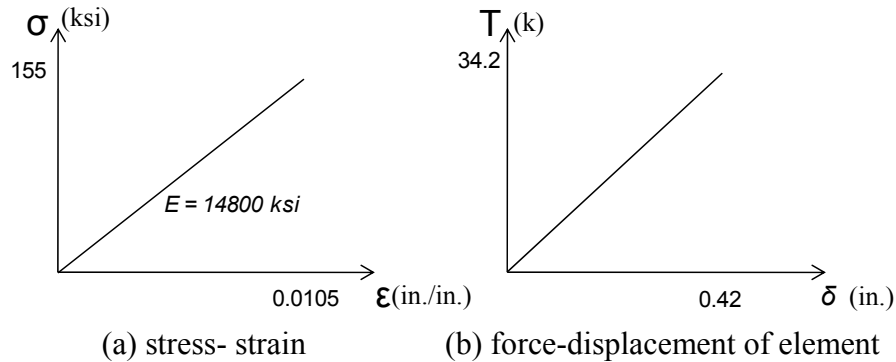(a) stress- strain   (b) force-displacement of element

Figure 5-31 Properties of FRP

5.5.4 Effects of Reinforcement Layout

Two reinforcement layouts (Cases A and B) are considered as shown in Figure 5-32. The difference between Case A and Case B is the location of the critical section with

respect to the vertical elements. The spacing of the vertical elements is constant, but shifted by $^S/_2$ in Case B.
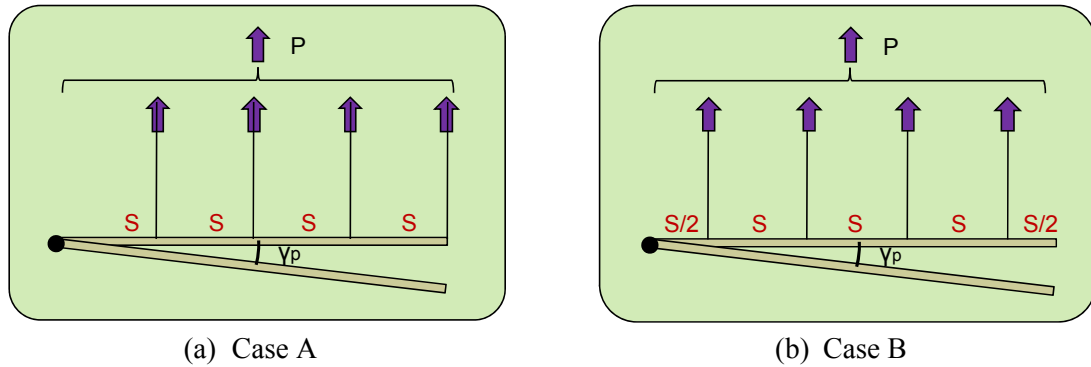

(a) Case A (b) Case B

Figure 5-32 Reinforcement layouts of simple shear behavior model

5.5.4.1 *Systems with Steel (ductile material) Elements*

The load versus shear strain responses of Cases A and B are shown in Figure 5-33. Due to the non-uniform strain distribution along the crack length, the yielding of stirrups occurs in sequence with increasing deformations. The first yielding in Case A occurred at Element 4 because the deformation of Element 4 is the largest (Figure 5-34). Element force is evaluated from force-deformation relationship. After yielding of Element 4, the force in Element 4 is constant.
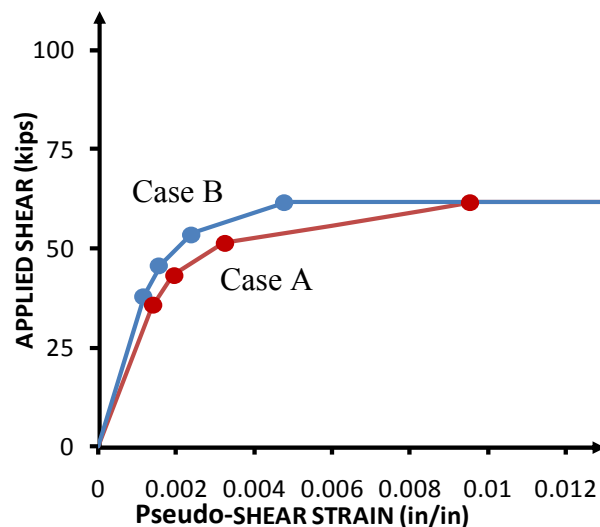

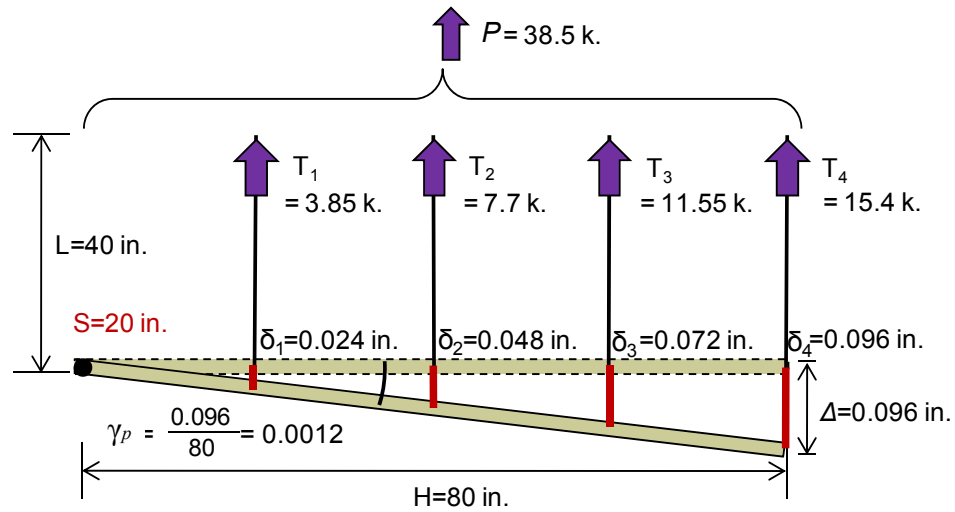***Figure 5-33 Shear strain-applied shear response of two cases***

208

Figure 5-34 Displacement configurations when first yielding (Case A)

Table 5-6 Summary of the load & shear strains when each stirrup yields (Case A)

Case A	γ_p	P	T_1	T_2	T_3	T_4
1st yielding	0.00121	38.5	3.85	7.7	11.55	15.4
2nd yielding	0.00161	46.2	5.13	10.27	15.4	15.4
3rd yielding	0.00241	53.9	7.7	15.4	15.4	15.4
4th yielding	0.00483	61.6	15.4	15.4	15.4	15.4

Note. Terms are defined in Figure 5-27 ,　Units : V and T in kips

Pseudo-shear strain, applied shear force, and element forces at the yield strain of each element are summarized in Table 5-6. Following the same procedure, the response of Case B was evaluated and the responses between two cases are compared in Table 5-7.

Table 5-7 Load-strain response in steel contribution of Case A and Case B

Steel	Case A		Case B	
	γ_p (in./in.)	P (k)	γ_p (in./in.)	P (k)
1st yielding	0.00121	38.5	0.00138	35.2
2nd yielding	0.00161	46.2	0.00193	43.12
3rd yielding	0.00241	53.9	0.00322	51.33
4th yielding	0.00483	61.6	0.00966	61.6

As shown in Figure 5-33, the stiffness of the two cases is slightly different but the maximum capacity of the two systems is identical after all stirrups yield. It is noted that if the pseudo-shear strain is not large enough to yield all elements, maximum capacity will differ.

5.5.4.2 Systems with FRP (brittle material) Elements

The pseudo-shear strain versus shear force response of Cases A and B with FRP vertical elements is shown in Figure 5-35. The displacement configurations of three different load phases for Case A are shown in Figure 5-36.

Unlike steel, FRP cannot sustain its capacity after rupture. In this case, the remaining capacity after first rupture does not exceed the shear force at first rupture. As a result, the failure would be abrupt and explosive with rupture of all elements if the loading was load-controlled. Under displacement control, the second rupture of another element can be monitored as shown in Figure 5-36 (c). With this procedure, the peak values at rupture of each strip are evaluated as shown in Table 5-8.
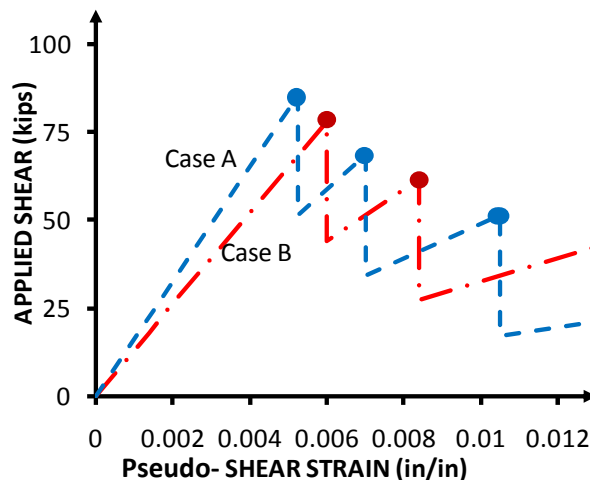

Figure 5-35 Shear strain vs. applied shear response of two cases with FRP

(a) Right before first rupture

(b) Right after first rupture

(c) Right before second rupture

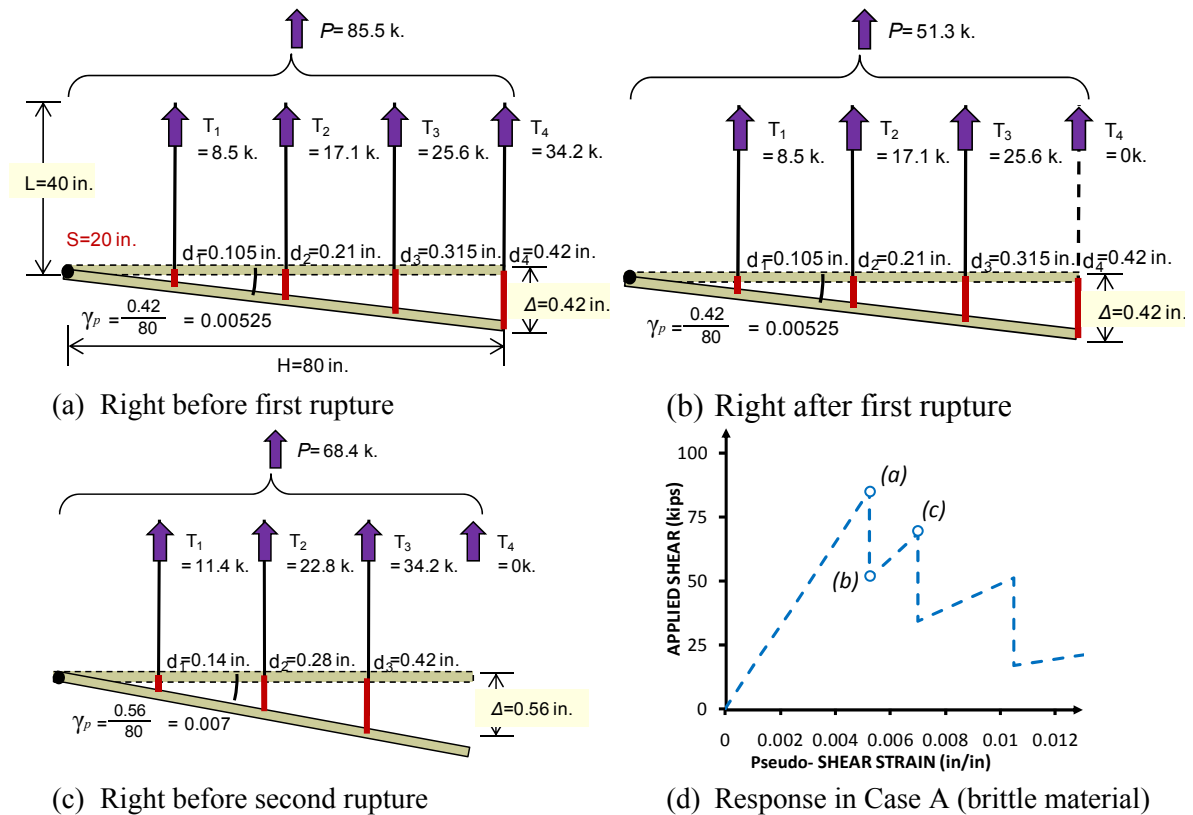(d) Response in Case A (brittle material)

Figure 5-36 Displacement configurations of different phases in FRP material

Table 5-8 Summary of load and shear strains when each element ruptures

	γ_p	P (k)		T_1 (k)	T_2 (k)	T_3 (k)	T_4 (k)
1st rupture	0.00525	85.47	51.28	8.55	17.09	25.64	34.19 → 0
2nd rupture	0.007	68.38	34.19	11.40	22.79	34.19 → 0	0
3rd rupture	0.0105	51.28	17.09	17.09	34.19 → 0	0	0
4th rupture	0.021	34.19	0	34.19 → 0	0	0	0

Several observations can be made from this example. The summation of all FRP element axial capacities is 136.75 k (34.19 k ×4 elements), but the maximum capacities of Cases A and B are 85.47 k and 78.14 k respectively (Table 5-9); which correspond to 62.5% and 57% of the maximum possible capacity. Two different layouts may therefore not give the same maximum capacity and these capacities cannot equal the sum of all element capacities. Furthermore, given that crack width profiles may also differ between

211

members with the same reinforcement layout, one can conclude that shear capacity using a brittle material can vary more than when steel stirrups are used. More conservative design recommendations may thus be warranted for FRP reinforced concrete beams.

Table 5-9 Load-strain response of Case A and Case B with FRP material

FRP	Case A			Case B		
	γ_p (in./in.)	P (k)		γ_p (in./in.)	P (k)	
1st rupture	0.00525	85.47	51.28	0.006	78.14	43.96
2nd rupture	0.007	68.38	34.19	0.0084	61.54	27.35
3rd rupture	0.0105	51.28	17.09	0.014	45.58	11.40
4th rupture	0.021	34.19	0	0.042	34.19	0

5.5.4.3 System with both Steel and FRP Elements

The combined shear force versus pseudo-shear strain response of Case A is shown in Figure 5-37 and key values presented in Table 5-10. The maximum shear contribution of steel occurred when all stirrups yielded, whereas the maximum shear contribution of FRP occurred when the first FRP strip ruptured. The maximum shear of the system occurred at the first FRP strip rupture. Such behavior is only valid when the pseudo-shear strain at first rupture is greater than the pseudo-shear strain at yielding of all stirrups.
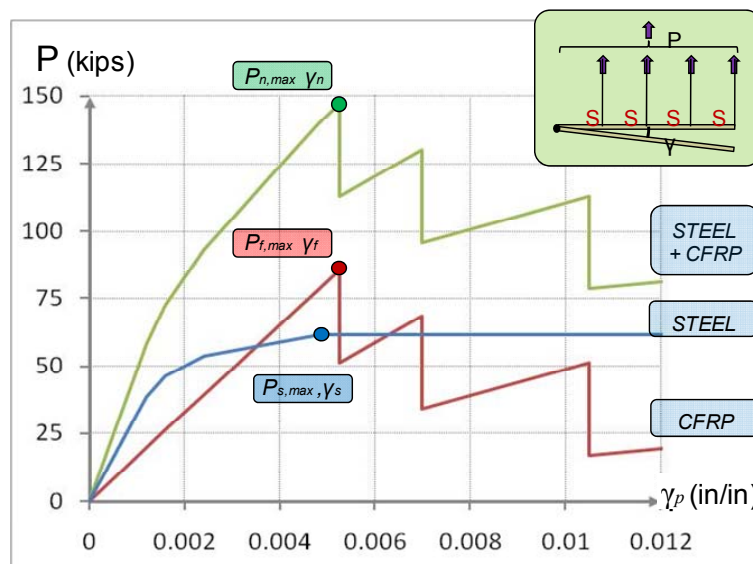

Figure 5-37 Combined behavior (Case A)

212

Table 5-10 Maximum capacity of steel, FRP, and combination (Case A)

	Steel	FRP	Combined	
Shear strain at max. contribution	$\gamma_s = 0.00483$	$\gamma_f = 0.00525$	$\gamma_n = 0.00525$	$\gamma_n = \gamma_f > \gamma_s$
Max. contribution	$P_{s,max} = 61.6\ k$	$P_{f,max} = 82.5\ k$	$P_{n,max} = 144.1k$	$P_{n,max} = P_{s,max} + P_{f,max}$

As shown in Figure 5-38 and

Table 5-11, the maximum shear contributions of both materials in Case B did not occur at the same time. As a result, the maximum capacity of the combined system is less than the sum of steel contribution and FRP contribution

The maximum capacity in Case B is obtained by adding the maximum FRP contribution and the steel contribution when the first FRP strip ruptured. The difference (ΔP) between the maximum steel contribution ($P_{s,max}$) and the actual steel contribution at maximum capacity (P_{s0}) is 5.8 k; which is a capacity loss due to deformation limitations that occur in members strengthened with brittle materials.
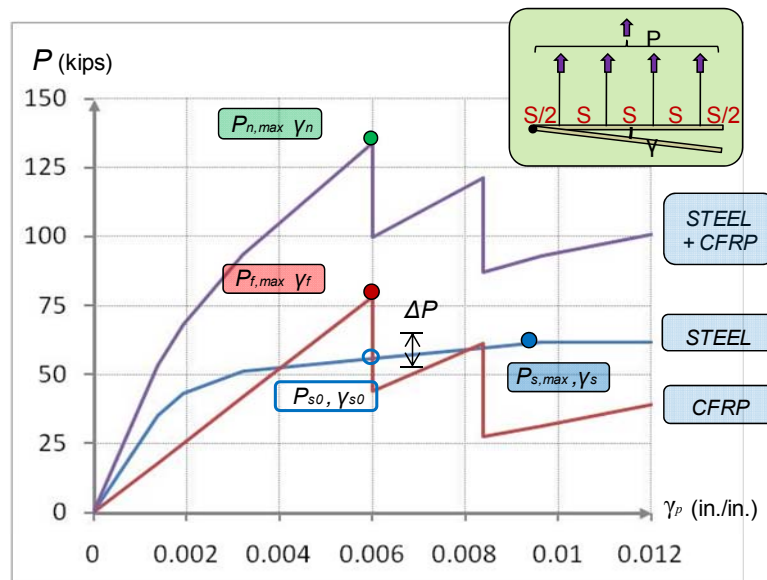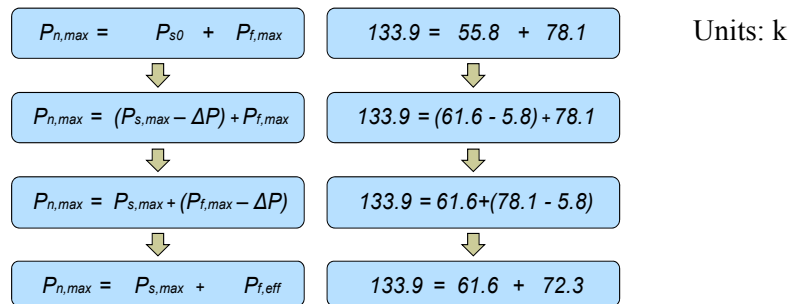

Figure 5-38 Combined behavior (Case B)

213

Table 5-11 Maximum capacity of steel, FRP and combination (Case B)

	Steel	FRP	Combined	
Shear strain at max. contribution	γ_s =0.00966	γ_f =0.006	γ_n = 0.006	$\gamma_n = \gamma_f < \gamma_s$
Max. contribution	$P_{s,max}$= 61.6k	$P_{f,max}$ =78.1k	$P_{n,max}$=133.9k	$P_{n,max} < P_{s,max}+P_{f,max}$

In design however, FRP is usually considered as the strengthening material and thus this loss in capacity is taken into account through a reduction in the FRP contribution instead of a reduction in steel contribution. The typical treatment of reduction in the steel contribution is illustrated in Figure 5-39. This reduction is determined by the FRP deformation limit and level of the steel contribution. For this reason, the maximum capacity of the combined system varies depending on deformation compatibility between steel and FRP.

$$P_{n,max} = P_{s0} + P_{f,max} \qquad 133.9 = 55.8 + 78.1 \qquad \text{Units: k}$$

$$P_{n,max} = (P_{s,max} - \Delta P) + P_{f,max} \qquad 133.9 = (61.6 - 5.8) + 78.1$$

$$P_{n,max} = P_{s,max} + (P_{f,max} - \Delta P) \qquad 133.9 = 61.6 + (78.1 - 5.8)$$

$$P_{n,max} = P_{s,max} + P_{f,eff} \qquad 133.9 = 61.6 + 72.3$$

P_{s0} : Steel contribution at the displacement of FRP maximum contribution
$\Delta P = P_{s,max} - P_{s0}$

Figure 5-39 Reduction in capacity due to FRP deformation limit

5.5.5 Debonding Failure (without anchorage)

In most cases of external FRP shear strengthening, debonding of the FRP from the concrete surface determines the maximum FRP shear contribution. Using the same system discussed in the previous section, the effects of debonding failure are studied.

5.5.5.1 System with FRP Elements

If a properly designed anchorage system is not provided for externally applied FRP, rupture strain is unlikely to be reached before debonding occurs. Typically, the debonding strain between FRP and concrete is around 0.004. Due to debonding, FRP material capacity is effectively reduced as shown in Figure 5-40. With these material properties, the response of Case B (discussed in Section 5.5.4) is investigated. As the usable FRP strain changes from the 0.0105 rupture strain to 0.004, element strength changes from 34.2 k to 13 k (2.7 times lower) while the deformation limit of FRP elements changes from 0.42 in. to 0.16 in.. With these element properties, the system response is shown in Figure 5-41. As can be seen in the figure, the initial stiffness of the system is not changed but strength and deformation at peak strength are decreased.
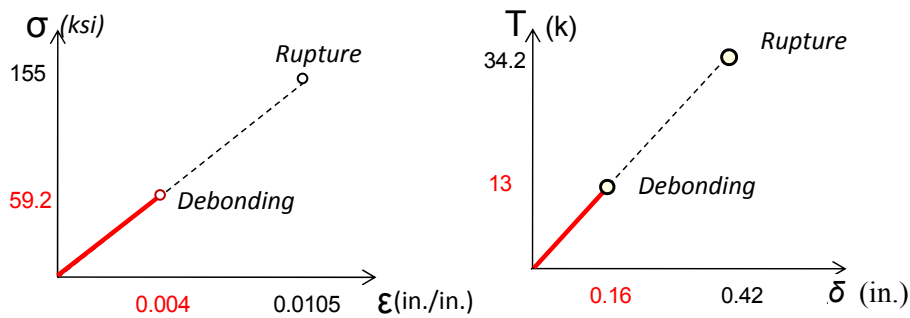
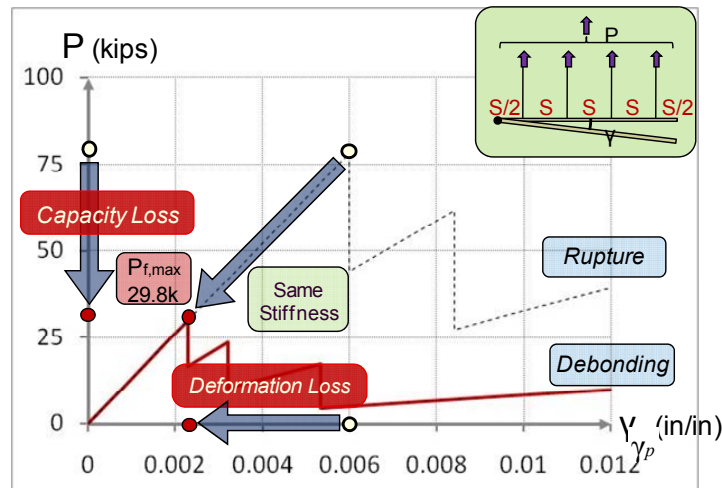**Figure 5-40 Element properties when FRP debonding**

Figure 5-41 Effect of FRP debonding on FRP shear contribution

215

5.5.5.2 System with Steel and FRP

Debonding failure reduces not only the strength contribution of the FRP, but also the deformation at peak strength. Such deformation reduction causes additional capacity loss due to a decrease in steel contribution when the combined steel/FRP system response is considered. As shown in Figure 5-42, the maximum strength of a combined system when debonding occurs is 75.2 k, which is 16.2 k less than the sum of the maximum steel and FRP strengths. The reduction in system strength is due to the FRP reaching debonding limits prior to yielding of all steel stirrups.

While the maximum strength of combined system with failure occurs at first debonding of FRP, subsequent strength peaks are at values that are close to the first peak. (Figure 5-42) The strengths at peak are summarized in Table 5-12.
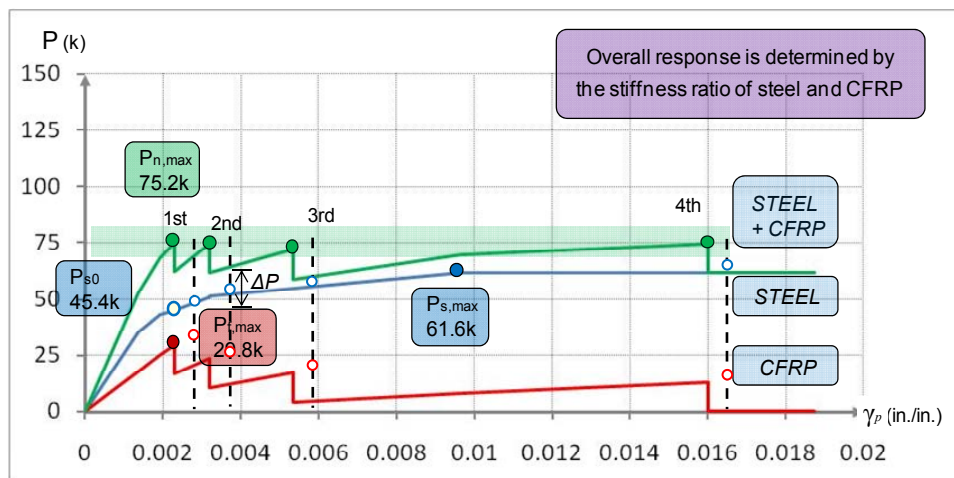
Figure 5-42 Combined response (with debonding)

Table 5-12 Steel, FRP, and combined capacity at debonding

	γ_p	$P_{s,i}$ (k)	$P_{f,i}$ (k)	$P_{n,i}$ (k)
1st debonding	0.00229	45.4	29.8	**75.2**
2nd debonding	0.0032	51.2	23.4	**74.7**
3rd debonding	0.00533	54.7	17.4	**72.1**
4th debonding	0.016	61.6	13.0	**74.6**

$P_{s,i}, P_{f,i}, P_{n,i}$: Steel contribution, FRP contribution, and overall strength at i-th peak

Small changes in FRP or steel area in this case can change the pseudo-shear strain at maximum strength significantly. In RC beams, concrete response also affects system response, possibly shifting maximum system strength to the shear strain at debonding failure of the second strip or even further. Such a shift was observed in several tests reported in Chapter 4, including tests 24-3-3, 24-3-4, 24-3-5, 24-3-9, and 24-2.1-1.

5.5.6 Shear Capacity Increase due to FRP Strengthening

FRP material is used for strengthening, so it is meaningful to evaluate strength increase with FRP. Two systems previously investigated with the same amount of FRP material are discussed. One system has FRP anchorage and the other does not. Both systems have the same layout as Case B of Section 5.5.4 and their responses were presented in Figure 5-38 and Figure 5-42. Strength increases in both cases due to FRP strengthening are presented in Figure 5-43 and Table 5-13. Since the maximum force an anchored FRP sheet can resist is about 2.5 times larger than that of an unanchored sheet (from the strain capacity ratio = 0.01/0.004 = 2.5), it is reasonable to expect that the shear strength increase of the beam strengthened with anchorage will be about 2.5 greater than that without anchorage. However, that is not the case because of capacity loss from various elements reaching their capacities at different deformations (as discussed in Section 5.5.2). As a result, the experimentally obtained strength increase of the beam strengthened without anchorage is 4 k, whereas the strength increase of the beam strengthened with anchorage was 47 k; which produces a ratio of strength increase of 47/4 = 11.75. The model captures that effect with unanchored beam strength gain of 13.6 k and anchored beam strength gain of 72.3 k; which produces a ratio of strength increase of 5.3.
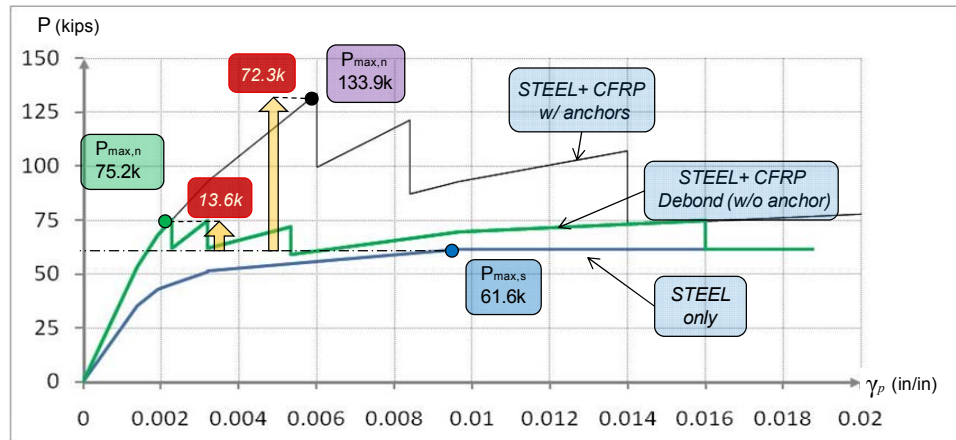
Figure 5-43 Strength increase of two cases (with anchors and without anchors)

Table 5-13 Comparison of the strength increases between a system with anchorage and a system without anchorage

	With anchorage (a)	Without anchorage (b)	Ratio (a) / (b)
FRP maximum usable strain	0.0105	0.004	2.625
FRP sum of element usable capacity	142.9k	52.1k	2.625
Maximum possible FRP shear contribution	78.1k (55%)	29.8k (55%)	2.625
Corresponding FRP average strain	0.0058	0.0022	
Capacity Loss due to peak material strengths at differing deformations	5.8k	16.2k	-
Net Strength increase	72.3k (51%)	13.6k (26%)	5.32
Corresponding FRP average strain (Effective FRP strain for design)	0.0053	0.0010	

Thus anchoring FRP sheets not only increases the usable strain and strength limits of the sheets but also has the potential of increasing the deformability of the member such that all steel stirrups across the critical section can yield; thus minimizing the loss of steel shear contributions.

Due to non-uniform strain distribution along the critical section, an effective FRP strain for design needs to be specified. The effective strain is a function of the shape of the strain distribution and the critical crack angle. In addition, the effect of steel

contribution reduction should be taken into account; most conveniently that reduction can be accounted for by reducing the effective FRP strain. In this example, the maximum usable FRP contribution in the case with anchors is 55% of the full element capacity. In other words, the average strain from element 1 to element 4 is comparable to 0.0058. However, after considering the capacity reduction due steel capacity loss, the net strength increase due to FRP strengthening is 72.3 k, which corresponds to 51% of FRP capacity or an effective FRP strain of 0.0053. (The average strain from tests results in Section 4.6 was 0.0051)

The same trends are observed in Table 5-13 for the un-anchored FRP system but with lower FRP contribution due to FRP debonding. In the unanchored case, the maximum possible FRP shear contribution is 21% of the full material capacity, which is equivalent to an average FRP strain of 0.0022. However, the estimated net capacity increase for the system is only 9.5% percent of the full material capacity (or 13.6 k) due to the loss in steel contribution; which corresponds to an effective FRP strain for design of 0.0010.

5.5.7 Continuous FRP Sheets

Because the shear capacity of the beam strengthened with FRP is different depending on the layout of FRP reinforcement, continuous sheet applications are likely to exhibit different behavior than discrete sheet applications.

A comparison was made between a model with continuous sheet application and Case B discussed in Section 5.5.4; the continuous sheet has equal FRP material quantity as the strip layout. As shown in Figure 5-44, the proposed model shows that the response of the continuous sheet application follows that of the discrete strip application without the large discontinuities the former exhibits. The initial stiffness with strips and continuous applications is identical, but the shear capacity of the strip layout is slightly greater than that of the continuous sheet application.
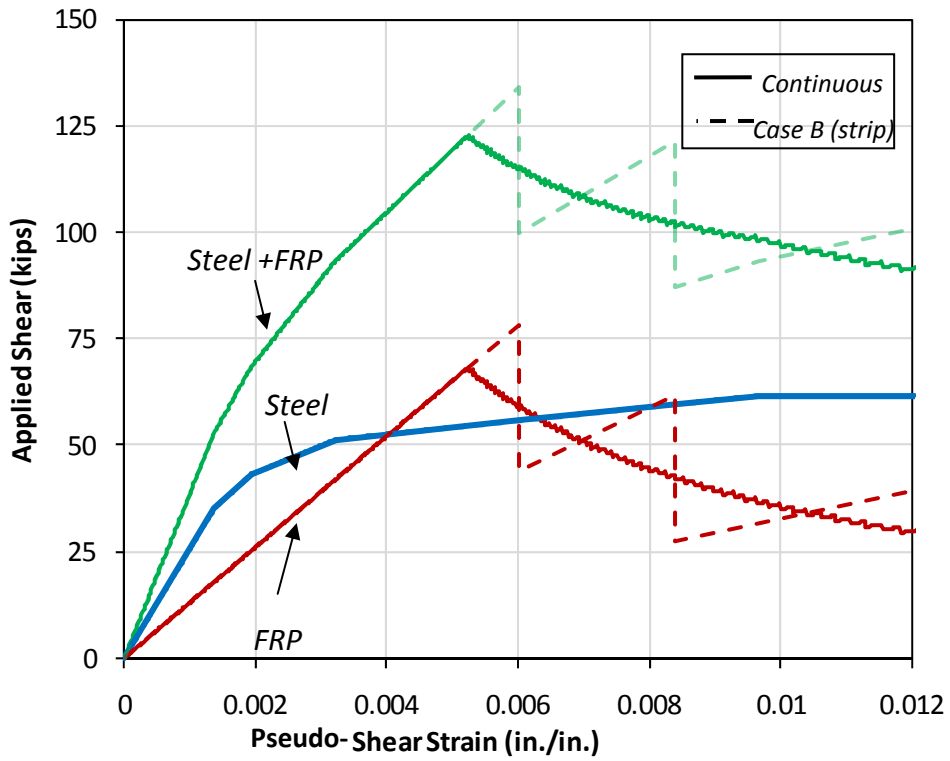
(a) With anchorage
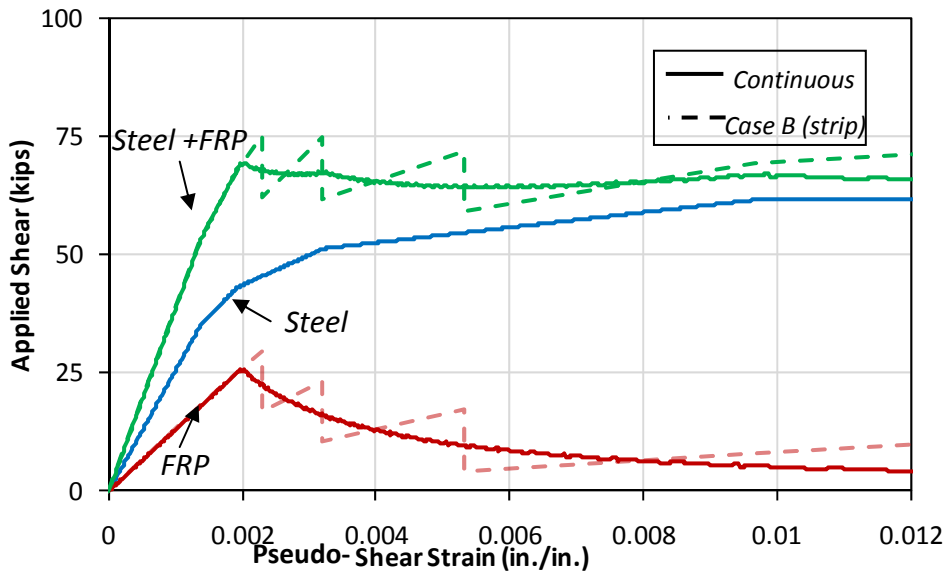
(b) Without anchorage

Figure 5-44 Response of continuous sheet compared with strip

220

Even though the FRP reinforcement ratio of both cases is the same, the FRP rupture occurs first in continuous sheets because of the larger strain variations along crack length. Because the strength of discrete strips depends on the strip layouts relative to the location of critical crack, the strength of continuous sheets can be used as a reference to get a reasonable strength estimate when the strip layout and the crack location are not specified.

Comparison between model and experimental results for continuous sheet applications was not possible. Tests 24-3-7 (continuous sheet) and 24-3-8 (2-layer strips) contained the same area of CFRP but in strip and continuous layouts. Unfortunately, beam 24-3-8 failed by the fracture of a CFRP anchor, such that the rupture strain in the CFRP was not reached.

5.5.8   Comparison with test results

The results from the model are compared with experimental results (Figure 5-45 and Table 5-14). The model response does not include the concrete contribution as discussed in Section 5.5.2. Therefore, the calculated concrete contribution to shear strength based on ACI 440.2R is added to the model response for comparison with experimental results.

(a) Response from tests   (b) Response from shear model
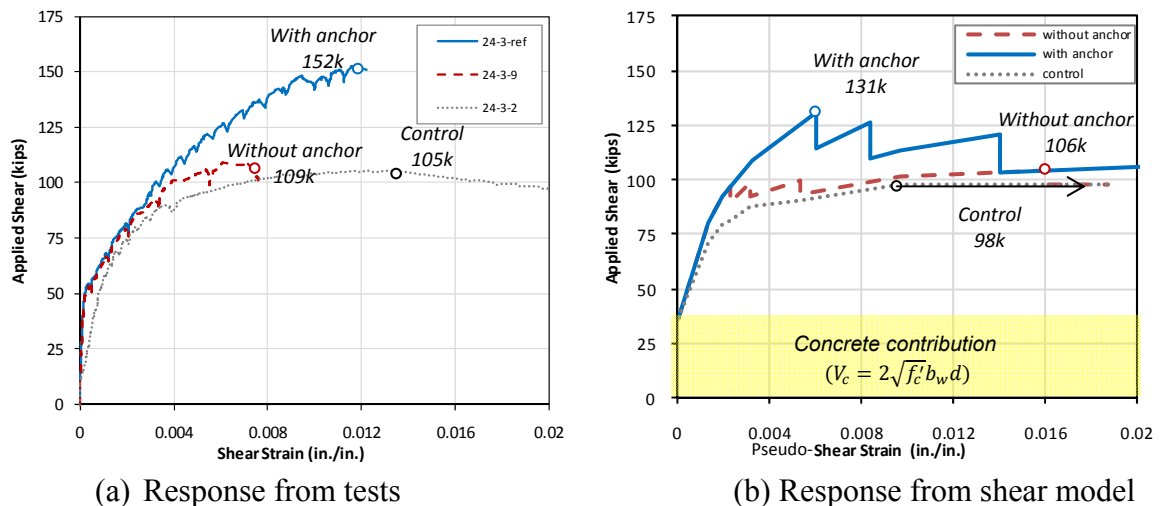
Figure 5-45 Comparison in response between tests and shear model

221

Table 5-14 Comparison of the strength increases between tests and shear model

	V (k) from ACI 440 EQ.		F (k) from TEST		F (k) from Shear Model*	
	Beam strength	Strength increase	Beam strength	Strength increase	Beam strength	Strength increase
Control (24-3-2)	64	-	105	-	**98**	
Unanchored (24-3-9)	74	10	109	4	106	8
Anchored (24-3-1r)	91	27	152	47	131	33

Note. Concrete contribution is evaluated based on ACI 440.2R   (Units: k)

Three tests (24-3-ref, 24-3-9 and 24-3-2) are used in model validation. Test observations indicate that FRP reinforced beams without FRP anchors can have lower deformation capacity than a nominally identical beam that is not reinforced with FRP (referred to as the control specimen; Figure 5-45). The proposed behavioral model captured the capacity loss due to interaction between steel and FRP. It is meaningless to compare shear strain values between tests and the model because the shear strain is not defined the same way. In addition, the bond effects are not included in this model. However, the general trends are quite similar.

5.6   SHEAR BEHAVIOR MODEL CONSIDERING BOND BEHAVIOR

In Section 5.5, the bond behavior was neglected to evaluate conservatively the ultimate strength of systems with adequately anchored FRP. To evaluate the effectiveness of the anchorage system, it is necessary to compare anchored system with bond-critical systems such as U-wrap and 2-sides bonded applications that necessitate the consideration of bond between the FRP and concrete. Moreover, while the effects of bond in anchored systems may be neglected at ultimate strength, when at service or design load levels, bond behavior becomes more critical and should be considered.

5.6.1 Comparison between 2-sides Bonded, U-wrap, and Completely Wrapped FRP Applications

FRP shear strengthening can be performed using separate bonded sheets on either side of a section (2-sides bonded), wrapping sheets on three sides of an element (U-wrap), and completely wrapping a section. To compare the effectiveness of these applications, bond behavior is included as it affects the stiffness of the bonded FRP and will be different for each of these applications.

5.6.1.1 Shear contribution in bond critical application

In Section 5.5.5, shear capacity at debonding failure was investigated and found to depend on the relative stiffness of each component. Stiffness variations due to change in the bond length were not considered in Section 5.5.5, but a constant stiffness neglecting bond behavior was used. The result was a conservative estimate of shear capacity.

5.6.1.2 Simplified response considering effect of bond

As shown in Figure 5-46, bond behavior can be simulated by using effective length instead of total member length and it can be compared with the dotted line that represents the response of shear reinforcement without considering bond behavior (as discussed in Section 5.4).
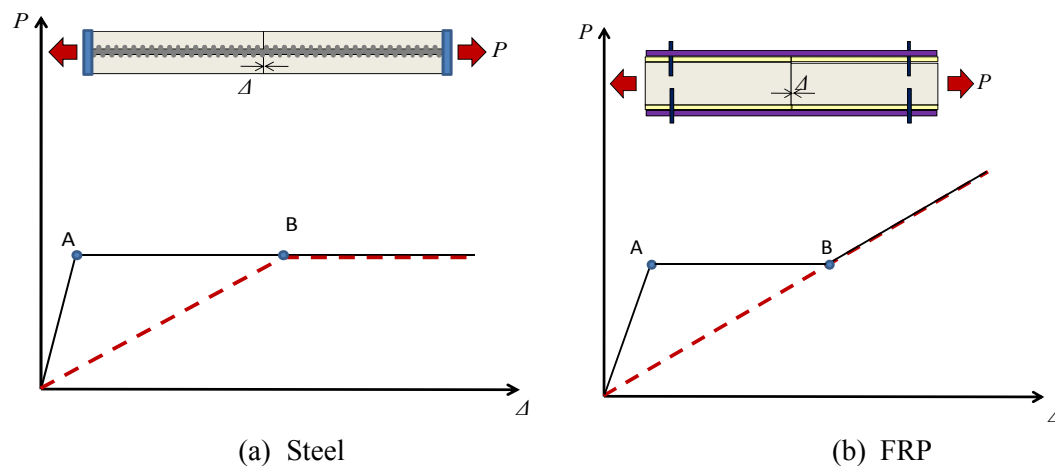
(a) Steel   (b) FRP
Figure 5-46 Simplified response considering bond effects

223

A concrete cracking Figure 5-46 initiated before debonding, which is at the low load level. Therefore, it is not important in developing shear contributions at ultimate load and change in stiffness due to concrete cracking was not considered. Point A of both responses in Figure 5-46 was evaluated using different definitions. For steel stirrups, Point A is determined by the effective length when steel reaches yield. Once the steel yields, the capacity of the member is constant regardless of bond behavior. For FRP, point A is from the stress (or strain) when debonding occurs. In region A-B, the deformation increases without any increase in stress due to debonding. The effective length also increases until debonding failure occurs. With adequate anchorage, stress in FRP will increase beyond point B until anchor failure or rupture because the effective length remains constant (anchor to anchor).

5.6.1.3   Strip-end debonding

In shear applications, FRP strips are subjected to different strains from the critical crack to the end of the strip. Once debonding starts, strip end-debonding is more critical when the distance from the crack to the strip end is short. In addition, once an end of a strip is totally debonded, there is no stress in the strip.

As shown in Figure 5-47, the strip-end debonding risk zone in U-wrap application would be smaller than that in sides-bonded application. In addition, a completely wrapped beam has no risk of strip-end debonding. In U-wrap with anchorage, the FRP anchor located at strip-end risk zone might be highly stressed.

(a) U-wrap application   (b) 2-side bond application
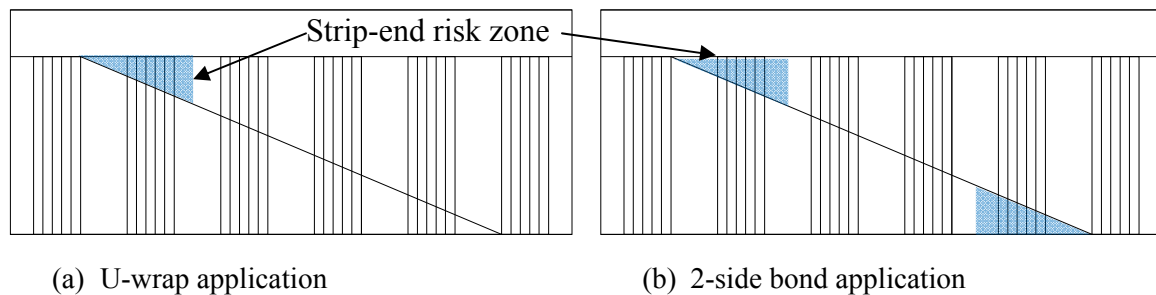
Figure 5-47 Strip-end debonding risk zone

5.6.1.4 Strip-end debonding and intermediate crack-induced debonding

Figure 5-48 and Figure 5-49 show the difference in response between strip-end debonding and intermediate crack-induced debonding. If the bond length is too short, debonding would start at a lower strain than the debonding strain as shown in Figure 5-48 (a). On the other hand, once the strain is greater than debonding strain (0.004 is assumed for debonding strain from test observations), debonding would start near the crack regardless of the bond length as shown in Figure 5-49 (a).

τ_{avg}

l_{bond}

σ_{max}

ε_{max}

Debonded length

(a) Before   (b) After
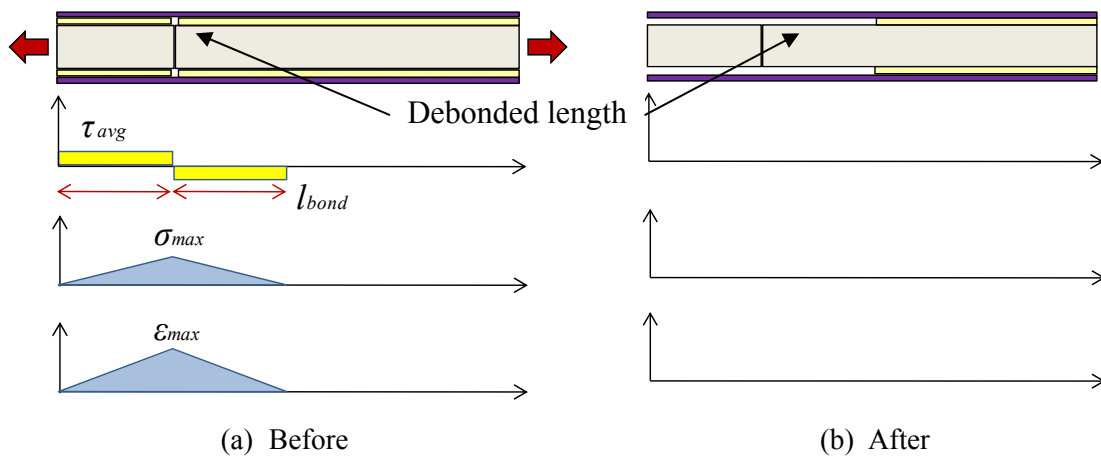
Figure 5-48 Strip-end debonding

τ_{avg}

l_{bond}

σ_{max}

ε_{max}

Debonded length

τ_{avg}

σ_{max}

ε_{max}

(a) Before   (b) After
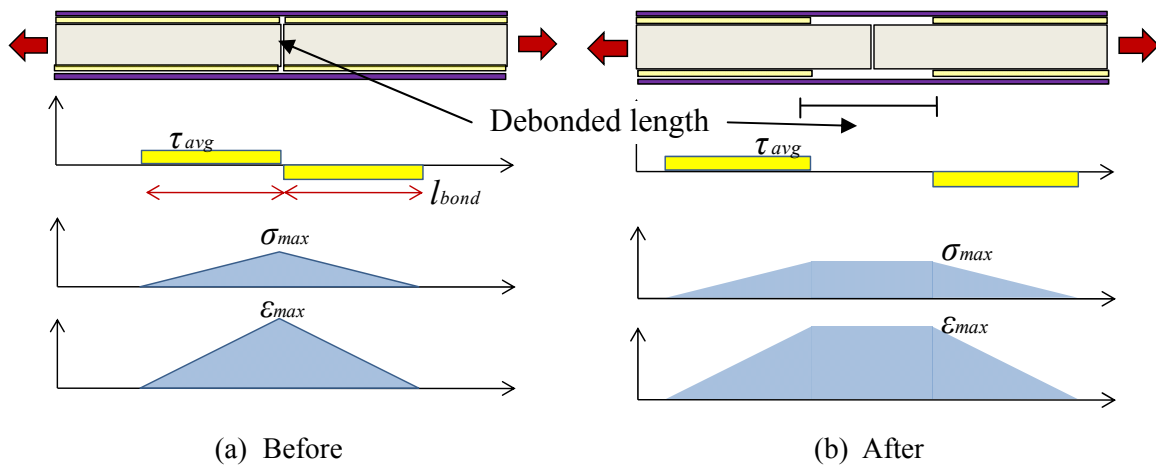
Figure 5-49 Intermediate crack-induced debonding

225

In strip-end debonding, the strain will be zero right after the initiation of debonding because the bond length is short. However, in intermediate crack-induced debonding, the strain is sustained until debonding extends to the strip end. Both responses would be the same eventually, but intermediate crack-induced debonding develops a larger deformation capacity than strip-end debonding. Because several strips across the critical section would contribute to the shear capacity simultaneously, intermediate crack-induced debonding allows other strips to have greater stress because a debonded strip has a larger deformation capacity.

5.6.1.5 *Debonding sequence in U-wrap*

The difference in shear capacity between U-wrap application and side-bond application can be explained by considering end and intermediate crack behavior. In both cases, the debonding of strips does not occur simultaneously because the distance from crack to strip-end varies from strip to strip across a diagonal shear crack.

When a linear strain distribution across the critical crack is assumed, the stress and shear resistance of FRP strips is linearly distributed across strips, but displacement distribution is not linear due to bond behavior.

Consider the example in Figure 5-50, strip-end debonding occurred at strip A and the maximum strain at debonding is lower than the debonding strain. In strip B, intermediate crack-induced debonding starts near crack and extends to the end of strip. In strip C, intermediate crack-induced debonding does not extend to the end of strip, but is close. In strips C and D, the strain can be sustained although the strain exists at the bottom end of strip because the FRP strip is continuous from side to side of beam and is continuous across the bottom of the beam. U-wrap application prevents debonding of the bottom end. If it was 2-sides bonded application, strip C and strip D would debond to strip-end at about the same load causes failure in strips A and B.

When strip B is debonded, other strips have a lower or equal strain. When strip A totally debonds, strip B already has totally debonded and contributes no shear. In other words, the overall shear contribution is less than the sum of the contributions of each strip.

226
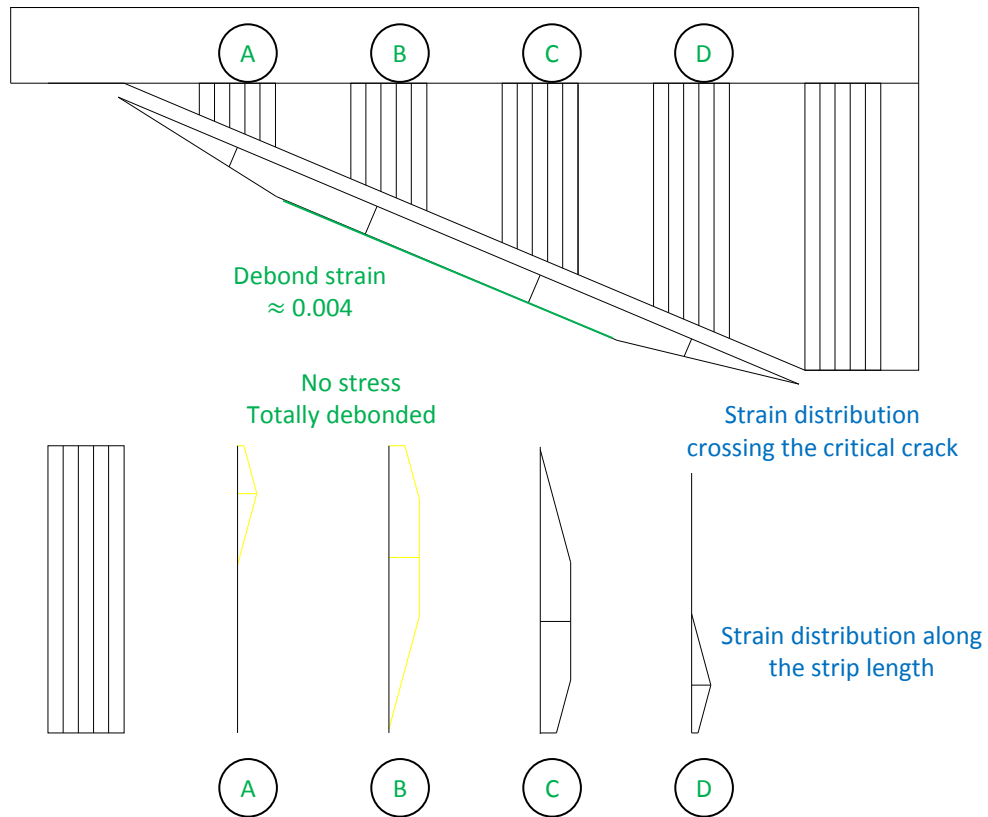
Figure 5-50 Strain distribution along the FRP at debonding

5.6.2 Case Study

5.6.2.1 Configuration of model

To evaluate the characteristic of the response considering bond behavior, the same configuration as the shear model in Section 5.5 is selected, but the effective length concept is added to the previous model as shown in Figure 5-51. Thus the location of the crack is a new parameter.
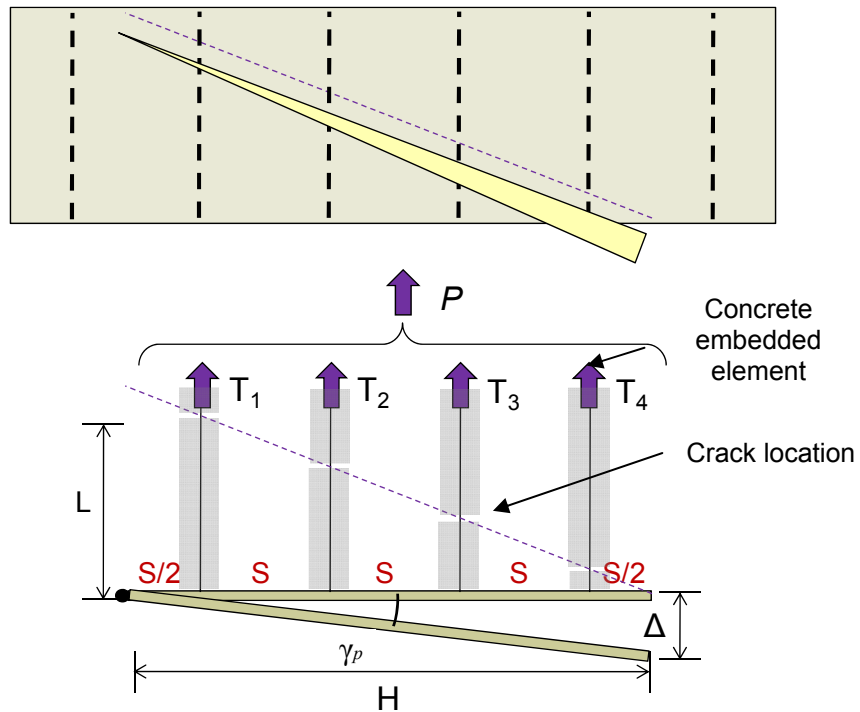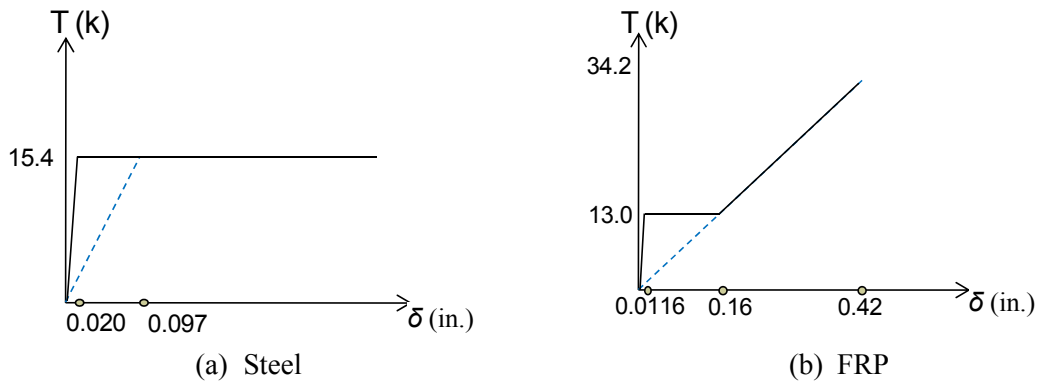
Figure 5-51 Shear behavior model considering bond behavior

(a) Steel   (b) FRP

Figure 5-52 Force-displacement response in steel and FRP material

Linear deformation distribution is assumed across a crack instead of linear strain distribution because the strain cannot be proportional to the displacement before total debonding. The results from Section 5.5 are based on a linear strain distribution, but the deformation distribution in that case was also linear because the element length was constant.

As shown in Figure 5-52, the ultimate strength does not change but the initial stiffness is greater when bond is considered (tension stiffening effect). The effective length at point A is calculated based on the development length for a stirrup with a standard hook (ACI 318-08) and the development length for a FRP strip from an ACI 440.2R Equation (13-2) (Teng et al. 2001). The following equations show the details of the calculations.

$$\Delta_{s,A} = l_{s,dh} \times \varepsilon_y = 8.3 \times 0.0024 = 0.02 \text{ in.}$$

$$\Delta_{f,A} = l_{s,dh} \times \varepsilon_{debond} = 2.9 \times 0.004 = 0.0116 \text{ in.}$$

where

$$l_{s,dh} = 0.02 \times \frac{f_y}{\sqrt{f_{ck}}} \times d_b = 0.02 \times \frac{70000}{\sqrt{4000}} \times \frac{3}{8} = 8.3 \text{ in.}$$

$$l_{f,dh} = 0.057 \sqrt{\frac{nE_f t_f}{\sqrt{f_c'}}} = 0.057 \sqrt{\frac{1 \times 14800 \times 1000 \times 0.011}{\sqrt{4000}}} = 2.9 \text{ in.}$$

ε_{debond} - Debonding strain (≈ 0.004)
$\Delta_{s,A}, \Delta_{f,A}$ - Steel and FRP deformation at Point A

5.6.2.2 Completely wrapped application

The overall response of a completely wrapped application considering bond behavior are evaluated and compared with the response discussed in Section 5.5 as shown in Figure 5-53 and Figure 5-54.

As expected, the overall response considering bond behavior is stiffer and the shear capacity is also greater. It is because other steel stirrups or FRP strips have greater resistance when the critical stirrup or strip reaches yielding or rupture capacity. Bond behavior should be considered in order to evaluate the shear behavior of FRP strengthening more accurately.
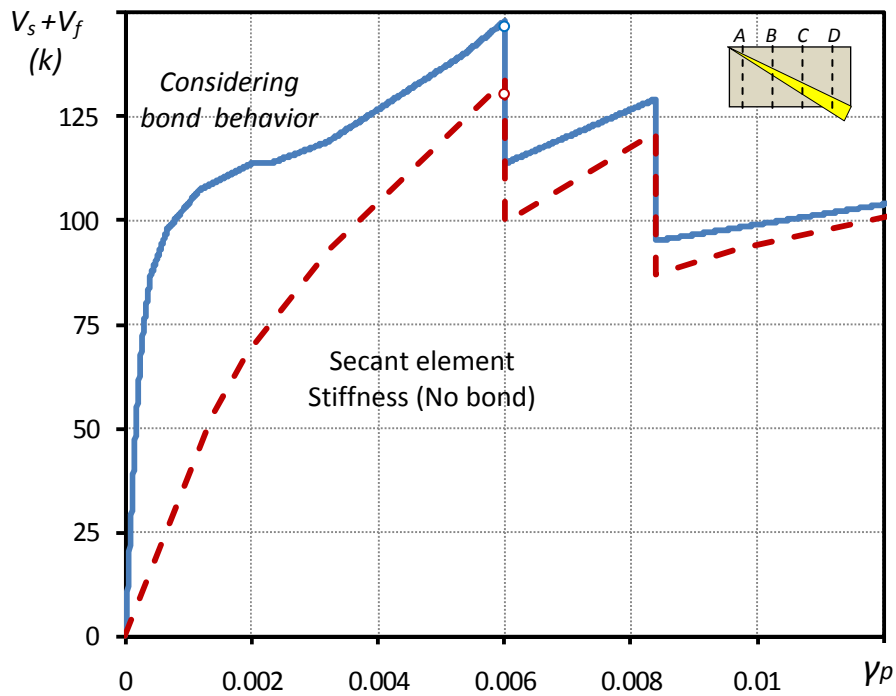
Figure 5-53 Difference in overall response with and without bond behavior

(a) Steel   (b) FRP
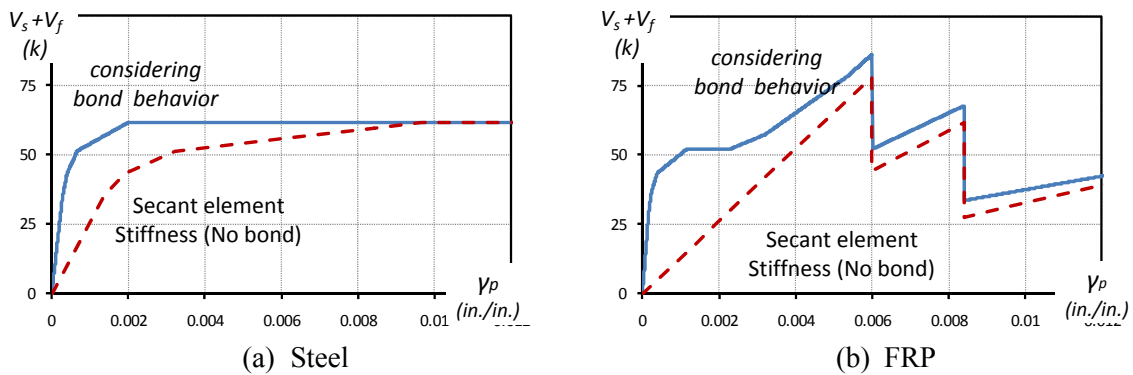
Figure 5-54 Difference in material response with and without the bond behavior

The maximum strain across a diagonal shear crack is likely to occur at mid-height of the beam instead of at the tension face of the section. When bond behavior is not considered, the crack width profile matters less because the overall response does not depend on crack location and the member stiffness is only determined by total element length, not effective length.

As the strain distribution changes (Figure 5-54), the relative shear contribution between strips changes as shown in Figure 5-55.
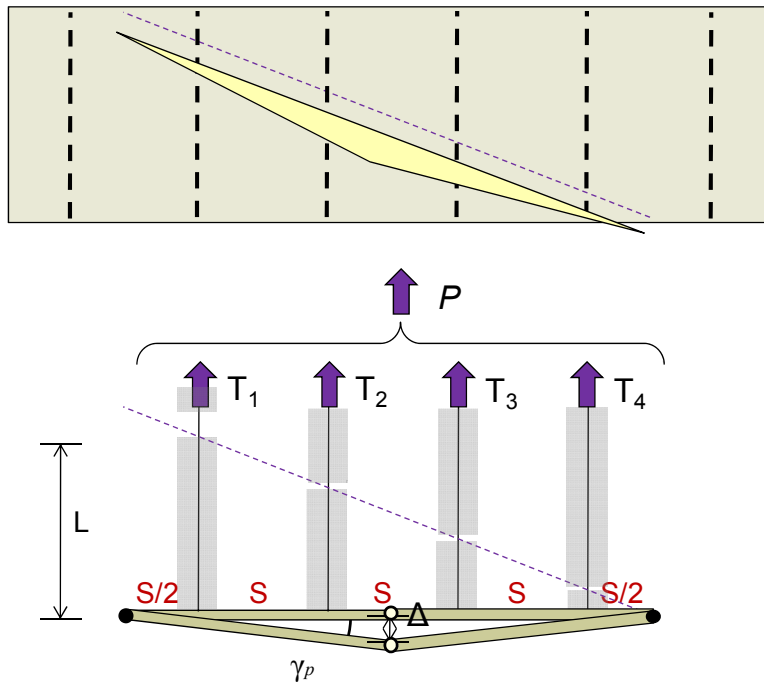
Figure 5-55 Shear behavior model considering bond behavior (maximum displacement at mid-height)
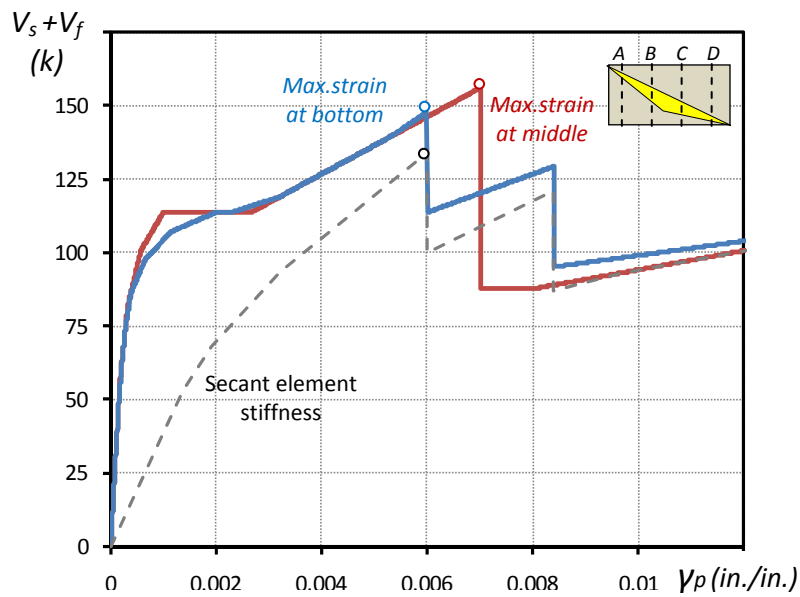
Figure 5-56 Comparison in response between maximum strain at mid-height and at tension face

The shear capacity is highest when maximum strain occurs at mid-height, but this result is specific to this example and cannot be generalized. Generally, as the strain distribution along the critical crack is more uniform than linear one, the shear capacity is higher.

5.6.2.3 Bond-critical Application (U-wrap and two-sides bonded)

As discussed in Section 5.6.1, the response of U-wrap and two-sides bonded application is likely to be determined by bond behavior. However, the characteristic of bond-critical applications cannot be simulated with the shear model used in Section 5.5.

(a) Maximum strain at bottom   (b) Maximum strain at middle
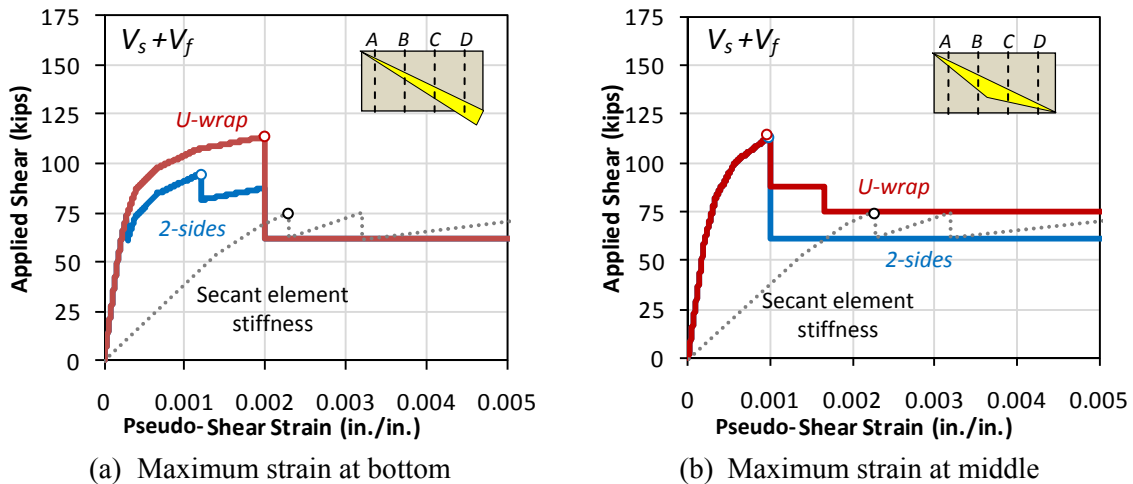
Figure 5-57 Responses of shear behavior model considering bond behavior in bond-critical applications

The difference in response between two-sides and U-wrap is studied in Figure 5-57. The shear capacity of the two-sides bonded application is always less or equal to that of the U-wrap application because the strip-end debonding risk zone is larger. The shear capacity considering bond behavior is greater than the shear capacity neglecting bond behavior because strain distribution is more uniform during debonding.

In the two-sides bonded case of Figure 5-57 (a), strip-end debonding occurred at strip D and intermediate crack-induced debonding occurred at strip C. The full debonding of strip A and strip B occurred at the same time because linear diagonal crack and linear displacement distribution is assumed. It is also the reason why all strips in a U-wrap

232

application debonded at the same time. In Figure 5-57 (b), shear capacities of U-wrap and two-sides bonded applications are identical because: 1) no strip-end debonding occurred until intermediate crack-induced debonding occurred, and 2) all strips across the critical crack reach the same strain that is the debonding strain. Post-peak responses of both applications are different however. All strips across the critical crack debond simultaneously in the two-sides bonded application, whereas the full debonding of strips is sequential in the U-wrap application. As shown in Figure 5-58, bond-critical applications (2-sides bonded and U-wrap) have a lower strength and deformation at peak than U-wrap with anchors (or complete wrapping).
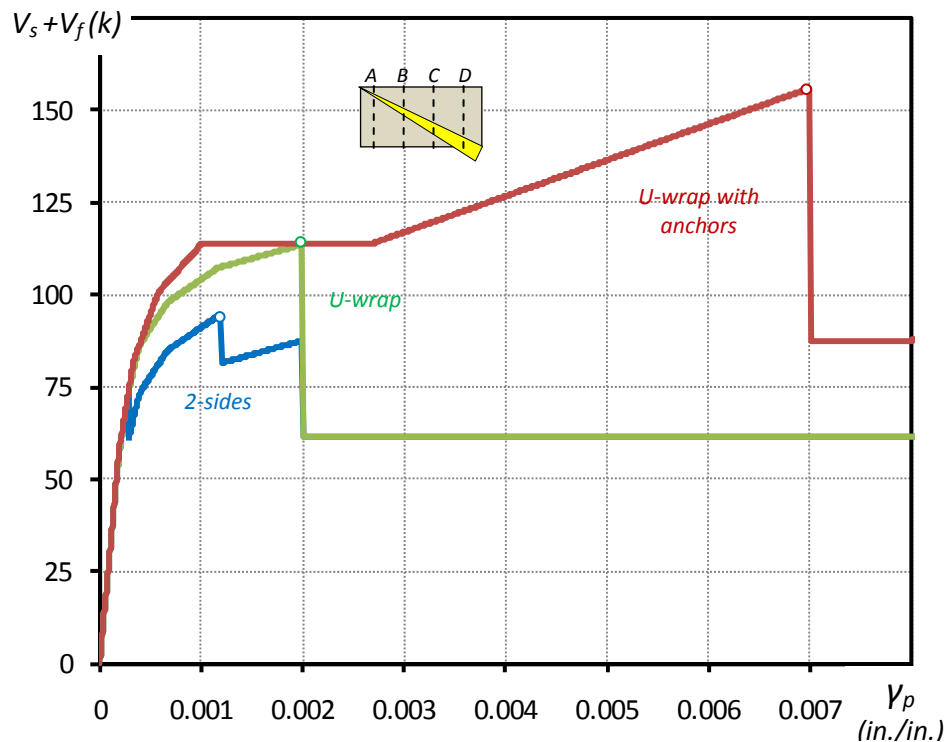
Figure 5-58 the responses of shear behavior model considering bond behavior

233

5.7 SUMMARY

To explain the shear behavior of beams strengthened with FRP, a simple behavioral model was developed. With ductile material, the strength capacity is the same for any crack and stress distribution because yield stress is sustained until all elements yield. Due to the nature of brittle material, the shear capacity is not proportional to the amount of material. The efficiency of FRP material depends on the stress distribution across and along strips. As the stress distribution becomes more uniform, rupture of strips becomes clustered and the ultimate strength of the system increases. Stress distribution across strips is not uniform in diagonal shear cracking cases. Therefore, the efficiency of FRP strengthening for shear is less than optimum.

FRP efficiency is not evaluated exactly unless the stress distribution is known. To calculate the stress of a FRP element, strains need to be known that are related to the stiffness of all elements. The stiffness of elements embedded in concrete depends on the bond behavior. Conservatively, bond behavior can be neglected for design purposes when an estimate of ultimate strength is required. When anchored FRP elements debond totally, the assumed stiffness neglecting bond effects is almost the same as the actual stiffness. Therefore, it is a reasonable and simple approach to neglect bond. When the FRP shear contribution is determined by debonding, bond behavior contributes significantly to the efficiency of FRP strengthening.

CHAPTER 6

Design Recommendations for Use of CFRP for Shear Strengthening

Design of strengthening scheme with CFRP strips anchors consists of following steps:

- Evaluate strength of existing beam
- Determine strength increase desired or needed
- Proportion CFRP material to provide desired strength
- Details of CFRP installation, especially CFRP anchor details
- Construction guidelines and specifications

6.1 EVALUATION OF EXISTING STRUCTURE OR ELEMENT

6.1.1 Strengthening Ratio and Existing Capacity

To determine the feasibility of shear strengthening with FRP, it is necessary to evaluate the shear capacity of the existing member. The strengthening ratio (α) is defined as the ratio of net capacity increase after strengthening compared with existing capacity. The strengthening ratio will differ as a function of existing capacity, especially transverse steel ratio as shown in Figure 6-1. The ratio of steel shear capacity compared with concrete shear capacity determines the maximum possible FRP shear capacity ($V_{f,max}$) because of design limits on total shear capacity ($V_{n,max}$) defined in terms of the concrete shear capacity (V_c). For this reason, the maximum possible strengthening ratio is 3/2 when $V_s = V_c$ (Case 1) and 2/3 when $V_s = 2V_c$ (Case 2). If the FRP shear contribution (V_f)

is specified as V_c, the strengthening ratio will be 1/2 for Case 1 and 1/3 for Case 2. The sum of the contributions must be less than $V_{n,max}$ $(= V_c + V_s + V_f \leq 5V_c)$

α=strengthening ratio
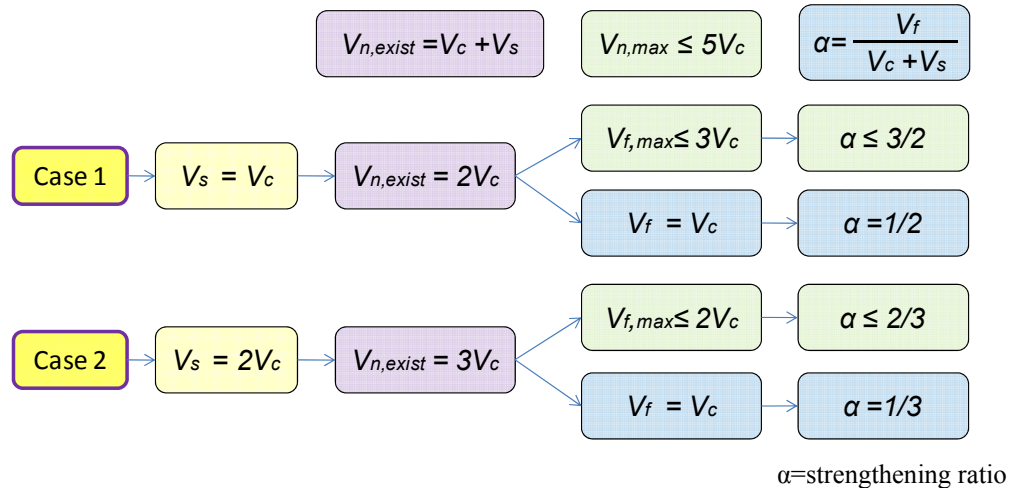
Figure 6-1 Effect on the existing capacity to the strengthening ratio

Due to the effects of interaction between steel and FRP, the actual FRP shear contribution may be less than estimated contribution at fracture shown in Figure 6-1 and the strengthening ratio may also decrease.

6.1.2 Flexural Capacity

Flexural capacity represents a target capacity after strengthening because once the mode of failure changes from shear to flexure, no additional strength is gained even if the shear capacity is increased. If the required capacity is greater than flexural capacity, flexural strengthening as well as shear strengthening must be considered. For this reason, the existing flexural capacity must be evaluated.

6.1.3 Shear Capacity Requirement

6.1.3.1 Before strengthening

As discussed in Section 2.2.6, the existing member capacity should satisfy Equation 2-1 and repeated Equation 6-1. Otherwise, other strengthening schemes such as increasing cross-sectional area should be considered.

236

$$(\phi R_n)_{existing} \geq (1.1DL + 0.75LL)_{new} \qquad (6\text{-}1)$$

6.1.3.2 Required strength

After strengthening the member must satisfy Equation 2-2

$$(\phi R_n)_{new} \geq (1.2DL + 1.6LL)_{new} \qquad (6\text{-}2)$$

6.1.4 Residual Stress

When applying CFRP, the residual stress should be considered. With residual stress, the CFRP shear contribution will be less at the same level of applied load because CFRP starts to contribute to the member capacity after strengthening.

6.2 DESIGN EQUATION

ACI 440.2R-08 was the basic guideline used to evaluate the data in this experimental program. NCHRP report 655 and NCHRP report 678 were published recently and are based on the AASHTO code. NCHRP report 655 covers use of FRP materials for a range of conditions whereas report 678 is more focused on shear applications.

6.2.1 Evaluation of ACI 440.2R-08 Shear Equations

The governing equations for shear capacity in ACI 440.2R-08 are shown in Figure 2-6 and are repeated in Figure 6-2. Although the guidelines for shear strengthening in ACI 440.2R are widely used, several disadvantages should be noted. First, there is no consideration for a U-wrap with anchorage in ACI 440.2R. The equation for U-wrap is complicated because it is a bond-critical application. Because properly designed anchors permit a U-wrap application to behave as if it were completely wrapped, the U-wrap with anchorage would increase the effective strain and makes it simpler to evaluate than U-wrap only. NCHRP report 655 and NCHRP report 678 published recently include design equations for U-wrap with anchorage, but have not been applied yet in ACI 440.2R.

$$V_n = \phi(V_c + V_s + \psi_f V_f)$$

where

ψ_f = additional reduction factors for FRP shear reinforcement

$\begin{cases} 0.95: \text{completely wrapped member} \\ 0.85: \text{U-wrap and 2 sided schemes} \end{cases}$

$$V_f = \frac{A_{vf} f_{fe}(\sin \alpha + \cos \alpha) d_{fv}}{s_f}$$

$$= \frac{A_{vf} f_{fe} d_{fv}}{s_f} \qquad (\alpha = 90°)$$

$$A_{vf} = 2n t_f w_f \ , \ f_{fe} = \varepsilon_{fe} E_f$$

where

$\begin{cases} \varepsilon_{fe} = 0.004 \le 0.75\varepsilon_{fu} & \text{(completely wrapped members)} \\ \varepsilon_{fe} = \kappa_v \varepsilon_{fu} \le 0.004 & \text{(Bonded U-wraps or bonded face plies)} \end{cases}$

$$\kappa_v = \frac{k_1 k_2 L_e}{468\varepsilon_{fu}} \le 0.75$$

$$L_e = \frac{2500}{\left(n_f t_f E_f\right)^{0.58}} \ , \ k_1 = \left(\frac{f_c'}{4000}\right)^{2/3}, k_2 = \begin{cases} \dfrac{d_{fv} - L_e}{d_{fv}} & \text{(U-wrap)} \\ \dfrac{d_{fv} - 2L_e}{d_{fv}} & \text{(2-sides)} \end{cases}$$

Figure 6-2 Current shear equation in ACI 440.2R (repeated)

Many previous studies (Chen et al 2010, Bousselham and Chaallal 2008, Pellegrino and Modena 2002, 2006, Grande et al. 2009) indicated that the FRP shear contribution is not proportional to the amount of FRP because the critical crack angle changes, but the ACI 440 shear equation does not reflect this observation. In addition, the CFRP shear contribution will be different depending on the transverse steel ratios although the same amount of CFRP material is used for strengthening. The current ACI 440 design equation does not reflect shear interaction between steel and CFRP. As a result, it is possible that ACI 440 equations may over-estimate the capacity of some

strengthened beam configurations (bond-critical case with large amount of CFRP, beams with high transverse steel ratio, small a/d ratio).

When the capacity of existing beams is estimated prior to strengthening, it should be as accurate as possible. As shown in Table 6-1, the measured capacity of strengthened beam was greater than estimated for the beam selected. However, in most cases the large strength margin was the result of a conservative estimate of the strength of the existing beam. However, the strength increase in an unanchored test was less than estimated. This is not acceptable because the FRP shear contribution will be overestimated. Therefore, the estimate of existing beam capacity needs to be more reliable so that a conservative estimate for design is based on an appropriate strength reduction factor.

Table 6-1 Comparison between design estimate and test capacity

	V (k) from ACI 440 EQ.		F (k) from TEST		Case without control test*	
	Beam strength	Strength increase	Beam strength	Strength increase	Beam strength	Strength increase
Control (24-3-2)	64	-	105	-	**64**	-
Unanchored (24-3-9)	74	10	109	4	109	45
Anchored (24-3-1r)	91	27	152	47	152	88

Note. Strength increase is based on strength of control beam

6.2.2 Evaluation of NCHRP Report 655 and NCHRP Report 678

As discussed in Sections 2.3.6 and 2.3.7, U-wraps with anchors are considered in the same design category as complete wrapping in both NCHRP report 655 and 678. In report 655, different strength reduction factors (0.65 for complete wrapping and 0.60 for U-wraps with anchors) because U-wraps with anchorage are less reliable than complete wrapping. The effective strain for side bonding and U-wrap is 0.004 and the effective strain for completely wrapping and U-wraps with anchors is greater than 0.004. In report 678, effective strain is determined by the FRP reinforcement ratio and FRP elastic modulus. It implies that the FRP contribution is a function of the amount of FRP material.

The effective strain of a complete wrap and U-wraps with anchors is greater than 0.004. In report 678, effective strain is determined by the FRP reinforcement ratio and FRP elastic modulus. It implies that the FRP contribution is a function of the amount of FRP material. The effective strain of complete wrap and U-wraps with anchors is 33% greater than that of side bonding and U-wrap.

6.2.3 Proposed Equation

The current shear design is too conservative because design estimate is quite not reliable value. However, CFRP contribution after strengthening evaluated from this design can be over-estimated because the margin of safety for concrete and steel contribution is considered as FRP contribution if the existing beam capacity is not estimated reasonably. Furthermore, CFRP contribution will depends on the configuration of existing beam, so the design estimate is less reliable without considering interaction between materials. With large strength reduction factor, design estimate can be determined, but it will not be smart approach.

As indicated in Table 4-8, the ratio of test to computed strength (F_n/V_n) is quite conservative (around 1.4). The conservative values are due to computed concrete and steel contributions being under-estimated. Furthermore, the CFRP contribution will depend on the characteristics of existing beam (a/d ratio, size and location of stirrups, and concrete strength), so the capacity of the strengthened beams depends on the interactions between materials.

For an unstrengthened beam, the calculated capacity represents a lower bound value. If this lower bound is used and a specific increase in strength is decided through the use of CFRP, the required incremental strength increase may not be realized due to the interaction between materials discussed above.

As shown in Figure 6-3, the ACI 440.2R shear design procedures was selected on the basis for design guidelines that include U-wraps with CFRP anchors. Three additional factors (k_a, k_s and k_f) are introduced; k_a is a factor considering shear-span-to-depth ratio. k_s and k_f are factors considering interaction between materials. The current shear

equations in ACI 440.2R for determining contribution of each material to shear capacity are considered as reference values (V_{c0}, V_{s0}, V_{f0}) for determining k_s and k_f. The capacity in proposed equations is calculated from the combination of V_{c0}, V_{s0}, V_{f0}, k_a , k_s, and k_f. Additions to ACI 440.2R procedure are shown in bold print.

The design shear capacity increase is the same, but anchored U-wraps are placed in the same category as complete wraps. New equations are introduced for the interactions between the concrete, steel, and FRP contribution through the factors k_s and k_f and will be discussed later.

$$\phi V_n = \phi(V_c + V_s + \psi_f V_f) \ , \ (\ 0 \leq V_{s0} + V_{f0} \leq 4V_{c0}) \tag{6-3}$$

where

$$\boldsymbol{V_c = (2 - k_a)V_{c0}} \quad \textbf{(6-4)}, \qquad \boldsymbol{V_s = k_a k_s V_{s0}} \quad \textbf{(6-5)}, \qquad \boldsymbol{V_f = k_a k_f V_{f0}} \quad \textbf{(6-6)}$$

V_c, V_s, V_f : concrete, steel, and FRP shear contribution considering interaction between materials

V_{c0}, V_{s0}, V_{f0} : concrete, steel, and FRP shear contribution without considering interaction between materials, same equations as ACI 440.2R

$$V_{c0} = 2\sqrt{f_c'}b_w d \tag{6-7}$$

$$V_{s0} = \frac{A_{sv}f_{sy}(\sin\alpha + \cos\alpha)d}{s} \tag{6-8}$$

$$= \frac{A_{sv}f_{sy}d}{s} \quad (\alpha = 90°)$$

$$V_{f0} = \frac{A_{vf}f_{fe}(\sin\alpha + \cos\alpha)d_{fv}}{s_f} \tag{6-9}$$

$$= \frac{A_{vf}f_{fe}d_{fv}}{s_f} \quad (\alpha = 90°)$$

$$A_{vf} = 2nt_f w_f \quad \text{(6-10)}, \qquad\qquad f_{fe} = \varepsilon_{fe}E_f \tag{6-11}$$

where

$\begin{cases} \varepsilon_{fe} = 0.004 \leq 0.75\varepsilon_{fu} \ \text{(completely wrapped and \textbf{U-wraps with anchorage})} \\ \varepsilon_{fe} = \kappa_v \varepsilon_{fu} \leq 0.004 \quad \text{(Bonded U-wraps or bonded face plies)} \end{cases}$

κ_v is evaluated according to the ACI440.2R equation (Fig. 2-6)

ψ_f = additional reduction factors for FRP shear reinforcement

$\begin{cases} \text{0.95: completely wrapped member} \\ \textbf{0.90: U-wrap with anchorage} \\ \textbf{0.75: Bonded U-wraps} \\ \textbf{0.60: bonded face plies} \end{cases}$

$\boldsymbol{k_a}$**: a transverse reinforcement contribution factor considering shear span to depth ratio in deep beam (FIB 1999)**

$\begin{cases} {}^a/_d \leq 0.5 : \quad \boldsymbol{k_a = 0} \\ \boldsymbol{0.5 \leq {}^a/_d \leq 2} \quad : \quad \boldsymbol{k_a = \dfrac{2({}^a/_d) - 1}{3}} \\ {}^a/_d \geq 2 \quad : \quad \boldsymbol{k_a = 1} \end{cases}$

$\boldsymbol{k_s}$**: steel interaction factor** $\quad \boldsymbol{k_f}$**: CFRP interaction factor**

$$\boldsymbol{k_s = \frac{8V_{c0}}{4V_{c0} + V_{s0} + V_{f0}}} \quad \text{(6-11)}, \qquad \boldsymbol{k_f = \frac{6V_{c0}}{4V_{c0} + V_{s0} + V_{f0}}} \tag{6-12}$$

Figure 6-3 Proposed updated format of design equation in ACI440.2R

6.2.3.1 Transverse reinforcement contribution factor considering a/d ratio (k_a)

The factor of k_a was included in FIP recommendations (1999). This factor adjusts the steel contribution efficiency according to the shear span to depth ratio (a/d ratio); $k_a=$ 0 when a/d $\leq$ 0.5 and all of the shear is carried by the concrete. $k_a = 1$ when a/d $\geq$ 2 and the steel contributes fully. This factor is linearly interpolated between those a/d ratios.

As a a/d ratio decreases in deep beam, the concrete contribution increases based on a database of test results of beams having no transverse reinforcement (Birrcher 2009). However, there is no adjustment of the concrete contribution in current US shear equation. Therefore, the modification factor (2- k_a) for concrete contribution is introduced using k_a discussed before. As indicated by beams in the database shown in Figure 6-4, this factor is still conservative.
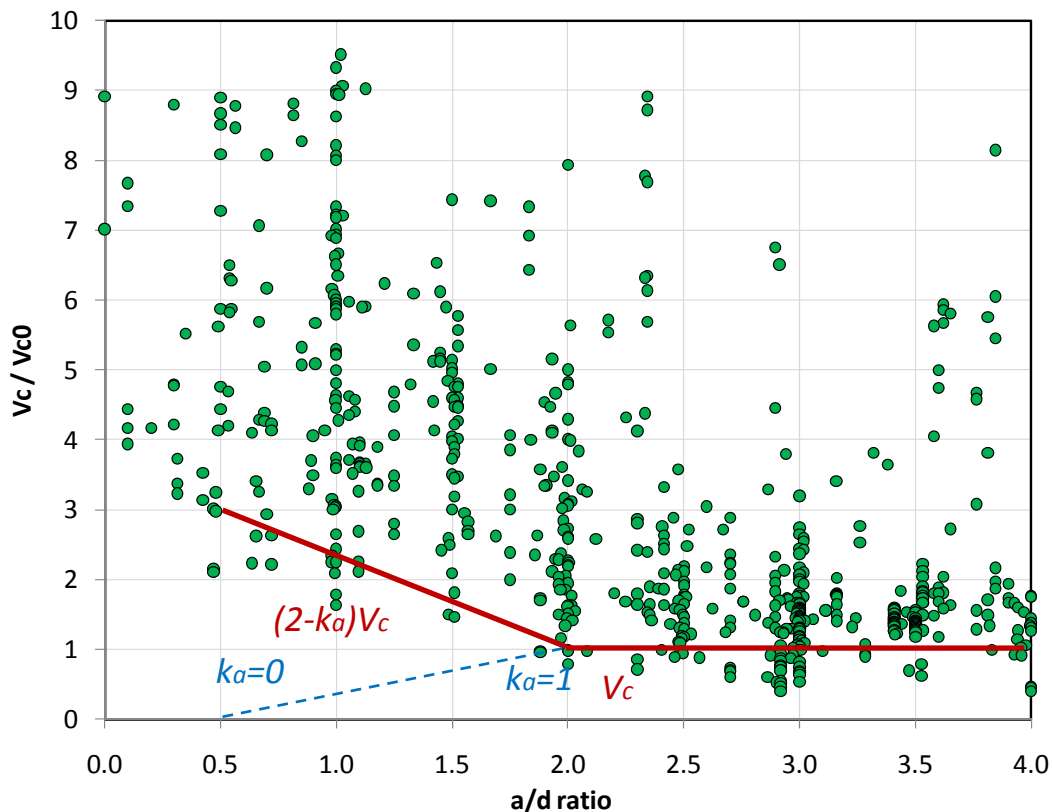
Figure 6-4 Test result of normalized shear strength according to a/d ratio in beam with no transverse reinforcement

243

6.2.3.2 Steel (k_s) and FRP (k_f) interaction factor

Basically, the steel and FRP capacity are proportional to the amount of material in the transverse reinforcement. However, the shear contribution of these materials as transverse reinforcement will not be proportional due to the change in the angle of the critical shear crack that is influenced by the amount of material.

In Figure 6-5, the database used by Birrcher (2009) was filtered to include only beams with a/d ratios greater than 2 and stirrup spacings less than d/2. For beams with a small steel contribution, the test results vary considerably because the beam capacity is determined primarily by the concrete capacity. A straight line determined from a regression analysis is drawn, but this line will not pass through the origin and does not follow the trend of the data. For this reason, a regression analysis using a logarithmic function was tried. The resulting curve fits the data better and reflects the finding from the research that the marginal strength increase decreased as the amount of material increased.
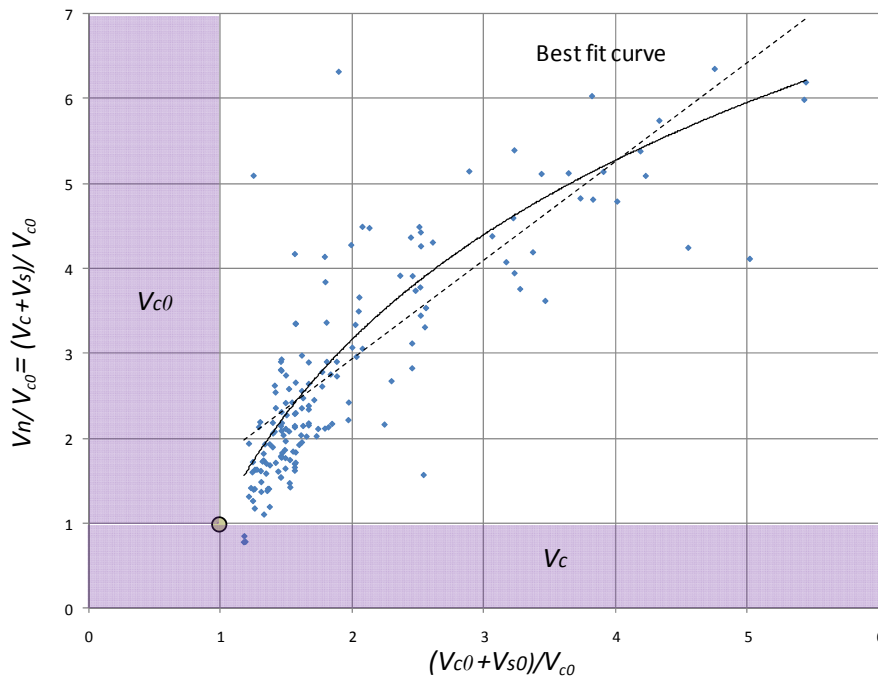
Figure 6-5 Comparison between linear function and log function for best fit curve of database (a/d ratio≥ 2.0, stirrup spacing ≤ d/2)

However, a logarithmic function is not easy for hand-calculations and the effects of the parameters are not transparent to the user. For this reason, the rational function show below was considered as an alternative for logarithmic function. The basic format for k_s is shown below.

$$y = \frac{a}{b+x}$$

$$a , b : \text{function coefficient}, \quad x : \text{variables} \left(\frac{V_s + V_f}{V_c} \right), \quad y : k_s$$

$$V_s = k_s V_{s0}$$

By trial-and-error, values of 8 and 4 were selected for a and b respectively, but these values do not result in a best-fit-curve, but are simple for use in design.

$$k_s = \frac{8}{4+\dfrac{V_{s0}+V_{f0}}{V_{c0}}} = \frac{8V_{c0}}{4V_{c0}+V_{s0}+V_{f0}} \quad , \quad V_s = k_s V_{s0} = \frac{8V_{c0}}{4V_{c0}+V_{s0}+V_{f0}} V_{s0}$$

The k_s factor will be a function of the ratio of steel or FRP contribution compared with concrete contribution. In addition, k_s decreases as a larger amount of steel used. At $V_{s0} = 4 V_{c0}$, the steel contribution will reach the limit of $V_n = 5 V_{c0}$ and k_s will be equal to 1. In this experimental program, the steel contribution was around $0.5V_{c0}$ for #3@18" in 48 in. beams and met the minimum ratio for steel stirrups required in ACI 318. With this layout, k_s is 1.78. When the steel contribution (V_{s0}) is equal to V_{c0}, which is a typical reinforcement layout, k_s is 1.6. These k_s values (1.78 and 1.6) are roughly comparable to the increase in the steel shear contribution when the critical angle changed from 45 degrees (cot 45°=1) to 30 degrees (cot 30°≈1.73). As shown in Figure 6-6. The linear relationships in ACI codes are shown by the dashed lines in Figure 6-6 (b). The k_s factor results in a higher steel contribution compared with the current ACI equation. More experimental data will be needed to construct a best-fit curve that applies to a wider range of beam geometry.

245

(a) k_s (b) $k_s(V_{s0})$
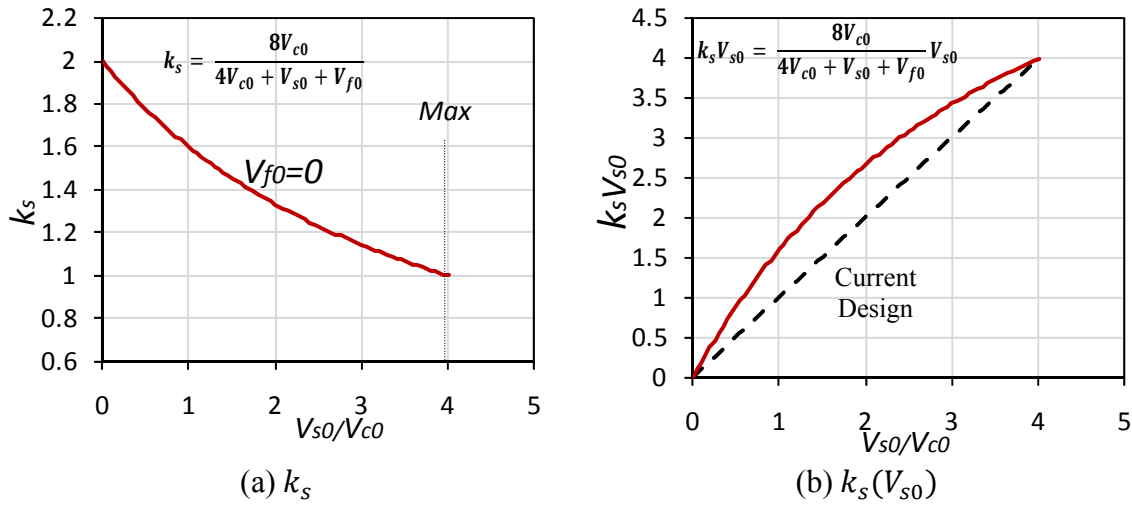
Figure 6-6 k_s and $V_s(= k_s V_{s0})$

The marginal increase in steel contribution keeps decreasing as steel stirrups are added as shown in Figure 6-7. Current code equations do not reflect this effect. Moreover, the steel contribution changes with the concrete capacity although the same amount of steel is placed because the ratio of steel capacity to concrete capacity changes. The FRP contribution factor (k_f) follows a similar interaction with the concrete.
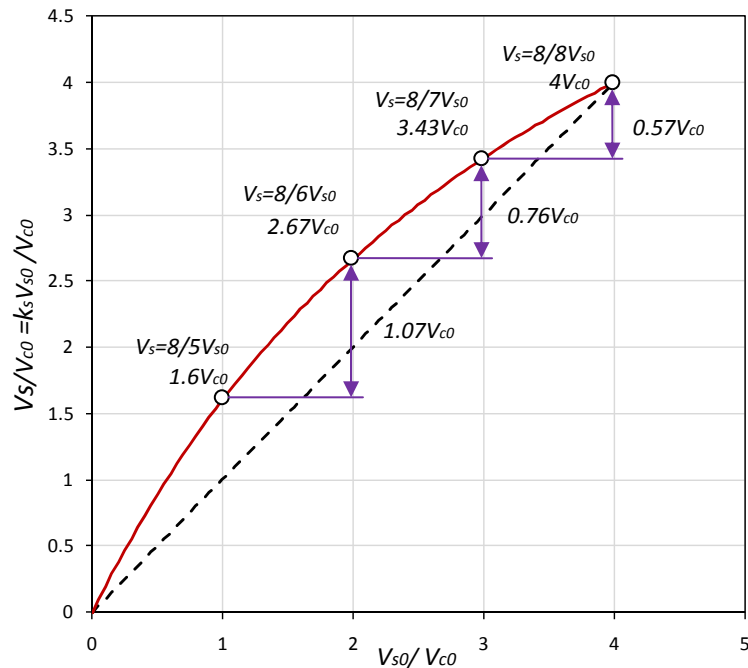
Figure 6-7 Marginal increase in steel contribution

246

In Figure 6-8, the equation for k_s is compared with both current ACI code provisions and data from previous studies. Both current and proposed equations are not conservative for a few test results, but design capacities after applying a strength reduction factor were generally acceptable. The test results shown in Figure 6-8 indicate that shear capacity was not proportional to the amount of steel, but the shear capacity increased as the amount of transverse steel increased.
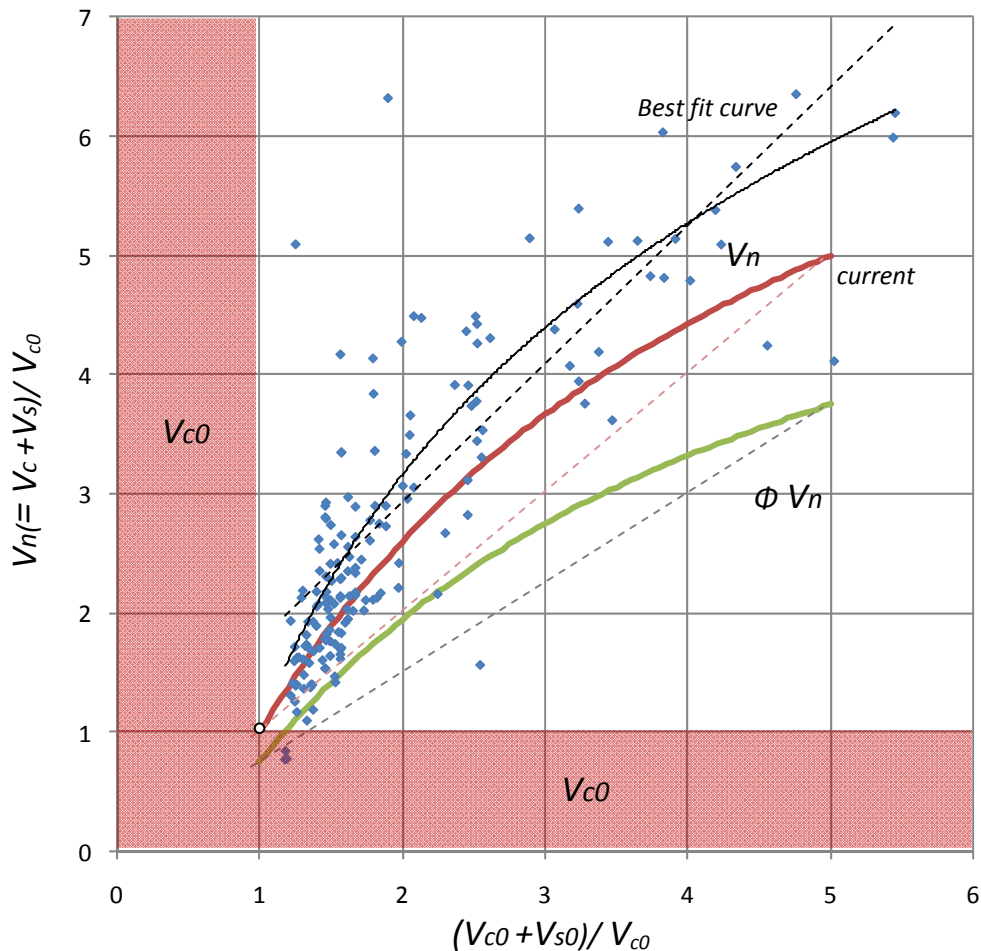
Figure 6-8 Comparison between estimate from proposed equation and test results of normalized shear (a/d ratio ≥ 2.0, stirrup spacing ≤ d/2)

As shown in Figure 6-9, the coefficient of k_f is assumed to be three-fourths of k_s. The contribution of the FRP strips will be similar to that of k_s except that k_f is reduced because redistribution of forces between FRP strips is unlikely in a brittle material. In

247

addition, it is intended to consider the capacity loss between concrete and FRP because the deformation at the maximum capacity will not be the same and the concrete contribution remains constant for all parameters. The value of k_f is close to current design when V_{f0} is $0\,V_{c0}$ to $2\,V_{c0}$. The value of k_f drops below 1.0 when V_{f0} is greater than $2\,V_{c0}$. As more experimental studies become available, the equation for k_f can be improved.

$$k_f = \frac{6V_{c0}}{4V_{c0} + V_{s0} + V_{f0}}$$

$$k_f V_{f0} = \frac{6V_{c0}}{4V_{c0} + V_{s0} + V_{f0}} V_{f0}$$

(a) k_f (b) $k_f(V_{f0})$
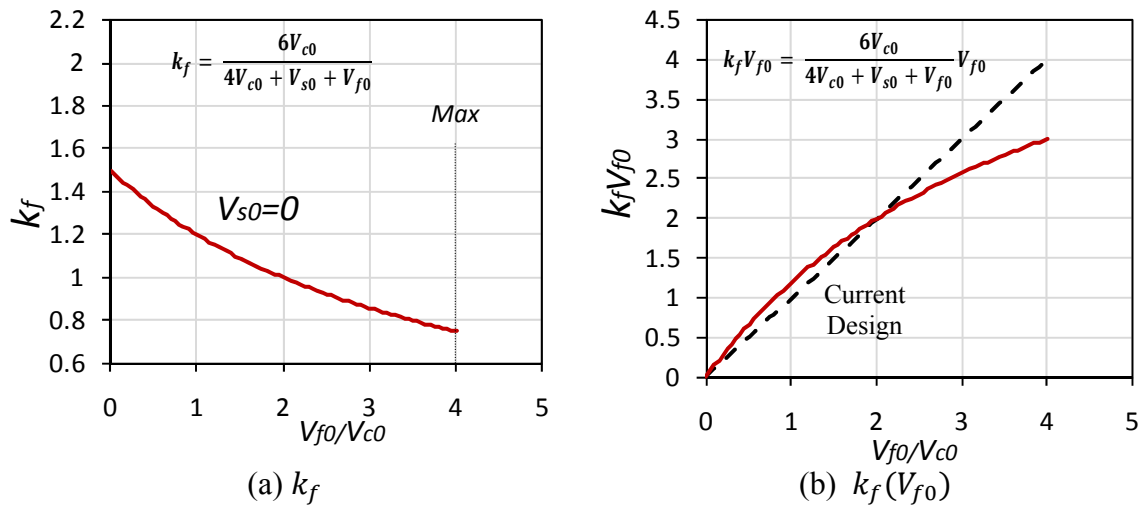
Figure 6-9 k_f and $V_f(= k_s V_{s0})$

In addition, k_s and k_f are also factors to account for the interaction between steel, FRP and concrete. The current steel and FRP shear equations are linear functions of cross-sectional areas and material properties. There is no interaction between steel capacity and FRP capacity as the contributions are simply added. However, the relationships are not linear and are interactive as observations from previous research and the experimental results of this research show. When the amount of FRP material was doubled, the FRP shear contribution was not doubled. In addition, the FRP shear contribution was proportionally less with the beam with high transverse steel ratio although the same amount of FRP material was applied. Nevertheless, the shear contribution of steel and CFRP was generally greater than estimated using current design equations because the critical crack angle is usually less than 45 degrees.

248

As shown in Figure 6-10, the presence of steel stirrups will affect k_f and the addition of FRP reinforcement will affect k_s because steel and FRP influence the shear transfer mechanism in the same manner. To reflect this interaction, both factors have the same terms in the denominators of Equations (6-11) and (6-12) and, in effect, V_{s0} and V_{f0} are interchangeable.

$$k_s = \frac{8V_{c0}}{4V_{c0} + V_{s0} + V_{f0}}$$

(a) k_s

$$k_f = \frac{6V_{c0}}{4V_{c0} + V_{s0} + V_{f0}}$$

(b) k_f

(c) $k_s(V_{s0})$

(d) $k_f(V_{f0})$
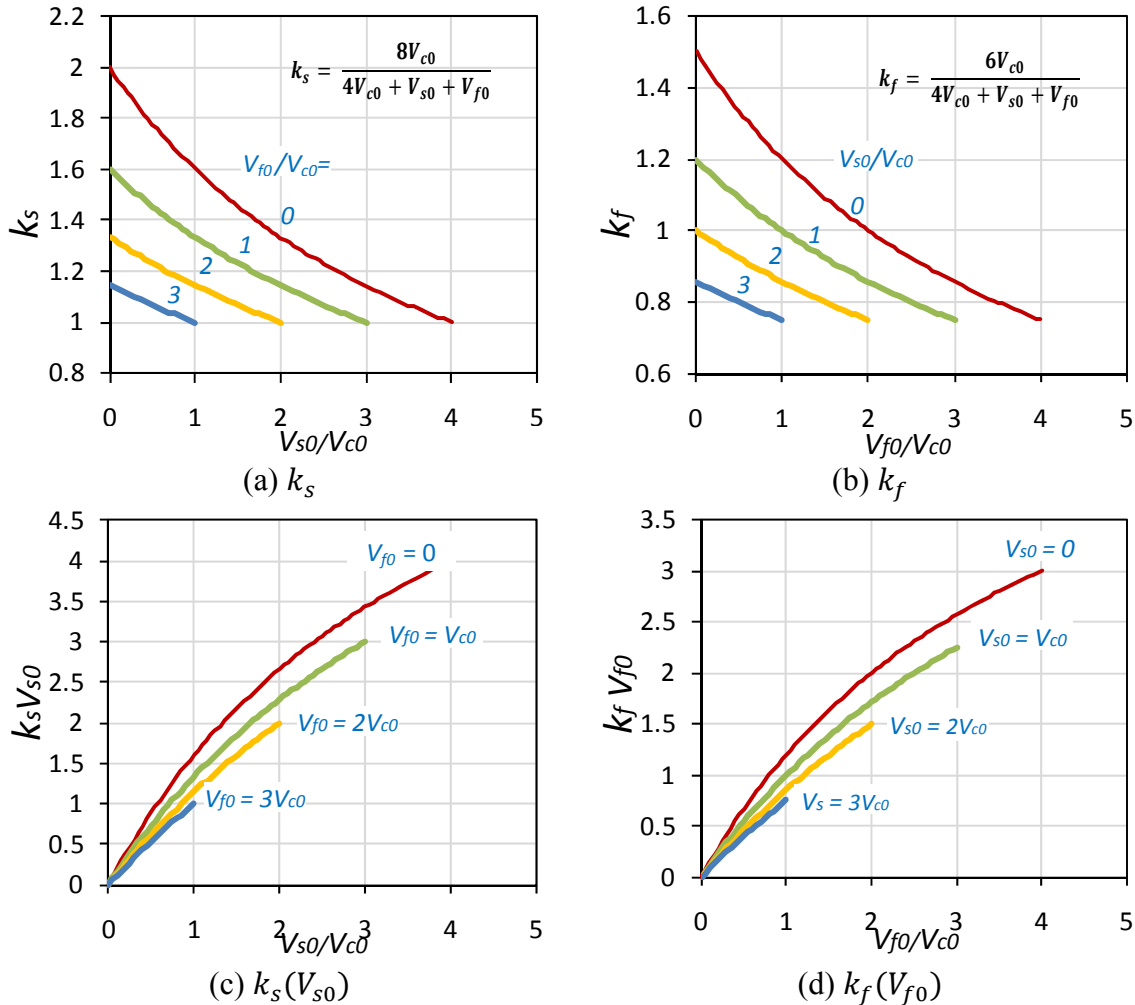
Figure 6-10 k_s and k_f and their contribution when existing interaction with other material

Figure 6-11 shows an example, for in two beams with $V_{f0} = 2V_{c0}$ and the steel stirrup contribution $V_{s0} = V_{c0}$ in one beam (Case 1) and $V_{s0} = 0$ in the other (Case 2). All calculations to evaluate the points shown in Figure 6-11 are listed in Figure 6-12.
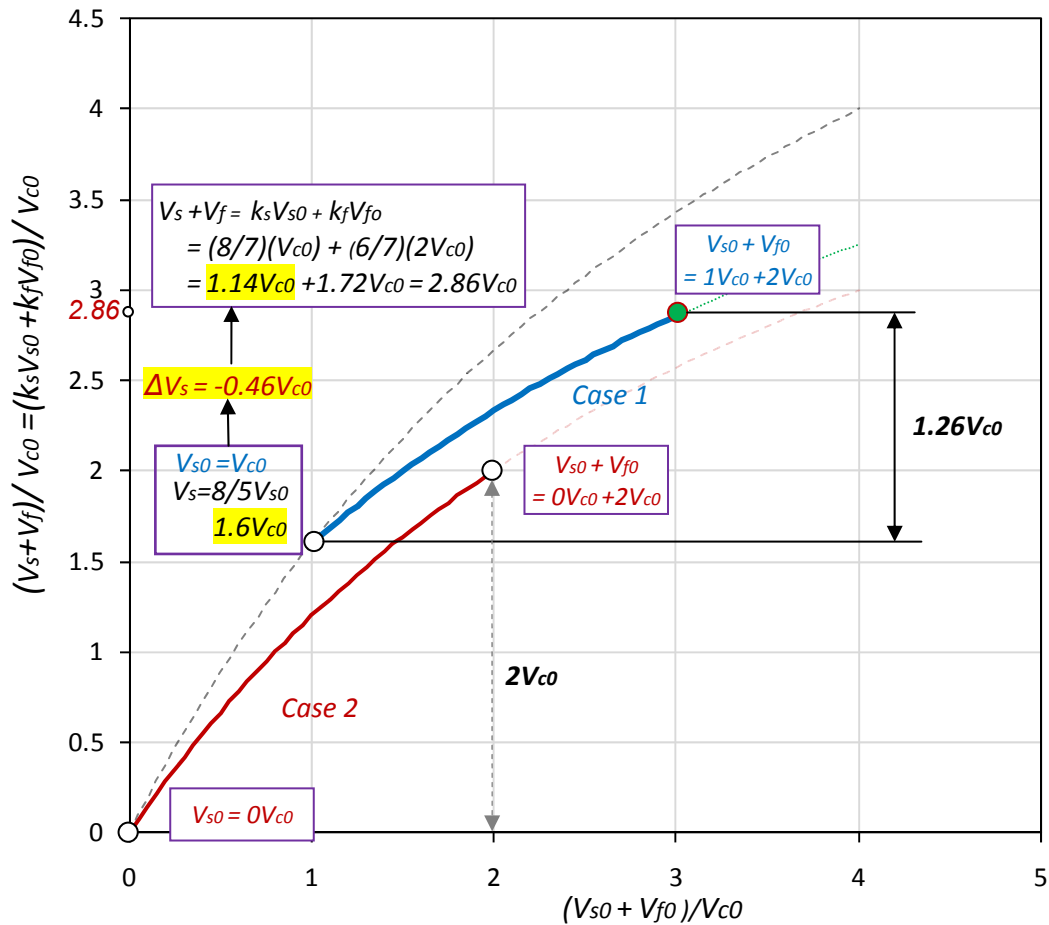
Figure 6-11 Case study of strength increase evaluation with two different existing steel capacities

The value of k_f will be 0.86 (=6/7) for Case 1 and 1 (=6/6) for Case 2 and V_f ($= k_f V_{f0}$) are equal to $1.72V_{c0}$ (Case 1) and $2V_{c0}$ (Case 2) which means that the existing steel reinforcement affect the effectiveness of FRP strengthening.

Case 1 : Existing beam : $V_{s0}=V_{c0}$ Strengthening: $V_{f0}= 2V_{c0}$

$$V_{n,exist} = V_c + \boldsymbol{V_s} = (2 - k_a)V_{c0} + k_a k_s V_{s0} = (2 - 1)V_{c0} + 1 \cdot \frac{8V_{c0}}{4V_{c0}+V_{s0}+V_{f0}} V_{s0}$$

$$=V_{c0} + \frac{8V_{c0}}{4V_{c0}+V_{c0}+0} V_{c0} = V_{c0} + \frac{8}{5} V_{c0} = V_{c0} + \boldsymbol{1.6\,V_{c0}}$$

$$V_{n,stregthening} = V_c + \boldsymbol{V_s} + \boldsymbol{V_f} = (2 - k_a)V_{c0} + k_a k_s V_{s0} + k_a k_f V_{f0}$$

$$= V_{c0} + 1 \cdot \frac{8V_{c0}}{4V_{c0}+V_{s0}+V_{f0}} V_{s0} + 1 \cdot \frac{6V_{c0}}{4V_{c0}+V_{s0}+V_{f0}}$$

$$= V_{c0} + 1 \cdot \frac{8V_{c0}}{4V_{c0}+1V_{c0}+2V_{c0}} V_{c0} + 1 \cdot \frac{6V_{c0}}{4V_{c0}+1V_{c0}+2V_{c0}} 2V_{c0}$$

$$= V_{c0} + \frac{8}{7} V_{c0} + \frac{6}{7} 2V_{c0} = V_{c0} + (1.14 + 1.72)V_{c0} = V_{c0} + \boldsymbol{2.86V_{c0}}$$

Case 2 : Existing beam : $V_{s0}=0V_{c0}$ Strengthening: $V_{f0}= 2V_{c0}$

$$V_{n,exist} = V_c + \boldsymbol{V_s} = (2 - k_a)V_{c0} + k_a k_s V_{s0} = (2 - 1)V_{c0} + 1 \cdot \frac{8V_{c0}}{4V_{c0}+V_{s0}+V_{f0}} V_{s0}$$

$$=V_{c0} + \frac{8V_{c0}}{4V_{c0}+0+0} 0V_{c0} = V_{c0} + \boldsymbol{0}$$

$$V_{n,stregthening} = V_c + \boldsymbol{V_s} + \boldsymbol{V_f} = (2 - k_a)V_{c0} + k_a k_s V_{s0} + k_a k_f V_{f0}$$

$$= V_{c0} + 1 \cdot \frac{8V_{c0}}{4V_{c0}+V_{s0}+V_{f0}} V_{s0} + 1 \cdot \frac{6V_{c0}}{4V_{c0}+V_{s0}+V_{f0}}$$

$$= V_{c0} + 1 \cdot \frac{8V_{c0}}{4V_{c0}+0V_{c0}+2V_{c0}} V_{c0} + 1 \cdot \frac{6V_{c0}}{4V_{c0}+0V_{c0}+2V_{c0}} 2V_{c0}$$

$$= V_{c0} + \frac{8}{6} 0V_{c0} + 1 \cdot \frac{6}{6} 2V_{c0} = V_{c0} + 0 + 1 \cdot \frac{6}{6} 2V_{c0} = V_{c0} + \boldsymbol{2V_{c0}}$$

Figure 6-12 Calculations of two cases shown in Figure 6-11

Furthermore, after FRP strengthening, V_s in Case 1 would decrease from $1.6V_{c0}$ to $1.14V_{c0}$ because k_f would be changed from 1.6 (= 8/5) to 1.14 (= 8/7). This change can simulate the condition where the stress redistribution was limited by FRP. The capacity loss of steel due to FRP was $0.46\,V_{c0}$ (=$1.6V_{c0} - 1.14V_{c0}$). It is important that the overall behavior can not be separate with V_s and V_f. Therefore, the net increase after strengthening would be $1.26\,V_{c0}$ (=$1.72\,V_{c0} - 0.46\,V_{c0}$). This value is lower FRP contribution comparing that the net increase of the case 2 is $2\,V_{c0}$. In addition,

strengthening ratio in both cases is also evaluated as shown in Table 6-2. Because the concrete contribution should be included when calculating strengthening ratio, the concrete contribution (V_c) of V_{c0} is added to $V_s + V_f$. Strengthening ratio are 1.48 for Case 1 and 3 for Case 2. As a result, the strengthening ratio cannot be generalized because it can be different with same amount of FRP material depending on the existing condition.

Table 6-2 Strengthening ratio of case study

	Before strengthening	Strengthening ($V_{f0} = 2V_{c0}$)	Strength increase due to CFRP	Strengthening ratio (included V_c)
Case 1 ($V_{s0} = V_{c0}$)	$1.6V_{c0}$	$2.86V_{c0}$	$1.26\ V_{c0}$	$\dfrac{2.86 + 1}{1.6 + 1} = 1.48$
Case 2 ($V_{s0} = 0$)	$0V_{c0}$	$2.0V_{c0}$	$2\ V_{c0}$	$\dfrac{2 + 1}{0 + 1} = 3$

6.2.3.3 *Effective strain for U-wrap with anchorage application*

The main purpose of this study was to evaluate the FRP shear capacity when U-wraps with anchorage are used for strengthening. To be compatible with current ACI 440.2R equations, the effective strain of 0.004 was selected although the average strain along the critical crack was greater than 0.004 based on test results. It is because the purpose of the U-wrap with anchorage is to provide a condition approaching that of complete wrapping which is the condition assumed in ACI 440 for an effective strain of 0.004.

Based on test results and the shear model discussed in Chapter 5, FRP average strain crossing the critical crack would be at least greater than half of the rupture strain if the mode of failure is rupture of strip. However, if rupture strain is greater than 0.01, the average strain might be lower than half of rupture strain because the concrete interlocking capacity would decrease at a strain of 0.01 in all strips. Therefore, the rupture strain should limited to 0.01 in calculating strength of CFRP strips. In addition, it is noted that in most cases ultimate stress and rupture strain are not used to evaluate the FRP contribution because the effective strain was specified for completely wrapped sections

and implies that the elastic modulus of the FRP is more important than the rupture stress/strain.

6.2.3.4 ψ_f *for U-wrap with anchorage application*

To reflect reliability of different FRP wrapping schemes compared with steel reinforcement, additional reduction factors (ψ_f) were introduced in ACI440.2R; ψ_f = 0.95 for complete wrapping and ψ_f = 0.85 for U-wrap. These values were based on test results of completely wrapped beams that were more consistent than those of U-wrapped beams. Therefore, ψ_f of 0.90 is proposed for U-wrap with anchorage because the strength of U-wrap with anchorage is more variable than complete wrapping and less variable than U-wrap. The same approach can be found in NCHRP report 655 in Section 4.3.1.

From test results, the strength increase in U-wrap application was substantially lower than that of U-wrap with anchorage not only because of effective strain, but also because of decrease in steel contribution due to lower deformation at failure. Therefore, additional reduction is proposed for U-wrap and 2-sides (bond-critical application). However, there is little data on which to base this factor. To be consistent with the ψ_f factors proposed for complete wrapping and U-wrap with anchorage, it is proposed that ψ_f is 0.60 for 2 sides and 0.75 for U-wrap because these values are likely comparable to NCHRP report 655. ($\phi \times \psi_f$: 0.75× 0.6=0.45, 0.75× 0.75=0.5625)

6.2.4 Comparison with Experimental Results

In Figure 6-13, the shear strength of the beams tested was calculated using the proposed equations and current ACI 440 equations.

(a) 48-3-1 ~4 (V_{s0}=0.41V_{c0})　　　　(b) 48-3-5~8 , 24-3-1~10 (V_{s0}=0.74 V_{c0})
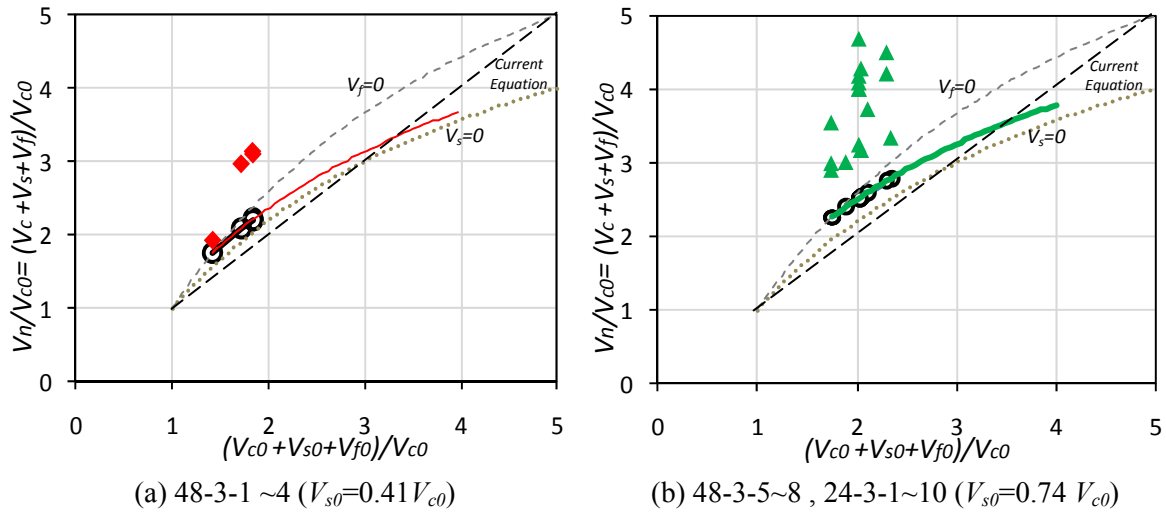
Figure 6-13 Comparison between test results and estimate from proposed equation

Because two transverse steel ratios were used, two graphs are plotted and one is for tests 48-3-1~4 and the other is for tests 48-3-5~8 and tests 24-3-1~10. Test capacities are shown in diamond and triangle symbols. Furthermore, the points (open circles) on design curve indicate the estimate from proposed equation at given area of FRP material. The ratios of measured to estimated strength are shown in Figure 6-14. The strengths computed from current ACI 440.2R and the proposed equations were conservative for all tests, but strengths computed from proposed equations exhibited less scatter than was noted using current ACI 440.2R equations.

The ratios of beams strengthened with FRP were generally greater than those of the control beams (48-3-1, 48-3-6, 24-3-2).　Because the loading on tests 48-3-1, 3, 5, 6 and 7 was stopped before the peak load was reached , the ratios for 48 in. beams was generally less than those for 24 in. beams. In addition, test 48-3-8 and 24-3-8 failed by fracture of anchors and test 24-3-9 failed by debonding, so the ratio for those beams was lower. The ratio of test 24-3-3 is excluded due to poor application of CFRP.
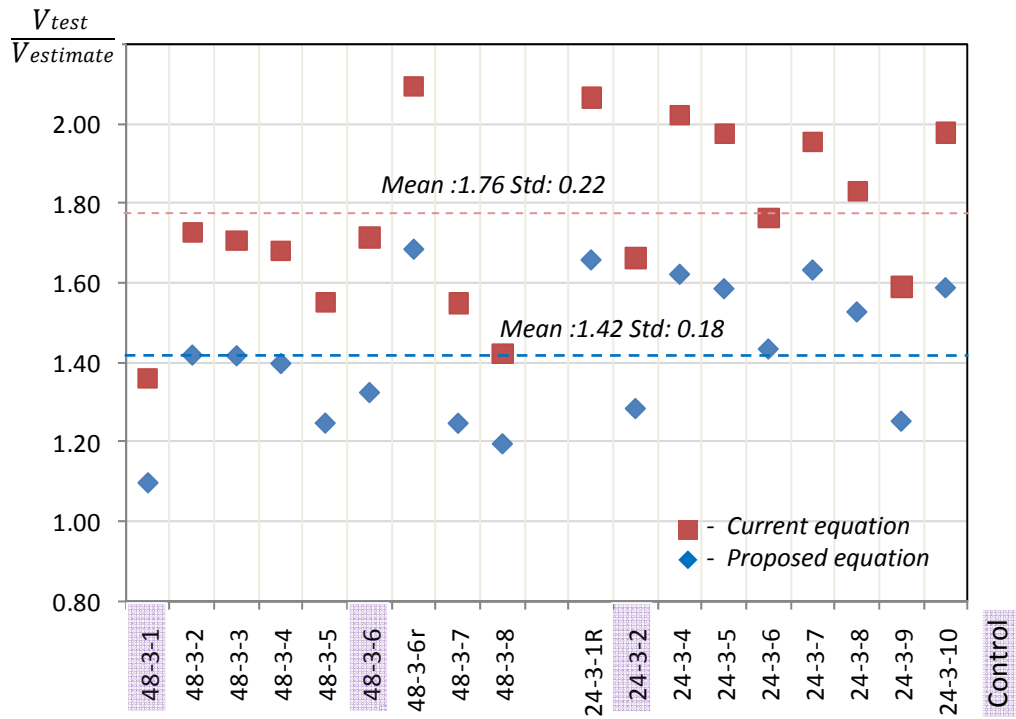
Figure 6-14 Comparison of max. capacity compared with estimate

After eliminating the tests discussed above, the results for the remaining tests are shown in Figure 6-15. Although the ratios varied considerable, the ratios for the proposed design equations were less conservative than current ACI 440 equations. The comparisons also indicate that the an effective strain of 0.004 intended for shear strengthening applications with completely wrapped sections appears to be a conservative approach for beams with anchored U-wraps. However, additional test results are needed to validate the proposed equation for a wider range of variables.

255
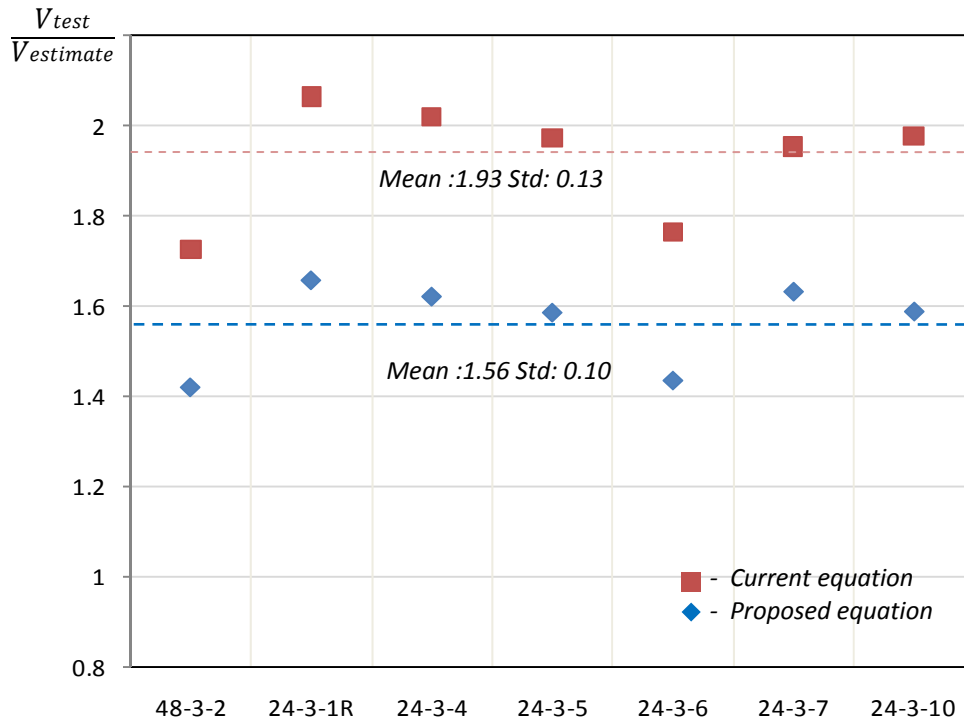
Figure 6-15 Comparison of max. capacity compared with estimate (U-wrap with anchor tests only)

Chaallal et al. (2002) studied the interaction of steel and FRP contributions to shear strength of T-Beams strengthened with FRP U-wraps (no anchorage). They tested the beams with four different stirrup ratios and strengthened with 1 to 3 layers of FRP per strip. As shown in Figure 6-16, the test results provide data in a wide range of variables for evaluating the proposed equations. As shown in Figure 6-17, the measured capacity was generally about twice the estimated strength for both the current ACI 440 and proposed equations. The standard deviation of the ratio of measured capacity compared to estimates from proposed equations was less than that using current equations. The ratio of test capacity compared to estimate was less as the number of FRP layers increased in both cases, but the variation in the ratio was less using the proposed equation indicating that the proposed equation is more consistent. When the stirrup ratio was lower, the variation of the ratios was greater because the shear capacity was determined by the interaction between concrete and FRP.

256
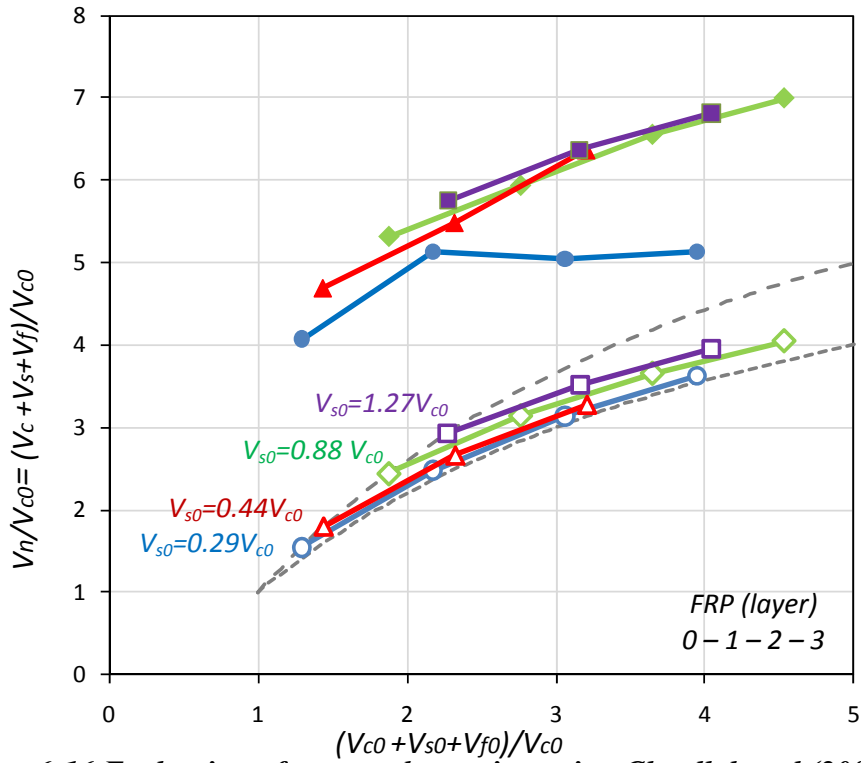
Figure 6-16 Evaluation of proposed equation using Chaallal et al.(2002)'s test result
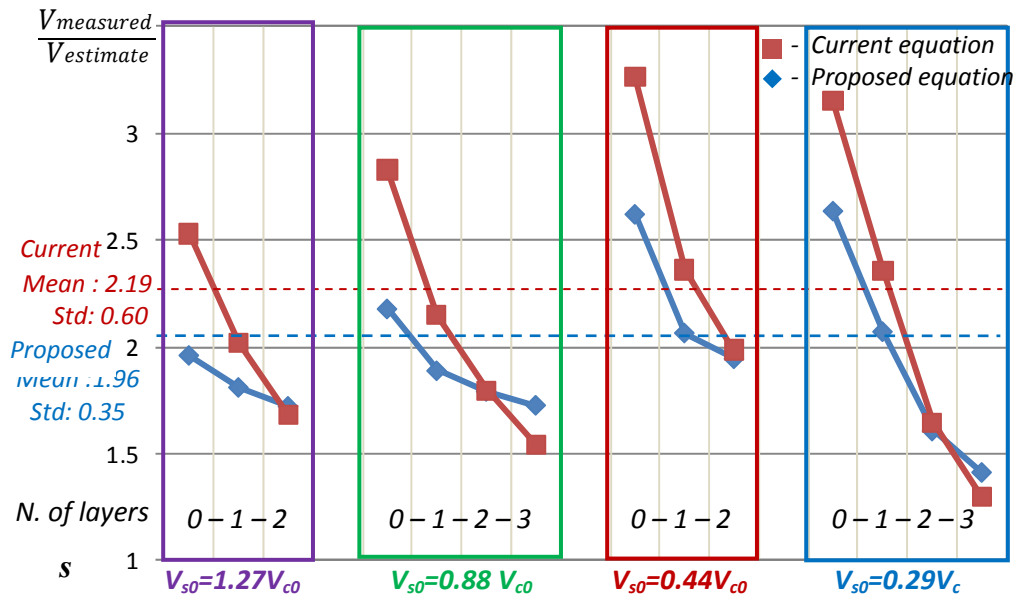
Figure 6-17 Comparison between current and proposed equation for tests reported by Chaallal et al (2002)

257

6.2.5   Design Example

A design example for beams with the same configuration as the 48 in. beams tested in this study was developed using the proposed modifications to ACI 440.2R and compared with current ACI 440.2R procedures for U-wraps and for complete wrapping. Because the U-wrap with anchors is considered to be equivalent to complete wrapping in the proposed equation, the calculations for both cases are the same. Because the shear span to depth ratio is 3, k_a is equal to 1. The material strengths (V_c , V_s , V_f) in ACI 440 are the base capacities (V_{c0} , V_{s0} , V_{f0}) in the proposed equations and the material contributions (V_c , V_s , V_f) are evaluated after considering the interaction factors k_s , k_f. It should be noted that the proposed equation using factors k_s , k_f can be applied to all strengthening schemes. However bond critical applications (unanchored U-wraps or only 2-sides bonded) are not recommended because debonding failure is not desirable and is highly variable. The proposed equation is only applied to the case of U-wraps with CFRP anchors. The detail calculations are shown in Appendix F.

One to three layers of CFRP strengthening are considered in the comparisons. Contributions for beams with #3 stirrups @10" or #3@18" are summarized in Table 6-3 and Table 6-4. The shear capacity, steel contribution, and CFRP contribution are plotted in Figure 6-18, Figure 6-19, and Figure 6-20 respectively.

Table 6-3 Comparison of contributions for #3@10" between proposed and ACI equation

V_S =56.9k	Current ACI 440 U-wrap (ε_{fe}=var.)				Current ACI 440 U-wrap+anchors (ε_{fe}=0.004)				Propose equation (ks, kf) U-wrap+anchors (ε_{fe}=0.004)			
	V_n	V_c	V_s	V_f	V_n	V_c	V_s	V_f	V_n	V_c	V_s	V_f
No CFRP	133	76.4	56.9		133	76.4	56.9		172	76.4	95.9	
1 layers	146	76.4	56.9	**12.6**	156	76.4	56.9	**22.8**	194	76.4	90.3	**27.1**
2 layers	150	76.4	56.9	**16.8**	179	76.4	56.9	**45.6**	213	76.4	85.2	**51.3**
3 layers	153	76.4	56.9	**19.9**	202	76.4	56.9	**68.4**	230	76.4	80.7	**72.8**

ε_{fe} =0.0021 (l layer), 0.0014(2layers) , 0.0011(3layers)

Table 6-4 Comparison of contributions for #3@18" between proposed and ACI equation

V_S =31.6k	Current ACI 440 U-wrap (ε_{fe}=var.)				Ccurrent ACI 440 U-wrap+anchors (ε_{fe}=0.004)				Propose equation (ks, kf) U-wrap+anchors (ε_{fe}=0.004)			
	V_n	V_c	V_s	V_f	V_n	V_c	V_s	V_f	V_n	V_c	V_s	V_f
No CFRP	105	76.4	28.5		105	76.4	28.5		134	76.4	57.2	
1 layers	117	76.4	28.5	**12.6**	128	76.4	28.5	**22.8**	159	76.4	53.6	**29.1**
2 layers	122	76.4	28.5	**16.8**	150	76.4	28.5	**45.6**	181	76.4	50.4	**54.6**
3 layers	125	76.4	28.5	**19.9**	173	76.4	28.5	**68.4**	201	76.4	47.6	**77.4**
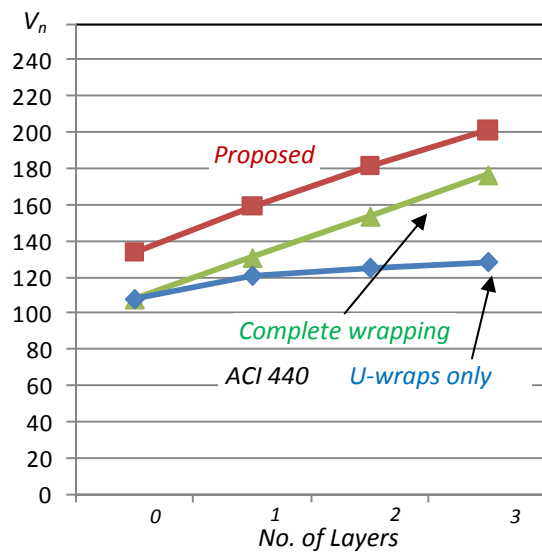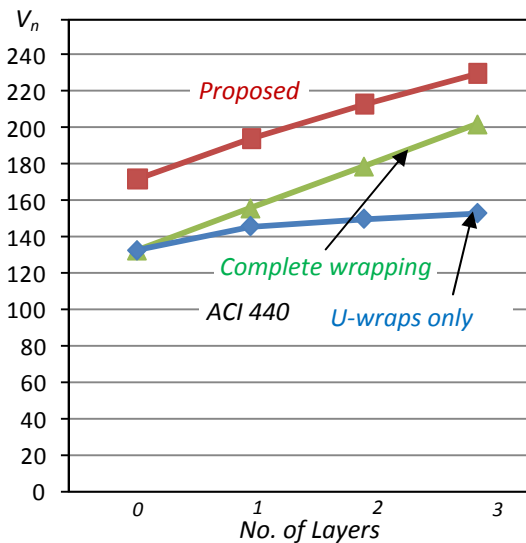
(a) #3@18"   (b) #3 @10

Figure 6-18 Comparison of shear capacity between proposed and ACI equation
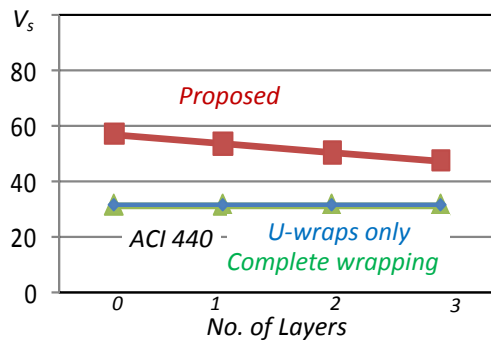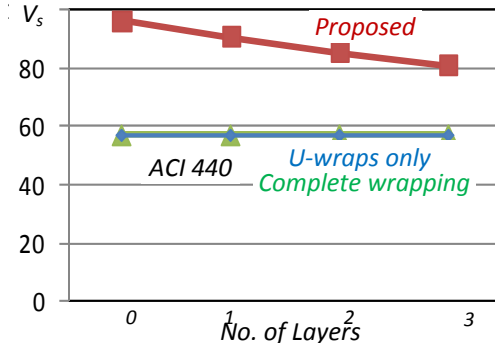
(a) #3@18"　　　　　　　　　　　　　(b) #3 @10

Figure 6-19 Comparison of steel contribution between proposed and ACI equation
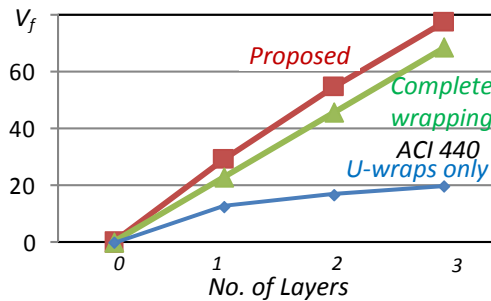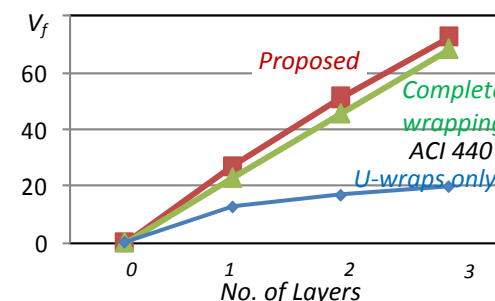
(a) #3@18"　　　　　　　　　　　　　(b) #3 @10

Figure 6-20 Comparison of CFRP contribution between proposed and ACI equation

In Figure 6-18, the CFRP contribution for a beam with #3 stirrups at 18 in. spacing is greater than that for a 10 in. spacing based on the proposed equation but is the same using the ACI 440.2R equation. In addition, the CFRP contribution of anchored strips is much greater than that of unanchored strips and that difference becomes more evident when the number of CFRP layers increases.

In Figure 6-19, the steel contribution using the proposed equation was greater when the number of FRP layer was smaller and the marginal change in the steel contribution was smaller when the existing beam had a higher transverse steel ratio. However, the steel contribution using ACI 440 procedures remained constant regardless of the amount of FRP.

260

In Figure 6-20, the marginal increase in FRP contribution from the proposed equation decreased as the number of FRP layer increased. In addition, the FRP contribution was lower when the existing beam had a higher transverse steel ratio. However, the CFRP contribution of U-wraps with anchors using ACI 440.2R was proportional to the amount of FRP material regardless of the amount of transverse steel reinforcement. The CFRP contribution of U-wraps in ACI 440.2R decreased as the number of layer increased due to a decrease in the effective strain.

In summary, the use of anchors can increase the CFRP contribution with very little increase in the amount of material needed for the anchors, thereby improving the effectiveness of the CFRP U-wraps. The proposed equation takes into account the change in critical angle as the amount of reinforcement changes. The interaction between the contributions to the shear capacity provided by the steel and CFRP is also taken in account using k_s , k_f. Therefore the proposed equation results in a more consistent safety of margin over a wide range of transverse reinforcement variations.

6.3 DESIGN CONSIDERATIONS

Although the required capacity of FRP is determined from the procedure discussed above, application of FRP in practice must be carefully monitored to realize the strengths calculated.

6.3.1 Design the Layout of CFRP Strip

6.3.1.1 Elastic modulus

High elastic modulus would be more helpful than high ultimate stress because ultimate stress would not be expected if the rupture strain is high (greater than 0.01). In addition, it is easy to apply FRP anchors when an FRP material with high elastic modulus is used because the cross-sectional area of the anchor is reduced. As shown in Figure 6-21, material A has lower ultimate stress, but higher elastic modulus. At the strain of 0.01,

material A has higher stress than material B. If the usable strain is assumed around 0.01, material A is more efficient (a larger fraction of its strength is developed) than material B.
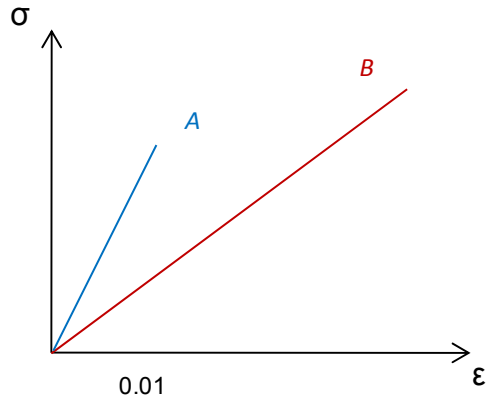
Figure 6-21 Cases of high stiffness and high rupture stress in brittle material

6.3.1.2   CFRP strip layout/spacing

At least one CFRP anchor is likely to be located close to the critical shear crack and this anchor will be subjected to high stress concentrations because the distance from the crack to anchor is short. As a result, the capacity of the CFRP strip resisted by this anchor may be lower than others and the anchor may rupture prematurely. Therefore, more FRP strips (more redundancy) across the critical crack would be better, but may not be practical. The current ACI 440.2R requires that the net spacing should be less than d/4 and represents a reasonable spacing requirement.

Continuous sheet application may be the best option because it provides continuity of the stress along the member. However, it is impossible to monitor cracking or any damage visually in this application. It is also unfavorable because the failure in brittle material is usually unpredictable and explosive. To reduce the possibility of a sudden catastrophic failure, a lower reduction factor might be considered for continuous sheet.
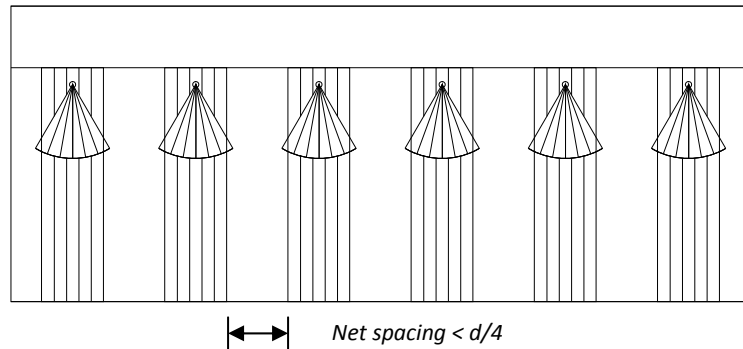
Net spacing < d/4

Figure 6-22 Net spacing between the strips

6.3.1.3 *Orientation of strip*

The most efficient use of FRP strip is to orient the strips perpendicular to the critical crack. However, the location and orientation of critical crack can not be specified before loading. In addition, the crack pattern might change after applying FRP because the load path was changed. As a result, the length of strip needs to be increased as the orientation of FRP strip is changed to cover the whole height. For this reason, the amount of FRP would increase although the shear capacity of FRP strip is increased by inclined application.

Inclined application of strip could be better for serviceability, but U-wrap scheme is not applicable in this application and additional consideration is needed to prevent the debonding failure at the bottom of the beam. Therefore, inclined application is not recommended unless the shear-span-to-depth ratio is less than 1, where the shear crack will occur from loading point to reaction point.

Horizontal FRP strips might help to distribute stress between the vertical strips. In addition, the horizontal strip can help satisfy equilibrium at local region near crack, not satisfying the equilibrium by longitudinal bars of member level. As a result, the crack width would be less and concrete strut capacity would increase when horizontal FRP strips are used. Therefore, the combination of vertical and horizontal FRP strip would be a good strategy in case where the concrete capacity needs to be increased.

263

6.3.2 Design of CFRP Anchors

The main purpose of this study was not the optimization of CFRP anchors but to provide anchors that are stronger than the strip being anchored. Because fracture of the anchor did not occur in most tests, current CFRP anchor details are considered to be feasible and to provide reliable strength. To optimize FRP anchor details, more parametric studies regarding anchor details would be needed.

6.3.2.1   The number of CFRP anchors

In general, it is better to increase the number of anchor and the number of strip across the critical section to provide more redundancy and reduce stress concentration. However, increasing the number of anchors will increase installation time.

One CFRP anchor per a side of CFRP strip is recommended. However, if the width of CFRP strip exceeds d_f/4, multiple anchors would be considered because of stress concentration at the anchor fan and key. For a continuous sheet, the number of CFRP anchors is determined by the width of CFRP strip per one anchor. It is recommended that this width not exceed d/4. As a result, at least four anchors would be provided within the critical section based on a 45 degree critical angle.

6.3.2.2   Fan length

The fan length is determined by the fan angle and overlapping length beyond CFRP width. However, overlapping length beyond CFRP width is specified as one-half inch, so fan length is determined by the fan angle. The small fan angle would perform better (Kobayashi, 2003), but the length will need to be increased to engage the width of the strip.

6.3.2.3   Fan angle

Kobayashi (2003) recommended that the fan angle should be less than 90 degrees and there are no adjustments needed for fan angle. However, a smaller fan angle requires more FRP material, so a fan angle of 90 degrees is most favorable. However, it is true

that the outer fibers of the anchor will be less efficient as the angle between strip and anchor increases. Therefore, more research is needed to evaluate the efficiency according to the fan angle. From this experimental program, the good performance of a 60 degree fan angle was verified. Furthermore, it is easy to calculate fan length because the fan length is always equal to the width plus 1-in. Therefore, a 60 degree fan angle is recommended.

6.3.2.4 The area of CFRP anchors compared with CFRP strip

With a typical hole diameter of ¼ to ¾ in. and ½ in. radius for the hole chamfer, the capacity of the strip would be reached if the area of the anchor is 2.5 to 3 times the area of the CFRP strip using Equation 2-4 in Section 2.4.5.2. However, the stress along the FRP strip length may be reduced due to shear friction between FRP and concrete surface and this stress reduction depends on the distance between crack and anchor. Therefore, the cross-sectional area of the FRP anchor is recommended as twice as the cross-sectional area of the FRP strip because anchors based on this value performed well in most tests.

6.3.2.5 Anchor hole diameter

After determining the amount of FRP material for anchors, the diameter of anchor can be calculated. To make the application of FRP anchor easier, it is recommended that the area of the anchor hole be 1.4 times of the area of the anchor. The diameter of hole will be from ¼ to ¾ in. Considering that most stirrups typically are No.3 or No.4 bars, the CFRP anchor hole can be angled not to interfere with steel stirrups and a small inclination of the key portion will not influence the performance of the anchor.

6.3.2.6 Details of anchor installation

Anchor embedment length may vary depending on the amount of material and the cover over the steel reinforcement, but 6 in. embedment will be sufficient for most cases. The anchor should extend into the confined core of the element. Hole chamfer radius is

an important detail to prevent stress concentration at the corner of the anchor fan and the key portion. A ½ in. radius worked well in this test program and follows recommendation of ACI 440.2R. A corner chamfer radius of ½ in. is also specified for the corner of the U-wrap. The overlapping length between anchors was 1 in. and is consistent with the recommendation that the anchor fan should extend a ½ in. beyond the strip width. Although the location of the anchor was 1-1/4 in. below the end of the strip in this experimental program, it performed well. Two additional patches in perpendicular directions were attached over the FRP anchors. The dimension of the patch is a square with sides equal to the strip width.

6.3.2.7 Final detail
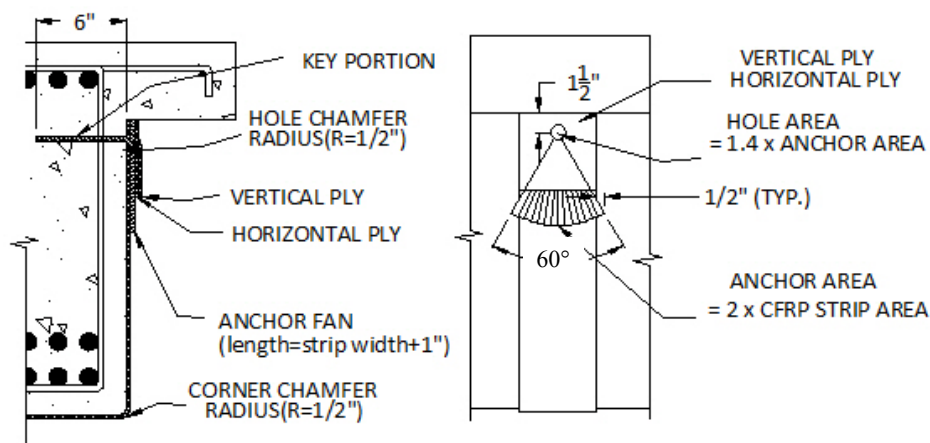
Figure 6-23 Recommended detail of CFRP anchor

6.4 SPECIFICATION

Because the FRP strengthening is applied under field condition, the expertise of the installers is important for a high quality. Specification sheet in NCHRP Report 514 provides guidance on application procedure and inspection. The quality assurance program (QAP) checklists in NCHRP Report 514 are listed below.

266

QAP1-6. Project Start-Up Requirements

        1. Project Start-Up Requirements / 2. Contract Documents /

        3. Specifications Review Checklist / 4. Drawing Review Checklist

        5. Staffing and Staff Qualification / 6. Miscellaneous Contractual Provisions

QAP 7. Material Qualification and Acceptance

QAP 8. Removal of Defective Concrete and Restoration of Section

QAP 9. Inspection - Surface Preparation

QAP 10. Application Conditions

QAP 11-13. FRP Application Process

        11. Wet Lay-up Systems / 12. Precured Systems

        13. Near Surface Mounted Systems

QAP 14. Identification of Defective Work

QAP 15. Postapplication - Quality Control Tests

QAP 16-20. General Job Administration

        16. Claims and Change Orders / 17. Schedule Monitoring

        18. Estimates and Payments / 19. Daily Inspectors Reports (DIR)

        20. Construction Close-Out

For the CFRP anchor installation, the overall procedure of installation CFRP anchors is described in Appendix A.4. The checklists for anchor installation are described below.

Anchor hole

1. Is the anchor hole at the specified location?
2. Is the embedment length greater than 6 in.?
3. Do any anchor holes interfere with steel reinforcement?
   If the hole is inclined to avoid reinforcement, is the angle less than 10 degrees from desired direction?
4. Is anchor hole clean?
5. Is the diameter of hole as specified?
6. Is the radius of anchor hole chamfer greater than 0.5 in.?
7. Are there any sharp edges around hole chamfer?

FRP anchor

1. Is FRP fiber cut carefully without loss of cross-sectional area?
2. Is the dimension of the anchor as specified?
3. Are all anchor holes saturated before application of FRP anchors?
4. Is the anchor fully saturated with epoxy resin before placement?
5. Is FRP anchor embedded fully into the hole?
6. Is the anchor fan spread uniformly?
7. Does the anchor fan extend half inch beyond the width of CFRP strip?
8. Is the dimension of the two additional patches as specified?
9. Are the patches perpendicular to each other?

Figure 6-24 Checklists for FRP anchor installation

CHAPTER 7

Conclusions

7.1 CONCLUSIONS

7.1.1 Findings from Experimental Results

To evaluate the performance of beams strengthened with CFRP anchors and CFRP U-wraps, experimental studies were carried out considering a number of parameters including depth of beam, shear span-to-depth ratio, transverse steel ratio, amount of CFRP material, CFRP material properties, concrete surface condition, anchor layout, and CFRP strip layout. The main findings from the test program are listed below.

1. The CFRP anchors enabled the CFRP U-wraps to reach rupture strain in strengthened beams because failure due to de-bonding was precluded.

2. The beams strengthened with U-wraps consisting of CFRP strips and anchors exhibited more shear deformation capacity and greater effective strains than beams strengthened with CFRP strips without anchors. Based on the test results, the net strength increase for beams strengthened with anchored CFRP was about 30~50% of the unstrengthened capacity. Similarly strengthened beam without anchors exhibited an increase in shear strength of less than 5%.

3. The critical crack angle became shallower as the applied load increased. Such behavior indicated that more stirrups and CFRP sheets contributed to shear strength than when a 45° crack angle is assumed, especially as the beams reached their shear capacity.

4. As the shear span to depth ratio decreases, the CFRP shear contribution decreased.

5. The strength increase after strengthening was greater as the transverse steel ratios of the existing beam decreases.

6. The capacity of members with shear-span-to-depth ratio less than two is generally controlled by the capacity of a concrete strut. Code provisions require that the maximum spacing of transverse reinforcement be reduced in deep members. As a result, the shear strengthening of members with low shear-span-to-depth ratios does not appear to be a viable approach.

7. The shear contribution of the CFRP material was not proportional to the amount of CFRP material used.

8. Bond between the CFRP laminates and concrete surface was not a critical parameter when CFRP anchors were provided. Bond did increase the overall stiffness because it decreased the length of the CFRP sheet over which strains were distributed. However, the ultimate capacity was not dependent on bond stress.

9. Beams strengthened with an FRP laminate having a high rupture strain were more likely to failure by concrete crushing or steel stirrups fracturing than by reaching the FRP rupture strain. Therefore, the effective rupture strain should not exceed 0.01.

10. U-wraps consisting of continuous sheets of CFRP exhibited a more uniform redistribution of stress than layouts consisting of individual spaced strips.

11. U-wraps placed diagonally were no more effective than vertical strips. The amount of material in diagonal strips increased because the length of strip increased. Therefore, wider vertical strip with the same amount of CFRP would be more efficient.

12. Poor quality CFRP installations exhibited marked reductions in the strengthened beam capacity.

7.1.2 Characteristics of Brittle Material

In ductile materials, the strains beyond yield do not result in any substantial change in the stress in the material. The maximum capacity of multiple elements can be easily evaluated by adding the capacity of each element under deformation large enough to yield all elements. However, the capacities cannot be added when brittle materials are combined. With brittle materials, the strain must be specified to calculate material stress. The maximum capacity of multiple brittle elements in material would be less than sum of each element unless all elements rupture simultaneously. Therefore, when an element ruptures, the maximum capacity would be different according to the strain on the other elements at the time the first element ruptures. The material characteristics of brittle materials must be taken into account when current designs used for steel reinforcement are modified to include the contribution of CFRP materials.

7.1.3 Shear Behavior in Brittle Materials

Because the location and orientation of critical cracks is not specified and bond behavior of the reinforcement embedded in concrete influences the strain in the reinforcement, strain compatibility cannot be used to define shear behavior. Therefore, in current code provisions, the steel contribution is evaluated assuming that the critical crack develops at 45 degrees and there is enough deformation to yield the steel stirrups. However, assumptions based on plasticity are not valid for brittle materials, so the shear behavior of beams strengthened with FPR materials is more complex.

Because strain distribution across a critical crack is not uniform, all FRP strips will not rupture simultaneously. As a result, the full capacity of FRP material cannot be used and an effective strain needs to be determined that represents the maximum possible FRP contribution. From the test results, it was found that when the FRP contribution reached maximum, the concrete contribution did not reach maximum because of interactions between the behavior of components with different material characteristics. Furthermore, some stirrups did not yield and the steel contribution can also be reduced when rupture or debonding failure of FRP limited the deformation capacity. An effective

271

strain was close to average strain across the critical crack was determined from the test data. In addition, when a beam is strengthened with CFRP, interactions between the contributions of the CFRP, steel or concrete must be taken into account.

7.1.4 CFRP Anchors

Because debonding of CFRP U-wraps occurred at strains (around 0.004) lower than the rupture strain (0.01), the contribution when debonding occurs would be low relative to the material capacity. Moreover, the strains would be insufficient to yield the steel and steel contribution decreased due to loss of deformation capacity.

In most tests, CFRP anchors prevented debonding failure of U-wrap application and enabled the CFRP strip to rupture. Therefore, CFRP anchors increased effective strain and maximized the material capacity. With anchors, the average strain in the CFRP strip across the critical crack exceeded 0.004 but is a function of the angle of the critical crack because the orientation of the crack determines the number of stirrups contributing to the shear capacity. Current code limitation on effective strain is too conservative when anchors are used but may be unconservative if debonding determines failure. The use of CFRP anchors resulted in U-wrap application to perform like continuous wrapping.

Beams strengthened with multiple-layers in the FRP strips failed by fracture of the anchors, but at higher effective strains compared with those at debonding failure.

7.1.5 Proposed Changes for Design using CFRP U-wraps with Anchors

7.1.5.1 Effective strain

To determine the FRP contribution, an effective strain must be specified. Current ACI 440.2R contains an equation for effective strain that is based on bond critical applications and specifies a reduction in the effective strain from 0.004 for complete wrapping. For bond critical applications (U-wraps and 2 sides bonded), the effective strain that can be mobilized in the CFRP is usually about 0.002; which is about half that of completely wrapped CFRP. However, there is no guideline for effective strain in U-wraps with anchorage. Based on the test results from this research program, a better

estimate of effective strain is 0.005, which represents the measured average strain across the critical crack.

However, an effective strain of 0.004 is proposed for U-wraps with anchorage. Because anchorage enables U-wraps to behave as well as complete wrapping, the effective strain of both cases for design should be identical even though the average strain from U-wraps tests results was greater than 0.004. Although the installation of CFRP anchors is more labor intensive, anchors can more than double the strength contribution of CFRP to shear.

7.1.6 Proposed modification of ACI 440.2R shear design

7.1.6.1 Adjustment factors: k_a , k_s, and k_f

To reflect the observations from this program and data from previous research, factors k_a, k_s and k_f are introduced. The change in concrete and steel contribution with the shear span to depth ratio (a/d ratio) is reflected by the k_a factor. For the concrete contribution, k_a is 2 if the a/d ratio is less than 0.5 and is 1.0 if the a/d ratio is greater than 2. Linear interpolation is used for values of a/d between 0.5 and 2.0.

The factor k_s is introduced to adjust the change in steel contribution due to the change of critical angle according to the amount of transverce reinforcement provided. When a low amount of transverse steel reinforcement was used, the critical angle was shallower than 45 degrees as is assumed in current design. Therefore, the number of stirrup contributing to shear capacity is under-estimated. For this reason, factor k_s increases as the transverse steel ratio decreases.

The interactions between steel and FRP transverse reinforcement are also represented by factors k_s and k_f. As the amount of either steel or FRP material increase, the efficiency of the other material decreases. As a result, the existing transverse steel ratio is an important factor for determining the FRP shear contribution.

7.2   FUTURE WORK

7.2.1   Anchor Detail

FRP anchor detail was not optimized in this study because the intent was to develop failure modes based on rupture of CFRP strips rather than the fracture of CFRP anchors. However, tests strengthened with two-layered FRP strips failed by the fracture of CFRP anchors and shear capacity was less than estimated. To apply FRP anchors to various strengthening situations, simple parametric studies of anchor details are needed including embedment length, diameter of anchor hole, chamfer radius, fan length, and fan angle. In addition, quality control procedures need to be developed because the performance of anchors depends on the expertise of workers and the quality of the installation.

7.2.2   Shear Design Equation

Although it is recommended that anchors be used in bond-critical CFRP shear installation, the proposed equations can be applied to cases with no FRP reinforcement, complete wrapping, U-wrapping with anchors, U-wrapping without anchors, and side-wrapping. However, the proposed equations need to be verified for these strengthening situations. Therefore, more data need to be collected and compared to verify the proposed equations, especially the k_s and k_f factors.

274

Appendix A

Construction of Test Specimen and CFRP Installation

In Appendix A, photos of the construction procedure including formwork, bar cages, strain gages, concrete cast and CFRP installation are listed.

A.1 FORMWORK

For 24 in. beams, a wood form was built by the project team. More details are described in Quinn's thesis (2009).
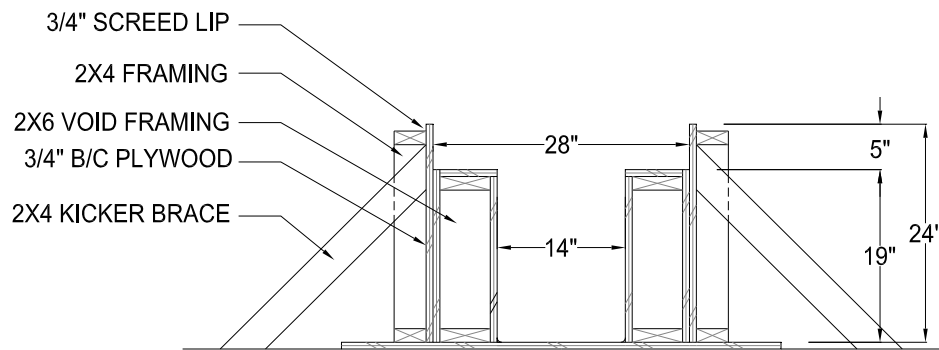
Figure A-1 Schematic cross-section of the form (24 in. beams)

(a) Cross-section of wood formwork   *(b) Corner chamfer*

Figure A-2 Photos of the form (24 in.)

Figure A-3 Photos of the reinforcement in form (24 in.)

276

A.2 BAR CAGES & STRAIN GAGE

A.2.1 24 in. Beams

Figure A-4 12 ft. and 16 ft. bar cages

Figure A-5 16 ft. bar cage for a/d=3 (#3@10")

Figure A-6 12 ft. bar cage for a/d=1.5 (#3@4")

Figure A-7 Strain gage layout for a/d=3 (left) and a/d=1.5 (right)

A.2.2 48 in. Beams

Figure A-8 Bar cage for 48 in. depth beam (#3@18")
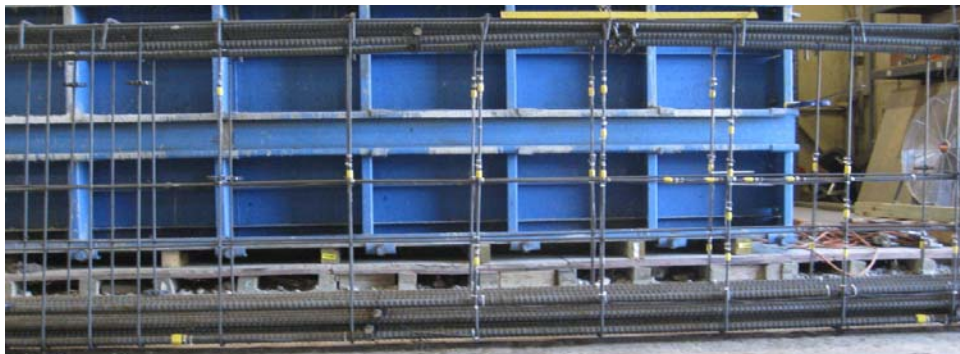
Figure A-9 Strain gage layout for 48-3-1 ~4 (#3@18")
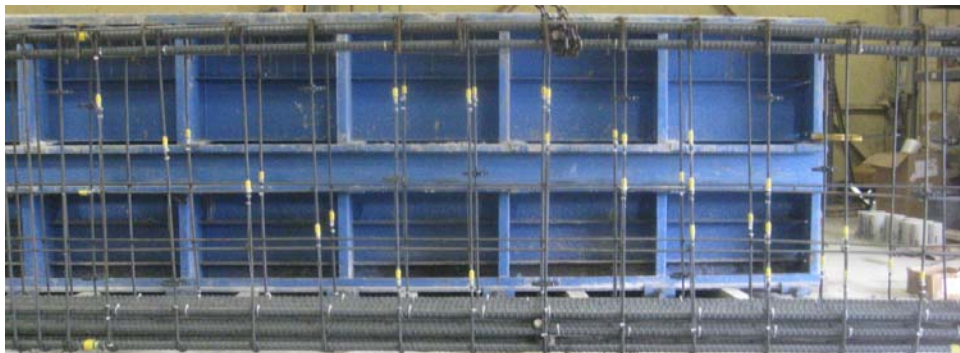
Figure A-10 Strain gage layout for 48-3-5 ~8 (#3@10")
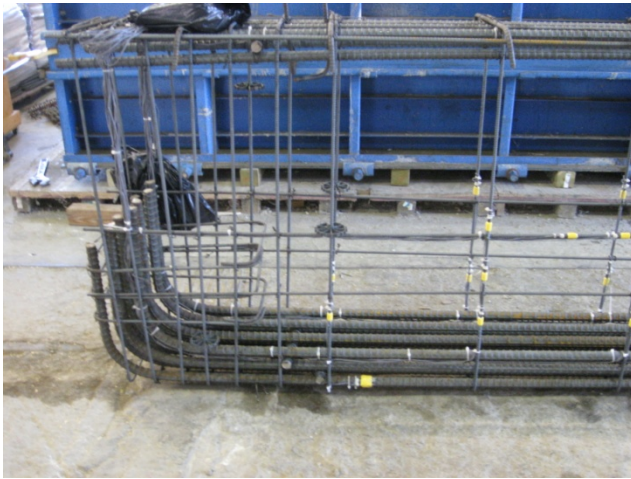
Figure A-11 Beam End Detail

A.3 CONCRETE PLACEMENT

Figure A-12 Concrete cast

A.4 CFRP INSTALLATION

A.4.1 Anchor Hole Preparation

Abrasive masonry bit was used to round the edge of all anchorage holes to a radius of 0.25 in. to 0.5 in. depending on the particular anchorage detail being studied. The anchorage holes need only be rounded to the required radius along the edge that contacts the anchorage fan. Because one-way CFRP anchors were used in all cases associated with this research project, the anchorage holes were only rounded along one side of the hole.

1) Drilling for anchor hole   2) Cleaning the hole

3) Rounding the edge of the hole   4) Completed CFRP anchor hole

Figure A-13 Surface preparation for anchor hole

A.4.2 Epoxy Resin Mix

Epoxy resin consists of two parts. The needed amount of Component A and component B was measured properly and mixed for five minutes.

1) Component A and Component B   2) Measuring the epoxy resin

3) Mix component A and B   4) Mixing (5 min.)   5) Complete mixing

Figure A-14 Epoxy resin mix

A.4.3 CFRP Strip and Anchor Installation

The procedure for CFRP strip and anchor installation are shown in Figure A-12; First, the concrete surface and anchor holes are saturated with epoxy (1~2), Then the CFRP strip is saturated by epoxy using rollers (3) and placed over the saturated location of concrete (4~5). Then the CFRP patch with perpendicular directional fibers is located over the strip end region (6). An opening to place CFRP anchor is created in the strip and patch (7). After impregnating anchor (8), the CFRP anchor is fully inserted into the hole (9~10). The anchor fan can be spread out uniformly by hand (11). If multiple anchors are used, repeat the procedures from (7) to (11). Cut bar tie used for placing the anchor (13) and cover the second patch over the anchor region (14).

When discrete strips of CFRP fabric are installed on the concrete surface, the anchor fan should extend past the edges of the CFRP strip by approximately 0.5-in. in order to ensure that every carbon fiber strand of the anchor intersects a fiber from the main CFRP strip.

| 1) Saturate the surface of concrete | 2) Saturate the anchor hole |

3) Impregnate CFRP strip

4) Attach CFRP strip to concrete surface

5) Removing excess epoxy

6) Attach the perpendicular directional patch

7) Creating an opening for CFRP anchor

8) Impregnated the CFRP anchor

9) Inserting the anchor into hole

10) Placing into the embedded length

11) Fan out the CFRP anchor

12) Repeating for another anchor

13) Cut the rebar tie
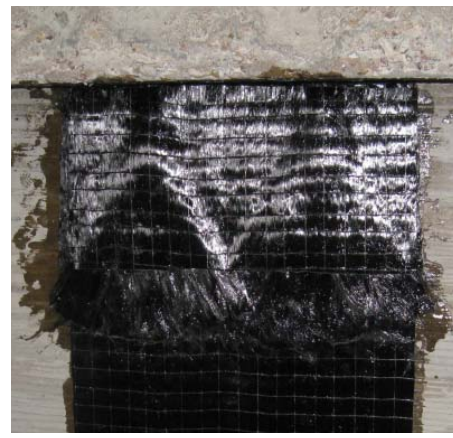
14) Attach another patch over CFRP anchor

Figure A-15 CFRP strip and anchor installation

284

A.4.4 CFRP Strain Gages

To monitor higher strain range of FRP than that of steel, different type of strain gage was used.
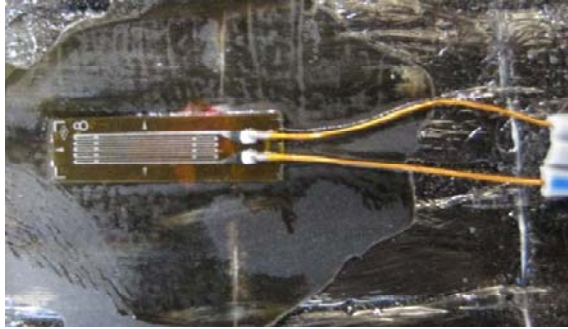
(a) CFRP strain gages   (b) Mechanical protection

Figure A-16 Photos of CFRP strain gages

A.4.5 Dry Lay-up Procedure

The dry lay-up installation procedures are as follows; first, a primer was applied to the concrete surface in order to seal cracks. Next, the two epoxy components were mixed and used to saturate both the location where CFRP strips were placed and the anchor holes. A dry CFRP strip was laid over the epoxy-coated concrete surface and epoxy was applied over the strip. Finally the CFRP strips were pressed into the epoxy with serrated roller. (Quinn 2009)

(a) Application of concrete surface primer   (b) Wetting the surface of the anchor holes
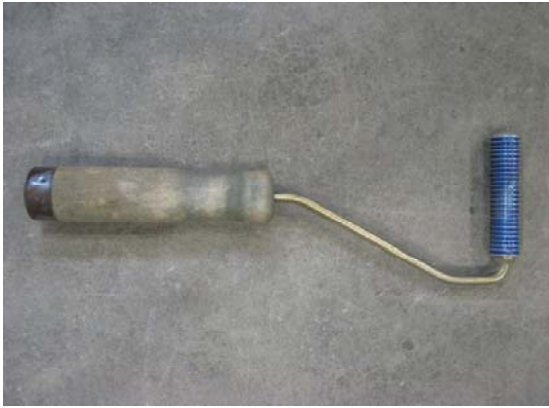
(c) Serrated roller

(d) Impregnating the CFRP strip

(e) Sealing the CFRP laminates with epoxy

(f) Completed installation

Figure A-17 Photos of dry lay-up procedure

Appendix B

Specimen Design Calculations

B.1.1 Shear Span to Depth Ratio of 3, 2.1 (#3@10")
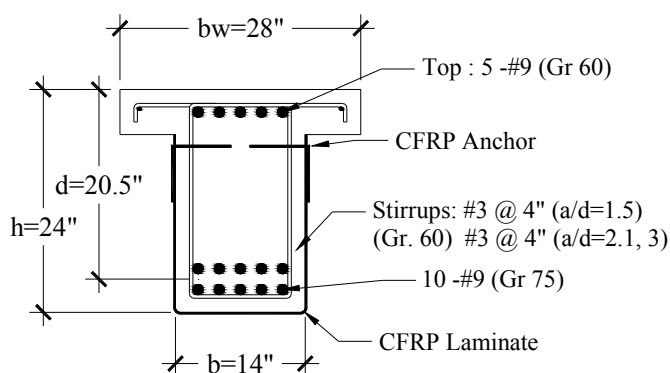
Figure B-1 Comparison of response between control test and strengthened test

1. Determine the shear capacity of section
   a) Calculate *Vc*

$$V_c = 2\sqrt{f'_c}b_w d = 2 \times \sqrt{4000} \times 14 \times 20.5 = 36.30 * 1000\ lbs = 36.30\ kips$$

The maximum allowable ACI318-08 Strength limit

$$V_{n,max} = 10\sqrt{f'_c}b_w d = \ 5\ V_c = 181.51\ kips$$

   b) Calculate *Vs*

Maximum spacing for stirrups

Check for #3 bar Gr. 60 ($A_s = 0.11\ in.^2$)

ACI318-08 11.4.6.3 – Spacing limits for shear reinforcement

$$S_1 = \frac{A_v \, f_{yt}}{0.75\sqrt{f'_c}b_w} = \frac{2\times0.11\times60000}{0.75\sqrt{4000}\times14} = 19.88 \; in \quad \text{from } A_{v,min} = 0.75\sqrt{f'_c}\frac{b_w s}{f_{yt}}$$

$$S_2 = \frac{A_v \, f_{yt}}{50 b_w} = \frac{2\times0.11\times60000}{50\times14} = 18.86 \; in \quad \text{from } A_{v,min} = \frac{50 b_w s}{f_{yt}}$$

ACI318-08 11.4.5 – spacing limits for shear reinforcement

$$S_3 = \frac{d}{2} = \frac{20.5}{2} = 10.25 \; in.$$

$$s = min.(\; s_1, s_2, s_3 \;) = 10.25 \; in. \qquad\qquad \rightarrow \quad \underline{\text{select} \quad s = 10 \; in.}$$

$$V_s = A_s f_y \frac{d}{s} = 2 \times 0.11 \times 60 \times \frac{20.5}{10} = 27.06 \; kips$$

Check $\quad V_s < 4\sqrt{f'_c}b_w d = 4 \times \sqrt{4000} / 1000 \times 14 \times 20.5 = 72.61 \; kips$

c) The expected shear capacity without CFRP

$$V_n = V_c + V_s = 36.30 + 27.06 = \underline{\textbf{63.36 k}}$$

2. CFRP Strengthening design

- **Basic assumption**

CFRP reaches the ultimate strain (=0.0105) when reaching the max. capacity

a) CFRP Properties

$$E_f = 1.48 \times 10^7 \; psi \; , \quad \varepsilon_{fu} = 0.0105 \; , t_f = 0.011 \; in.^2$$

$$f_{fe} = E_f \, \varepsilon_f = 1.48 \times \frac{10^7}{1000} \times 0.0105 = 155 \; ksi$$

b) Design equation

$$V_f = A_{fv} f_{fe}(\sin\alpha + \cos\alpha)\frac{d_f}{s_f} \qquad \text{(ACI 440.2R Eqn.11-3)}$$

(24-3-1R/3/4/10, 24-2.1-1)

Use 5 in. wide 1 layer at 10 in. spacing / $w_f = 5 \; in., \; s_f = 10 \; in., \; \alpha = 90°$

$$s_f < w_f + \frac{d}{4} \qquad\qquad \text{(ACI 440.2R 11.1)}$$

$$10 < 10.125 \; (= 5 + \frac{20.5}{4})$$

$$A_{fv} = 2 \, t_f w_f = 2 \times 0.011 \times 5 = 0.11 \; in.^2$$

$$d_f = d - h_f = 20.5 - 5 = 15.5 \; in.$$

288

$$V_f = A_{fv}f_{fe}\frac{d_f}{s_f} = A_{fv}f_{fe}\frac{d_f}{s_f} = 0.11 \times 155 \times \frac{15.5}{10} = 26.43 \; kips$$

(24-3-8: 2 layers)

$$V_f = A_{fv}f_{fe}\frac{d_f}{s_f} = A_{fv}f_{fe}\frac{d_f}{s_f} = (2 \times 0.11) \times 155 \times \frac{15.5}{10} = 52.86 \; kips$$

(24-3-7: Continuous sheet)

Use 1 sheet / $w_f = 5 \; in.$, $s_f = \mathbf{5 \; in.}$, $\alpha = 90\,°$

$$V_f = A_{fv}f_{fe}\frac{d_f}{s_f} = A_{fv}f_{fe}\frac{d_f}{s_f} = 0.11 \times 155 \times \frac{15.5}{5} = 52.86 \; kips$$

(24-3-9: No CFRP anchor)

$$E_c = 57000\sqrt{f_c'} = 57000\sqrt{4000} = 3.605 \times 10^6 \; psi$$

$$n_f = \frac{E_f}{E_c} = \frac{14.8}{3.605} = 4.1$$

$$\kappa_v = \frac{k_1 k_2 L_e}{468\varepsilon_{fu}} = \frac{k_1 k_2 L_e 1 \times 0.932 \times 1.05}{468 \times 0.0105} = 0.20 \qquad \leq 0.75$$

$$L_e = \frac{2500}{(n_f t_f E_f)^{0.58}} = \frac{2500}{(4.1 \times 0.011 \times 1.48 \times 10^7)^{0.58}} = 1.05$$

$$k_1 = \left(\frac{f_c'}{4000}\right)^{2/3} = \left(\frac{4000}{4000}\right)^{2/3} = 1 \quad , \qquad k_2 = \frac{d_{fv} - L_e}{d_{fv}} = \frac{15.5 - 1.05}{15.5} = 0.93$$

$$\varepsilon_{fe} = \kappa_v \, \varepsilon_{fu} = 0.20 \times 0.0105 = 0.0021$$

$$f_{fe} = E_f \, \varepsilon_{fe} = 1.48 \times \frac{10^7}{1000} \times 0.0021 = 31.1 \; ksi$$

$$V_f = A_{fv}f_{fe}\frac{d_f}{s_f} = A_{fv}f_{fe}\frac{d_f}{s_f} = 0.11 \times 31.1 \times \frac{15.5}{10} = 5.3 \; kips$$

However, debonding strain (=0.004) is used for unanchored test because anchored tests used rupture strain (=0.01) to compare each other in this study.

$$f_{fe} = E_f \, \varepsilon_{fe} = 1.48 \times \frac{10^7}{1000} \times 0.004 = 59.2 ksi$$

$$V_f = A_{fv}f_{fe}\frac{d_f}{s_f} = A_{fv}f_{fe}\frac{d_f}{s_f} = 0.11 \times 59.2 \times \frac{15.5}{10} = 10.1 \; kips$$

(24-3-5: laminate B)

$$E_f = 0.82 \times 10^7 \, psi \,, \quad \varepsilon_{fu} = 0.01 \,, t_f = 0.02 \, in^2$$

$$f_{fe} = E_f \, \varepsilon_f = 0.82 \times \frac{10^7}{1000} \times 0.01 = 82 \, ksi$$

$$w_f = 5 \, in \,, s_f = 10 \, in, \alpha = 90\,°$$

$$A_{fv} = 2 \, t_f w_f = 2 \times 0.02 \times 5 = 0.2 \, in.^2$$

$$V_f = A_{fv} f_{fe} \frac{d_f}{s_f} = A_{fv} f_{fe} \frac{d_f}{s_f} = 0.2 \times 82 \times \frac{15.5}{10} = 25.42 \, kips$$

(24-3-6: laminate C)

$$E_f = 3.3 \times 10^7 \, psi \,, \quad \varepsilon_{fu} = 0.0167 \,, t_f = 0.0065 \, in^2$$

$$f_{fe} = E_f \, \varepsilon_f = 3.3 \times \frac{10^7}{1000} \times 0.0167 = 551.1 \, ksi$$

$$w_f = 5 \, in \,, s_f = 10 \, in, \alpha = 90\,°$$

$$A_{fv} = 2 \, t_f w_f = 2 \times 0.0065 \times 5 = 0.065 \, in.^2$$

$$V_f = A_{fv} f_{fe} \frac{d_f}{s_f} = A_{fv} f_{fe} \frac{d_f}{s_f} = 0.065 \times 551.1 \times \frac{15.5}{10} = 55.5 \, kips$$

(This shear capacity was doubted before testing due to high rupture strain.)

c) The expected shear capacity with CFRP (maximum shear :24-3-7 or -8)

$$V_n = V_c + V_s + V_f = 36.30 + 27.06 + 52.86 = 116.2 \, kips< V_{n,max} \, (= 181.5 \, kips)$$

B.1.2 Shear Span to Depth Ratio of 1.5 (#3@4")

1. Determine the shear capacity of section

   a) Calculate Vc

$$V_c = 2\sqrt{f'_c} b_w d = 2 \times \sqrt{4000} \times 14 \times 20.5 = 36.30 * 1000 \, lbs = 36.30 \, kips$$

   b) Calculate Vs

    Maximum spacing for stirrups

   Check for #3 bar Gr. 60 ($A_s = 0.11 \, in.^2$)

        ACI 318-08 11.4.6.3 – spacing limits for shear reinforcement

$$S_1 = \frac{A_v\, f_{yt}}{0.75\sqrt{f'_c}\,b_w} = \frac{2\times0.11\times60000}{0.75\sqrt{4000}\times14} = 19.88 \; in \quad \text{from} \quad A_{v,min} = 0.75\sqrt{f'_c}\,\frac{b_w s}{f_{yt}}$$

$$S_2 = \frac{A_v\, f_{yt}}{50 b_w} = \frac{2\times0.11\times60000}{50\times14} = 18.86 \; in \quad \text{from} \quad A_{v,min} = \frac{50 b_w s}{f_{yt}}$$

ACI 11.7.4 – spacing limits for shear reinforcement (deep beam)

$$S_3 = \min\left(\frac{d}{5}, 12\right) = \min\left(\frac{20.5}{5}, 12\right) = 4.1 \; in.$$

$$s = min.\left(s_1, s_2, s_3\right) = 4.1 \; in. \qquad\qquad \underline{\text{Select} \quad s = 4 \; in.}$$

$$V_s = A_s f_y \frac{d}{s} = 2\times 0.11\times 60\times\frac{20.5}{4} = 67.65 \; kips$$

c) The expected shear capacity without CFRP

$$V_n = V_c + V_s = 36.30 + 67.65 = 103.95 \; k$$

2. CFRP design

a) CFRP Properties

$$E_f = 1.48 \times 10^7 \; psi \;, \quad \varepsilon_{fu} = 0.0105 \;, \; t_f = 0.011 \; in.^2$$

$$f_{fe} = E_f\,\varepsilon_f = 1.48 \times \frac{10^7}{1000} \times 0.0105 = 155 \; ksi$$

b) Design equation

$$V_f = A_{fv} f_{fe}(\sin\alpha + \cos\alpha)\frac{d_f}{s_f} \qquad \text{(ACI 440.2R Eqn.11-3)}$$

(24-1.5-4)

Use 5 in.wide 1layer at 10 in. spacing / $w_f = 5 \; in.$, $s_f = 10 \; in.$, $\alpha = 90\,°$

$$s_f < w_f + \frac{d}{4} \qquad\qquad \text{(ACI 440.2R 11.1)}$$

$$10 < 10.125 \left(= 5 + \frac{20.5}{4}\right)$$

$$A_{fv} = 2\, t_f w_f = 2\times 0.011\times 5 = 0.11 \; in.^2$$

$$d_f = d - h_f = 20.5 - 5 = 15.5 \; in.$$

$$V_f = A_{fv} f_{fe}\frac{d_f}{s_f} = A_{fv} f_{fe}\frac{d_f}{s_f} = 0.11\times 155\times\frac{15.5}{10} = 26.43 \; kips$$

(24-1.5-1r: 2 layers)

$$V_f = A_{fv}f_{fe}\frac{d_f}{s_f} = A_{fv}f_{fe}\frac{d_f}{s_f} = (2 \times 0.11) \times 155 \times \frac{15.5}{10} = 52.86 \; kips$$

(24-1.5-2 : No CFRP anchor)

$$E_c = 57000\sqrt{f_c'} = 57000\sqrt{4000} = 3.605 \times 10^6 \; psi$$

$$n_f = \frac{E_f}{E_c} = \frac{14.8}{3.605} = 4.1$$

$$\kappa_v = \frac{k_1 k_2 L_e}{468\varepsilon_{fu}} = \frac{1 \times 0.955 \times 0.7}{468 \times 0.0105} = 0.136 \quad \leq 0.75$$

$$L_e = \frac{2500}{(n_f t_f E_f)^{0.58}} = \frac{2500}{(4.1 \times 0.022 \times 1.48 \times 10^7)^{0.58}} = 0.7$$

$$k_1 = \left(\frac{f_c'}{4000}\right)^{2/3} = \left(\frac{4000}{4000}\right)^{2/3} = 1 \quad , \qquad k_2 = \frac{d_{fv} - L_e}{d_{fv}} = \frac{15.5 - 0.7}{15.5} = 0.955$$

$$\varepsilon_{fe} = \kappa_v \, \varepsilon_{fu} = 0.136 \times 0.0105 = 0.00143$$

$$f_{fe} = E_f \, \varepsilon_{fe} = 1.48 \times \frac{10^7}{1000} \times 0.00143 = 21.1 \; ksi$$

$$V_f = A_{fv}f_{fe}\frac{d_f}{s_f} = A_{fv}f_{fe}\frac{d_f}{s_f} = (2 \times 0.11 \times 2) \times 21.1 \times \frac{15.5}{10} = 7.2 \; kips$$

c) The expected shear capacity with CFRP (maximum shear :24-1.5-1r)

$$V_n = V_c + V_s + V_f = 36.30 + 67.65 + 52.86 = 156.9 \; \text{kips}$$

B.1.3 Flexural Capacity (for all 24 in. Beams)

1. Determine the neutral axis

   - Assume a is located in the slab (as a rectangular section, a = 0.85c < t_f)

   $$T = A_s f_y = 10 \times 1 \times 75 = 750 \; \text{kips}$$

   C_{s1} - Compression force due to reinforcement of the beam (5 -#9)

   C_{s2} - Compression force due to reinforcement of the slab (4- #3)

   $$C_{s1} = A_s f_s = 5 \times 1 \times 87\left(1 - \frac{2.44}{c}\right) = 435\left(1 - \frac{2.44}{c}\right)$$

   $$C_{s2} = A_s f_s = 4 \times 0.11 \times 87\left(1 - \frac{2.1875}{c}\right) = 38.28\left(1 - \frac{2.1875}{c}\right)$$

$$f_s = E_s\varepsilon_s = E_s \frac{c-d'}{c}\varepsilon_{cu} = 29000 \times \left(1 - \frac{2.44}{c}\right) \times 0.003 = 87\left(1 - \frac{2.44}{c}\right)$$

$$C_c = 0.85f'_c ab_f = 0.85 \times 4 \times 0.85c \times 28 = \quad 80.9c$$

(No consideration of substraction of compressive steel area)

To satisfy the equilibrium

$$T = C_{s1} + C_{s2} + C_c$$

$c = \quad 5.843$ in.

Check for assumptions

$a = \quad 0.85 \cdot c = 0.85 \times 5.843 = 4.97\ in \quad < \quad 5\ in.$ (as a rectangular beam)

$f_{s1} = 50.647\ kips\ , \quad f_{s2} = 54.405\ kips\ < \ f_y$

(Approximate solution: No consideration for compressive reinforcement)

$$M = A_s f_y \left(d - \frac{a}{2}\right) = 750 \times \left(20.5 - \frac{4.97}{2}\right) = 13512.5\ kips \cdot in.$$

Corresponding shear capacity

(a/d=3) $V = \frac{M}{d \times 3} = \frac{13512.5}{20.5 \times 3} = 219.7\ k$ /(a/d =2.1) $V = \frac{M}{d \times 2.1} = \frac{13512.5}{20.5 \times 2.1} = 318.9k$

(a/d=1.5) $V = \frac{M}{d \times 1.5} = \frac{13512.5}{20.5 \times 1.5} = 439.4\ k$

Table B-1 Shear capacity vs. required shear capacity corresponding moment

	$V_c + V_s$	$V_c + V_s + V_f$	Shear capacity corresponding Moment	Safety margin	5 Vc code limit
a/d =1.5 (#3@4")	104 k	157 k	439 k	2.8	
a/d=2.1 (#3@10")	63 k	116 k	319 k	2.75	181.5 k
a/d=3 (#3@10")	63 k	116 k	220 k	1.9	

- Anchorage Design

  Based on the moment diagram, there is no moment at the reaction point in simple beam. However, 2-ft development length was provided for tensile stress unexpectedly due to shear shift

- Local zone

  No local zone failure were observed because of enough steel bearing plates were
  used.

B.1.4 Test Setup

Applied load capacity: 600 kips (= 300k/ram× 2 rams)

Reaction capacity: 240 kips (= 30k/rod × 8 rods)

Applied load corresponding reaction

(a/d=3) 240 × $\frac{144}{68}$ = 455k / (a/d=2.1) 240 × $\frac{96}{48}$ = 480k /(a/d=1.5) 240 × $\frac{96}{58}$ = 397k

- Reaction capacity control the capacity of loading setup and member capacity
does not exceed reaction capacity (safety margin : 240/157 = 1.53 for most unsafe
condition – a/d=1.5)

In addition, in the capacity of 12-ft loading setup is less than the flexural capacity
of specimen (a/d=1.5 and 2.1). the limit of loading setup could be reached first.
For this reason, the test capacity exceeded test 24-1.5-1r, so test 24-3-1r2 and 24-
3-4 were conducted with 48-inch beam loading setup.

B.2 48 IN. BEAMS

B.2.1 Minimum Transverse Steel Ratio (#3@18")

1. Determine the shear capacity of section
   a) Calculate V_c

$$V_c = 2\sqrt{f'_c}b_w d = 2 \times \sqrt{4000} \times 14 \times 43.125$$

$$= 76.369 * 1kip\ /1000\ lbs = 76.38\ kips$$

The maximum allowable CODE Strength limit

$$V_{n,max} = 10\sqrt{f'_c}b_w d = 5\ V_c = 381.8\ kips$$

b) Calculate V_s

Maximum spacing for stirrups

Check for #3 bar Gr 60 ($A_s = 0.11\ in.^2$)

ACI 11.4.6.3 – spacing limits for shear reinforcement

$$S_1 = \frac{A_v\,f_{yt}}{0.75\sqrt{f'_c}\,b_w} = \frac{2\times0.11\times60000}{0.75\sqrt{4000}\times14} = 19.88\ in. \quad \text{from}\quad A_{v,min} = 0.75\sqrt{f'_c}\,\frac{b_w s}{f_{yt}}$$

$$S_2 = \frac{A_v\,f_{yt}}{50 b_w} = \frac{2\times0.11\times60000}{50\times14} = 18.86\ in. \qquad \text{from}\quad A_{v,min} = \frac{50 b_w s}{f_{yt}}$$

ACI 11.4.5 – spacing limits for shear reinforcement

$$S_3 = \frac{d}{2} = \frac{43.5}{2} = 21.75\ in.$$

$s = min.\ (\ s_1, s_2, s_3\ ) = 18.86\ in.$ ->   Select s = 18 in.

$$V_s = A_s f_y \frac{d}{s} = 2\times 0.11\times 60\times \frac{43.125}{18} = 31.625\ kips$$

Check $V_s < 4\sqrt{f'_c}\,b_w d = 4\times\sqrt{4000}\,/1000\times 14\times 20.5 = 154.06\ kips$

c) The expected shear capacity without CFRP

$$V_n = V_c + V_s = 76.37 + 31.625 = \mathbf{108.00\ k}$$

2. CFRP design

- **Basic assumption**

  CFRP laminate reaches the ultimate strain ($\varepsilon_f = 0.0105$)

  when the section reach the max. capacity

a) CFRP Properties

$$E_f = 1.48\times 10^7\ psi\ ,\ \varepsilon_{fu} = 0.0105\ , t_f = 0.011\ in.^2$$

$$f_{fe} = E_f\,\varepsilon_f = 1.48\times \frac{10^7}{1000}\times 0.0105 = 155\ ksi$$

b) Design equation

$$V_f = A_{fv} f_{fe}(\sin\alpha + \cos\alpha)\frac{d_f}{s_f} \qquad \text{(ACI 440R eq (11-3))}$$

Use 1 sheet / $w_f = 10\ in.$, $s_f = 20\ in.$, $\alpha = 90\,°$

$s_f < w_f + \frac{d}{4} = 10 + \frac{43.125}{4} = 20.875$ in.   (ACI 440R 11.1)

$A_{fv} = 2 \, t_f w_f = 2 \times 0.011 \times 10 = 0.22 \; in.^2$

$d_f = d - h_f = 43.125 - 8 = 35.125 \; in.$

$V_f = A_{fv} f_{fe} \frac{d_f}{s_f} = A_{fv} f_{fe} \frac{d_f}{s_f} = 0.22 \times 155 \times \frac{35.125}{20} = 59.89 \; kips$

c) The expected shear capacity with CFRP

$V_n = V_c + V_s + V_f = 77.0 + 31.9 + 60.5 = 169.4$ kips

B.2.2 Same Transverse Steel Ratio as 24 in. beams (a/d=3, #3@10")

1. Determine the shear capacity of section

   a) Calculate Vc

$$V_c = 2\sqrt{f'_c} b_w d = 2 \times \sqrt{4000} \times 14 \times 43.125$$

$$= 76.369 * 1kip \, /1000 \; lbs = 76.38 \; kips$$

   b) Calculate Vs

$s = min.(\, s_1, s_2, s_3 \,) = 18.86$ in.   (from previous calculation)

<u>s = 10 in.</u>   (to make same transverse ratio with 24 in. depth beams)

$$V_s = A_s f_y \frac{d}{s} = 2 \times 0.11 \times 60 \times \frac{43.125}{10} = 56.925 \; kips$$

Check $V_s < 4\sqrt{f'_c} b_w d = 4 \times \sqrt{4000} \, / 1000 \times 14 \times 20.5 = 154.06 \; kips$

   c) The expected shear capacity without CFRP

$V_n = V_c + V_s + V_f = 77.0 + 57.4 + 60.5 = 194.9$ kips

B.2.3 Flexural Capacity

1. Determine the neutral axis

Assume a is located in the slab (as a rectangular section, a = 0.85c < t_f)

$T = A_s f_y = 12 \times 1.27 \times 75 = 1143$ kips

C_s - Compression force due to top bar of the beam   (6 -#9)

$$C_{s1} = A_s f_{s1} = 4 \times 1 \times 87 \left(1 - \frac{3.5}{c}\right) = 348 \left(1 - \frac{3.5}{c}\right)$$

296

$$C_{s2} = A_s f_{s2} = 2 \times 1 \times 87 \left(1 - \frac{5.5}{c}\right) = 174 \left(1 - \frac{5.5}{c}\right)$$

$$f_{s1} = E_s \varepsilon_{s1} = E_s \frac{c - d'_1}{c} \varepsilon_{cu} = 29000 \times \left(1 - \frac{3.5}{c}\right) \times 0.003 = 87 \left(1 - \frac{3.5}{c}\right)$$

$$f_{s2} = E_s \varepsilon_{s2} = E_s \frac{c - d'_2}{c} \varepsilon_{cu} = 29000 \times \left(1 - \frac{5.5}{c}\right) \times 0.003 = 87 \left(1 - \frac{5.5}{c}\right)$$

$$C_c = 0.85 f'_c a b_f = 0.85 \times 4 \times 0.85c \times 21 = \quad 60.69c$$

To satisfy the equilibrium

$$T = C_{s1} + C_{s2} + C_c$$

Solve $c = 13$ in.

Check the rectangular section assumption

$$a = 0.85 \cdot c = 0.85 \times 13 = 11.05 \; in. \; > \; 8 \; in. \quad \text{N.G (as a T-beam)}$$

$$C_{c1} = 0.85 f'_c t_f (b_f - b_w) = 0.85 \times 4 \times 8 \times (21 - 14) = \quad 190.4 kips$$

$$C_{c2} = 0.85 f'_c a b_f = 0.85 \times 4 \times 0.85c \times 14 = \quad 40.46c$$

To satisfy the equilibrium

$$T = C_{s1} + C_{s2} + C_{c1} + C_{c2}$$

Solve $c = 14.38$ in.

$$a = 0.85 \cdot c = 0.85 \times 14.38 = 12.22 \; in.$$

Maximum extreme tensile strain when reach 0.003 of concrete strain: 0.0063

➔ Tension controlled, but lower ductility. Need to be monitored for concrete crushing

$$M = A_s f_y \left(d - \frac{a}{2}\right) = 1143 \times \left(43.5 - \frac{12.22}{2}\right) = 42737 \; kips \cdot in$$

shear capacity corresponding moment

$$(a/d=3) \; V = \frac{M}{d \times 3} = \frac{42737}{43.5 \times 3} = 327 \; kips$$

Table B-2 Shear capacity vs. required shear capacity corresponding moment

	$V_c + V_s$	$V_c + V_s + V_f$	Shear capacity corresponding Moment	Safety margin	5 Vc code maximum
1~4 (#3@18")	108 k	168k	327	1.55	381.8
5~8 (#3@10")	133 k	193k		1.45	

From test observation in 24 in. beams, development length was reduced to fit the steel formwork dimension and additional hoops were placed. It is difficult to get the great safety margin because the depth of beam was doubled. Therefore, safety margin were reduced because the flexural reinforcement were too closed located despite three layers of No. 10 bars.

No local zone failure observed.

B.2.4 Test Setup

The column capacity = 800 kips (4EA × 200 kips/EA) control the capacity of loading setup

Corresponding shear = $800 \times \frac{159}{296} = 430$ kips

This capacity is greater than flexural capacity of all 48 in. specimen. Therefore there was no issue of testing setup.

Appendix C

Design of CFRP Anchors

C.1 24-IN. BEAMS

All 24 in beams had a one anchor per 5 in. wide strip. The area for CFRP anchor was twice the area of the strip. If the material for anchor is the same as the material for strip, the area of the anchor is simply evaluated by doubling the width of strip to . Otherwise, elastic modulus and thickness of strip is also considered to calculate the required area for anchor. Depending on the area of the strip, the diameter of anchor hole need to be calculated.

1. Area of the anchor

$$A_{fv} = t_f w_f = 0.011 \times 5 = 0.055 \ in.^2$$

To make the CFRP anchor stronger than strip, the area for CFRP anchor was twice the area of the strip.

$$A_{f,anchor} = 2 \ A_{f,v} = 2 \times 0.055 = 0.11 \ in.^2$$

$$w_{f,anchor} = \frac{A_{f,anchor}}{w_{f,anchor}} = \frac{0.11}{0.041} = 2.68 \ in.$$

Laminate A-1 (0.041in.) was used for anchors instead of laminate A (0.011 in.)

If the laminate for anchor is the same as the laminate for strip, the width will be doubled.

$$A_{f,anchor} = 2 \ A_{f,v} = 2 \times 0.055 = 0.11 \ in.^2$$

$$w_{f,anchor} = \frac{A_{f,anchor}}{w_{f,anchor}} = \frac{0.11}{0.011} = 10 \ in.$$

2. Anchor length

Fan angle: <u>select = 60 degrees</u> (easy to calculate)

Fan length = Fan width (when the fan angle is 60 degrees)

2 × (Overlapping width) + (Strip width) = 2 × 0. 5+ 5 = 6 in.

Total length for anchor = Embedment length + Fan length = 6+6 =12 in.

CFRP anchor dimension : 2.68 in. × 0.041 in. × 12 in.

However, A CFRP anchor was folded to put into the hole easily.

Thus, final CFRP anchor cutting dimension : **1.34 in. × 0.041 in. × 24 in.**

(See Figure 2-13)

3. Anchor hole design

$$A_{hole,anchor} = 1.4\ A_{f,anchor} = 1.4 \times 0.11\ = 0.154\ in.^2$$

$$d_{hole,anchor} = \ 2\sqrt{\frac{A_{hole,anchor}}{\pi}}\ = 2\sqrt{\frac{0.154}{\pi}} = 0.443 in \cong {}^7\!/_{16}\, in.$$

(24-3-5, Laminate B, lower elastic modulus than laminate A)

$$A_{fv} = \ t_f w_f = 0.02\ \times 5 = 0.1\ in.^2$$

$$A_{f,anchor} = 2\ A_{f,v} = 2\ \times 0.1 = 0.2\ in.^2$$

$$w_{f,anchor} = \frac{A_{f,anchor}}{w_{f,anchor}} = \frac{0.2}{0.02} = 10\ in.$$

Fan angle and strip width is same. Anchor length = 12 in.

Anchor dimension: 10 in. × 0.02 in. × 12 in. → 5 in. × 0.02 in. × 24 in.

$$A_{hole,anchor} = 1.4 A_{f,anchor} = 1.4 \times 0.2 = 0.28\ in.^2$$

$$d_{hole,anchor} = \ 2\sqrt{\frac{A_{hole,anchor}}{\pi}}\ = 2\sqrt{\frac{0.28}{\pi}} = 0.597 in. \cong {}^5\!/_8\, in.$$

(24-3-6, Laminate C, high rupture strain, and dry lay-up)

$$A_{fv} = \ t_f w_f = 0.0065\ \times 5 = 0.0325\ in.^2$$

$$A_{f,anchor} = 2\ A_{f,v} = 2\ \times 0.0325 = 0.065\ in.^2$$

$$w_{f,anchor} = \frac{A_{f,anchor}}{w_{f,anchor}} = \frac{0.065}{0.0065} = 10\ in.$$

300

Fan angle and strip width is same. Anchor length = 12 in.

Anchor dimension: 10 in. × 0.02 in. × 12 in. → 5 in. × 0.02 in. × 24 in.

$$A_{hole,anchor} = 1.4 A_{f,anchor} = 1.4 \times 0.0625 = 0.0875 \; in.^2$$

$$d_{hole,anchor} = 2\sqrt{\frac{A_{hole,anchor}}{\pi}} = 2\sqrt{\frac{0.0875}{\pi}} = 0.334 in \cong \frac{3}{8} in.$$

(24-3-8, 2 layers)

$$A_{fv} = t_f w_f = 2 \times 0.011 \times 5 = 0.11 \; in^2$$

$$A_{f,anchor} = 2 A_{f,v} = 2 \times 0.11 = 0.22 \; in^2$$

$$w_{f,anchor} = \frac{A_{f,anchor}}{w_{f,anchor}} = \frac{0.22}{0.041} = 5.37 \; in.$$

Fan angle and strip width is same. Anchor length = 12 in.

Anchor dimension: 5.37 in. × 0.041 in. × 12 in. → 2.68 in. × 0.041 in. × 24 in.

$$A_{hole,anchor} = 1.4 A_{f,anchor} = 1.4 \times 0.22 = 0.308 \; in.^2$$

$$d_{hole,anchor} = 2\sqrt{\frac{A_{hole,anchor}}{\pi}} = 2\sqrt{\frac{0.308}{\pi}} = 0.626 in \cong \frac{5}{8} in.$$

C.2 48 IN. BEAMS

In 48 in beams, two anchors per each strip (10 in. wide) were used. Each anchor transferred the force of 5 in. wide strip. Therefore, basically the same anchor detail as 24 in.beams was used.

48-3-3 (14 in. wide, 2 anchors / strip)

$$A_{fv} = t_f w_f = 0.011 \times 14 \; / \; 2 = 0.077 \; in.^2$$

$$A_{f,anchor} = 2 A_{f,v} = 2 \times 0.077 = 0.154 \; in.^2$$

$$w_{f,anchor} = \frac{A_{f,anchor}}{w_{f,anchor}} = \frac{0.154}{0.041} = 3.36 \; in.$$

The fan length =2 × overlapping width + strip width =2 × 0. 5 + 7 = 8 in.

Total length for anchor = embedment length + fan length = 6+8 =14 in.

Anchor dimension: 3.36 in. $\times$ 0.041 in.$\times$ 14in. $\rightarrow$ 1.68 in. $\times$ 0.041 in. $\times$ 24 in.

$$A_{hole,anchor} = 1.4A_{f,anchor} = 1.4 \times 0.154 = 0.2156 \ in.^2$$

$$d_{hole,anchor} = 2\sqrt{\frac{A_{hole,anchor}}{\pi}} = 2\sqrt{\frac{0.2156}{\pi}} = 0.524 in. \cong \frac{1}{2}in.$$

48-3-7 (10 in. wide, two anchors / strip, intermediate anchor)

Unlike typical anchor detail, anchor fan spreaded in both directions $\rightarrow$ 2 anchors in the one hole for intermediate anchor. the dimension for an anchor is the **same dimension as 24-3-8.**

48-3-8 (2 layers , 2anchors/ strip)

Same dimension as 24-3-8

Appendix D
Material Testing Data

D.1 CONCRETE

Typical concrete mix design (used by the ready mix provider)

- 4-1/4 Sack (A measure of how much portland cement to include within the mix)

- 25% Fly Ash

- ¾ in. Maximum Aggregate Size

- 6 to 8 in. Slump
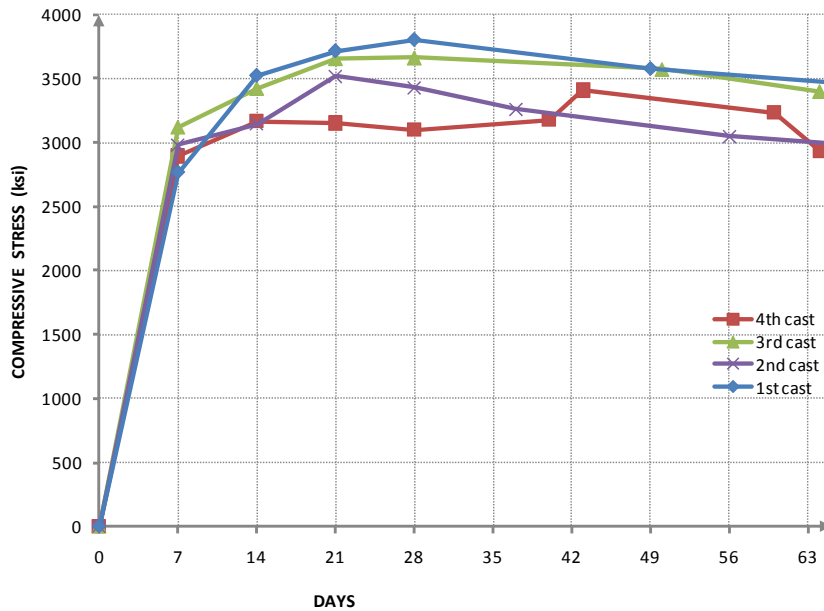
Figure D-1 Concrete test results for casts 1 to 4 (24 in. beams)
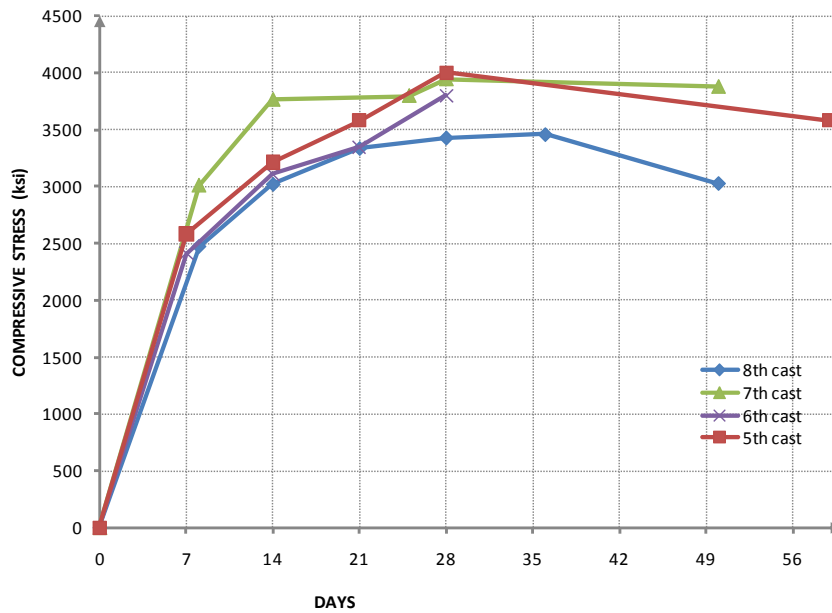
Figure D-2 Concrete test results for casts 5 to 8 (48 in. beams)

Table D-1 Compressive strength of concrete according to the cast

cast	Test	Average stress (10 x 3 psi)	Tensile stress (10 x 3 psi)
1	24-1.5-1/2 , 24-3-1/2	3.6	0.43
2	24-1.5-3/4 , 24-3-3/4	3.3	0.37
3	24-2.1-1/2 , 24-3-5/6	3.5	0.32
4	24-3- 7 / 8 / 9 / 10	3.2	0.34
	24 in.	**3.4**	**0.37**
5	48-3- 1/2	3.9	0.32
6	48-3- 3/4	3.9	0.35
7	48-3- 5/6	3.9	0.41
8	48-3- 7/8	3.4	0.39
	48 in.	**3.8**	**0.37**

- Average compressive stress were calculated from all data after 28th days

D.2 STEEL
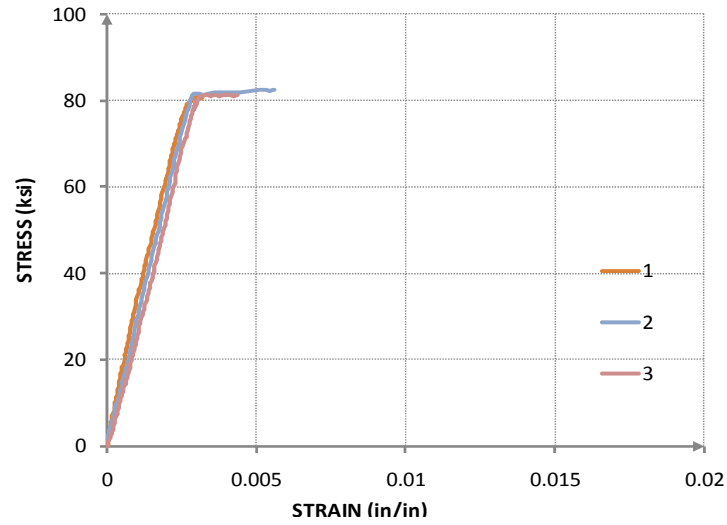
Figure D-3 Stress-strain relationship in No.9 grade 75 bar in 24 in. beams
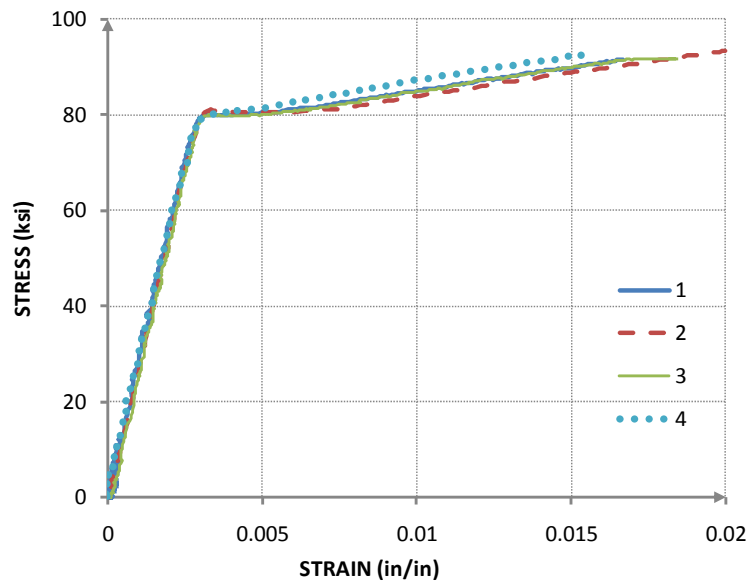
Figure D-4 Stress-strain relationship in No.10 bar (grade 75) in 48 in. beams
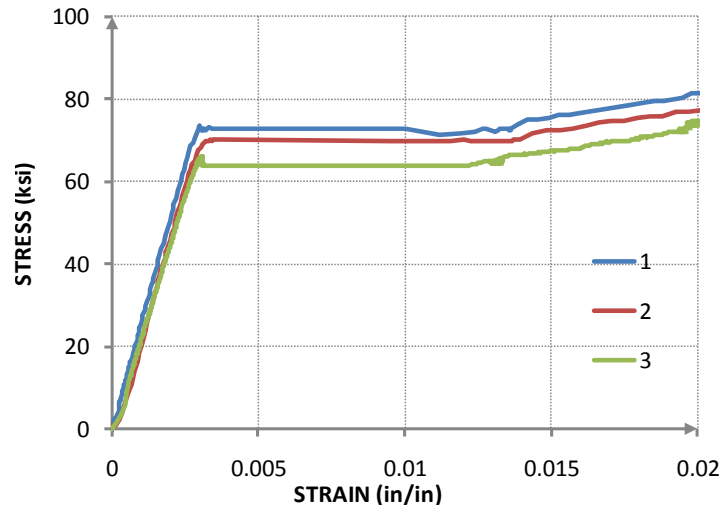
Figure D-5 Stress-strain relationship in No.3 grade 60 bar in 24 in. beams
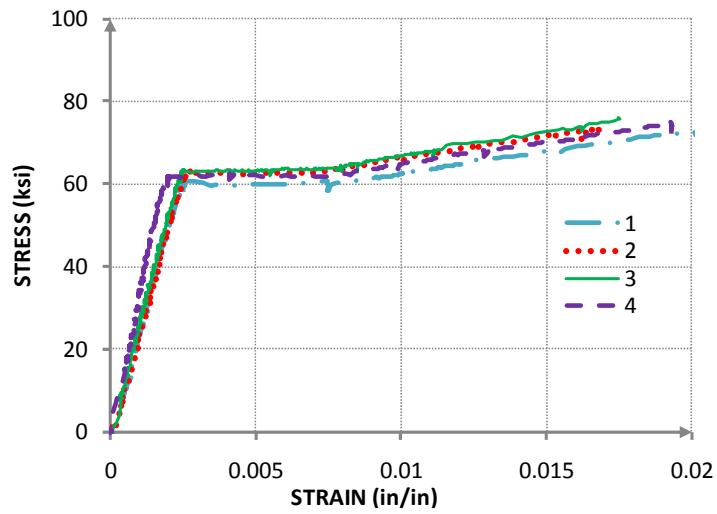
Figure D-6 Stress-strain relationship in No.3 bar (grade 60) in 48 in. beams

D.3 CFRP

Three laminates(A, B, C) were used, but laminate A was used for most specimens.
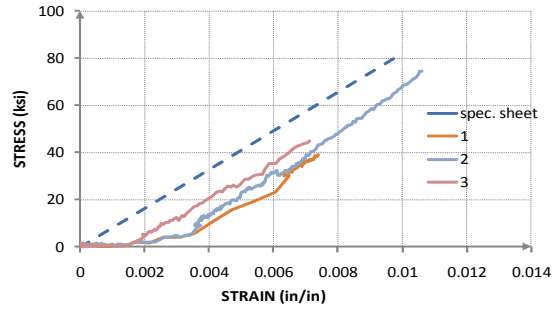
Figure D-7 Stress-strain curves of CFRP laminate A
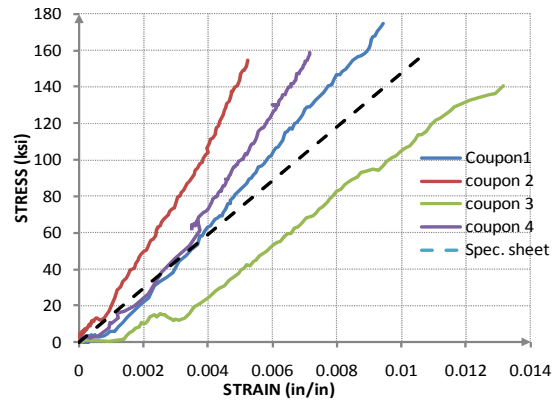
Figure D-8 Stress-strain relationship of CFRP material B
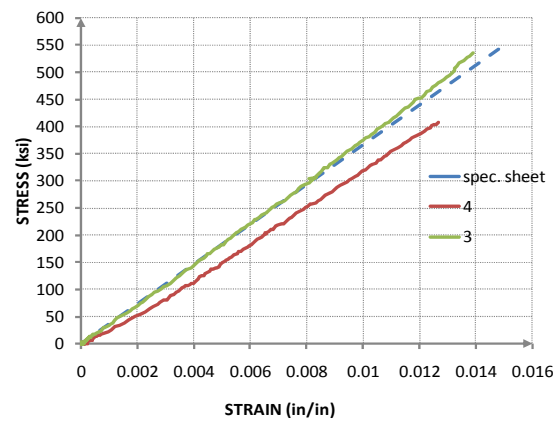
Figure D-9 Stress-strain relationship of CFRP material C

Unfortunately, two coupon tests of laminate C were lost due to a malfunction of data acquisition system (Figure D-9).

Appendix E

Shear Contribution Calculations

In appendix E, the crack patterns of all test and the location of strain gages selected to evaluate shear contribution of each material at ultimate. All shear contributions seen in Chapter 4 were evaluated when the strengthened beam reached maximum strength.

Calculation procedure: Example (24-3-1r)

  1) Steel shear contribution

Table E-1 Force calculations from measured strains in the steel (See pages 3 and 4)

	FRONT SIDE				BACK SIDE			
	3C	2D	3E	4F	3CR	2DR	3ER	4FR
strain	0.0014	0.0022	0.0042	0.0082	0.0055	0.0027	0.0032	0.0003
stress	40.7	62.2	70	70	70	70	70	9.5
force	4.5	6.8	7.7	7.7	7.7	7.7	7.7	1.1

$\sigma_{3C} = E\varepsilon_{3C} = 29000 \times 0.0014 = 40.7$ ksi

If this stress exceeded the yield stress, yield stress was used (3E, 4F, 3CR, 2DR and 3ER).

$F_{3C} = A_s\sigma_{3C} = 0.11 \times 40.7 = 4.5$ kips (Nominal area of No.3 bars is 0.11in.^{2})

All other forces in the stirrup can be easily calculated as the same way.

$F_s = \sum F_{s,i} = 4.5 + 6.8 + 7.7 + 7.7 + 7.7 + 7.7 + 7.7 + 1.1 = 50.9$ kips

2) CFRP shear contribution

Table E-2 Force calculations from measured strains in the FRP (See pages 5 and 6)

	FRONT SIDE				BACK SIDE			
	F1C	F1D	F2E	F2F	F1Cr	F1Dr	F1Er	F2F
strain	0.0002	0.0122	0.0076	0.0027	0.0009	0.0074	0.0071	0.0027
stress	3.4	181.3	112.0	39.8	13.7	110.1	105.0	39.8
force	0.2	10.0	6.2	2.2	0.7	6.1	5.8	2.2

$$\sigma_{F1C} = E\varepsilon_{F1C} = 14800 \times 0.0002 = 3.4 \text{ ksi}$$

$$F_{F1C} = A_f\sigma_{F1C} = (5 \times 0.011) \times 3.4 = 0.2 \text{ kips}$$

$$(\text{Width} = 5 \text{ in.}, \text{ Thickness} = 0.011\text{in.})$$

All other forces in the CFRP strip can be easily calculated as the same way.

$$F_f = \sum F_{f,i} = 0.2 + 10 + 6.2 + 2.2 + 0.7 + 6.1 + 5.8 + 2.2 = 33.2\text{kips}$$

3) Concrete shear contribution

The applied load at evaluation point : 287.3 kips

Applied shear can be calculated from equilibrium equation

$$F_n = \frac{144 - 68}{144 \text{ in}} \times 287.3 = 151.6 \text{ kips}$$

(total span : 12 ft. = 12 ft. × 12in./ft. = 144 in.)

$$F_c = F_n - F_s - F_f = 151.6 - 50.9 - 33.2 = 67.5 \text{ kips}$$

In the same manner, all material shear contributions during loading were evaluated from strain gages. The locations of gages selected to estimated shear contribution are shown in drawings of the crack patterns. The measured strains from those gages are plotted belows.

Parameters	Pre-cracked, Strengthened / 1 Layer, 5"@10"	Steel	Front
		CFRP	Back

4F

3C   3E

2D

3C

2D

3E

4F

Note. Blue:24-3-1 / Red:24-3-1r

Parameters	Pre-cracked, Strengthened / 1 Layer, 5"@10"	Steel	Front
		CFRP	Back

4Fr

3Er

3Cr

2Dr

3CR

2DR

3ER

4FR

Note. Blue:24-3-1 / Red:24-3-1r

Parameters	Pre-cracked, Strengthened / 1 Layer, 5"@10"	Steel	Front
		CFRP	Back

F2E   F2F*

F1C   F1D

F1C

APPLIED SHEAR (kips)

175
150
125
100
75
50
25
0

-0.002   0   0.002   0.004   0.006   0.008   0.01   0.012

STRAIN (in/in)

F1D

APPLIED SHEAR (kips)

175
150
125
100
75
50
25
0

-0.002   0   0.002   0.004   0.006   0.008   0.01   0.012

STRAIN (in/in)

F2E

APPLIED SHEAR (kips)

175
150
125
100
75
50
25
0

-0.002   0   0.002   0.004   0.006   0.008   0.01   0.012

STRAIN (in/in)

F2F

APPLIED SHEAR (kips)

175
150
125
100
75
50
25
0

-0.002   0   0.002   0.004   0.006   0.008   0.01   0.012

STRAIN (in/in)

Note.

Parameters	Pre-cracked, Strengthened / 1 Layer, 5"@10"	Steel	Front
		CFRP	Back

F1Cr

F1Dr

F1Er

Note. There is no record from straingage located at the last strip (strip F), so F2F value double-counted for both sides.

Parameters	No CFRP / control	Steel	Front
		CFRP	Back

2C

2D

3E

4F

Note. The strain value of one side is significantly lower than the other side, so used just one side and double-count it.

Parameters	No CFRP / control	Steel	Front
		CFRP	Back

Note.

Parameters	No bond, bad application (1 Layer, 5"@10")	Steel	Front
		CFRP	Back

2C

2D

4F

Note. 3Er – double count for both sides

Parameters	No bond, poor application (1 Layer, 5"@10")	Steel	Front
		CFRP	Back

3DR

3ER

4FR

Note. C1- double count

Parameters	No bond, poor application (1 Layer, 5"@10")	Steel	Front
		CFRP	Back

F2F, F1E, F1D, F1C

F1C

F1D

F1E

F2F

Note.

Parameters	No bond, poor application (1 Layer, 5"@10")	Steel	Front
		CFRP	Back

F2Fr

F1Cr   F1Dr   F1Er

F1CR

APPLIED SHEAR (kips) vs STRAIN (in/in)

F1DR

APPLIED SHEAR (kips) vs STRAIN (in/in)

F1ER

APPLIED SHEAR (kips) vs STRAIN (in/in)

F2FR

APPLIED SHEAR (kips) vs STRAIN (in/in)

Note.

Parameters	No bond, proper application (1 Layer, 5"@10")	Steel	Front
		CFRP	Back

3C

2D

4F

3C

APPLIED SHEAR (kips)

STRAIN (in/in)

2D

APPLIED SHEAR (kips)

STRAIN (in/in)

4F

APPLIED SHEAR (kips)

STRAIN (in/in)

Note. The contribution of 3ER is double counted

Parameters	No bond, proper application (1 Layer, 5"@10")	Steel	Front
		CFRP	Back

3Er

2Dr

2DR

APPLIED SHEAR (kips)

STRAIN (in/in)

3ER

APPLIED SHEAR (kips)

STRAIN (in/in)

Note.   the contributoin of 3C, 4F was double counted

Parameters	No bond, proper application (1 Layer, 5"@10")	Steel	Front
		CFRP	Back

F1C

F1D

F2E

F2F

Note.

Parameters	No bond, proper application (1 Layer, 5"@10")	Steel	Front
		CFRP	Back

F1CR

F1DR

F1ER

F1ER

Note.

Parameters	Laminate B (1 Layer, 5"@10")	Steel	Front
		CFRP	Back

3C

4D

4E

4F

Note.

Parameters	Laminate B (1 Layer, 5"@10")	Steel	Front
		CFRP	Back

3CR

2DR

3ER

4FR

Note.

Parameters	Laminate B (1 Layer, 5"@10")	Steel	Front
		CFRP	Back

F2F

F1E F1D F1C

F1C

APPLIED SHEAR (kips)

STRAIN (in/in)

F1D

APPLIED SHEAR (kips)

STRAIN (in/in)

F1E

APPLIED SHEAR (kips)

STRAIN (in/in)

F2F

APPLIED SHEAR (kips)

STRAIN (in/in)

Note.

Parameters	Laminate B (1 Layer, 5"@10")	Steel	Front
		CFRP	Back

F2Fr

F1Cr   F1Dr   F1Er

F1CR

APPLIED SHEAR (kips)

175
150
125
100
75
50
25
0

-0.002   0   0.002   0.004   0.006   0.008   0.01   0.012

STRAIN (in/in)

F1DR

APPLIED SHEAR (kips)

175
150
125
100
75
50
25
0

-0.002   0   0.002   0.004   0.006   0.008   0.01   0.012

STRAIN (in/in)

F1ER

APPLIED SHEAR (kips)

175
150
125
100
75
50
25
0

-0.002   0   0.002   0.004   0.006   0.008   0.01   0.012

STRAIN (in/in)

F2FR

APPLIED SHEAR (kips)

175
150
125
100
75
50
25
0

-0.002   0   0.002   0.004   0.006   0.008   0.01   0.012

STRAIN (in/in)

Note.

Parameters	Laminate C (1 Layer, 5"@10")	Steel	Front
		CFRP	Back

3C

2D

4E

Note. 4Fr double counted

Parameters	Laminate C (1 Layer, 5"@10")	Steel	Front
		CFRP	Back

4Fr
3Er
3Cr
2Dr

3CR

APPLIEDSHEAR (kips)
STRAIN (in/in)

2DR

APPLIEDSHEAR (kips)
STRAIN (in/in)

3ER

APPLIED SHEAR (kips)
STRAIN (in/in)

4FR

APPLIED SHEAR (kips)
STRAIN (in/in)

Note. 4Fr double counted

329

Parameters	Laminate C (1 Layer, 5"@10")	Steel	Front
		CFRP	Back

F2E F2F

F1C F1D

F1C

F1D

F2E

F2F

Note.

Parameters	Laminate C (1 Layer, 5"@10")	Steel	Front
		CFRP	Back

F2Fr
F1Er F1Dr F1Cr

F1CR

APPLIED SHEAR (kips)

175
150
125
100
75
50
25
0

-0.002   0   0.002   0.004   0.006   0.008   0.01   0.012

STRAIN (in/in)

F1DR

APPLIED SHEAR (kips)

175
150
125
100
75
50
25
0

-0.002   0   0.002   0.004   0.006   0.008   0.01   0.012

STRAIN (in/in)

F1ER

APPLIED SHEAR (kips)

175
150
125
100
75
50
25
0

-0.002   0   0.002   0.004   0.006   0.008   0.01   0.012

STRAIN (in/in)

F2FR

APPLIED SHEAR (kips)

175
150
125
100
75
50
25
0

-0.002   0   0.002   0.004   0.006   0.008   0.01   0.012

STRAIN (in/in)

Note.

Parameters	Continuous Sheet	Steel	Front
		CFRP	Back

3C

3D

4E

4F

3CR

3DR

3ER

4FR

Note.

Parameters	Continuous Sheet	Steel	Front
		CFRP	Back

F1D

F1E

F2F

F1CR

F1DR

F1ER

F2FR

Note.   F1Cr double counted

Parameters	2 Layers, 5"@10"	Steel	Front
		CFRP	Back

4E 4F

3C 3D

3C

APPLIED SHEAR (kips)

STRAIN (in/in)

3D

APPLIED SHEAR (kips)

STRAIN (in/in)

4E

APPLIED SHEAR (kips)

STRAIN (in/in)

4F

APPLIED SHEAR (kips)

STRAIN (in/in)

Note.

Parameters	2 Layers, 5"@10"	Steel	Front
		CFRP	Back

4Fr
3Er   3Dr   3Cr

3CR

3DR

3ER

4FR

APPLIED SHEAR (kips)
STRAIN (in/in)

Note.

Parameters	2 Layers, 5"@10"	Steel	Front
		CFRP	Back

F1C

F1D

F1E

F2F

Note.

Parameters	2 Layers, 5"@10"	Steel	Front
		CFRP	Back

F2Fr

F1Er

F1Cr

F1CR

APPLIED SHEAR (kips)

STRAIN (in/in)

F1ER

APPLIED SHEAR (kips)

STRAIN (in/in)

F2FR

APPLIED SHEAR (kips)

STRAIN (in/in)

Note.

Parameters	Unanchored (1 Layer, 5"@10")	Steel	Front
		CFRP	Back

3C

3D

4E

4F

Note.

Parameters	Unanchored (1 Layer, 5"@10")	Steel	Front
		CFRP	Back

3CR

3DR

4FR

Note. 4E double counted

| Parameters | Unanchored (1 Layer, 5"@10") | Steel | Front |
| | | CFRP | Back |

F1C

F1D

F2E

F2F

Note.

Parameters	Unanchored (1 Layer, 5"@10")	Steel	Front
		CFRP	Back

F2Fr

F1Cr

F1Er

F3Dr

F1CR

APPLIED SHEAR (kips)

STRAIN (in/in)

F3DR

APPLIED SHEAR (kips)

STRAIN (in/in)

F1ER

APPLIED SHEAR (kips)

STRAIN (in/in)

F2FR

APPLIED SHEAR (kips)

STRAIN (in/in)

Note.

Parameters	Inclined anchor (1 Layer, 5"@10")	Steel	Front
		CFRP	Back

3C

3D

4E

4F

Note.

Parameters	Inclined anchor (1 Layer, 5"@10")	Steel	Front
		CFRP	Back

4Fr

3Er 3Dr 3Cr

3CR

APPLIED SHEAR (kips)

STRAIN (in/in)

3DR

APPLIED SHEAR (kips)

STRAIN (in/in)

3ER

APPLIED SHEAR (kips)

STRAIN (in/in)

4FR

APPLIED SHEAR (kips)

STRAIN (in/in)

Note.

Parameters	Inclined anchor (1 Layer, 5"@10")	Steel	Front
		CFRP	Back

F1C

F1D

F1E

F2F

Note.

Parameters	Inclined anchor (1 Layer, 5"@10")	Steel	Front
		CFRP	Back

F1CR

F1DR

F1ER

F2FR

Note.

Parameters	1 Layer, 5"@10"	Steel	Front
		CFRP	Back

2A

3B

3C

4D

Note. No straingage in redandant side. The contribution of test side was double counted

Parameters	1 Layer, 5"@10"	Steel	Front
		CFRP	Back

F1A

F1B

F1C

F2D

F1BR

F1CR

Note.

Parameters	Control, No CFRP	Steel	Front
		CFRP	Back

3B
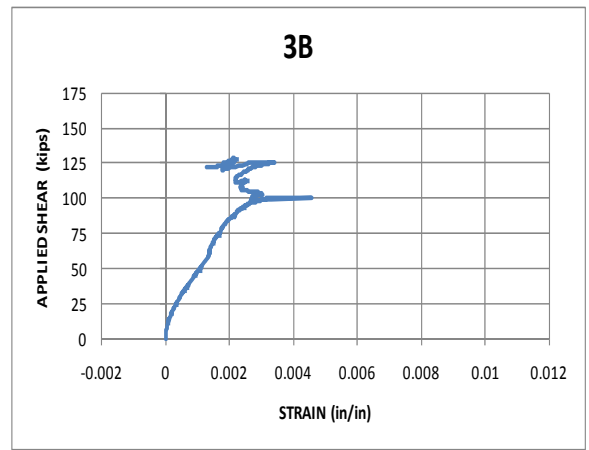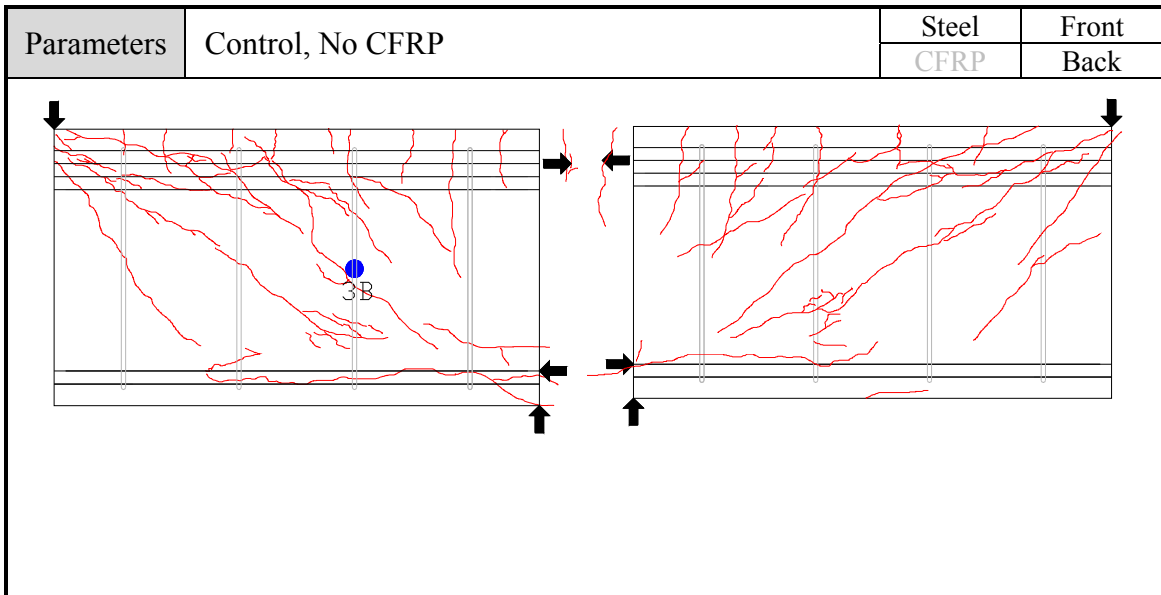
 Note. A few gage were mounted and most of gages were not working. Therefore, from one monitored value, steel contribution was calculated and it might not be accurate.

Parameters	2 Layers, 5" Strip@10"	Steel	Front
		CFRP	Back

2B

2C

2D

4F

2AR

3ER

Note.

Parameters	2 Layers, 5" Strip@10"	Steel	Front
		CFRP	Back

F1A

F1B

F1C

F1Ar

F1Br

F1Cr

Note.

Parameters	2 Layers, 5" Strip@10", No Anchor	Steel	Front
		CFRP	Back

4F 4E 4D
3D
2C 2B 2A

2A

APPLIED SHEAR (kips)
STRAIN (in/in)

2B

APPLIED SHEAR (kips)
STRAIN (in/in)

2C

APPLIED SHEAR (kips)
STRAIN (in/in)

3D

APPLIED SHEAR (kips)
STRAIN (in/in)

4D

APPLIED SHEAR (kips)
STRAIN (in/in)

4E

APPLIED SHEAR (kips)
STRAIN (in/in)

Note.

Parameters	2 Layers, 5" Strip@10", No Anchor	Steel	Front
		CFRP	Back

Note.

Parameters	2 Layers, 5" Strip@10", No Anchor	Steel	Front
		CFRP	Back

F3A

F1B

F2C

F3Ar

F1Br

F2Cr

Note.

Parameters	No CFRP / Control	Steel	Front
		CFRP	Back

2A

3B

3C

4D

4E

4F

Note.

Parameters	No CFRP / Control	Steel	Front
		CFRP	Back

2AR

3BR

3CR

3DR

3ER

4FR

Note.

Parameters	1 Layer, 5" Strip@10", 1 Anchor	Steel	Front
		CFRP	Back

3B

3C

3D

4E

4F

Note. 4Fr: double counted

Parameters	1 Layer, 5" Strip@10", 1 Anchor	Steel	Front
		CFRP	Back

2AR

3BR

3CR

3DR

3ER

4FR

Note.

Parameters	1 Layer, 5" Strip@10", 1 Anchor	Steel	Front
		CFRP	Back

F1A

F1B

F2C

F1AR

F1BR

F2CR

Note.

Parameters	1 Layer, 10" Strip@20", 2 anchors./strip	Steel	Front
		CFRP	Back

D2

E3

F4

G5

Note.

Parameters	1 Layer, 10" Strip@20", 2 anchors./strip	Steel	Front
		CFRP	Back

C1r D2r E3r F4r

C1R

APPLIED SHEAR (kips)

STRAIN (in/in)

D3R

APPLIED SHEAR (kips)

STRAIN (in/in)

E3R

APPLIED SHEAR (kips)

STRAIN (in/in)

F5R

APPLIED SHEAR (kips)

STRAIN (in/in)

Note.

360

Parameters	10" wide strip @ 20"	Steel	Front
		CFRP	Back

C1

D2

E3

G5

Note.

Parameters	10" wide strip @ 20"	Steel	Front
		CFRP	Back

C1R

D1R

E3R

F5R

Note.

Parameters	10" wide strip @ 20"	Steel	Front
		CFRP	Back

FC1
FD1
FE3
FF5

FC1

FD1

FE3

FF5

Note.

Parameters		Steel	Front
		CFRP	Back

FC1R

FD2R

FE4R

FF5R

Note.

Parameters	14" wide strip @ 20"	Steel	Front
		CFRP	Back

C1

D2

E4

F5

Note.

Parameters	14" wide strip @ 20"	Steel	Front
		CFRP	Back

C1R

D1R

E3R

F5R

Note.

Parameters	14" wide strip @ 20"	Steel	Front
		CFRP	Back

FC1

FD2.2

FE4

FF5

Note.

Parameters	14" wide strip @ 20"	Steel	Front
		CFRP	Back

FC1r
FD2r
FE4r
FF5r

FC1R

FD2R

FE4R

FF5R

Note.

Parameters	diagonal application (10" wide strip @ 20")	Steel	Front
		CFRP	Back

A1

C1

D3

E5

Note.

Parameters	diagonal application (10" wide strip @ 20")	Steel	Front
		CFRP	Back

C1R

D3R

E5R

F5R

Note.

Parameters	diagonal application (10" wide strip @ 20")	Steel	Front
		CFRP	Back

FA2

FB4

FC1

FD5

Note.

Parameters	diagonal application (10" wide strip @ 20")	Steel	Front
		CFRP	Back

FE4

(Plot: APPLIED SHEAR (kips) vs STRAIN (in/in))

FB4R

(Plot: APPLIED LOAD (kips) vs STRAIN (in/in))

FC5R

(Plot: APPLIED SHEAR (kips) vs STRAIN (in/in))

FD5R

(Plot: APPLIED SHEAR (kips) vs STRAIN (in/in))

Note.

Parameters	Stirrup spacing 18" –> 10" (10" wide strip @ 20")	Steel	Front
		CFRP	Back

E1

F1

G2

H3

Note.

| Parameters | Stirrup spacing 18" –> 10" (10" wide strip @ 20") | Steel | Front |
| | | CFRP | Back |

I4

J4

K5

L5

Note.

| Parameters | Stirrup spacing 18" –> 10" (10" wide strip @ 20") | Steel | Front |
| | | CFRP | Back |

FC1

FD2

FE4

FF5

Note.

| Parameters | Stirrup spacing 18" –> 10" (10" wide strip @ 20") | Steel | Front |
| | | CFRP | Back |

FC1r
FD2r
FE4r
FE5r

FC1R

APPLIED SHEAR (kips)

STRAIN (in/in)

FD2R

APPLIED SHEAR (kips)

STRAIN (in/in)

FE4R

APPLIED SHEAR (kips)

STRAIN (in/in)

FF5R

APPLIED SHEAR (kips)

STRAIN (in/in)

Note.

Parameters	Control ,w/o CFRP, 10-inch stirrup spacing	Steel	Front
		CFRP	Back

E1

F1

G2

H3

Note.

Parameters	Control ,w/o CFRP,10-inch stirrup spacing	Steel	Front
		CFRP	Back

I4

J4

K5

L5

Note.

Parameters	**repair** (10" wide strip @ 20")	Steel	Front
		CFRP	Back

E5

G1

H3

I4

Note.

Parameters	**repair** (10" wide strip @ 20")	Steel	Front
		CFRP	Back

J5

B2R

D4R

K5R

Note.

Parameters	**repair** (10" wide strip @ 20")	Steel	Front
		CFRP	Back

FC2

FD3

FE4

FF5

Note.

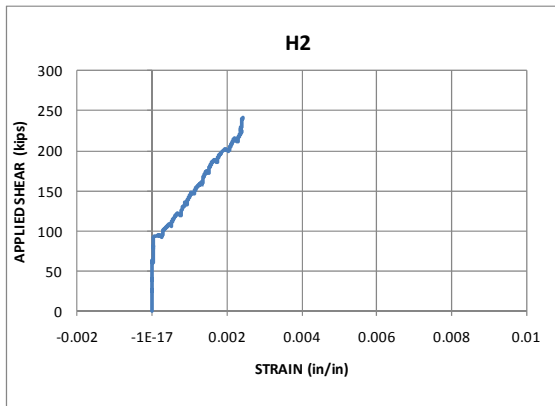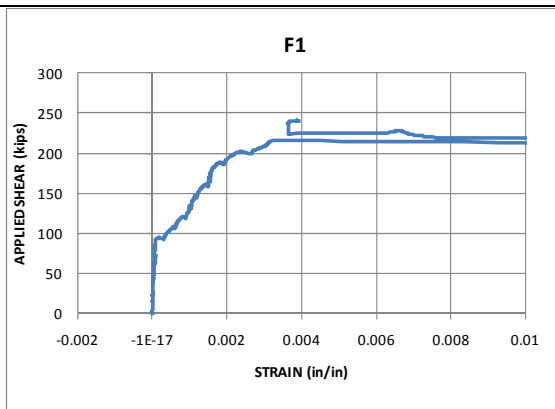| Parameters	repair (10" wide strip @ 20")	Steel	Front
		CFRP	Back

FC2R

FD3R

FE4R

FF5R

Note.

Parameters	intermediate anchor (10" wide strip @ 20")	Steel	Front
		CFRP	Back

F1

G2

H2

J4

Note.

Parameters	intermediate anchor (10" wide strip @ 20")	Steel	Front
		CFRP	Back

E1r
I3r
L5r

K5

APPLIED SHEAR (kips)
STRAIN (in/in)

E1R

APPLIED SHEAR (kips)
STRAIN (in/in)

I3R

APPLIED SHEAR (kips)
STRAIN (in/in)

L5R

APPLIED SHEAR (kips)
STRAIN (in/in)

Note.

Parameters	intermediate anchor (10" wide strip @ 20")	Steel	Front
		CFRP	Back

FD2

FC1

FE3

FF5

FC1

APPLIED SHEAR (kips)

STRAIN (in/in)

FD2

APPLIED SHEAR (kips)

STRAIN (in/in)

FE3

APPLIED SHEAR (kips)

STRAIN (in/in)

FF5

APPLIED SHEAR (kips)

STRAIN (in/in)

Note.

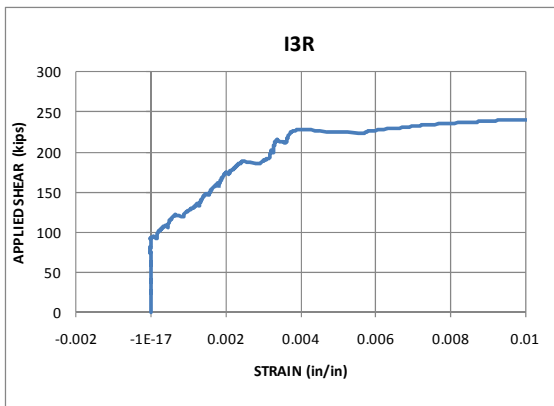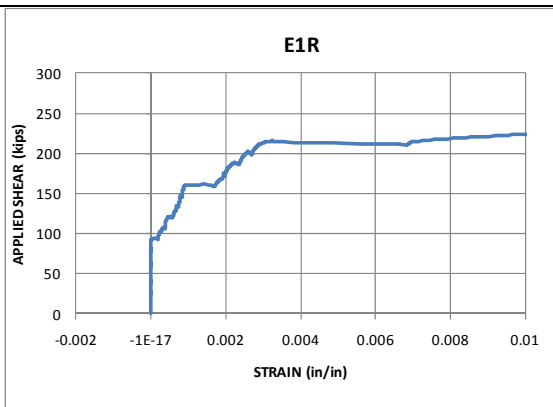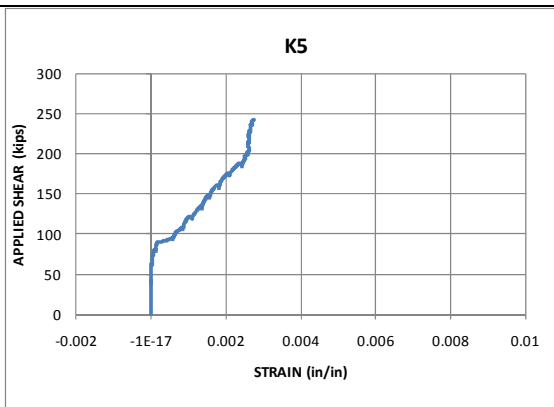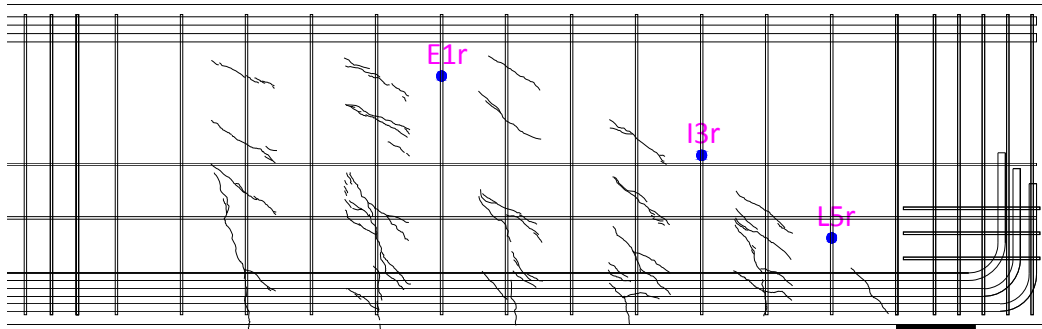| Parameters	intermediate anchor (10" wide strip @ 20")	Steel	Front
		CFRP	Back

FC1r FD2r FE4r FE5r

FC1R

APPLIED SHEAR (kips)

STRAIN (in/in)

FD2R

APPLIED SHEAR (kips)

STRAIN (in/in)

FE4R

APPLIED SHEAR (kips)

STRAIN (in/in)

FF5R

APPLIED SHEAR (kips)

STRAIN (in/in)

Note.

Parameters	2 layers (10" wide strip @ 20")	Steel	Front
		CFRP	Back

E1

F1

G2

H3

Note. Straingage values were selected one side and the values of other side were considered as the same value.

| Parameters | 2 layers (10" wide strip @ 20") | Steel | Front |
| | | CFRP | Back |

I4

J4

K4

L5

Note. Straingage values were selected one side and the values of other side were considered as the same value.

Parameters	2 layers (10" wide strip @ 20")	Steel	Front
		CFRP	Back

FC1

FD2

FE4

FF5

Note.

Parameters	2 layers (10" wide strip @ 20")	Steel	Front
		CFRP	Back

FC1r
FD2r
FE3r
FF5r

FC1R

FD2R

FE3R

FF5R

Note.

Appendix F

Design Example using Proposed Modifications to ACI 440.2R
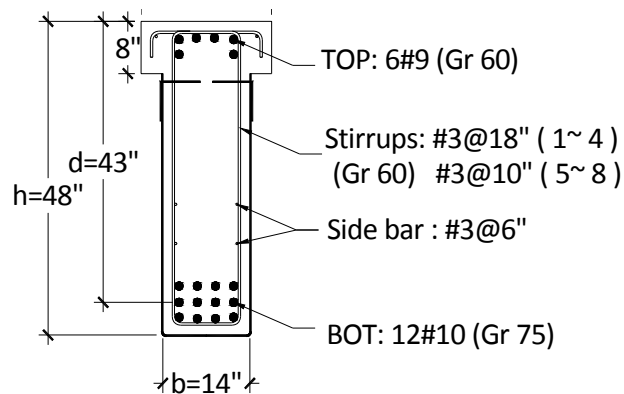
F.1 Debonding Case Using ACI 440.2R

a) Calculate V_c $f'_c = 4000$ psi

$$V_c = 2\sqrt{f'_c}b_w d = 2 \times \sqrt{4000} \times 14 \times 43.125$$

$$= 76369 * 1\text{kip} / 1000 \text{ lbs} = 76.38 \text{ k}$$

b) Calculate V_s

$$V_s = A_s f_y \frac{d}{s} =$$

Grade 60 #3@18"	Grade 60 #3@10"
$2 \times 0.11 \times 60 \times \dfrac{43.125}{18} = 31.625 \text{ k}$	$2 \times 0.11 \times 60 \times \dfrac{43.125}{10} = 56.925 \text{ k}$

Existing beam

$$V_{n,exist} = V_c + V_s + V_f=$$

Grade 60 #3@18"	Grade 60 #3@10"
76.4 + 31.6 + 0 = 108 k	76.4 + 56.9 + 0 = 133 k

c) Calculate V_f

10" wide @20" CFRP strips

$$E_f = 1.48 \times 10^7 \text{ psi} , \quad \varepsilon_{fu} = 0.0105 , \quad t_f = 0.011 \text{ in.}^2$$

$$E_c = 57000\sqrt{f_c'} = 57000\sqrt{4000} = 3.605 \times 10^6 \text{ psi}$$

$$n_f = \frac{E_f}{E_c} = \frac{14.8}{3.605} = 4.1$$

$$\kappa_v = \frac{k_1 k_2 L_e}{468\varepsilon_{fu}} = \frac{1\times0.97\times1.05}{468\times0.0105} = 0.21 \qquad \leq 0.75$$

$$L_e = \frac{2500}{(n_f t_f E_f)^{0.58}} = \frac{2500}{(4.1\times0.011\times1.48\times10^7)^{0.58}} = 1.05$$

$$k_1 = \left(\frac{f_c'}{4000}\right)^{2/3} = \left(\frac{4000}{4000}\right)^{2/3} = 1 \quad , \qquad k_2 = \frac{d_{fv}-L_e}{d_{fv}} = \frac{35.5-1.05}{35.5} = 0.97$$

$$\varepsilon_{fe} = \kappa_v \, \varepsilon_{fu} = 0.21 \times 0.0105 = 0.0022$$

$$f_{fe} = E_f \, \varepsilon_{fe} = 1.48 \times \frac{10^7}{1000} \times 0.0022 = 31.1 \text{ ksi}$$

$$V_f = A_{fv}f_{fe}\frac{d_f}{s_f} = A_{fv}f_{fe}\frac{d_f}{s_f} = 0.22 \times 31.1 \times \frac{35.125}{20} = 12.55 \text{ k}$$

After strengthening

$$V_{n,strengthening} = V_c + V_s + V_f=$$

Grade 60 #3@18"	Grade 60 #3@10"
76.4 + 31.6+ 12.5 = 120.6 k	76.4 + 56.9+ 12.5 = 146 k

Net CFRP contribution or strength increase

Grade 60 #3@18"	Grade 60 #3@10"
$120.6 - 108 = 12.5, \quad \frac{12.5}{108} = 11.7\%$	$146 - 133 = 12.5k , \quad \frac{12.5}{133} = 9.5\%$

F.2 Complete Wrapping (U-Wraps with CFRP Anchors) Case in ACI 440.2R

a) V_c and V_s is same value with debonding.

b) Calculate V_f

    10" wide @20" CFRP strips

$$f_{fe} = E_f\, \varepsilon_f = 1.48 \times \frac{10^7}{1000} \times 0.004 = 59.2 \text{ ksi}$$

$$V_f = A_{fv}f_{fe}\frac{d_f}{s_f} = A_{fv}f_{fe}\frac{d_f}{s_f} = 0.22 \times 59.2 \times \frac{35.125}{20} = 22.8 \text{ k}$$

After strengthening

$V_{n,strengthening} = V_c + V_s + V_f =$

Grade 60 #3@18"	Grade 60 #3@10"
= 76.4 + 31.6+ 22.8 = 130.8 k	= 76.4 + 56.9+ 22.8 = 156 k

Net CFRP contribution or strength increase

Grade 60 #3@18"	Grade 60 #3@10"
$130.8 - 108 = 22.8k$, $\frac{12.5}{108} = 21.1\%$	$156 - 133 = 22.8k$, $\frac{12.5}{133} = 17.1\%$

F.3 Proposed Equation for U-Wraps with CFRP Anchors

Proposed equation using factors k_s , k_f can be applied to all strengthening schemes. However bond critical applications – U-wraps and 2-sides bonded- are not recommended because debonding failure is not desirable. The proposed equation is only applied to the case of U-wraps with CFRP anchors.

$V_{c0} = 76.4\text{k}$, $V_{f0} = 22.8\text{k}$

Because $k_a = 1$,

$V_c = V_{c0}, V_s = k_s V_{s0}\ V_f = k_f V_{f0}$

- Calculate k_s , k_f and shear contributions ($V_s V_f$)

Grade 60 #3@18	Grade 60 #3@10
$V_{s0} = 31.6k$	$V_{s0} = 56.9k$
Existing beam	*Existing beam*
$k_s = \dfrac{8V_{c0}}{4V_{c0}+V_{s0}+V_{f0}}$	$k_s = \dfrac{8V_{c0}}{4V_{c0}+V_{s0}+V_{f0}}$
$= \dfrac{8\times76.4}{4\times76.4+31.6+0} = 1.81$	$= \dfrac{8\times76.4}{4\times76.4+56.9+0} = 1.69$
$k_f = \dfrac{6V_{c0}}{4V_{c0}+V_{s0}+V_{f0}}$	$k_f = \dfrac{6V_{c0}}{4V_{c0}+V_{s0}+V_{f0}}$
$= \dfrac{6\times76.4}{4\times76.4+31.6+0} = 1.36$	$= \dfrac{6\times76.4}{4\times76.4+56.9+0} = 1.26$
$V_s = k_sV_{s0} = 1.81 \times 31.6 = 57.3k$	$V_s = k_sV_{s0} = 1.69 \times 56.9 = 95.9k$
$V_f = k_fV_{f0} = 1.26 \times 0 = 0k$	$V_f = k_fV_{f0} = 1.26 \times 0 = 0k$
$V_{n,exist} = V_c + V_s + V_f$	$V_{n,exist} = V_c + V_s + V_f$
$= 76.4 + 57.3 + 0 = 133.7k$	$= 76.4 + 95.9 + 0 = 172.3 \text{ k}$
After strengthening	*After strengthening*
$k_s = \dfrac{8V_{c0}}{4V_{c0}+V_{s0}+V_{f0}}$	$k_s = \dfrac{8V_{c0}}{4V_{c0}+V_{s0}+V_{f0}}$
$= \dfrac{8\times76.4}{4\times76.4+31.6+22.8} = 1.70$	$= \dfrac{8\times76.4}{4\times76.4+56.9+22.8} = 1.59$
$k_f = \dfrac{6V_{c0}}{4V_{c0}+V_{s0}+V_{f0}}$	$k_f = \dfrac{6V_{c0}}{4V_{c0}+V_{s0}+V_{f0}}$
$= \dfrac{6\times76.4}{4\times76.4+31.6+22.8} = 1.27$	$= \dfrac{6\times76.4}{4\times76.4+56.9+22.8} = 1.19$
$V_s = k_sV_{s0} = 1.70 \times 31.6 = 53.6k$	$V_s = k_sV_{s0} = 1.59 \times 56.9 = 90.3k$
$V_f = k_fV_{f0} = 1.27 \times 22.8 = 29.0k$	$V_f = k_fV_{f0} = 1.19 \times 22.8 = 27.1k$
$V_{n,strengthening} = V_c + V_s + V_f$	$V_{n,strengthening} = V_c + V_s + V_f$
$= 76.4 + 53.6 + 29.0 = 159.1 \text{ k}$	$= 76.4 + 90.3 + 27.1 = 193.8 \text{ k}$
Net CFRP contribution or strength increase	Net CFRP contribution or strength increase
$159 - 134 = 25k$, $\dfrac{159-134}{134} = 19.0\%$	$194 - 172 = 22k$, $\dfrac{194-172}{172} = 12.8\%$

References

AASHTO (2007), *AASHTO LRFD Bridge Design Specifications*, 4th edition, Washington, DC, USA.

ACI-ASCE Committee 445 (1998). Recent Approaches to Shear Design of Structural Concrete. *Journal of Structural Engineering*, Vol. 124, No. 12, pp. 1375-1417.

ACI Committee 318 (2008). Building Code Requirements for Structural Concrete (ACI 318-08), American Concrete Institute, Farmington Hills, Michigan, USA

ACI Committee 440 (2004). Guide Test Methods for Fiber-Reinforced Polymers (FRPs) for Reinforcing or Strengthening Concrete Structures.(ACI 440.3R-04), American Concrete Institute, Farmington Hills, Michigan, USA

ACI Committee 440 (2006). Guide for the Design and Construction of Structural Concrete Reinforced with FRP Bars (ACI 440.1R-06), American Concrete Institute, Farmington Hills, MI, USA.

ACI Committee 440 (2007) Report on Fiber-Reinforced Polymer (FRP) Reinforcement for Concrete Structures.(ACI 440R-07), American Concrete Institute. Farmington Hills, MI, USA

ACI Committee 440 (2008). Guide for the Design and Construction of Externally Bonded FRP Systems for Strengthening Concrete Structures (ACI 440.2R-08), American Concrete Institute, Farmington Hills, Michigan, USA

Adhikary, Bimal Babu and Mutsuyoshi, Hiroshi (2006). "Shear strengthening of RC beams with web-bonded continuous steel plates," *Construction and Building Materials*, Vol. 20, No. 5, pp. 296-307.

Ahmed, Ehab A., El-Salakawy, Ehab F. et al. (2008). "Tensile Capacity of GFRP Postinstalled Adhesive Anchors in Concrete," *Journal of Composites for Construction,* Vol. 12, No. 6, pp. 596-607.

Arduini, Marco and Nanni, Antonio (1997). "Behavior of Precracked RC Beams Strengthened with Carbon FRP Sheets," *Journal of Composites for Construction,* Vol. 1, No. 2, pp. 63-70.

Alrousan, R. Z. et al.,"Size Effect of Reinforce Beams on Shear Contribution of CFRP Composite," *The Ninth International Symposium on Fiber Reinforced Polymer Reinforcement for Concrete Structures*. Sydney, Australia, FRPRCS-9, pp.1-4

ASTM D3039-07 (2007), *Standard Test Method for Tensile Properties of Polymer Matrix Composite Materials*, American Society for Testing Materials, (ASTM International).

Bakis, C. E., Bank, L. C., Brown, Vol. L., Cosenza, E., Davalos, J. F., Lesko, J. J., Machida, A., Rizkalla, S. H., and Trianatfillou, T. C. (2002), ―Fiber-Reinforced Polymer Composites for Construction – State of the Art Review, *Journal of Composites for Construction*, Vol. 6, No. 2, pp. 73-87.

Bank, Lawrence C. (2006), Composites for Construction – Structural Design with FRP Materials, John Wiley and Sons, Inc., Hoboken, New Jersey.

Barros, J., and Dias, S. (2003), ―Shear Strengthening of Reinforced Concrete Beams with Laminate Strips of CFRP, *Proceedings*, International Conference on Composites in Constructions (CCC2003), Italy, pp. 289-294.

Barros, J., and Dias, S. (2006), "Near Surface Mounted CFRP Laminates for Shear Strengthening of Concrete Beams," *Cement & Concrete Composites*, Vol. 28, No. 3, pp. 276-292.

Birrcher, David (2009). Design of Reinforced Concrete Deep Beams for Strength and Serviceability, The Univesity of Texas at Austin, Ph.D Dissertation

Bonacci, J. F. and Maalej, M. (2001). "Behavioral Trends of RC Beams Strengthened with Externally Bonded FRP," *Journal of Composites for Construction,* Vol. 5, No. 2, pp. 102-113.

Bousselham, Abdelhak and Chaallal, Omar (2004). "Shear Strengthening of Reinforced Concrete Beams with Fiber Reinforced Polymer: Assessment of Influencing Parameters and Required Research," *ACI Structural Journal*, Vol. 101, No. 2, pp. 219-227.

Bousselham, Abdelhak and Chaallal, Omar (2006a). "Behavior of Reinforced Concrete T-Beams Strengthened in Shear with Carbon Fiber Reinforced Polymer - An Experimental Study. ," *ACI Structural Journal*, Vol. 103, No. 3, pp. 339-347.

Bousselham, Abdelhak and Chaallal, Omar (2006b). "Effect of transverse steel and shear span on the performance of RC beams strengthened in shear with CFRP," *Composites Part B: Engineering*, Vol. 37, No. 1, pp. 37-46.

Bousselham, Abdelhak and Chaallal, Omar (2008). "Mechanisms of Shear Resistance of Concrete Beams Strengthened in Shear with Externally Bonded FRP," *Journal of Composites for Construction,* Vol. 12, No. 5, pp. 499-512.

Cao, S. Y., Chen, J. F. et al. (2005). "Debonding in RC Beams Shear Strengthened with Complete FRP Wraps," *Journal of Composites for Construction*, Vol. 9, No. 5, pp. 417-428.

Carolin, Anders and Taljsten, Bjorn (2005a). "Experimental Study of Strengthening for Increased Shear Bearing Capacity," *Journal of Composites for Construction*, Vol. 9, No. 6, pp. 488-496.

Carolin, Anders and Taljsten, Bjorn (2005b). "Theoretical Study of Strengthening for Increased Shear Bearing Capacity," *Journal of Composites for Construction,* Vol. 9, No. 6, pp. 497-506.

Ceroni, Francesca, Pecce, Marisa et al. (2008). "Debonding Strength and Anchorage Devices for Reinforced Concrete Elements Strengthened with FRP Sheets," *Composites Part B: Engineering*, Vol. 39, No. 3, pp. 429-441.

Ceroni, Francesca and Pecce, Marisa (2010). "Evaluation of Bond Strength in Concrete Elements Externally Reinforced with CFRP Sheets and Anchoring Devices," *Journal of Composites for Construction,* Vol. 14, No. 5, pp. 521-530.

Chaallal, O., Shahawy, M. et al. (2002). "Performance of reinforced concrete T-girders strengthened in shear with carbon fiber-reinforced polymer fabric," *ACI Structural Journal*, Vol. 99, No. 3, pp. 335-343.

Chajes, Michael J. et al. (1994). "Flexural strengthening of concrete beams using externally bonded composite materials," *Construction and Building Materials*, Vol. 8, No. 3, pp. 191-201.

Chajes, Michael J. et al. (1995). "Shear Strengthening of Reinforced Concrete Beams Using Externally Applied Composite Fabrics," *ACI Structural Journal*, Vol. 92, No. 3, pp. 295-303.

Chen, J. F. and Teng, J. G. (2001). "Anchorage Strength Models for FRP and Steel Plates Bonded to Concrete," *Journal of Structural Engineering*, Vol. 127, No. 7, pp. 784-791.

Chen, J. F. and Teng, J. G. (2003a). "Shear Capacity of Fiber-Reinforced Polymer-Strengthened Reinforced Concrete Beams: Fiber Reinforced Polymer Rupture," *Journal of Structural Engineering*, Vol. 129, No. 5, pp. 615-625.

Chen, J. F. and Teng, J. G. (2003b). "Shear capacity of FRP-strengthened RC beams: FRP debonding," *Construction and Building Materials*, Vol. 17, No. 1, pp. 27-41.

Chen, G. M., Teng, J. G. et al. (2010). "Interaction between Steel Stirrups and Shear-Strengthening FRP Strips in RC Beams," *Journal of Composites for Construction,* Vol. 14, No. 5, pp. 498-509.

De Lorenzis, L., and Nanni, A. (2001a), "Shear Strengthening of Reinforced Concrete Beams with Near-Surface Mounted Fiber-Reinforced Polymer Rods," *ACI Structural Journal*, Vol. 98, No. 1, pp. 60-68.

De Lorenzis, L., and Nanni, A. (2001b), "Characterization of NSM FRP Rods as Near Surface Mounted Reinforcement," *Journal of Composites for Construction*, Vol. 4, pp. 114-121.

Deifalla, A. and Ghobarah, A.(2006). Calculating the Thickness of FRP Jacket for Shear and Torsion Strengthening of RC Girders T-Girders. *Third International Conference on FRP Composites in Civil Engineering. CICE 2006*. Miami, Florida.

Deniaud, C. and Cheng, J. J. Roger (2001). "Shear Behavior of Reinforced Concrete T-Beams with Externally Bonded Fiber-Reinforced Polymer Sheets," *ACI Structural Journal*, Vol. 98, No. 3, pp. 386-394.

Deniaud, C. and Cheng, J. J. Roger (2003). "Reinforced Concrete T-beams Strengthened in Shear with Fiber Reinforced Polymer Sheets," *Journal of Composites for Construction,* Vol. 7, No. 4, pp. 302-310.

Deniaud, Christophe and Cheng, J. J. Roger (2004). "Simplified Shear Design Method for Concrete Beams Strengthened with Fiber Reinforced Polymer Sheets," *Journal of Composites for Construction*, Vol. 8, No. 5, pp. 425-433.

Eshwar, N., Nanni, A. et al. (2008). "Performance of Two Anchor Systems of Externally Bonded Fiber-reinforced Polymer Laminates," *ACI Materials Journal*, Vol. 105, No. 1, pp. 72-80.

Grande, E., Imbimbo, M. et al. (2009). "Effect of Transverse Steel on the Response of RC Beams Strengthened in Shear by FRP: Experimental Study," *Journal of Composites for Construction,* Vol. 13, No. 5, pp. 405-414.

Hoult, N. A. and Lees, J. M. (2009). "Efficient CFRP Strap Configurations for the Shear Strengthening of Reinforced Concrete T-Beams," *Journal of Composites for Construction,* Vol. 13 No. 1, pp. 45-52.

Islam, M. R., Mansur, M. A. et al. (2005). "Shear Strengthening of RC Deep beams Using Externally Bonded FRP Systems," *Cement and Concrete Composites*, Vol. 27, No. 3, pp. 413-420.

Japanese Society of Civil Engineers (JSCE). (1997). "Recommendations for Design and Construction of Concrete Structures Using Continuous Fiber Reinforcing Materials," *Concrete Engineering Series , 23* . (A. Machida, Ed.), Tokyo, Japan.

Jirsa, James O and Kim, Yungon et al. (2011) "Shear Strengthening of Bridge Girders Using Cfrp Sheets and Anchors," fib Symposium, Prague, 2011, pp.1137-1140

Khalifa, A., Alkhrdaji, T. et al. (1999). "Anchorage of Surface Mounted FRP Reinforcement," *Concrete International*, Vol. 21, No. 10, pp. 49-54.

Khalifa, Ahmed, Gold, William J. et al. (1998). "Contribution of Externally Bonded FRP to Shear Capacity of RC Flexural Members," *Journal of Composites for Construction,* Vol. 2, No. 4, pp. 195-202.

Khalifa, Ahmed and Nanni, Antonio (2000). "Improving shear capacity of existing RC T-section beams using CFRP composites," *Cement and Concrete Composites*, Vol. 22, No. 3, pp. 165-174.

Khalifa, Ahmed and Nanni, Antonio (2002). "Rehabilitation of rectangular simply supported RC beams with shear deficiencies using CFRP composites," *Construction and Building Materials*, Vol. 16, No. 3, pp. 135-146.

Kim, Insung (2008). Use of CFRP to Provide Continuity in Existing Reinforced Concrete Members Subjected to Extreme Loads. Deparment of Civil, Environmental and

Architectural Engineering. Austin, Texas, The University of Texas at Austin. Ph.D Dissertation.

Kim, S. J. and Smith, S. T. (2009). Shear Strength and Behavior of FRP Spike Anchors in Cracked Concrete. (CD-ROM). *Ninth International Symposium on Fiber Reinforced Polymer Reinforcement for Concrete Structures.* Sydney, Australia, FRPRCS-9**: pp.** 1-4.

Kim, S. J. and Smith, S. T. (2010). "Pullout Strength Models for FRP Anchors in Uncracked Concrete," *Journal of Composites for Construction,* Vol. 14, No. 4, pp 406-414.

Kim, Yungon et al. (2011) "Shear Strengthening RC T-beams Using CFRP Laminates and Anchors," *Proceedings of the 10th International Symposium on Fiber-Reinforced Polymer (FRP) Reinforcement for Concrete Structures,.FRPRCS- 10 (ACI SP275-36),* Tampa, Florida, April, 2011, pp. 1- 17

Kobayashi, K., Fujii, S., Yabe, Y., Tsukagoshi, H., & Sugiyama, T. (2001). Advanced Wrapping System with CF-Anchor. *FRP-128 ,* pp.1-10.

Kobayashi, K., Fujii, S. et al.(2001). Advanced Wrapping System with CF Anchor-Stress Transfer Mechanism of CF Anchor. *Proceedings of the 5th International Symposium on Fiber-Reinforced Polymer (FRP) Reinforcement for Concrete Structures,.* FRPRCS-5. Cambridge, U.K. , pp. 379-388.

Leung, C., Chen, Z., Lee, S., Mandy, N., Ming, X., and Tang, J. (2007), "Effect of Size on the Failure of Geometrically Similar Concrete Beams Strengthened in Shear with FRP Strips," *Journal of Composites for Construction*, Vol. 11, No. 5, pp. 487-496.

Lu, X. Z., Chen, J. F., et al. (2009). "RC Beams Shear-strengthened with FRP: Stress Distributions in the FRP Reinforcement," *Construction and Building Materials*, Vol. 23, No. 4, pp. 1544-1554.

Maalej, M. and Bian, Y. (2001). "Interfacial Shear Stress Concentration in FRP-strengthened Beams," *Composite Structures*, Vol. 54, No. 4, pp. 417-426.

Maalej, M. and Leong, K. S. (2005). "Effect of Beam Size and FRP Thickness on Interfacial Shear Stress Concentration and Failure Mode of FRP-strengthened Beams," *Composites Science and Technology*, Vol. 65, No. 7-8, pp. 1148-1158.

Maeda, T., Asano, Y. et al. (1997). "A Study on Bond Mechanism of Carbon Fiber Sheets, Proceedings of the 3rd International Symposium," *Non-Metallic (FRP) reinforcement for concrete structures*, Vol., No. 1, pp 279-286.

Malek, A. M. Saadatmanesh, Hamid (1998a). "Analytical Study of Reinforced Concrete Beams Strengthened with Web-Bonded Fiber Reinforced Plastic Plates or Fabrics " *ACI Structural Journal*, Vol. 95, No. 3, pp. 343-352.

Malek, Amir M. and Saasatmanesh, Hamid (1998b). "Ultimate Shear Capacity of Reinforced Concrete Beams Strengthened with Web-Bonded Fiber-Reinforced Plastic Plates," *ACI Structural Journal*, Vol. 95, No. 4, pp. 391-399.

Martin, Jeremy A. and Lamanna, Anthony J. (2008). "Performance of Mechanically Fastened FRP Strengthened Concrete Beams in Flexure," *Journal of Composites for Construction,* Vol. 12, No. 3, pp 257-265.

Monti, G., and Liotta, M. A. (2005), "FRP-Strengthening in Shear: Tests and Design Equations," *Proceedings*, *7th International RILEM Symposium on Non-Metallic (FRP) Reinforcement for Concrete Structures (FRPRCS-7)*, Kansas City, Missouri, USA, pp. 543-562.

NCHRP Report 514 (2004). "Bonded Repair and Retrofit of Concrete Structures Using FRP Composites—Recommended Construction Specifications and Process Control Manual ". Transportation Research Board. Washington, DC, USA.

NCHRP Report 655 (2010). Recommended Guide Specification for the Design of Externally Bonded FRP Systems for Repair and Strengthening of Concrete Bridge Elements. Transportation Research Board. Washington, DC, USA.

NCHRP Report 678 (2011). Design of FRP Systems for Strengthening Concrete Girders in Shear, Transportation Research Board. Washington, DC, USA.

Nozaka, Katsuyoshi, Shield, Carol K. et al. (2005). "Effective Bond Length of Carbon-Fiber-Reinforced Polymer Strips Bonded to Fatigued Steel Bridge I-Girders," *Journal of Bridge Engineering*, Vol. 10, No. 2, pp. 195-205.

Ortega, C. A., Belarbi, A. et al. (2009). End Anchorage of Externally Bonded FRP Sheets for the Case of Shear Strengthening of Concrete Girders. *The Ninth International*

Symposium on Fiber Reinforced Polymer Reinforcement for Concrete Structures, FRPRCS-9 . Sydney, Australia**:** 4 p.

Orton, S. L. (2007). Development of a CFRP System to Provide Continuity in Existing Reinforced Concrete Structures Vulnerable to Progressive Collapse. Department of Civil, Environmental and Architectural Engineering. Austin, Texas, The University of Texas at Austin. Ph.D Dissertation.

Orton, Sarah L., Jirsa, James O. et al. (2008). "Design Considerations of Carbon Fiber Anchors," *Journal of Composites for Construction,* Vol. 12, No. 6, pp. 608-616.

Ouezdou, Mongi Ben, Belarbi, Abdeldjelil et al. (2009). "Effective Bond Length of FRP Sheets Externally Bonded to Concrete," *International Journal of Concrete Structures and Materials*, Vol. 3, No. 2, pp. 127-131.

Ozbakkaloglu, Togay and Saatcioglu, Murat (2009). "Tensile Behavior of FRP Anchors in Concrete," *Journal of Composites for Construction,* Vol. 13, No. 2, pp. 82-92.

Pellegrino, C. and Modena, C. (2006). "Fiber-reinforced Polymer Shear Strengthening of Reinforced Concrete Beams: Experimental Study and Analytical Modeling," *ACI Structural Journal*, Vol. 103, No. 5, pp. 720-728.

Pellegrino, Carlo and Modena, Claudio (2002). "Fiber Reinforced Polymer Shear Strengthening of Reinforced Concrete Beams with Transverse Steel Reinforcement," *Journal of Composites for Construction,* Vol. 6, No. 2, pp. 104-111.

Pellegrino, Carlo, Tinazzi, Davide et al. (2008). "Experimental Study on Bond Behavior between Concrete and FRP Reinforcement," *Journal of Composites for Construction,* Vol. 12, No. 2, pp. 180-189.

Quinn, Kevin (2009). Shear Strengthening of Reinforced Concrete Beams with Carbon Fiber Reinforced Polymer (CFRP) and Improved Anchor Details. Austin, TX, University of Texas at Austin, Master Thesis.

Saadatmanesh, Hamid and Ehsani, Mohammad R. (1991). "RC Beams Strengthened with GFRP Plates. I: Experimental Study," *Journal of Structural Engineering*, Vol. 117, No. 11, pp. 3417-3433.

Sas, G., Taljsten, B. et al. (2009). "Are Available Models Reliable for Predicting the FRP Contribution to the Shear Resistance of RC Beams?," *Journal of Composites for Construction,* Vol. 13, No. 6, pp. 514-534.

Sato, Y., Ueda, T., Kakuta, Y., and Tanaka, T. (1996), "Shear Reinforcing Effect of Carbon Fiber Sheet Attached to the Side of Reinforced Concrete Beams," *Proceedings*, 3rd International Conference on Advanced Composite Materials in Bridges and Structures, Montreal, Canada, pp. 621-628.

Schuman, P. M. (2004), Mechanical Anchorage for Shear Rehabilitation of Reinforced Concrete Structures with FRP: An Appropriate Design Approach, Ph.D. Dissertation, Department of Structural Engineering, University of California, UCSD, San Diego, CA,USA.

Teng, J. G., Smith, S. T., et al. (2003). "Intermediate Crack-Induced Debonding in RC Beams and Slabs," *Construction and Building Materials*, Vol. 17, No. 6-7, pp. 447-462.

Teng, J. G., Lam, L., and Chen, J. F. (2004), ―Shear Strengthening of RC Beams with FRP Composites, *Progress in Structural Engineering Materials*, Vol. 6, pp. 173-184.

Teng, J. G. and Yao, J. (2007). "Plate End Debonding in FRP-plated RC Beams -II: Strength Model," *Engineering Structures*, Vol. 29, No. 10, pp. 2472-2486.

Triantafillou, Thanasis C. (1998). "Shear Strengthening of Reinforced Concrete Beams Using Epoxy-bonded FRP Composites," *ACI Structural Journal*, Vol. 95, No. 2, pp. 107-115.

Triantafillou, Thanasis C. (1998). "Composites: A New Possibility for the Shear Strengthening of Concrete, Masonry and Wood," *Composites Science and Technology*, Vol. 58, No. 8, pp. 1285-1295.

Triantafillou, Thanasis C. and Antonopoulos, Costas P. (2000). "Design of Concrete Flexural Members Strengthened in Shear with FRP," *Journal of Composites for Construction,* Vol. 4, No. 4, pp. 198-205.

Ueda, T. and Dai, J. (2005). "Interface Bond between FRP Sheets and Concrete Substrates: Properties, Numerical Modeling and Roles in Member Behavior," *Progress in Structural Engineering and Materials John Wiley & Sons Ltd.*, Vol. 7, No. 1, pp. 27-43.

Uji, K. (1992). "Improving Shear Capacity of Existing RC Concrete Members by Applying Carbon Fiber Sheets," *Transactions of the Japan Concrete Institute*, Vol. 14, pp. 253-256.

Wu, Zhishen, Shao, Yixin, et al. (2007). "Strengthening of Preloaded RC Beams Using Hybrid Carbon Sheets," *Journal of Composites for Construction,* Vol. 11, No. 3, pp. 299-307.

Zhang, Z. and Hsu, C.-T. T (2005). "Shear Strengthening of Reinforced Concrete Beams Using Carbon-fibre-reinforced Polymer Laminates," *Journal of Composite for Construstion*, Vol. 9, No. 2, pp. 158-169.

Vita

Yungon Kim was born in Seoul, South Korea in 1977, the son of Raebok Kim and Kyungsoon Cho. He graduated Hansung Science high school for gifted students in 1996. He entered Yonsei University. He served military service from 1997 to 1999. He received the degree of Bachelor of Science in Architectural Engineering in 2002. He then continued graduate school at the Seoul National University and got the degree of Master of Science in 2004. Since then, he worked for Hyundai Engineering and Construction as a structural engineer. In 2007, he attended the graduate school at the University of Texas at Austin.

Permanent address: 130-24, Junnong-dong,

Dongdaemun-gu, Seoul

South Korea   (130 - 020)

emptyspace@utexas.edu

This dissertation was typed by the author.